

Evaluation of the ECCO-Darwin Ocean Biogeochemistry State Estimate vs. In-situ Observations

Dustin Carroll^{1,2}, Dimitris Menemenlis², Hong Zhang², Matt Mazloff³, Galen McKinley⁴,
Amanda Fay⁴, Stephanie Dutkiewicz⁵, Jonathan Lauderdale⁵, Ian Fenty²,
and ECCO consortium members

¹Moss Landing Marine Laboratories, San José State University

²Jet Propulsion Laboratory, California Institute of Technology

³Scripps Institution of Oceanography, University of California San Diego

⁴Columbia University and Lamont Doherty Earth Observatory

⁵Massachusetts Institute of Technology

Last updated: 02/06/2024

Summary

This document provides 1) a brief introduction to ECCO-Darwin v05 and 2) evaluation of the model against a suite of *in-situ* ocean observations. ECCO-Darwin is an ongoing global-ocean biogeochemistry state estimate in the framework of Carroll et al. (2020).

ECCO-Darwin model output is available at the ECCO Data Portal and ECCO Drive:

https://data.nas.nasa.gov/ecco/data.php?dir=/eccodata/llc_270/ecco_darwin_v5/
https://ecco.jpl.nasa.gov/drive/files/ECCO2/LLC270/ECCO-Darwin_extension

The ECCO Data Portal is used to host input and output files for published solutions, while ECCO Drive is used to host the latest time extensions of the model.

Each user must first register for a NASA Earthdata account at

<https://urs.earthdata.nasa.gov/users/new> in order to access the files in ECCO Drive.

Model code and platform-independent instructions for running ECCO-Darwin simulations are available at: https://github.com/MITgcm-contrib/ecco_darwin

Fork of MITgcm with Darwin ecosystem model added is available at:

<https://github.com/darwinproject/darwin3>

Darwin package documentation is available at:

https://darwin3.readthedocs.io/en/latest/phys_pkgs/darwin.html

Code for generating the figures shown this document is available at:

https://github.com/MITgcm-contrib/ecco_darwin/tree/master/code_util/evaluation/

1. Period of analysis

The latest v05 ECCO-Darwin solution spans January 1992 to December 2022. Future extensions covering 1992 to near-present are planned on a semi-annual basis.

2. Model configuration

A detailed description of the ECCO-Darwin model setup, observational constraints, and optimization methodology is presented in Carroll et al. (2020). The latest ECCO-Darwin solution (v05) is based on ocean circulation and physical tracers (i.e., temperature, salinity, and sea ice) from the Estimating the Circulation and Climate of the Ocean (ECCO) LLC270 global-ocean and sea-ice data synthesis (Zhang et al., 2018).

The “Lat-Lon-Cap” (LLC) grid topology is described in Forget et al. (2015). Horizontal grid spacing varies spatially from 12 km at high latitudes to 28 km at mid-latitudes. The vertical grid spacing increases from 10 m near the surface to 457 m near the deepest ocean seafloor. The model resolution is too coarse to properly resolve mesoscale eddies. To account for resolved tracer mixing associated with unresolved mesoscale eddies, the model employs the Redi (1982) and Gent and McWilliams (1990) schemes. Vertical mixing is parameterized with a combination of the Gaspar et al. (1990) scheme and a constant background diffusivity.

The LLC270 ocean state estimate is used at each time step (1200 s) to drive an online biogeochemistry and ecosystem model provided by the Massachusetts Institute of Technology Darwin Project (Dutkiewicz et al., 2015, 2020; Follows et al., 2007); taken together these components form ECCO-Darwin. The Darwin model includes the cycling of carbon, phosphorus (PO_4), iron (Fe), silica (SiO_2), oxygen (O_2), and alkalinity. Matter is cycled from inorganic nutrients, through living and dead organic matter, and remineralized back to inorganic forms. All particulates are instantly removed once they reach the seafloor as a crude parameterization of sedimentation and to prevent model instability due to the accumulation of particulates at the bottom. Nitrogen cycling explicitly includes nitrate (NO_3), nitrite (NO_2), and ammonium pools (NH_4). Carbonate chemistry is based on the efficient solver of Follows et al. (2006). Air-sea CO_2 flux is computed using the parameterization of Wanninkhof (1992) and forced with apCO_2 from the zonally-averaged National Oceanic and Atmospheric Administration Marine Boundary Layer Reference (NOAA MBL) product (Andrews et al., 2014). Atmospheric iron dust deposition at the ocean surface and terrestrial runoff along coastal boundaries is forced using the monthly climatology of Mahowald et al. (2009) and Fekete et al. (2002), respectively. Terrestrial runoff consists of freshwater only and does not include nutrients nor carbon.

The Darwin ecology includes five large-to-small phytoplankton functional types (diatoms, other large eukaryotes, *Synechococcus*, and low- and high-light adapted *Prochlorococcus*), along with two zooplankton types that graze preferentially on either large eukaryotes or small picoplankton. Biogeochemical properties (i.e., inorganic carbon and nutrients, phytoplankton and zooplankton, dissolved organic matter, and detrital particles) are treated as prognostic variables and are advected and mixed by the LLC270 ocean circulation.

3. Observational constraints and data assimilation

Physical observations are assimilated using the adjoint method (i.e., 4-D-Var; Wunsch et al., 2009; Wunsch and Heimbach, 2013), which minimizes a weighted least squares sum of model-data misfit (the cost function) to optimize initial conditions, time-varying surface-ocean boundary conditions, and time-invariant, three-dimensional mixing coefficients for along-isopycnal, cross-isopycnal, and isopycnal thickness diffusivity. Because the initial conditions, surface boundary conditions, and mixing coefficients are estimated as part of the adjoint-method optimization, the ECCO LLC270 ocean circulation estimate has negligible drift.

The biogeochemical initial conditions and model parameters are optimized using a low-dimensional Green's Functions approach (Menemenlis et al., 2005) after the optimization of the physical model. The mixing coefficients from the adjoint optimization are applied to both the physical and biogeochemical fields. The biogeochemical observations used to evaluate and adjust ECCO-Darwin include: (1) surface ocean fugacity ($f\text{CO}_2$) from the monthly-gridded Surface Ocean CO_2 Atlas (SOCATv5 2023, Bakker et al., 2016), (2) GLODAP ship-based profiles of NO_3 , PO_4 , SiO_2 , O_2 , Dissolved Inorganic Carbon (DIC), and alkalinity (Key et al., 2015; Olsen et al., 2016), and (3) BGC-Argo float profiles of NO_3 and O_2 (Riser et al., 2016; Riser et al., 2018).

What sets the ECCO LLC270 and ECCO-Darwin solutions apart from conventional discrete or gridded observational products, is that, in addition to good agreement with observational data, ECCO products provide a complete suite of ocean and sea ice variables that describe the entire physical and biogeochemical state of the ocean and sea ice (such as 3-D temperature, salinity, and carbon, 3-D velocity, sea level, bottom pressure). Furthermore, in contrast to most other ocean reanalyses, the ECCO product fields, by design, are physically consistent with each other and with the air-sea fluxes, allowing for a full physical accounting of their temporal evolution, fundamental to studies of attribution and causation. For a description of ECCO-Darwin biogeochemical budgets and analysis, see Carroll et al. (2022).

4. Model-data evaluation

In the accompanying figures, we compare monthly-mean ECCO-Darwin values vs. *in-situ* observations in 1) the global ocean at various depth levels and 2) spatially-averaged in the open-ocean biomes from Fay and McKinley (2014) and 5 superbiomes defined in Carroll et al. (2020). Observations include SOCATv2023 (Bakker et al., 2023), GLODAPv2.2023 (Lauvset et al. 2024), and BGC-Argo (M. Mazloff, pers. comm.) data. Monthly-mean model values are paired with closest space-time-located (x,y,z,t) *in-situ* data. All map plots show values at model grid cell locations. All values shown in individual superbiomes/biomes represent area-weighted and volume-weighted means for surface ocean and depth-range analysis, respectively; vertical profiles represent area-weighted means at each vertical level. To avoid spin-up drift, all maps, scatter plots, vertical profiles, and seasonal climatology plots start in January 1995. All time-series plots begin in January 1992 (instead of January 1995) to show the complete model spin-up period (when observations are available).

5. Description of figures

The table below shows a list and description of all figures. The leftmost column color provides a quick index for the type of observation (orange = SOCAT, blue = GLODAP, and gray = BGC-Argo).

Quick Index	Page #	Description	Analysis	Notes
	11–12	Maps of Fay and McKinley (2014) biome regions and superbiomes		Superbiomes are constructed by combining individual biomes. For details see Carroll et al. (2022).
	14	ECCO-Darwin vs. SOCAT model-data difference map	Time-mean from 1995–2022, surface ocean	
	16–24	ECCO-Darwin vs. GLODAP model-data difference map	Time-mean from 1995–2022, 0 to 100-m depth	
	26–34	ECCO-Darwin vs. GLODAP model-data difference map	Time-mean from 1995–2022, 100 to 500-m depth	
	36–44	ECCO-Darwin vs. GLODAP model-data difference map	Time-mean from 1995–2022, 500 to 6000-m depth	
	46–48	ECCO-Darwin vs. BGC-Argo model-data difference map	Time-mean from 1995–2022, 0 to 100-m depth	
	50–52	ECCO-Darwin vs. BGC-Argo model-data difference map	Time-mean from 1995–2022, 100 to 500-m depth	
	54–56	ECCO-Darwin vs. BGC-Argo model-data difference map	Time-mean from 1995–2022, 500 to 2000-m depth	
	58	ECCO-Darwin vs. SOCAT scatter plot	All data from 1995–2022	
	60–68	ECCO-Darwin vs. GLODAP scatter plot	All data from 1995–2022	
	70–72	ECCO-Darwin vs. BGC-Argo scatter plot	All data from 1995–2022	
	74–80	ECCO-Darwin vs. GLODAP vertical profiles	All data from 1995–2022	
	82–84	ECCO-Darwin vs.	All data from 1995–2022	

		BGC-Argo vertical profiles		
	86	ECCO-Darwin vs. SOCAT seasonal climatology	All data from 1995–2022, surface ocean	Circles show all model-data pairs; solid lines show monthly climatological values
	88–96	ECCO-Darwin vs. GLODAP seasonal climatology	All data from 1995–2022, 0 to 100-m depth	Circles show all model-data pairs; solid lines show monthly climatological values
	98–106	ECCO-Darwin vs. GLODAP seasonal climatology	All data from 1995–2022, 100 to 500-m depth	Circles show all model-data pairs; solid lines show monthly climatological values
	108–116	ECCO-Darwin vs. GLODAP seasonal climatology	All data from 1995–2022, 500 to 6000-m depth	Circles show all model-data pairs; solid lines show monthly climatological values
	118–120	ECCO-Darwin vs. BGC-Argo seasonal climatology	All data from 1995–2022, 0 to 100-m depth	Circles show all model-data pairs; solid lines show monthly climatological values
	122–124	ECCO-Darwin vs. BGC-Argo seasonal climatology	All data from 1995–2022, 100 to 500-m depth	Circles show all model-data pairs; solid lines show monthly climatological values
	126–128	ECCO-Darwin vs. BGC-Argo seasonal climatology	All data from 1995–2022, 500 to 2000-m depth	Circles show all model-data pairs; solid lines show monthly climatological values
	130	ECCO-Darwin vs. SOCAT time series	All data from 1992–2022, surface-ocean	Blue and grey circles show all data and model values, respectively; blue and red lines show annual-mean data and model values, respectively
	132–140	ECCO-Darwin vs. GLODAP time series	All data from 1992–2022, 0 to 100-m depth	Blue and grey circles show all data and model values, respectively; blue and red lines show annual-mean data and model values, respectively
	142–150	ECCO-Darwin vs. GLODAP time series	All data from 1992–2022,	Blue and grey circles show all data and

			100 to 500-m depth	model values, respectively; blue and red lines show annual-mean data and model values, respectively
	152–160	ECCO-Darwin vs. GLODAP time series	All data from 1992–2022, 500 to 6000-m depth	Blue and grey circles show all data and model values, respectively; blue and red lines show annual-mean data and model values, respectively
	162–164	ECCO-Darwin vs. BGC-Argo time series	All data from 1992–2022, 0 to 100-m depth	Blue and grey circles show all data and model values, respectively; blue and red lines show annual-mean data and model values, respectively
	166–168	ECCO-Darwin vs. BGC-Argo time series	All data from 1992–2022, 100 to 500-m depth	Blue and grey circles show all data and model values, respectively; blue and red lines show annual-mean data and model values, respectively
	170–172	ECCO-Darwin vs. BGC-Argo time series	All data from 1992–2022, 500 to 6000-m depth	Blue and grey circles show all data and model values, respectively; blue and red lines show annual-mean data and model values, respectively

Acknowledgements

We acknowledge support from the NASA Ocean Biology and Biogeochemistry (OBB), Physical Oceanography (PO), Modeling, Analysis, and Prediction (MAP), Interdisciplinary Research in Earth Science (IDS), and Carbon Monitoring Systems (CMS) programs. A portion of this study was carried out at the Jet Propulsion Laboratory, California Institute of Technology, under contract with NASA. High-end computing resources were provided by the NASA Advanced Supercomputing (NAS) Division of the Ames Research Center.

References

- Andrews, A. E., Kofler, J. D., Trudeau, M. E., Williams, J. C., Neff, D. H., Masarie, K. A., et al. (2014). CO₂, CO, and CH₄ measurements from tall towers in the NOAA Earth system research laboratory's global greenhouse gas reference network: Instrumentation, uncertainty analysis, and recommendations for future high-accuracy greenhouse gas monitoring efforts. *Atmospheric Measurement Techniques*, 7(2), 647–687.
- Bakker, D. C. E., Pfeil, B., Landa, C. S., Metzl, N., O'Brien, K. M., Olsen, A., and Xu, S. (2016). A multi-decade record of high-quality fCO₂ data in version 3 of the Surface Ocean CO₂ Atlas (SOCAT). *Earth System Science Data*, 8(2), 383–413.
- Bakker, D. C. E., et al. (2023). Surface Ocean CO₂ Atlas Database Version 2023 (SOCATv2023) (NCEI Accession 0278913. NOAA National Centers for Environmental Information. Dataset. <https://doi.org/10.25921/r7xa-bt92>. Accessed 02/06/2024.
- Carroll, D., Menemenlis, D., Adkins, J. F., Bowman, K. W., Brix, H., Dutkiewicz, S., et al. (2020). The ECCO-Darwin data-assimilative global ocean biogeochemistry model: Estimates of seasonal to multidecadal Surface Ocean pCO₂ and air-sea CO₂ flux. *Journal of Advances in Modeling Earth Systems*, 12(10), 1–28.
- Carroll, D., Menemenlis, D., Dutkiewicz, S., Lauderdale, J. M., Adkins, J. F., Bowman, K. W., et al. (2022). Attribution of space-time variability in global-ocean dissolved inorganic carbon. *Global Biogeochemical Cycles*, 36, e2021GB007162.
- Dutkiewicz, S., Hickman, A. E., Jahn, O., Gregg, W. W., Mouw, C. B., and Follows, M. J. (2015). Capturing optically important constituents and properties in a marine biogeochemical and ecosystem model. *Biogeosciences*, 12(14), 4447–4481.
- Dutkiewicz, S., Cermenio, P., Jahn, O., Follows, M. J., Hickman, A. E., Taniguchi, D. A. A., and Ward, B. A. (2020). Dimensions of marine phytoplankton diversity. *Biogeosciences*, 17(3), 609–634.
- Fekete, B. M., Vörösmarty, C. J., and Grabs, W. (2002). High-resolution fields of global runoff combining observed river discharge and simulated water balances. *Global Biogeochemical Cycles*, 16(3), 15–1.
- Fay, A. R., and McKinley, G. A. (2014). Global open-ocean biomes: Mean and temporal variability. *Earth System Science Data*, 6(2), 273–284.
- Follows, M. J., Ito, T., and Dutkiewicz, S. (2006). On the solution of the carbonate chemistry system in ocean biogeochemistry models. *Ocean Modelling*, 12(3), 290–301.
- Follows, M. J., Dutkiewicz, S., Grant, S., and Chisholm, S. W. (2007). Emergent biogeography of microbial communities in a model ocean. *Science*, 315(5820), 1843–1846.

Forget G., J. Campin, P. Heimbach, C. N. Hill, R. Ponte, and C. Wunsch. (2015). ECCO version 4: an integrated framework for non-linear inverse modeling and global ocean state estimation, *Geoscientific Model Development*, 8(10), 3071–3104.

Gaspar, P., Grégoris, Y., and Lefevre, J.-M. (1990). A simple eddy kinetic energy model for simulations of the oceanic vertical mixing: Tests at station papa and long-term upper ocean study site. *Journal of Geophysical Research: Oceans*, 95(C9), 16179–16193.

Gent, P. R., and McWilliams, J. C. (1990). Isopycnal mixing in ocean circulation models. *Journal of Physical Oceanography*, 20(1), 150–155.

Key, R., et al. (2015). Global Ocean Data Analysis Project, Version 2 (GLODAPv2), *ORNL/CDIAC-162, ND-P093*, Carbon Dioxide Inf. Anal. Cent., Oak Ridge Natl. Lab., U.S. Dep. of Energy, Oak Ridge, Tenn.

Lauvset, S. K., et al. (2024). The annual update GLODAPv2.2023: the global interior ocean biogeochemical data product. *Earth System Science Data Discussion*, <https://doi.org/10.5194/essd-2023-468>.

Mahowald, N. M., Engelstaedter, S., Luo, C., Sealy, A., Artaxo, P., Benitez-Nelson, C., et al. (2009). Atmospheric iron deposition: Global distribution, variability, and human perturbations. *Annual Review of Marine Science*, 1(1), 245–278.

Menemenlis, D., Fukumori, I., and Lee, T. (2005). Using Green's Functions to calibrate an ocean general circulation model. *Monthly Weather Review*, 133(5), 1224–1240.

Olsen, A., Lange, N., Key, R. M., Tanhua, T., Bittig, H. C., Kozyr, A., et al. (2020). An updated version of the global interior ocean biogeochemical data product, GLODAPv2.2020. *Earth System Science Data*, 12(4), 3653–3678.

Redi, M. H. (1982). Oceanic isopycnal mixing by coordinate rotation. *Journal of Physical Oceanography*, 12(10), 1154–1158.

Riser, S. C., et al. (2016). Fifteen years of ocean observations with the global Argo array, *Nature Climate Change*, 6, 145–153.

Riser, S. C., Swift, D., and R. Drucker. (2018). Profiling floats in SOCCOM: Technical capabilities for studying the Southern Ocean, *Journal of Geophysical Research: Oceans*, 123(6), 4055–4073.

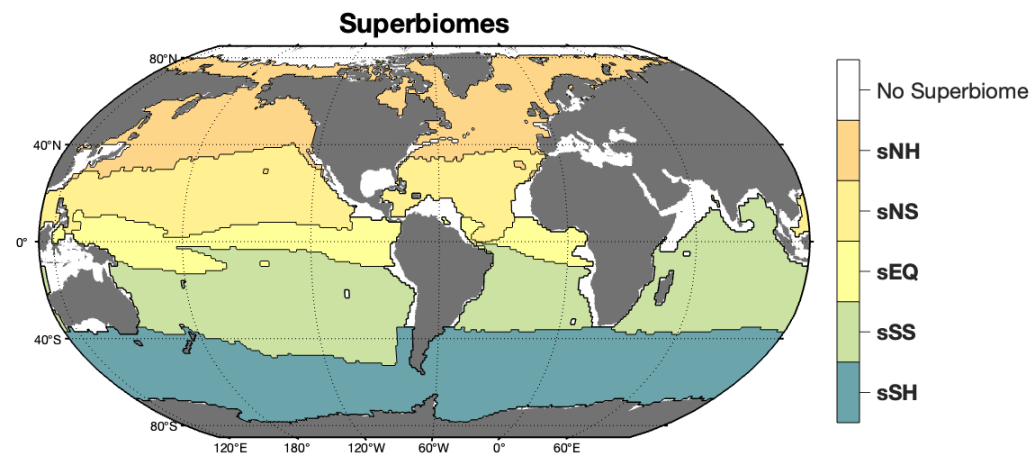
Wanninkhof, R. (1992). Relationship between wind speed and gas exchange over the ocean. *Journal of Geophysical Research: Oceans*, 97(C5), 7373–7382.

Wunsch, C., Heimbach, P., Ponte, R., and Fukumori, I. (2009). The global general circulation of the ocean estimated by the ECCO-consortium. *Oceanography*, 22(2), 88–103.

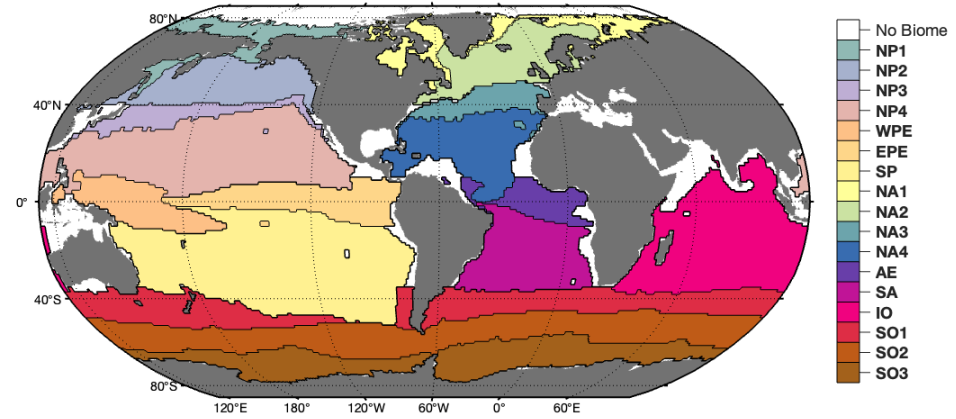
Wunsch, C., and Heimbach, P. (2013). Dynamically and kinematically consistent global ocean circulation and ice state estimates. In G. Siedler, S. M. Griffies, J. Gould, and J. A. Church (Eds.), *Ocean circulation and climate: A 21st century perspective* (Vol. 103, pp. 553–579). Academic Press.

Zhang, H., Menemenlis, D., and Fenty, I. G. (2018). ECCO LLC270 ocean-ice state estimate (Tech. Rep.). Jet Propulsion Laboratory. California Institute of Technology. Available at: <http://hdl.handle.net/1721.1/119821>

Superbiome and biome regions

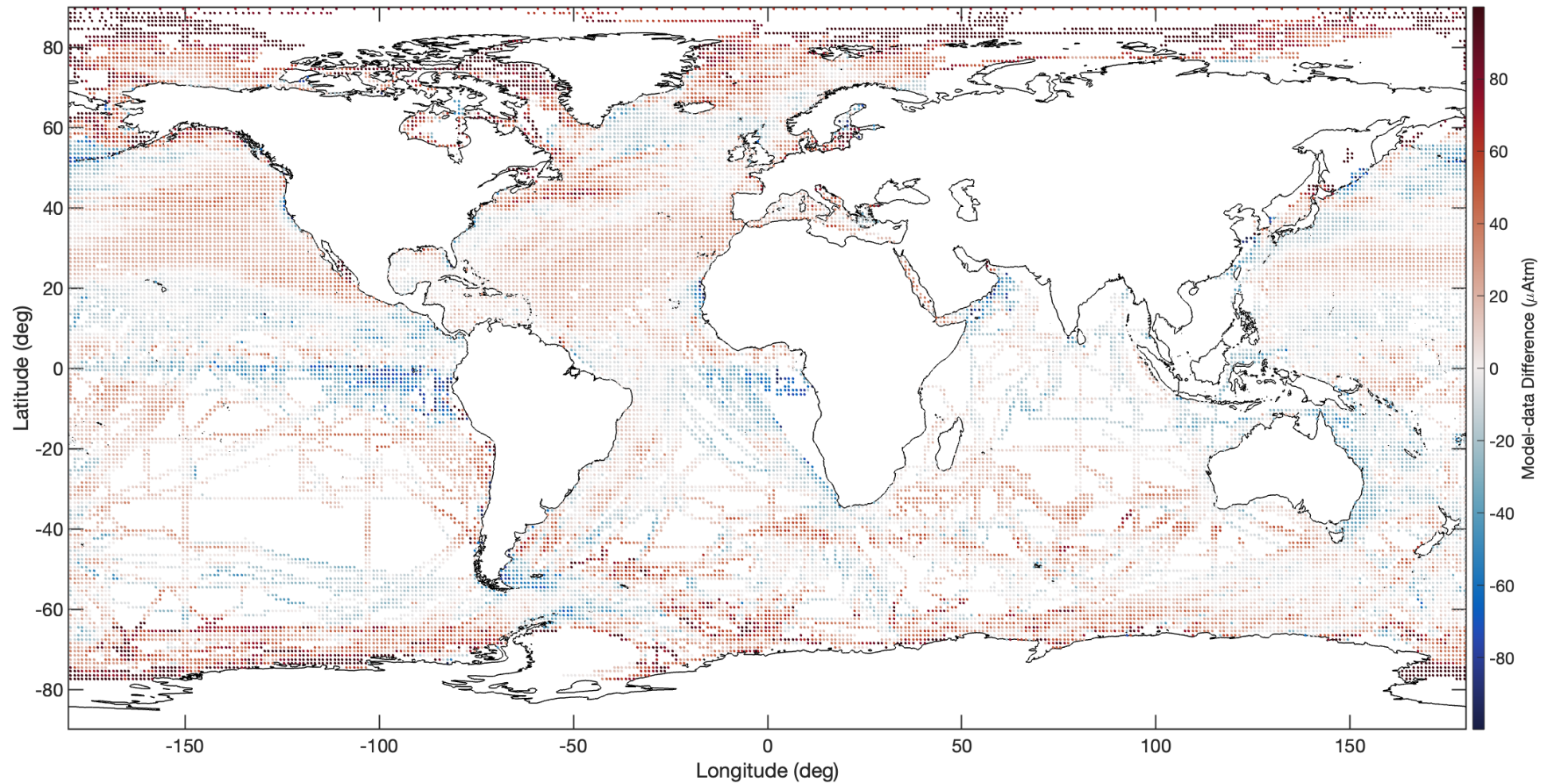


Biomes



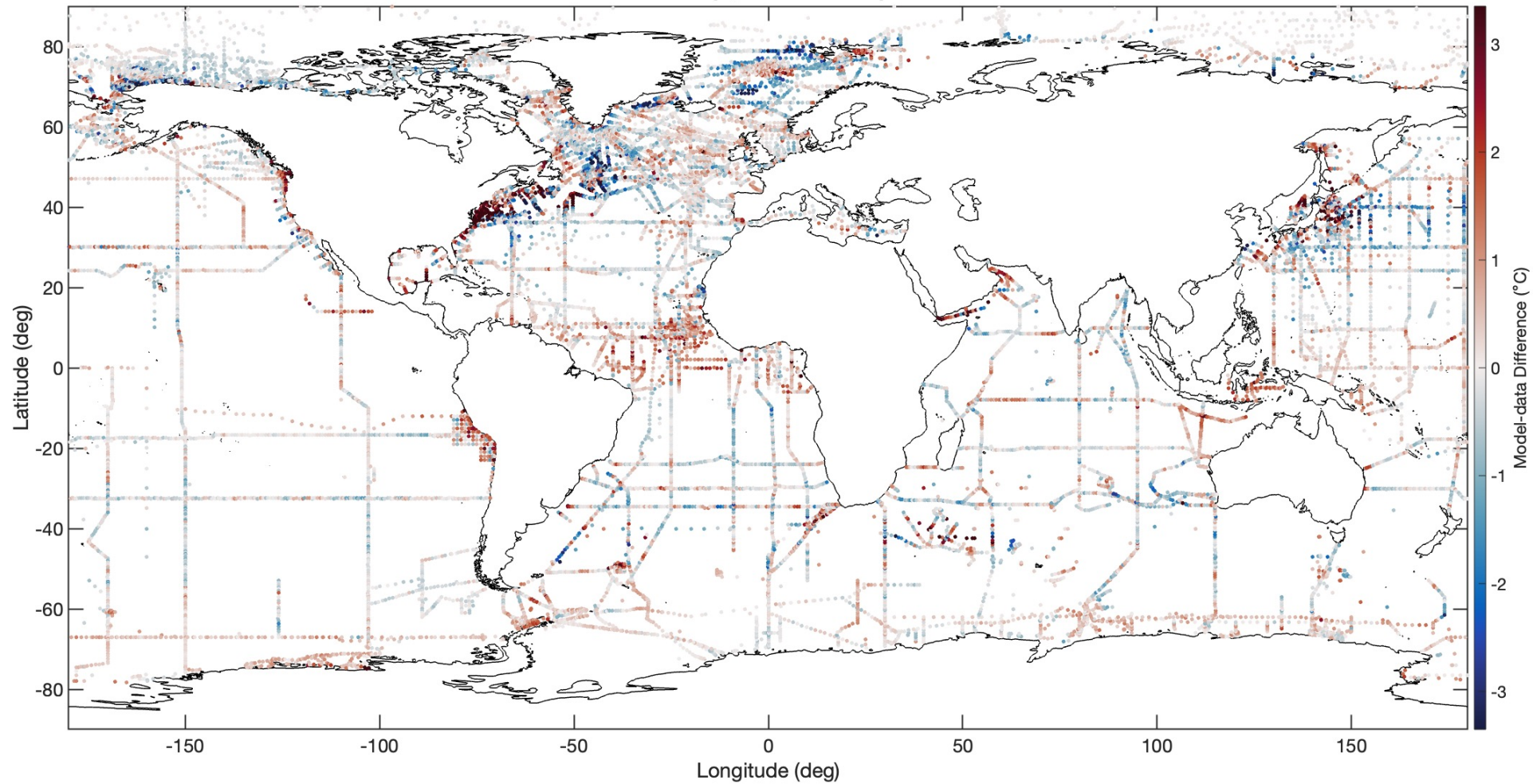
ECCO-Darwin vs. SOCAT model-data difference map: surface ocean

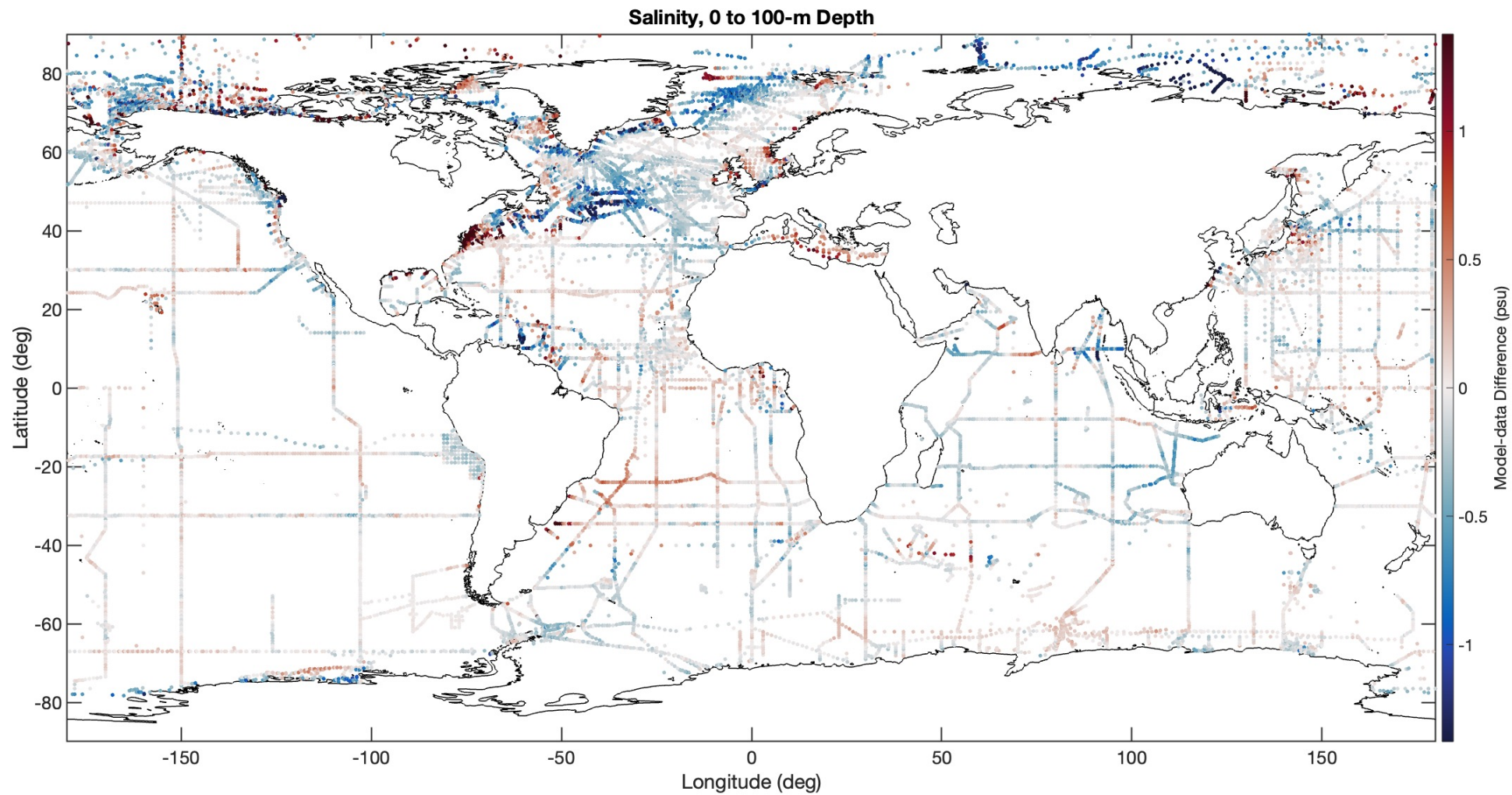
Surface-ocean $f\text{CO}_2$



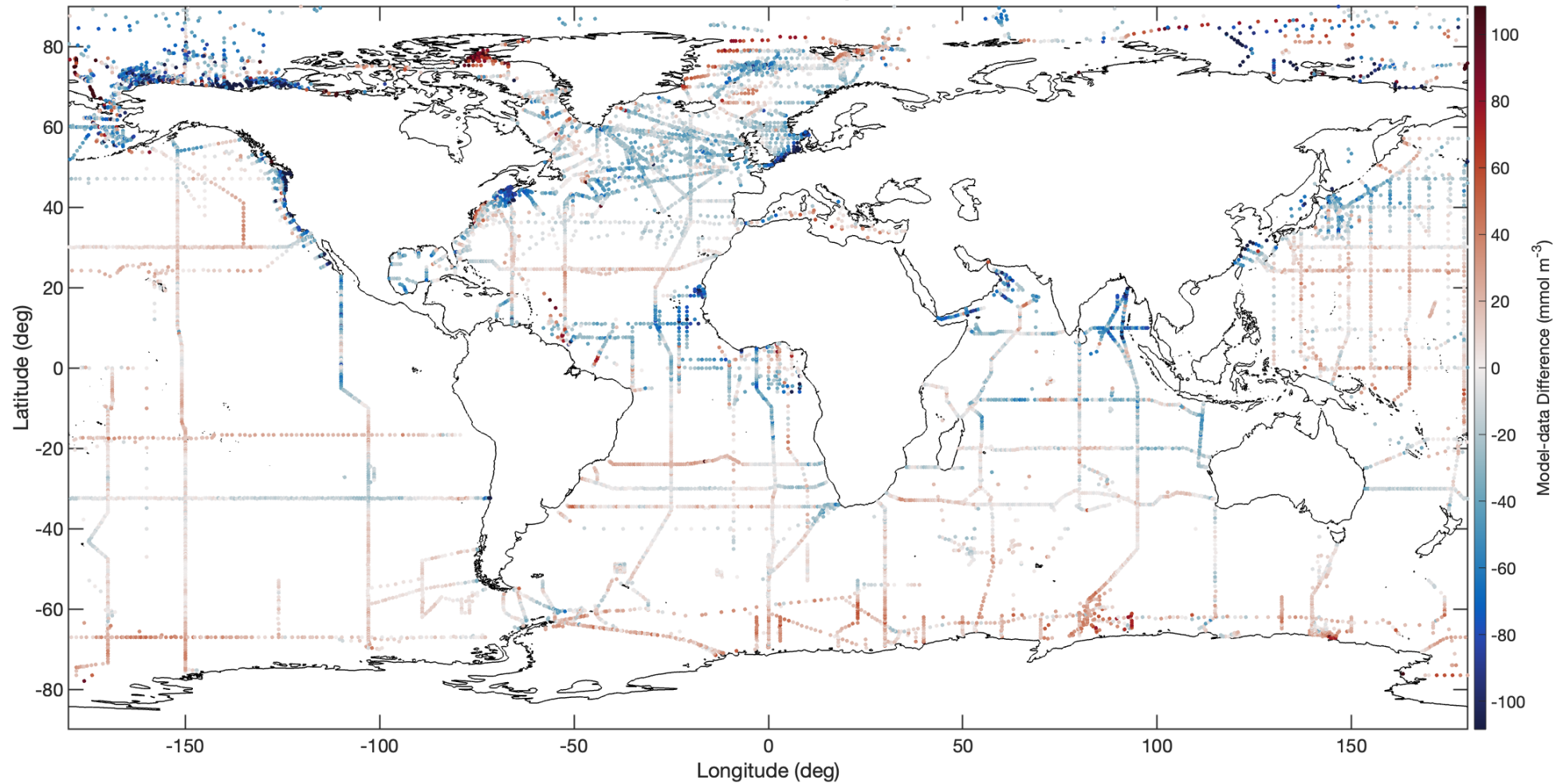
ECCO-Darwin vs. GLODAP model-data difference map: 0 to 100-m depth

Pot. Temp., 0 to 100-m Depth

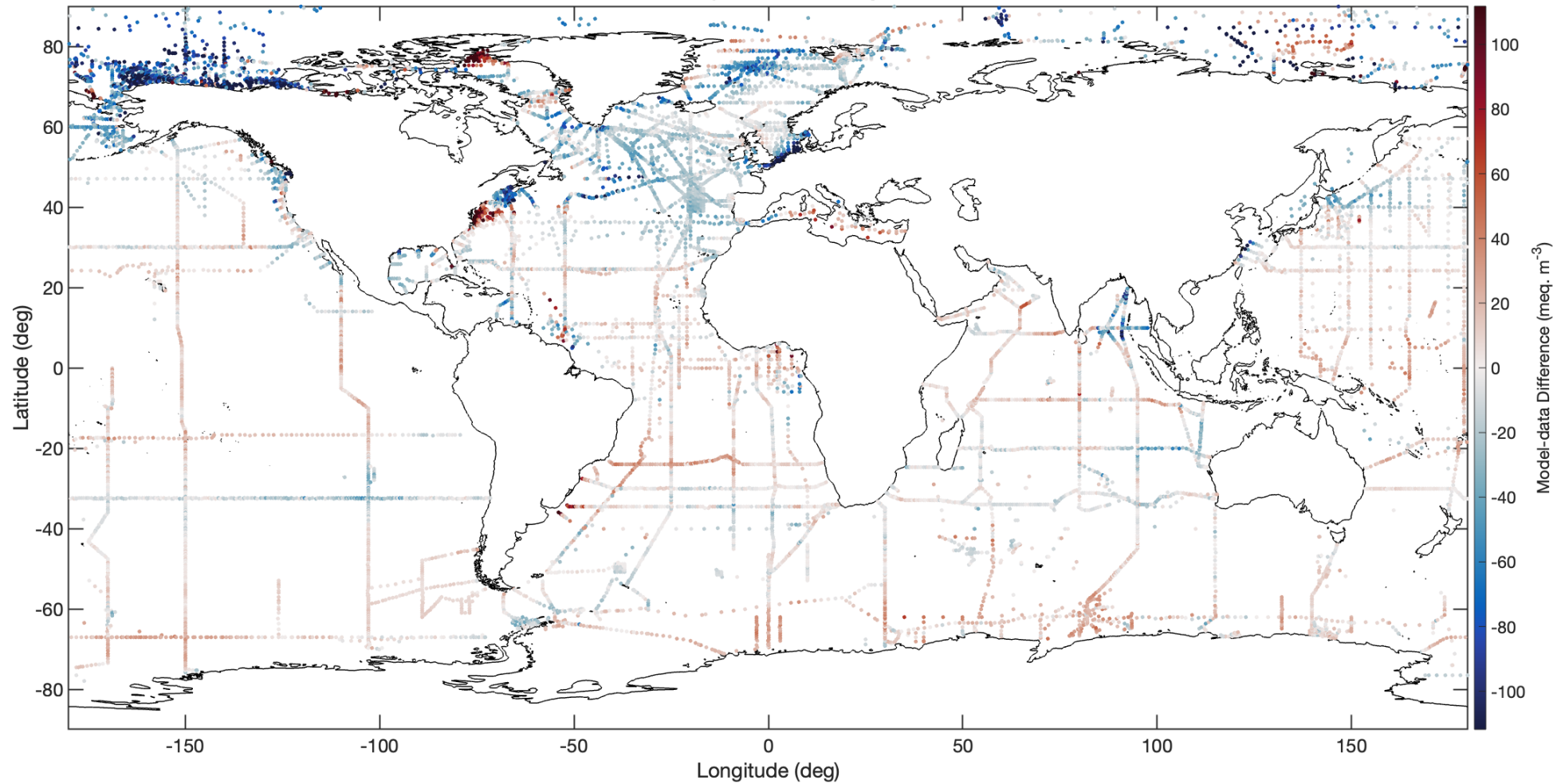


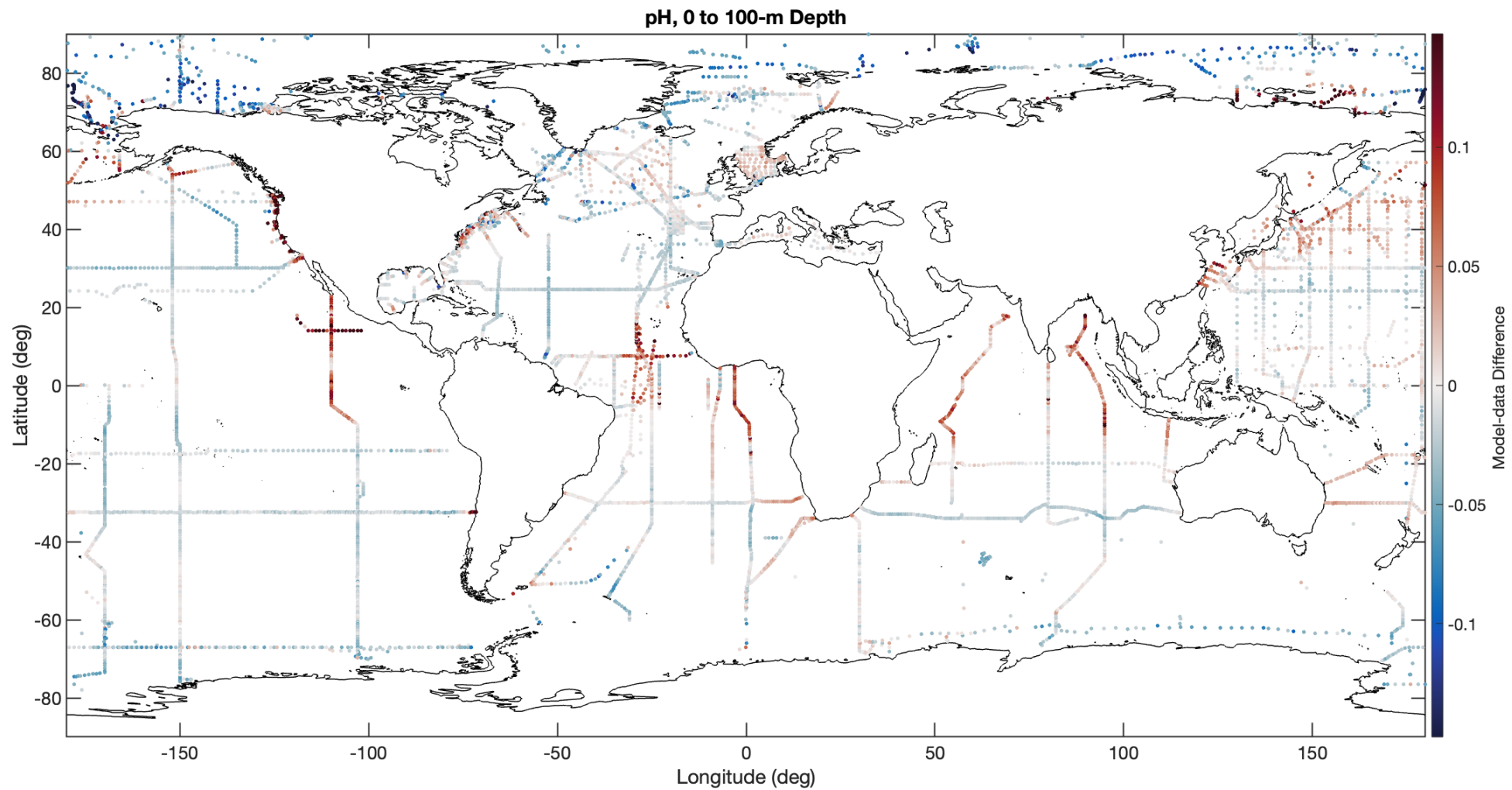


DIC, 0 to 100-m Depth

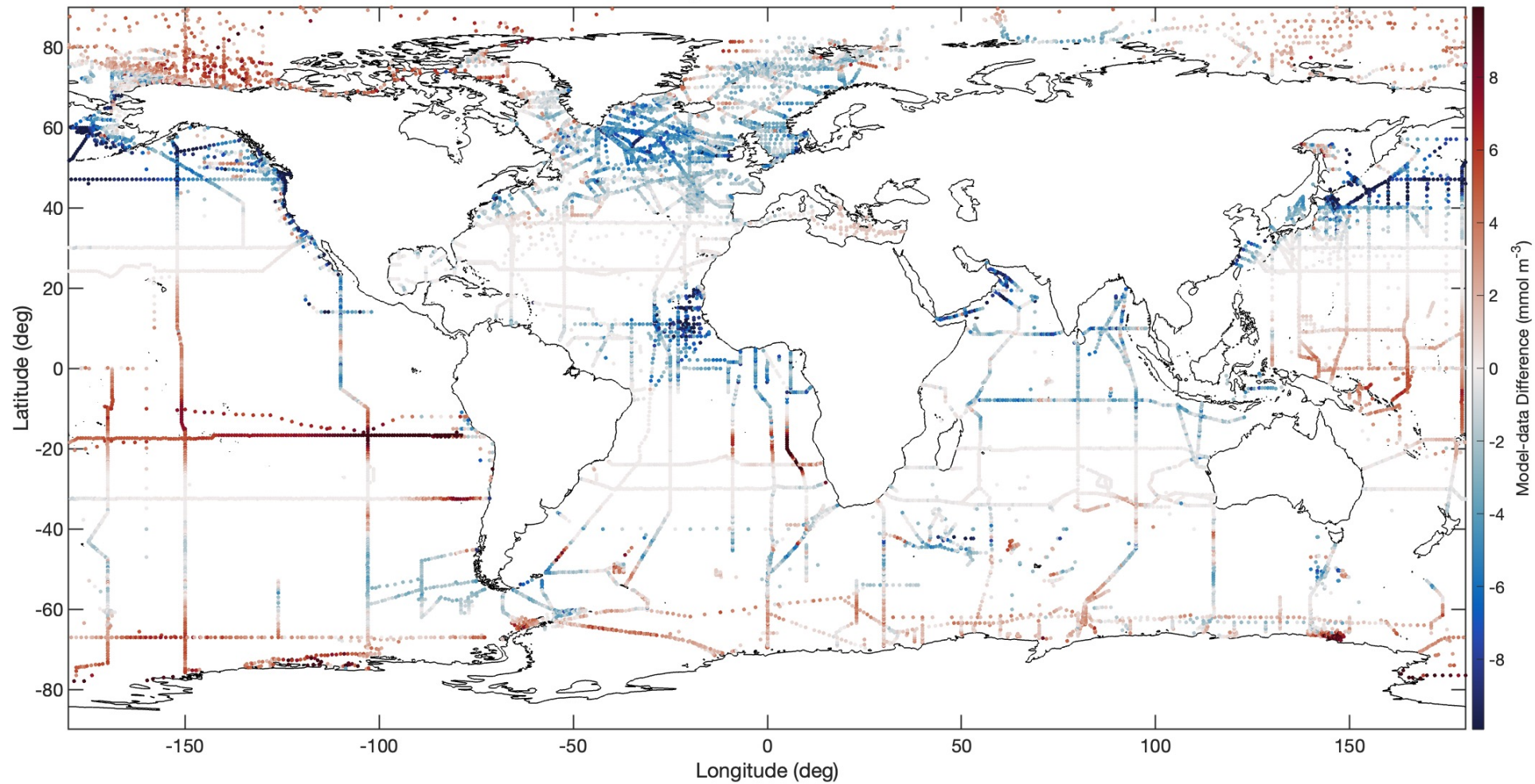


Alkalinity, 0 to 100-m Depth

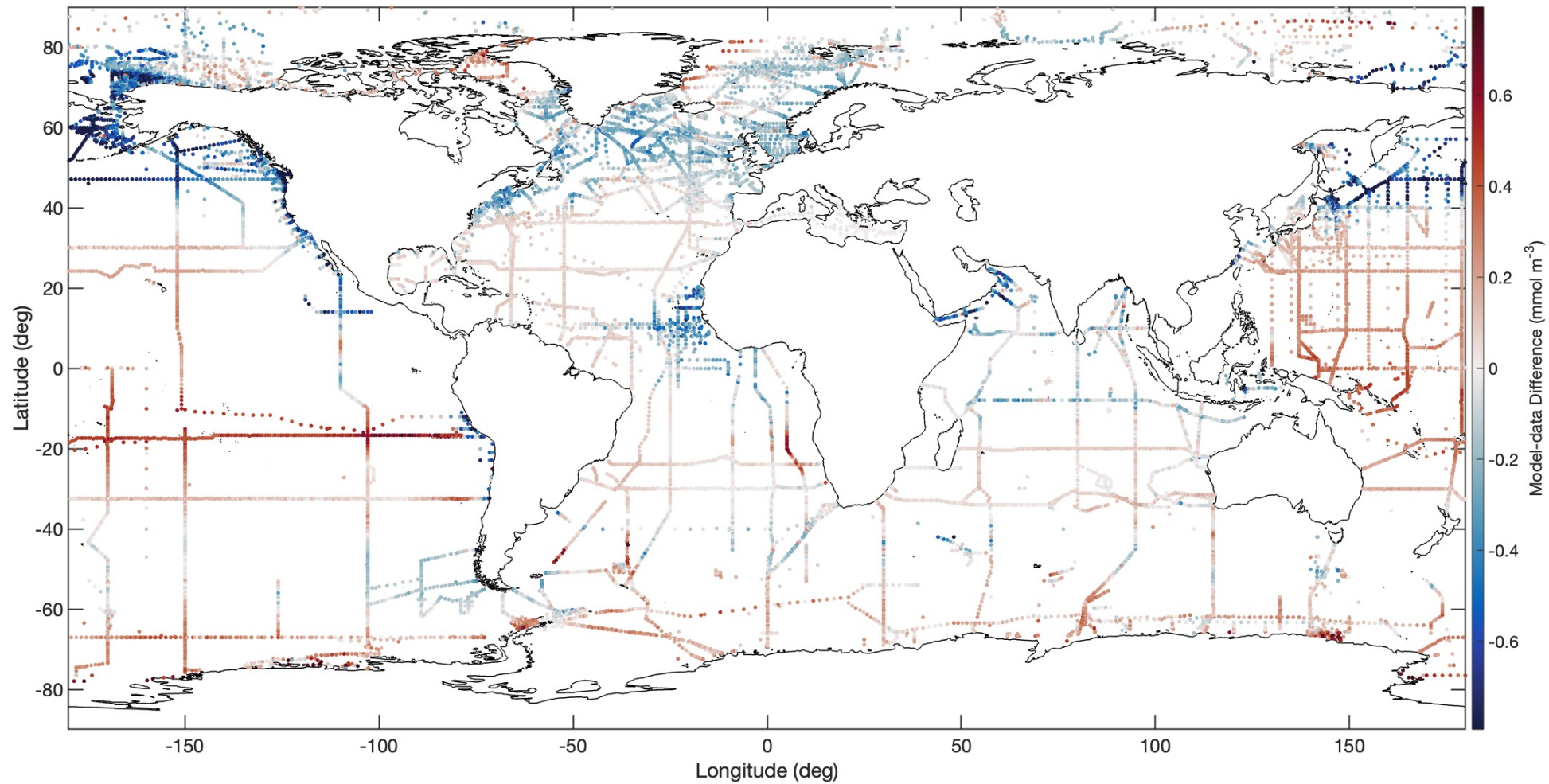




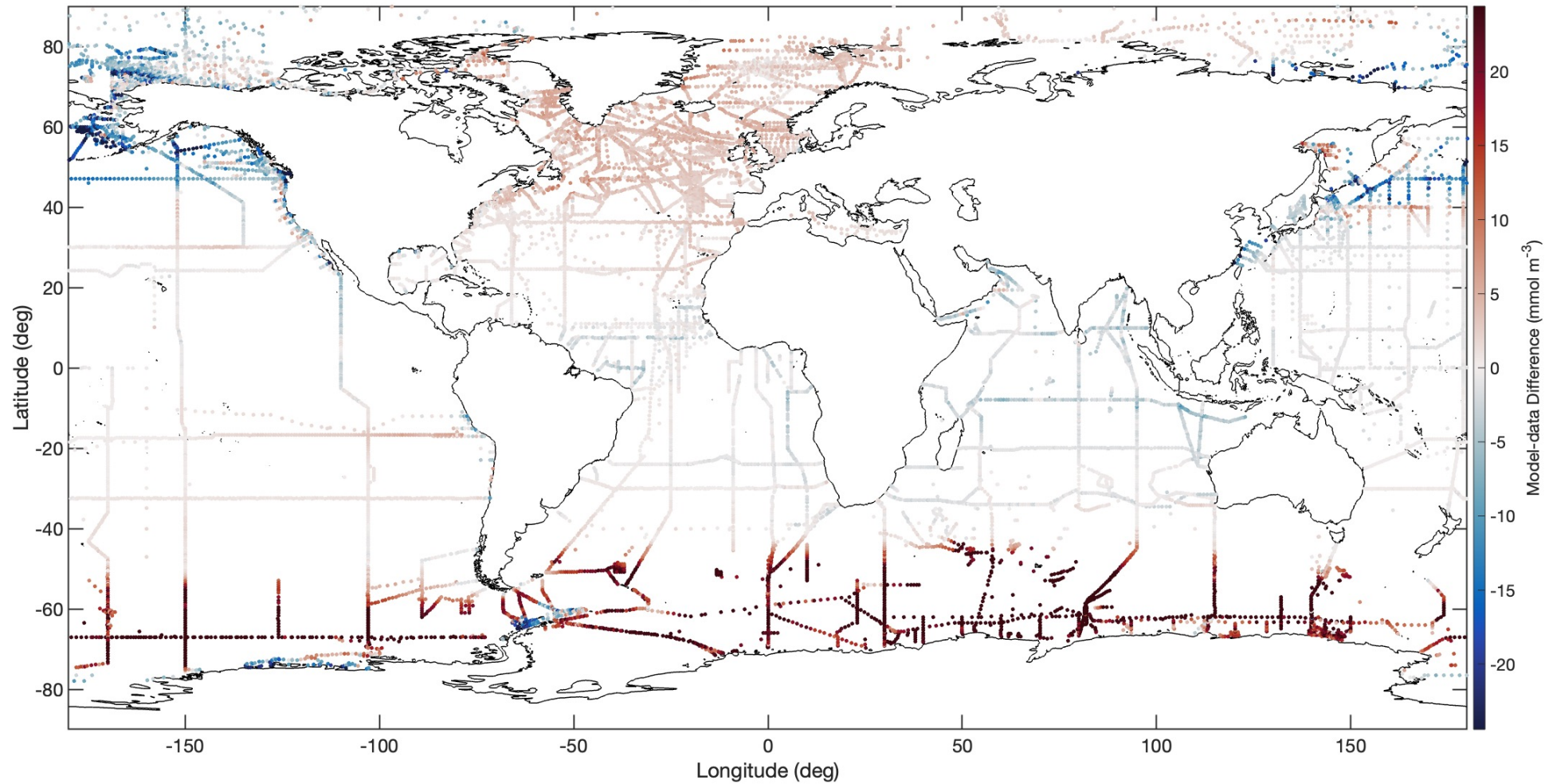
NO_3^- , 0 to 100-m Depth



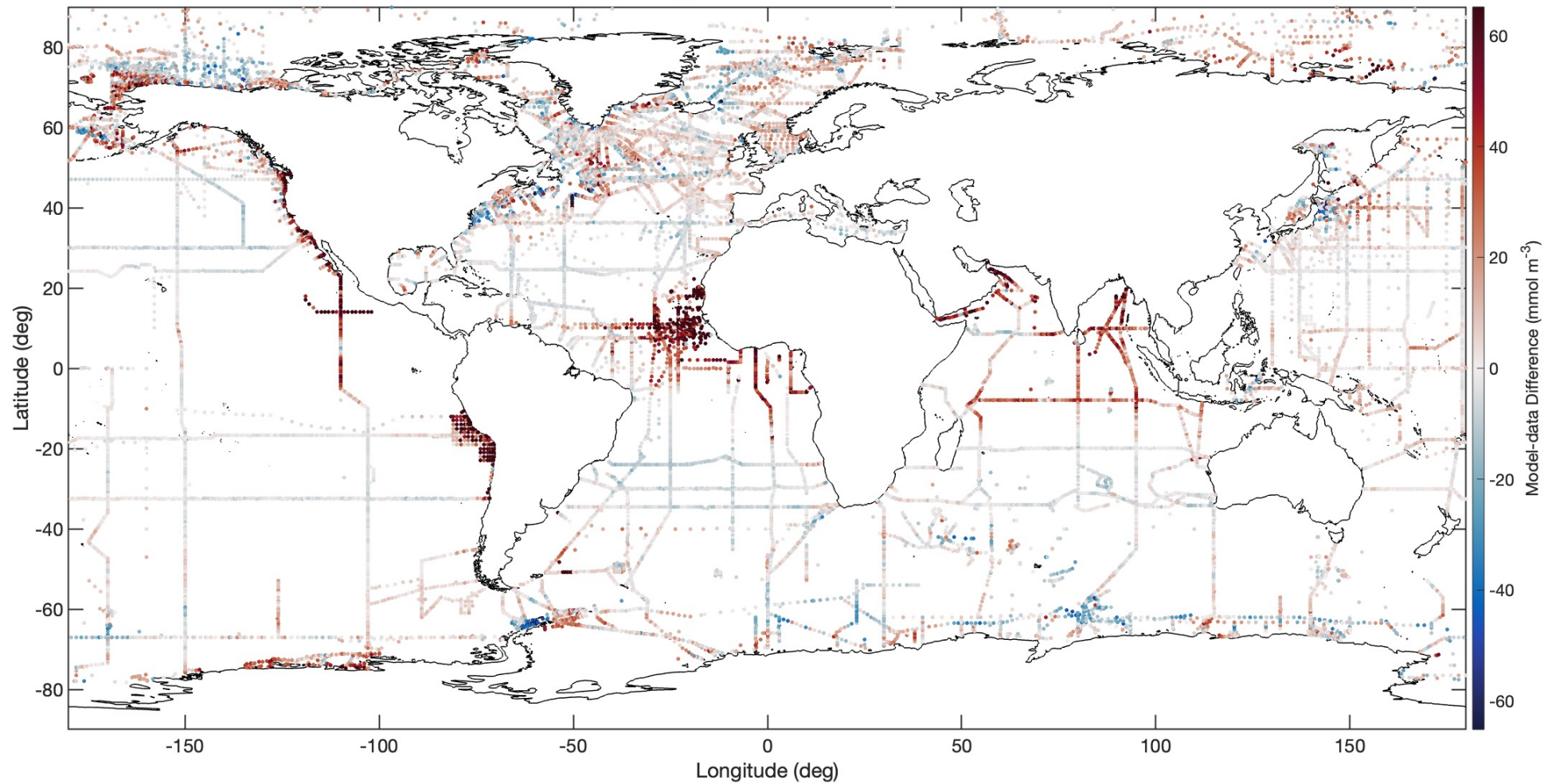
PO_4 , 0 to 100-m Depth



SiO_2 , 0 to 100-m Depth

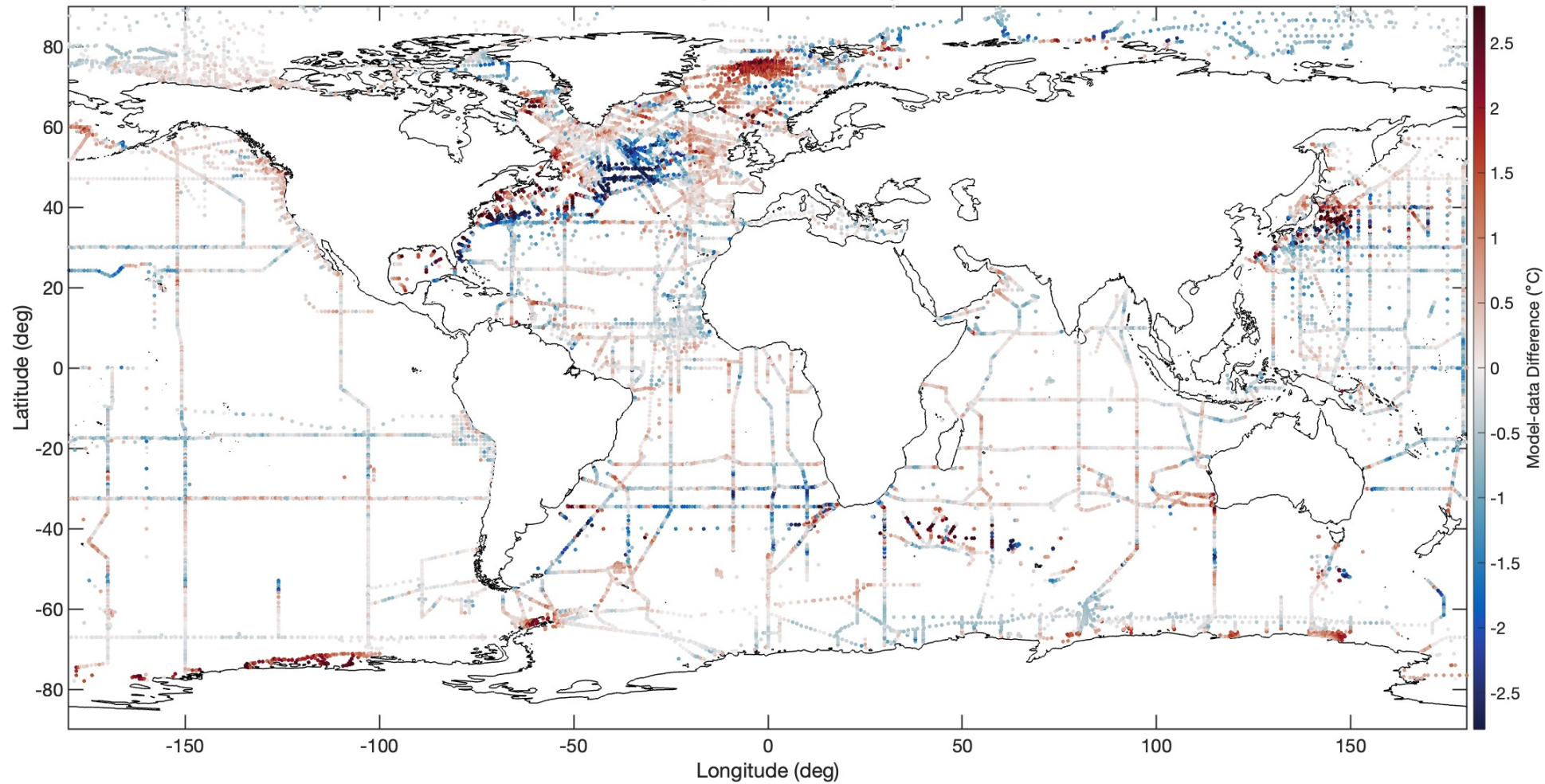


O_2 , 0 to 100-m Depth

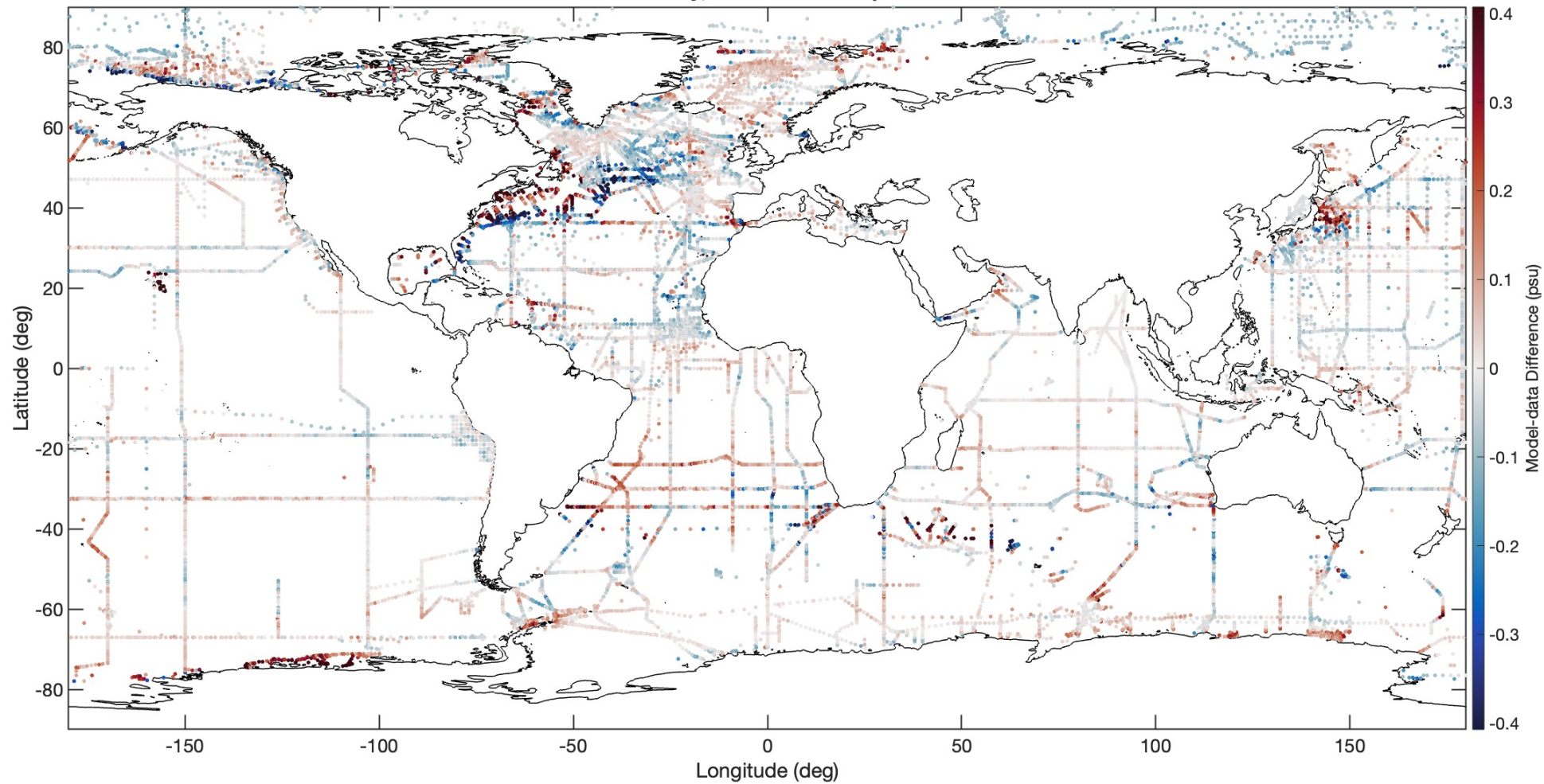


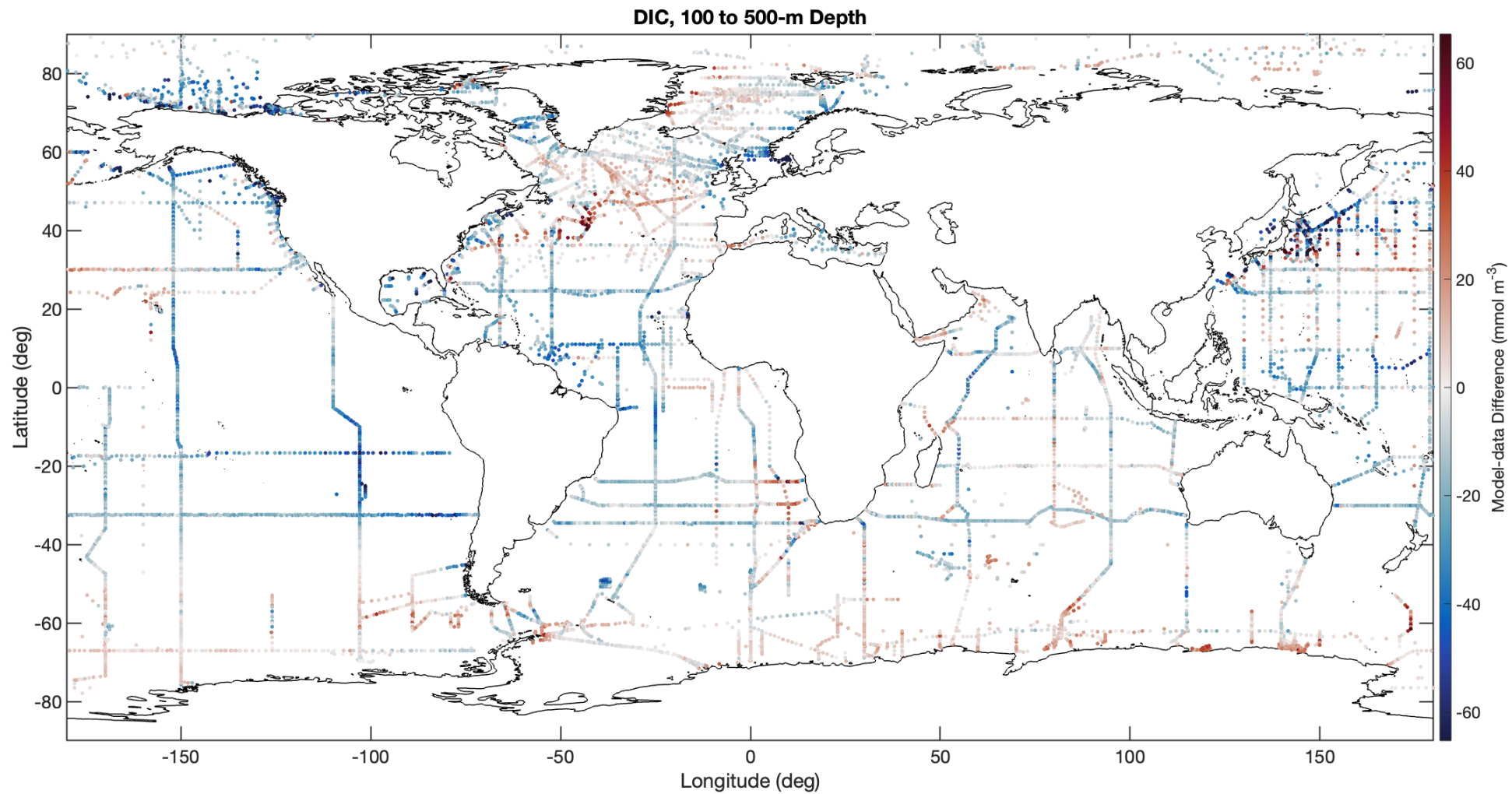
ECCO-Darwin vs. GLODAP model-data difference map: 100 to 500-m depth

Pot. Temp., 100 to 500-m Depth

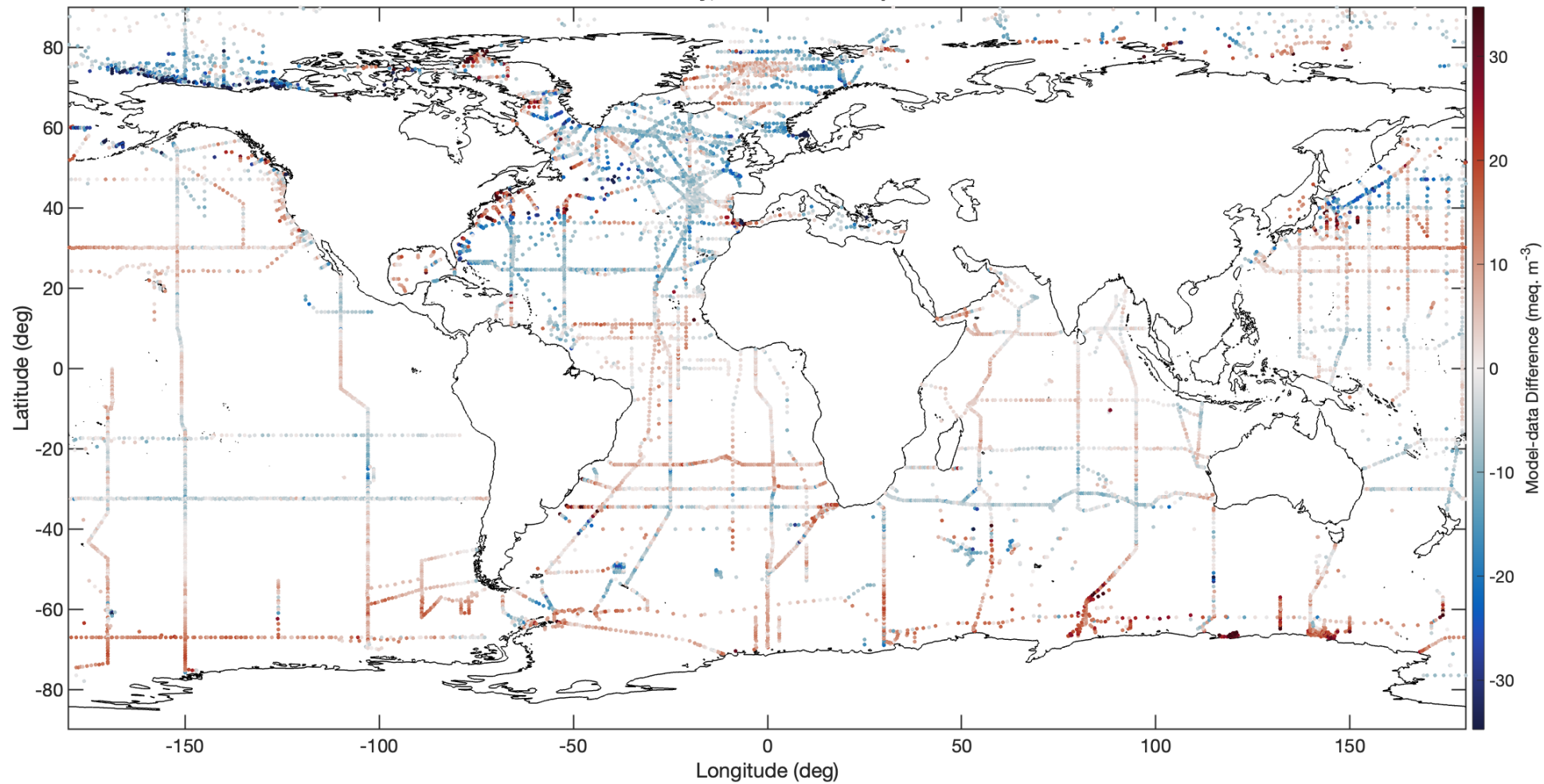


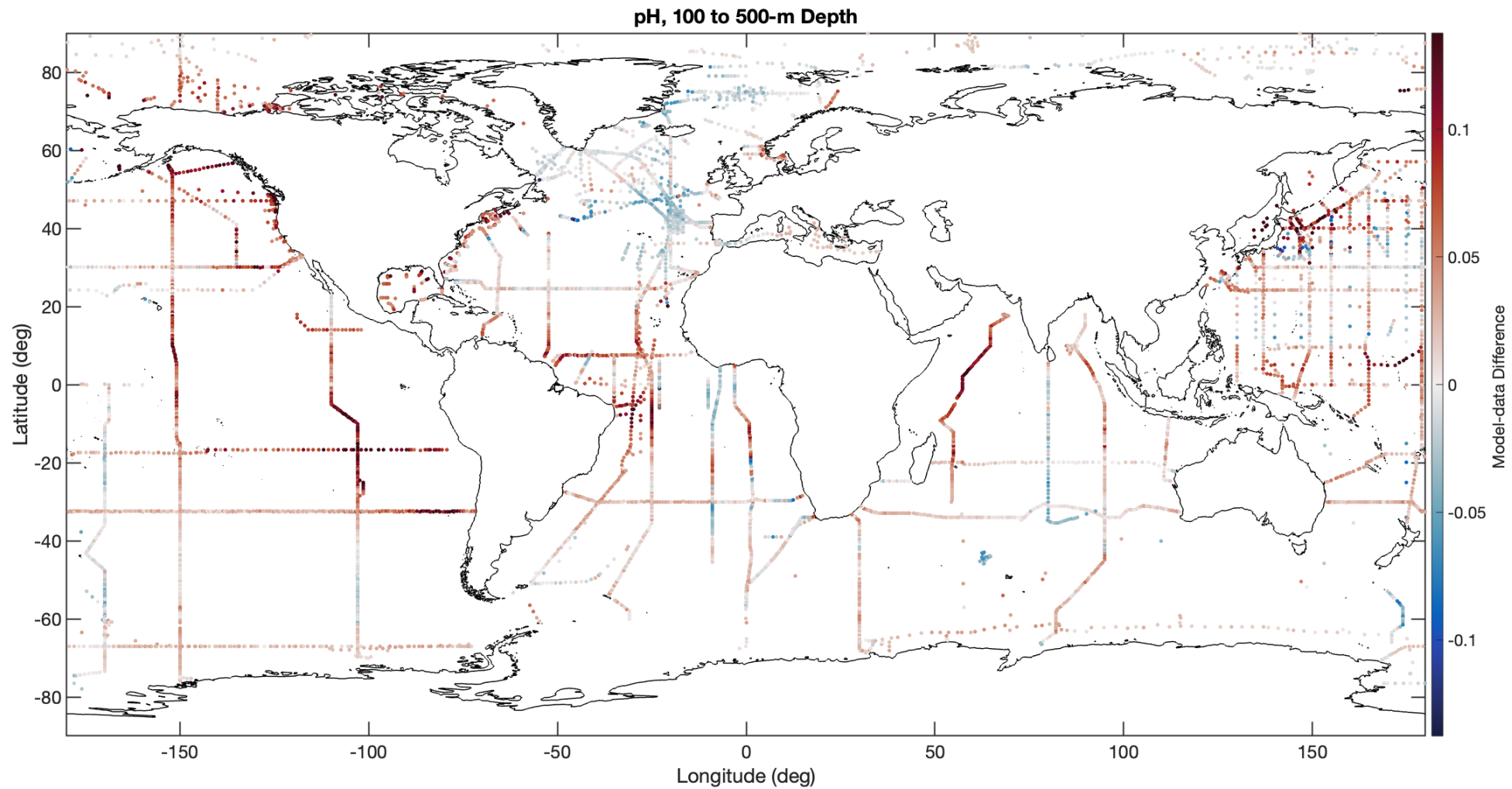
Salinity, 100 to 500-m Depth



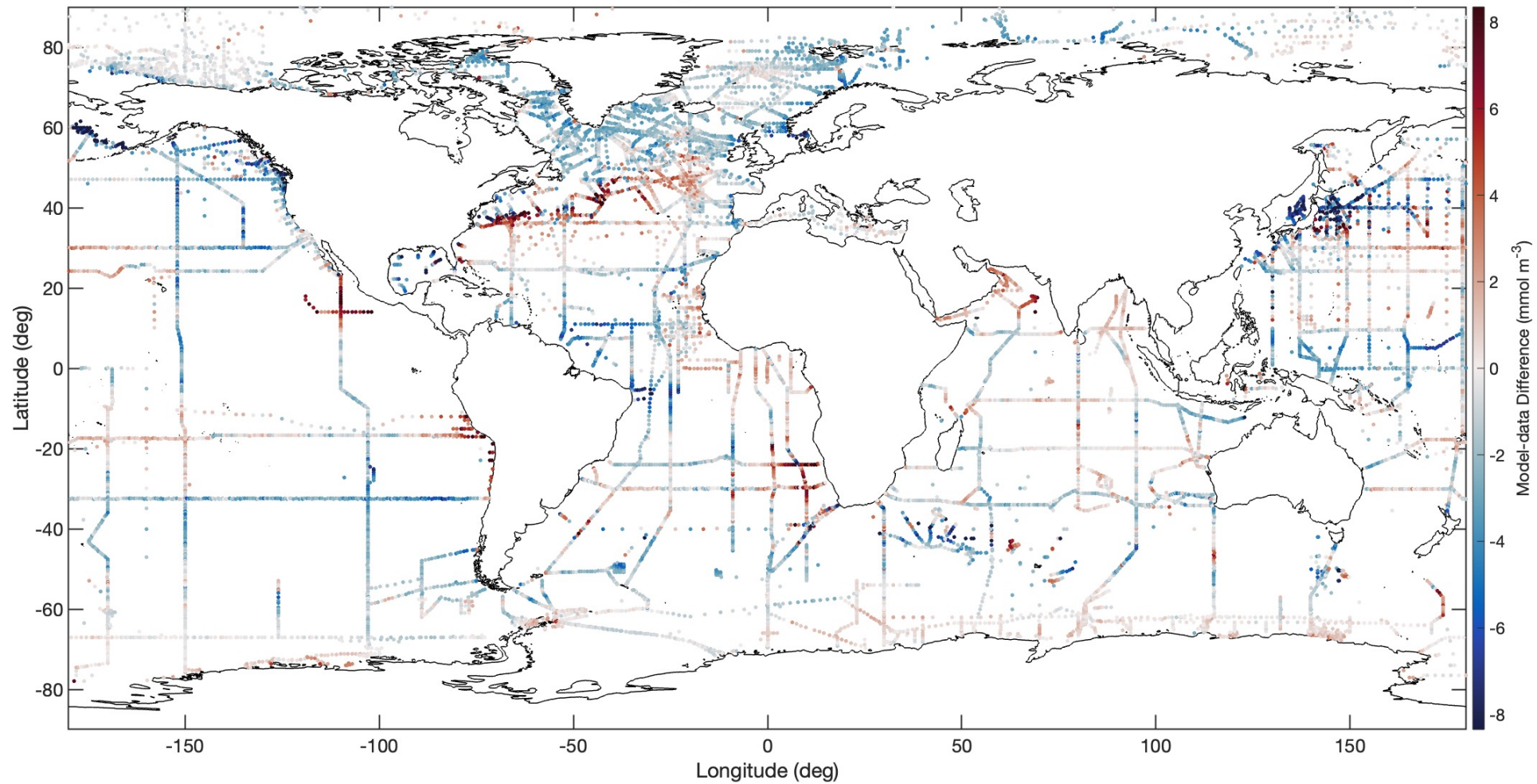


Alkalinity, 100 to 500-m Depth

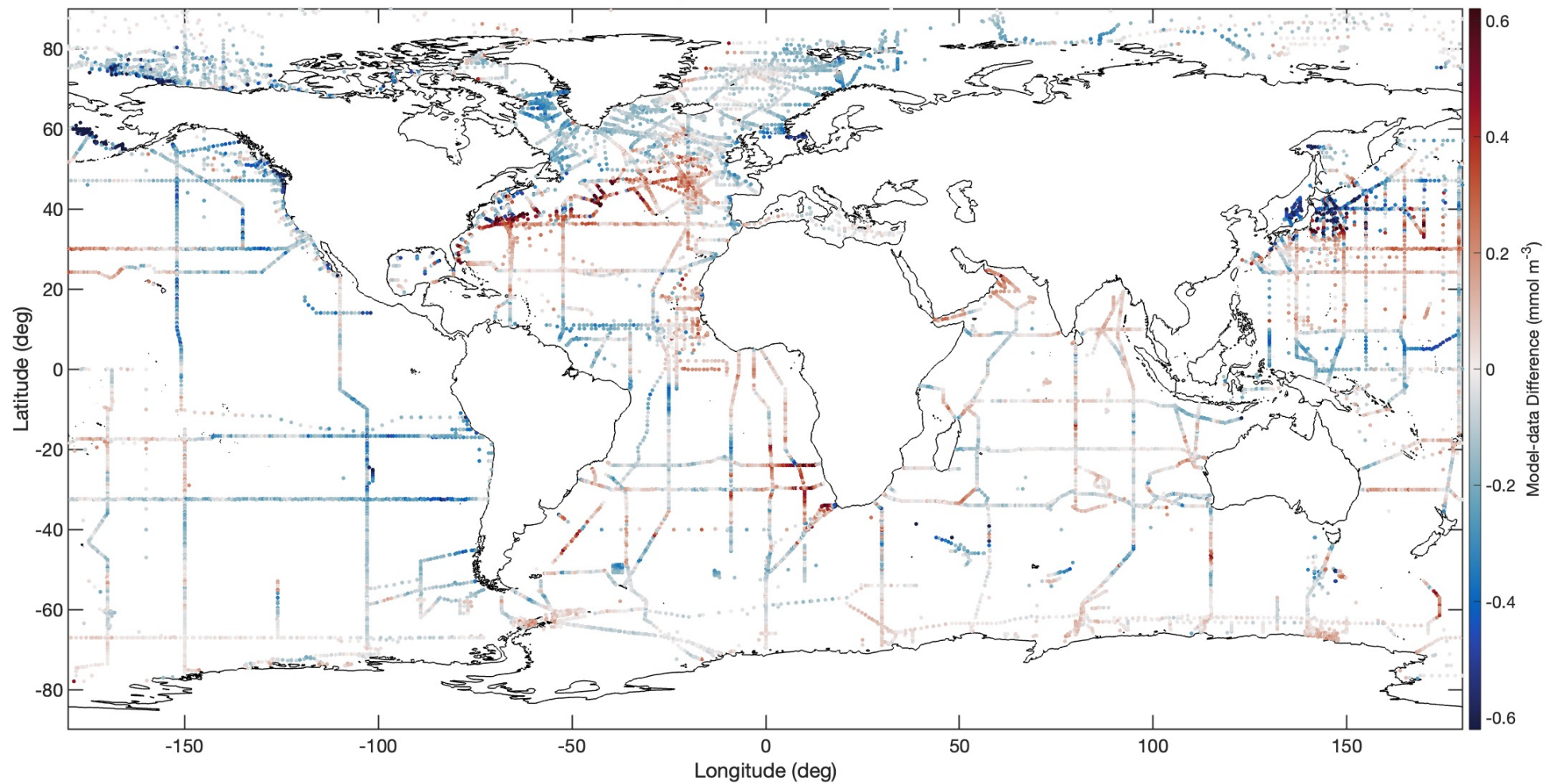




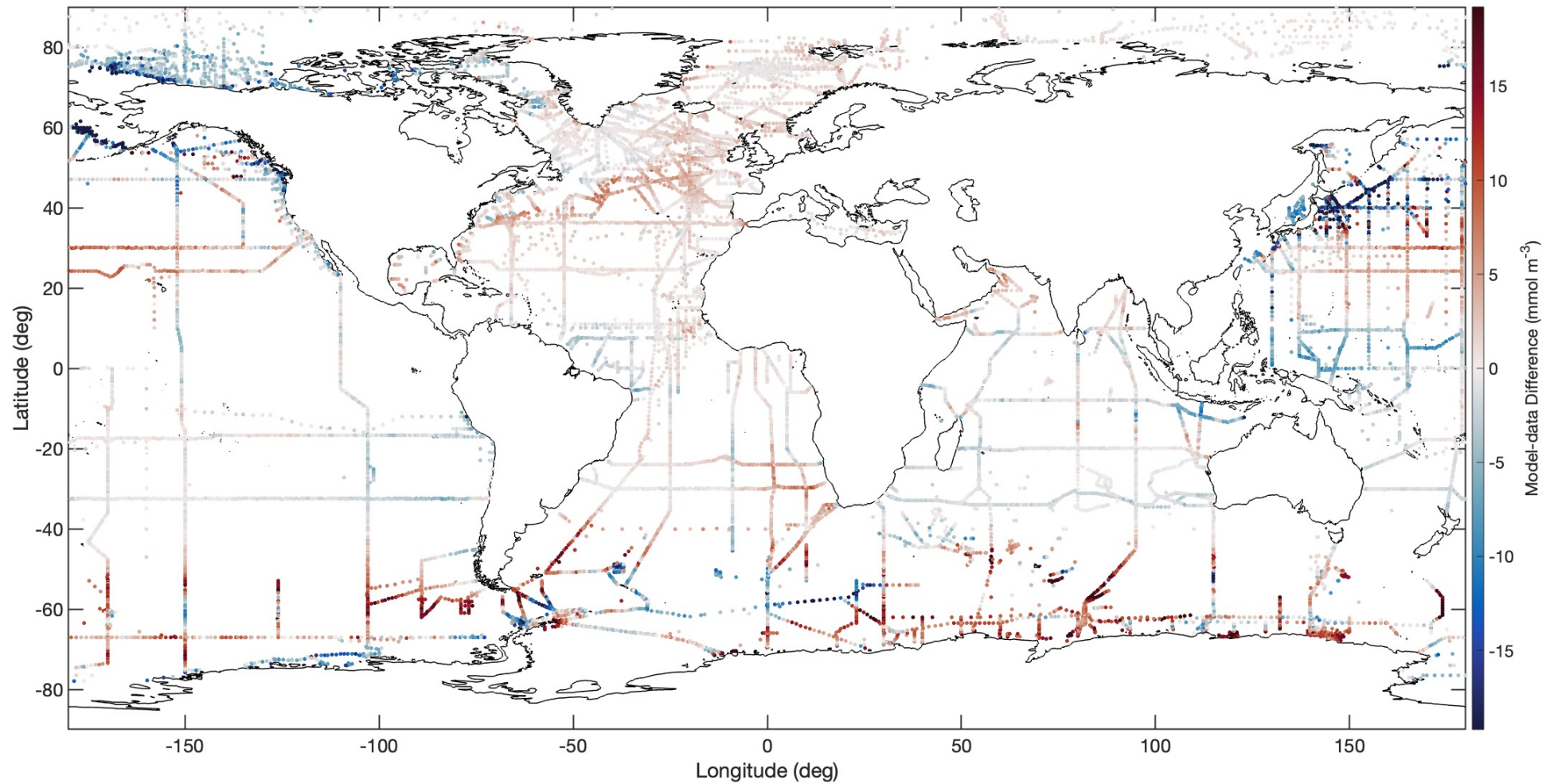
NO_3^- , 100 to 500-m Depth



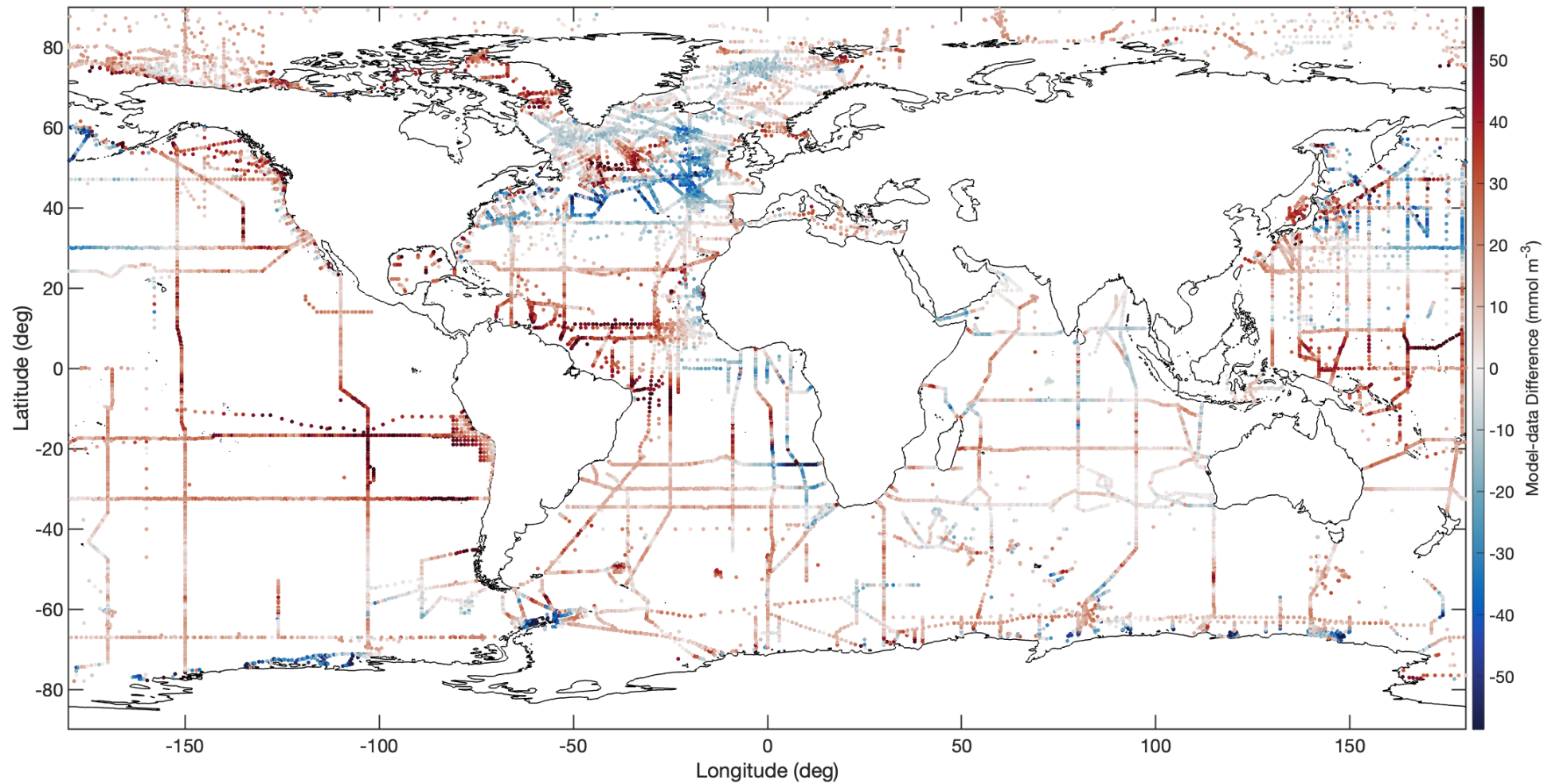
PO_4 , 100 to 500-m Depth



SiO_2 , 100 to 500-m Depth

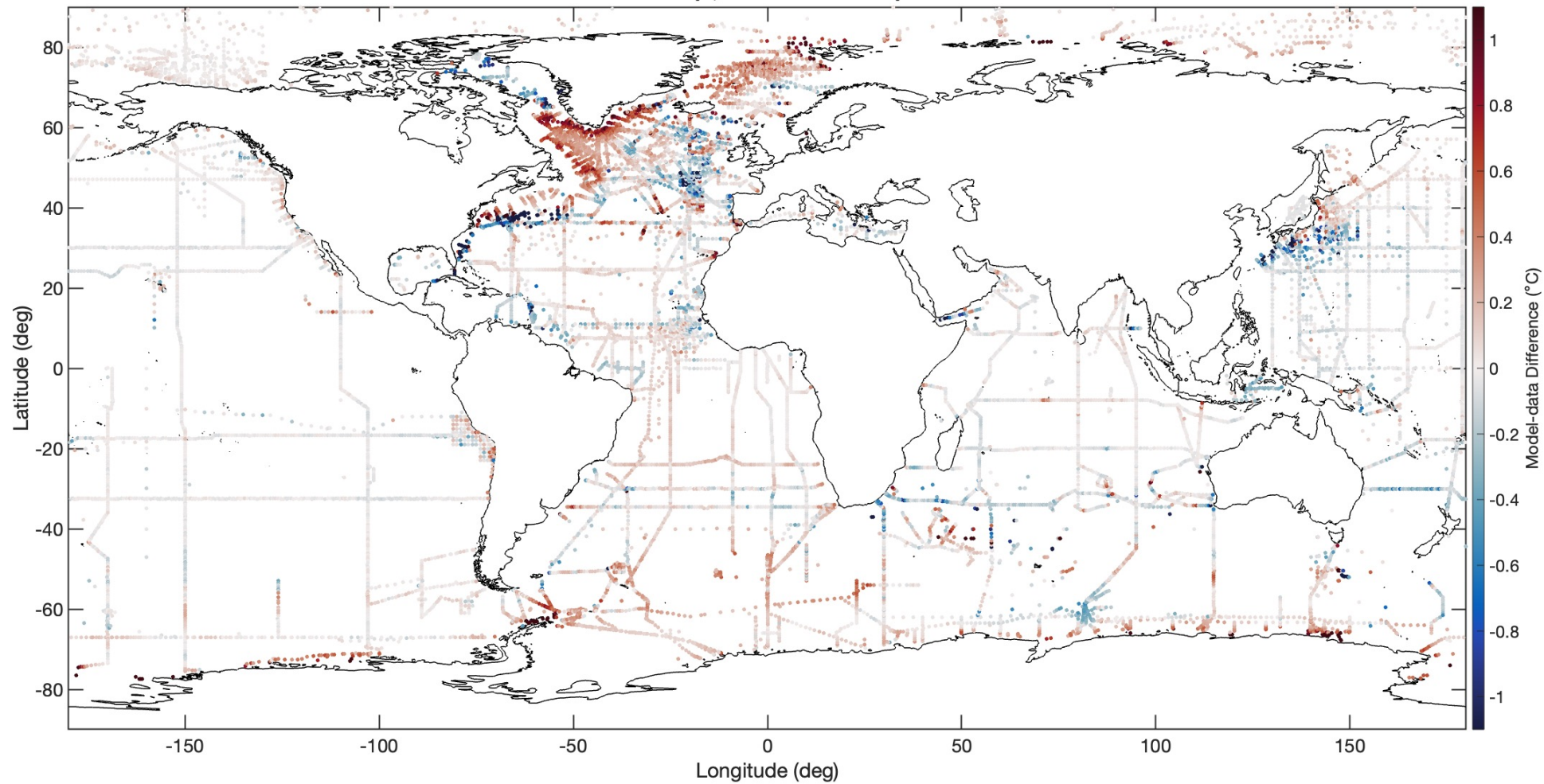


O₂, 100 to 500-m Depth

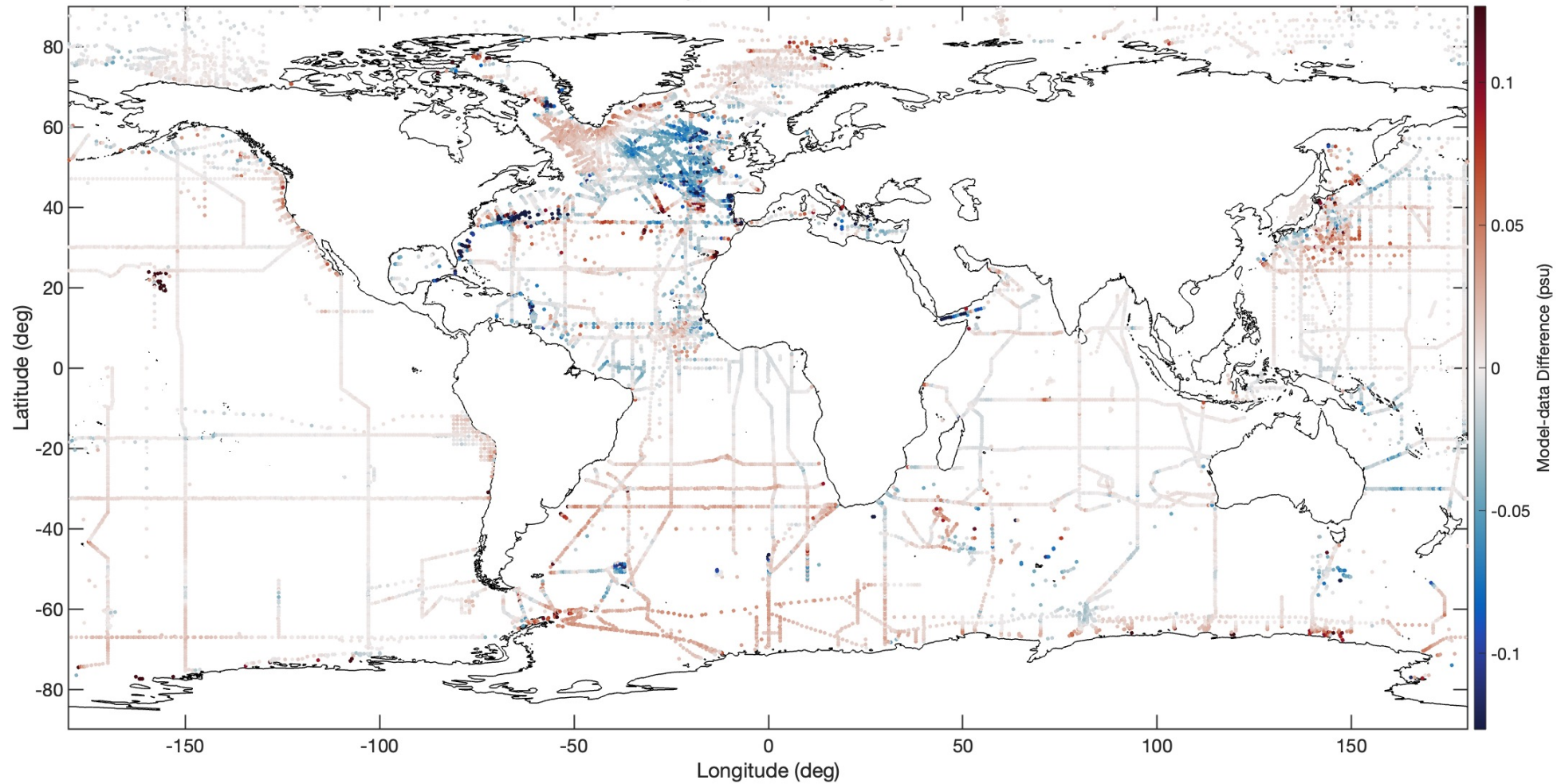


ECCO-Darwin vs. GLODAP model-data difference map: 500 to 6000-m depth

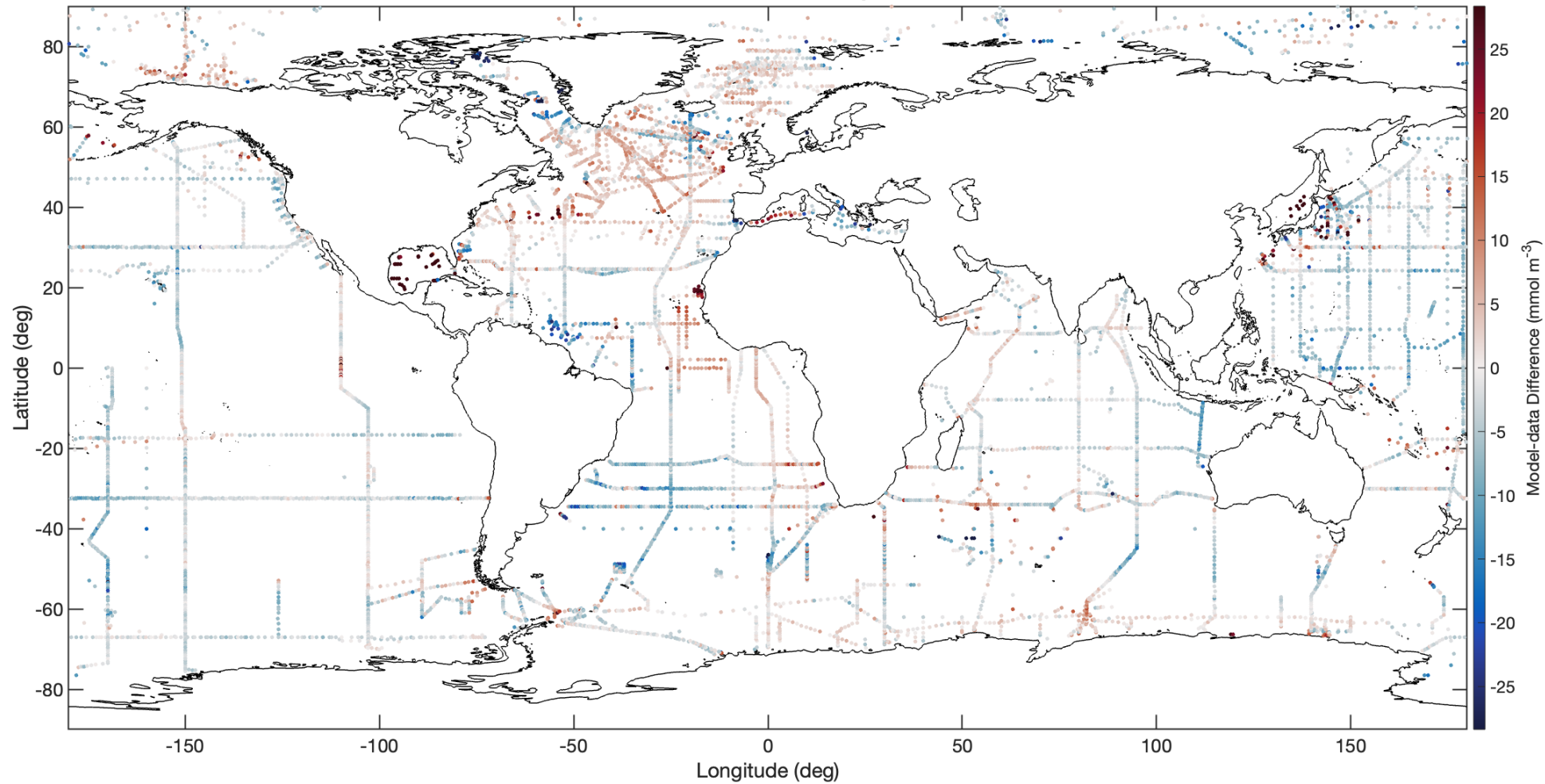
Pot. Temp., 500 to 6000-m Depth



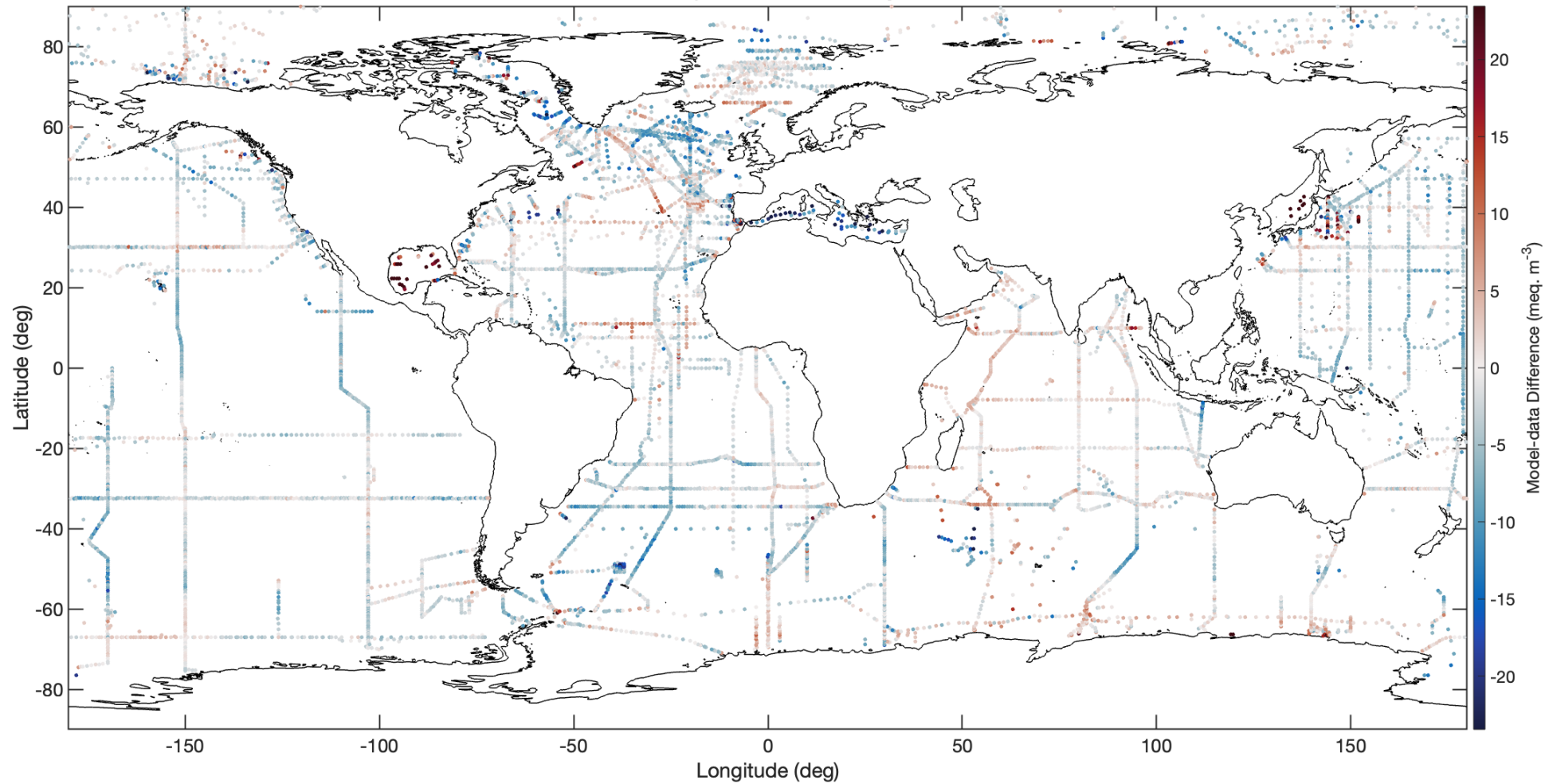
Salinity, 500 to 6000-m Depth



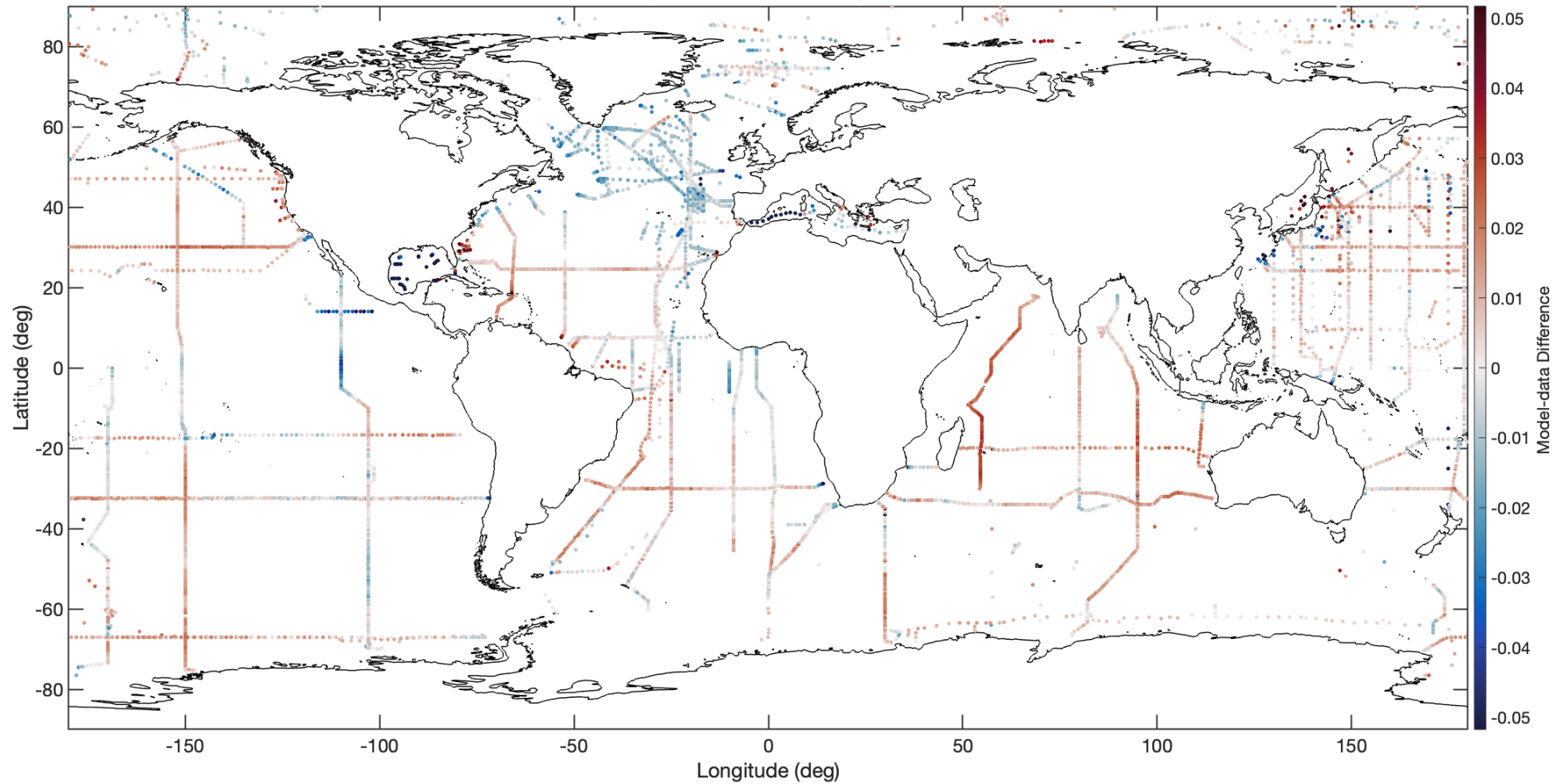
DIC, 500 to 6000-m Depth



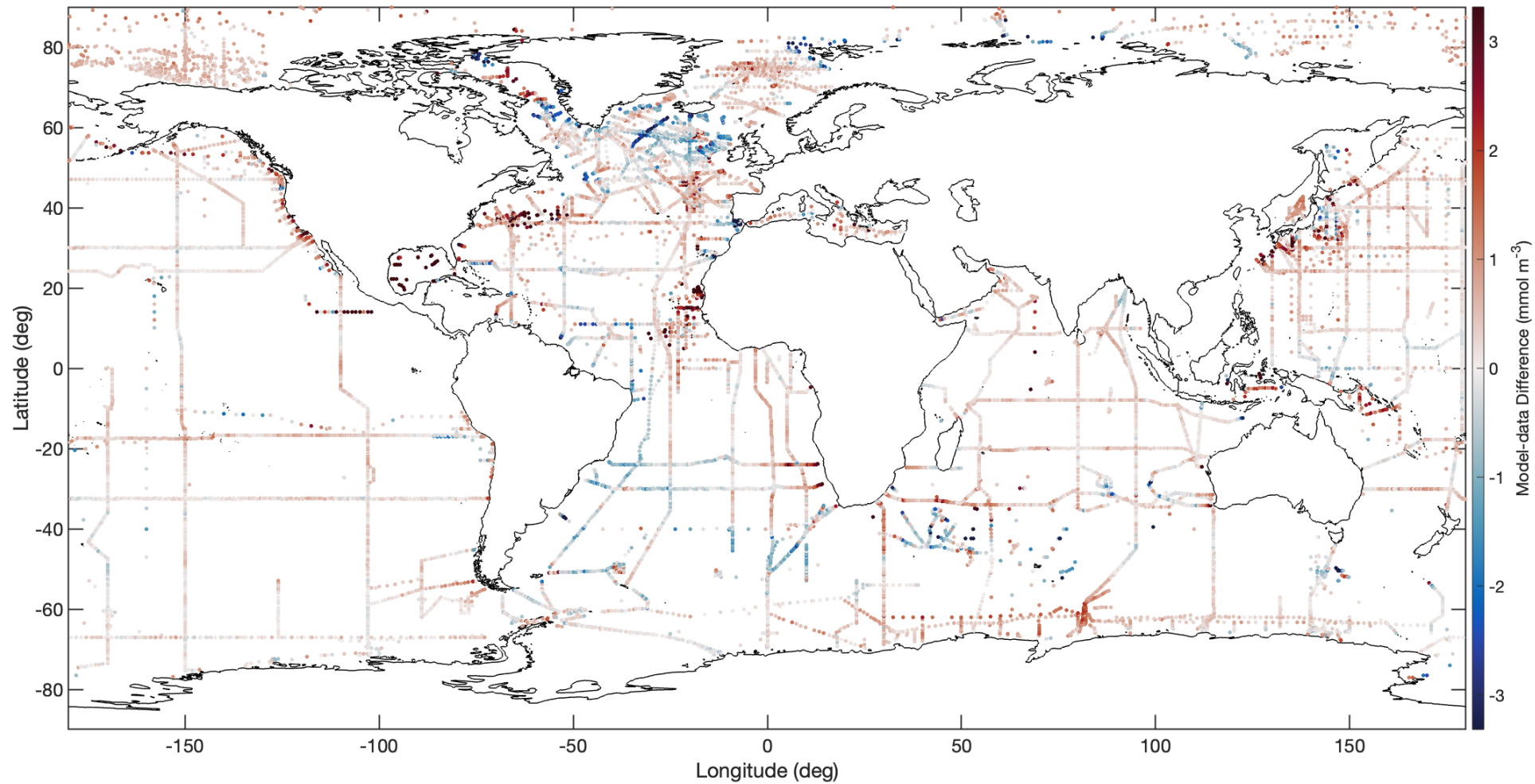
Alkalinity, 500 to 6000-m Depth



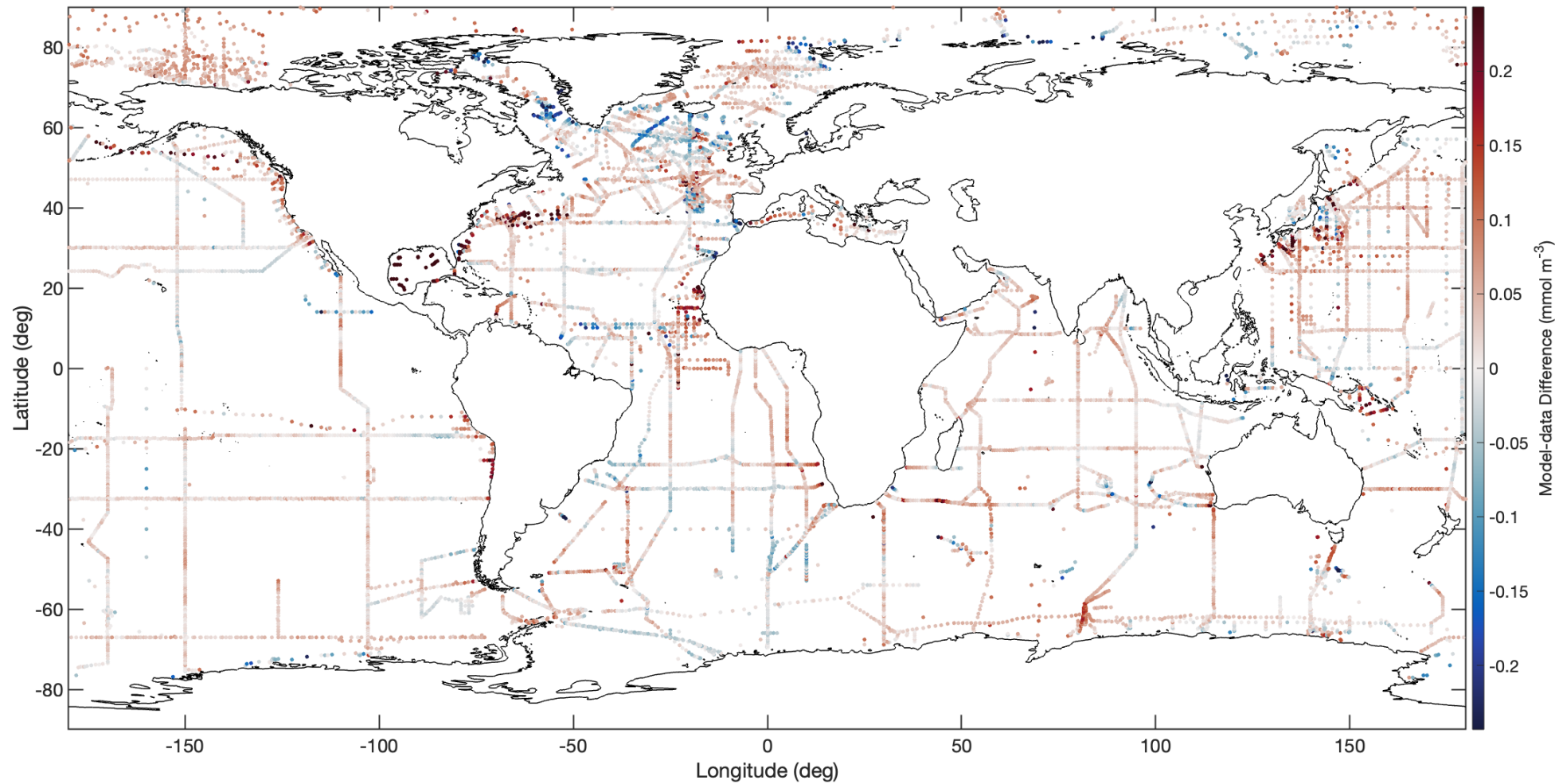
pH, 500 to 6000-m Depth



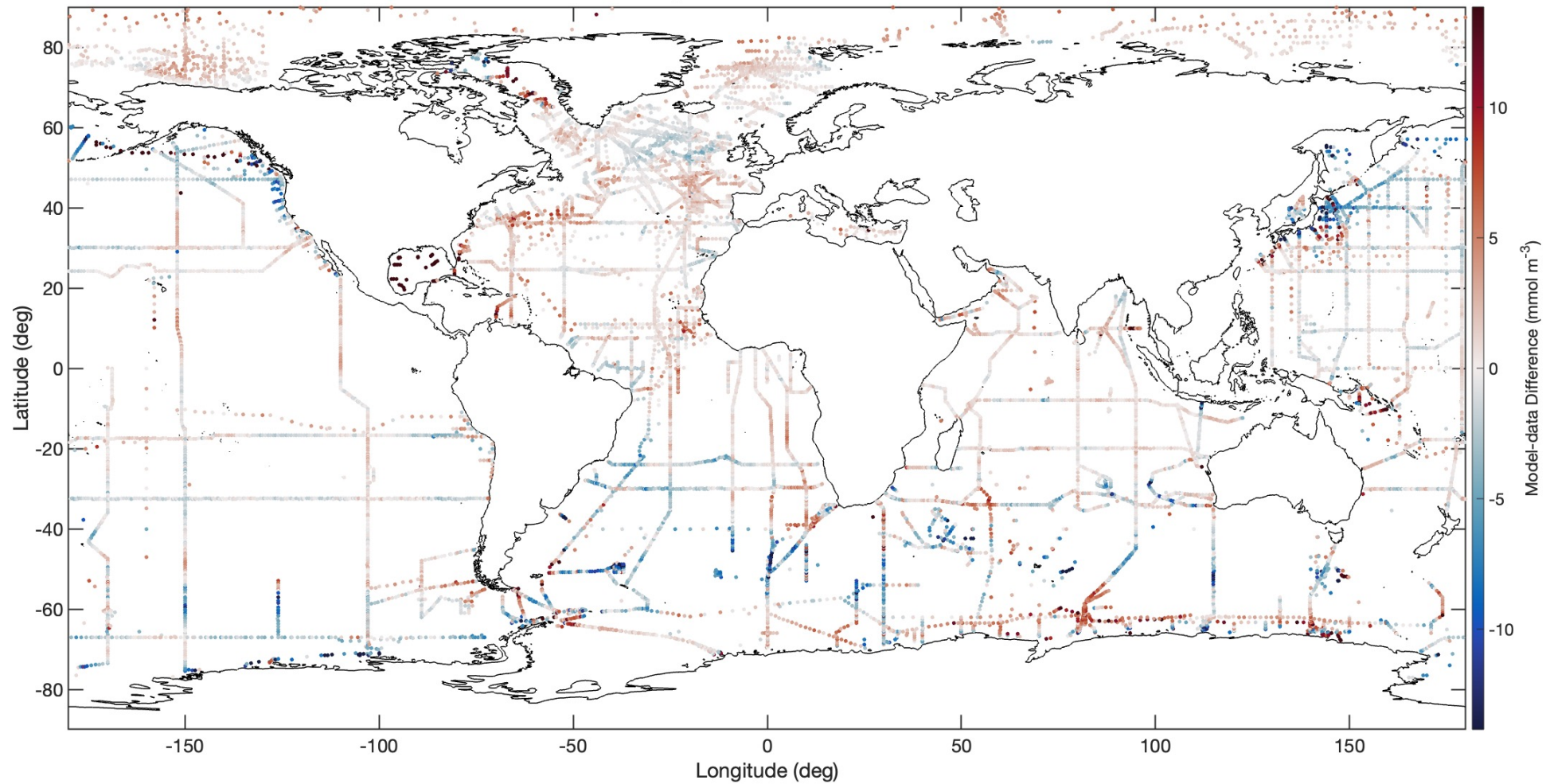
NO_3^- , 500 to 6000-m Depth



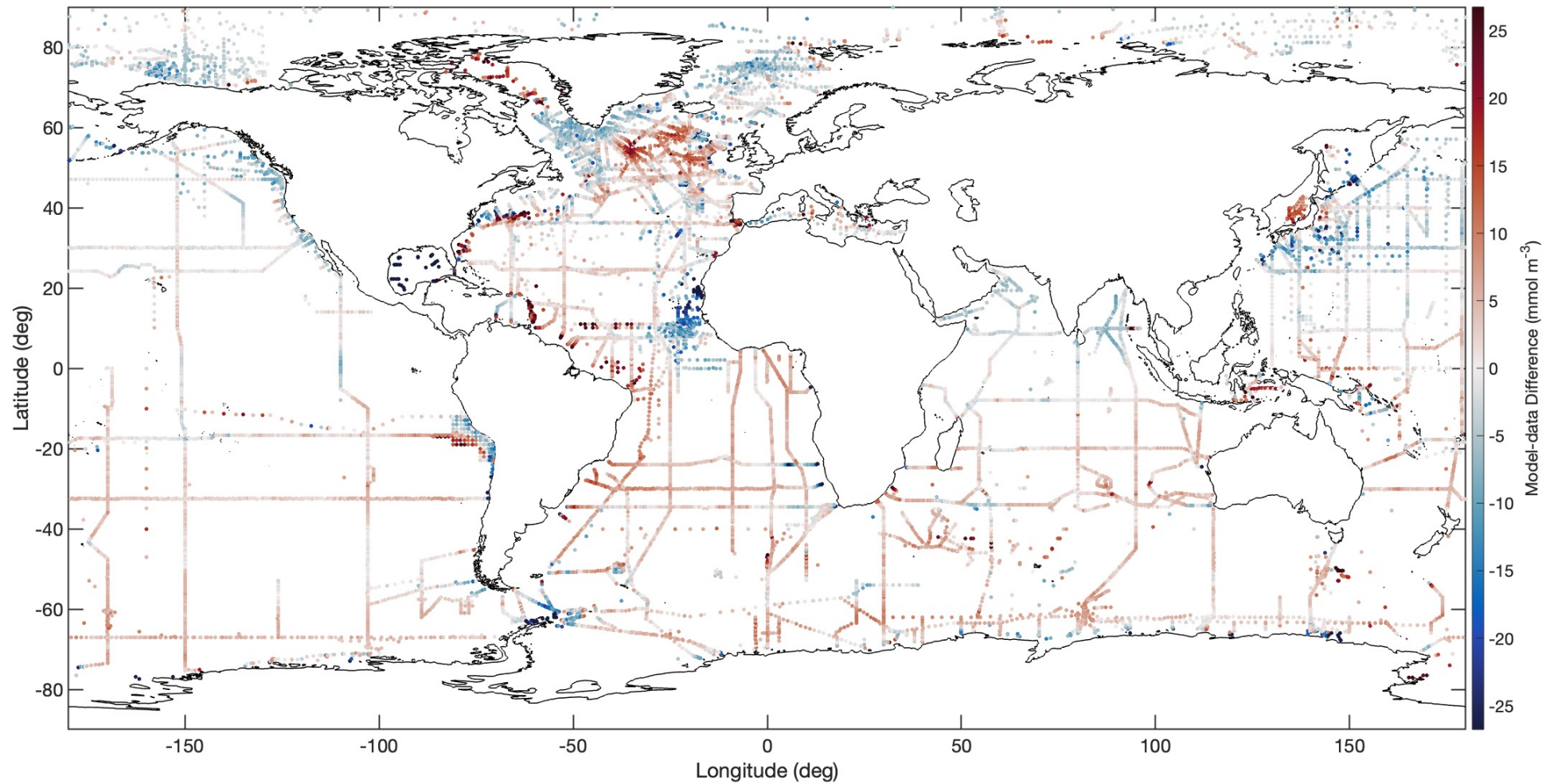
PO_4 , 500 to 6000-m Depth



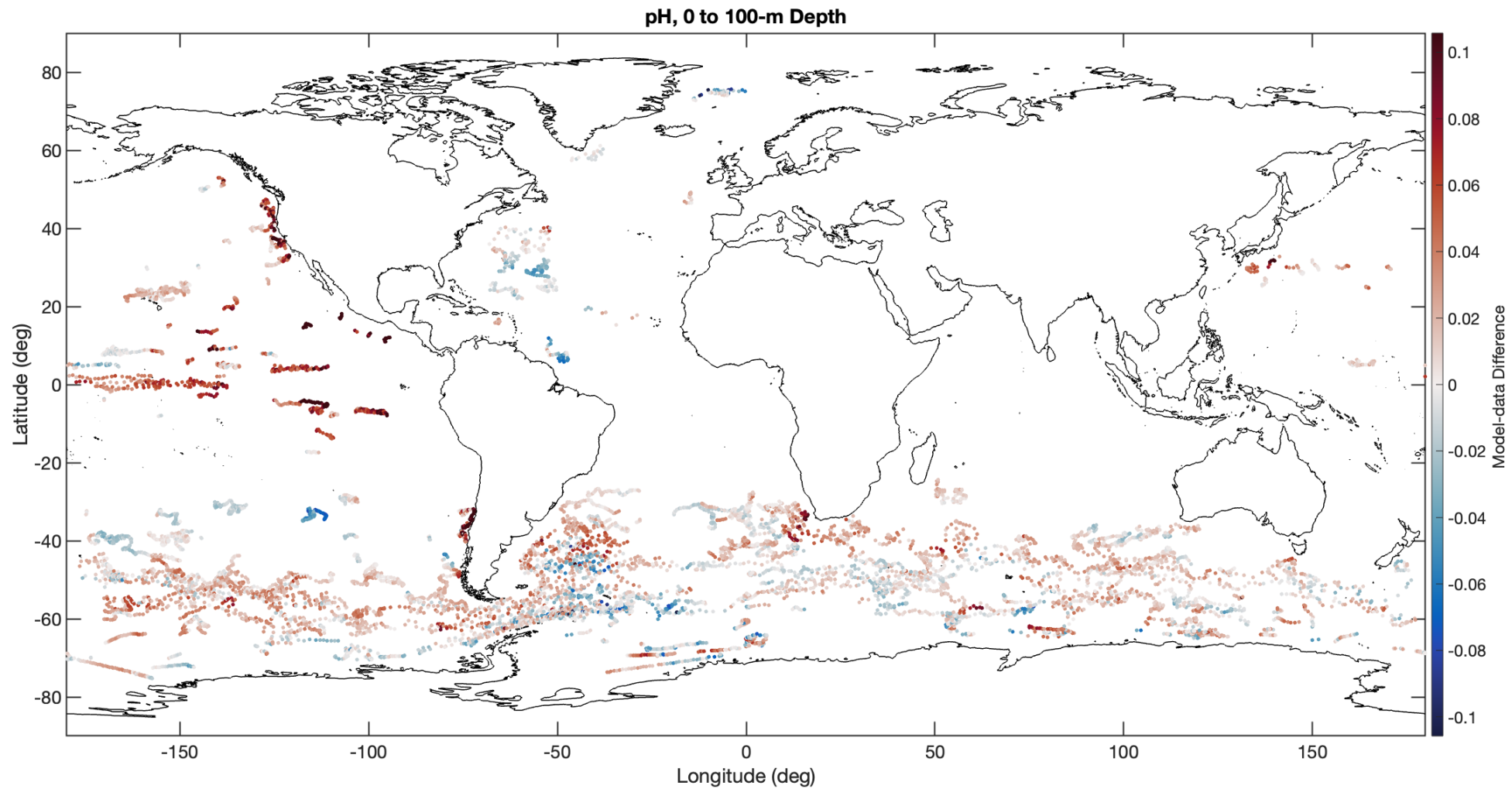
SiO_2 , 500 to 6000-m Depth



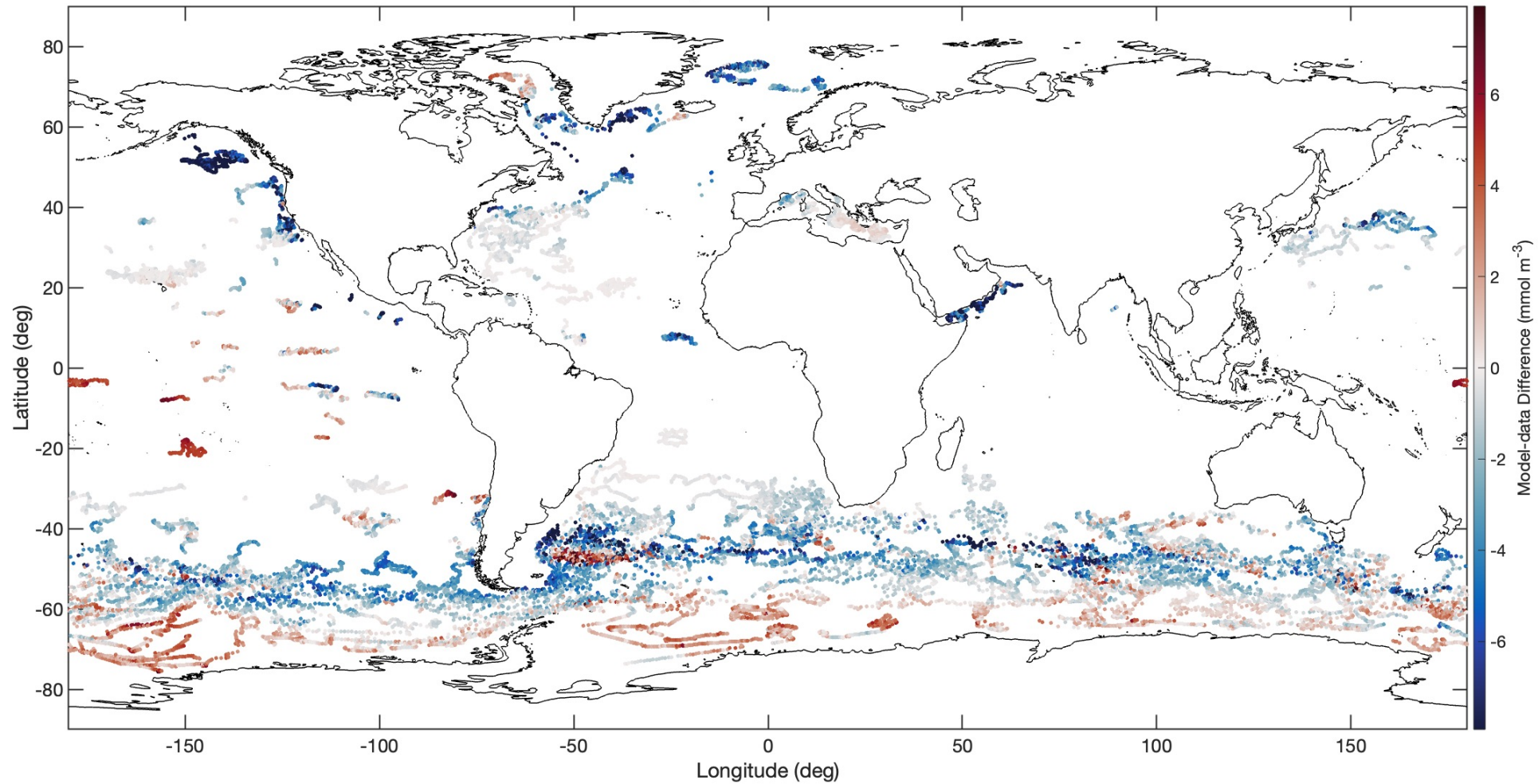
O₂, 500 to 6000-m Depth



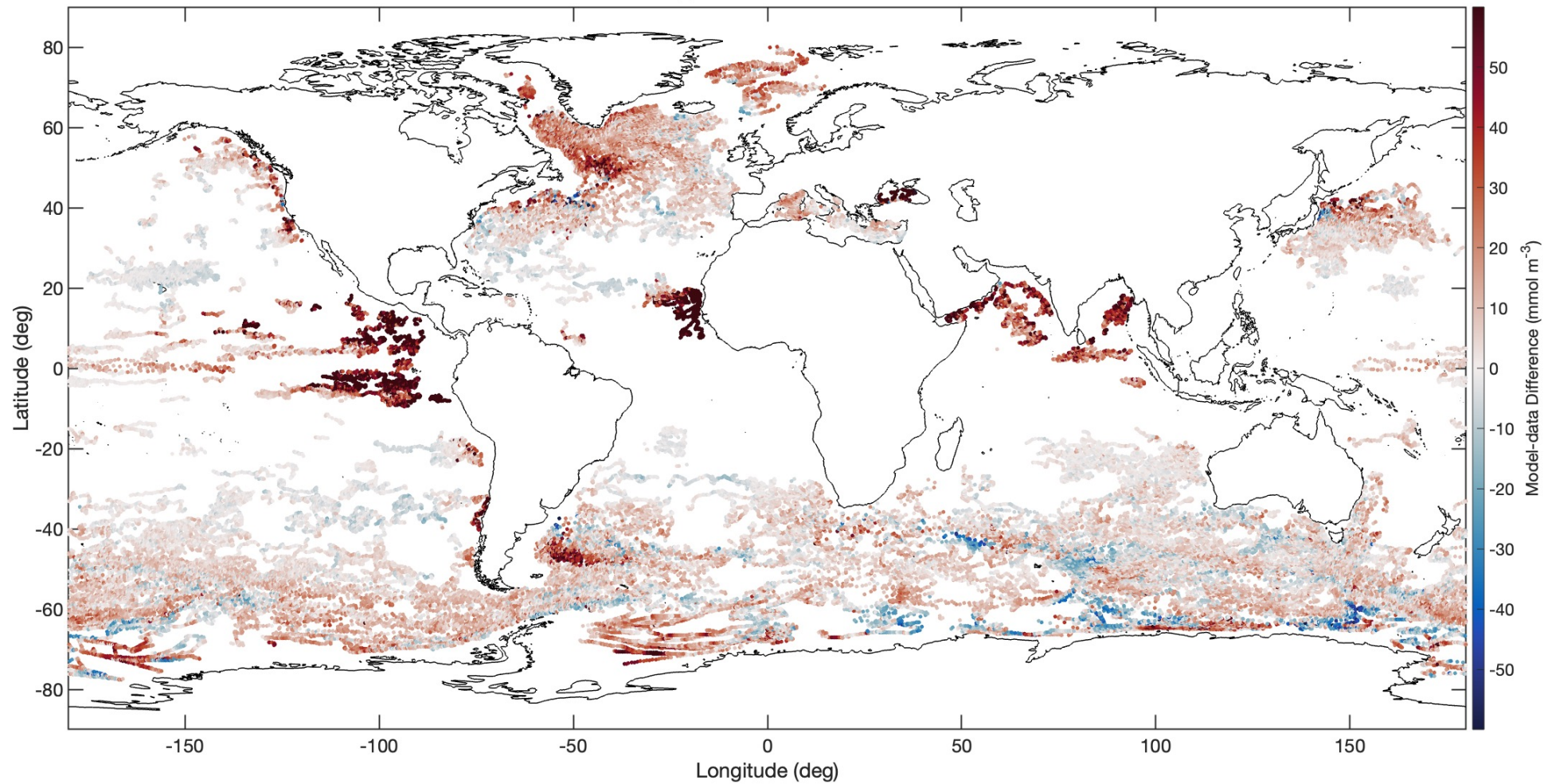
ECCO-Darwin vs. BGC-Argo model-data difference map: 0 to 100-m depth



NO_3^- , 0 to 100-m Depth

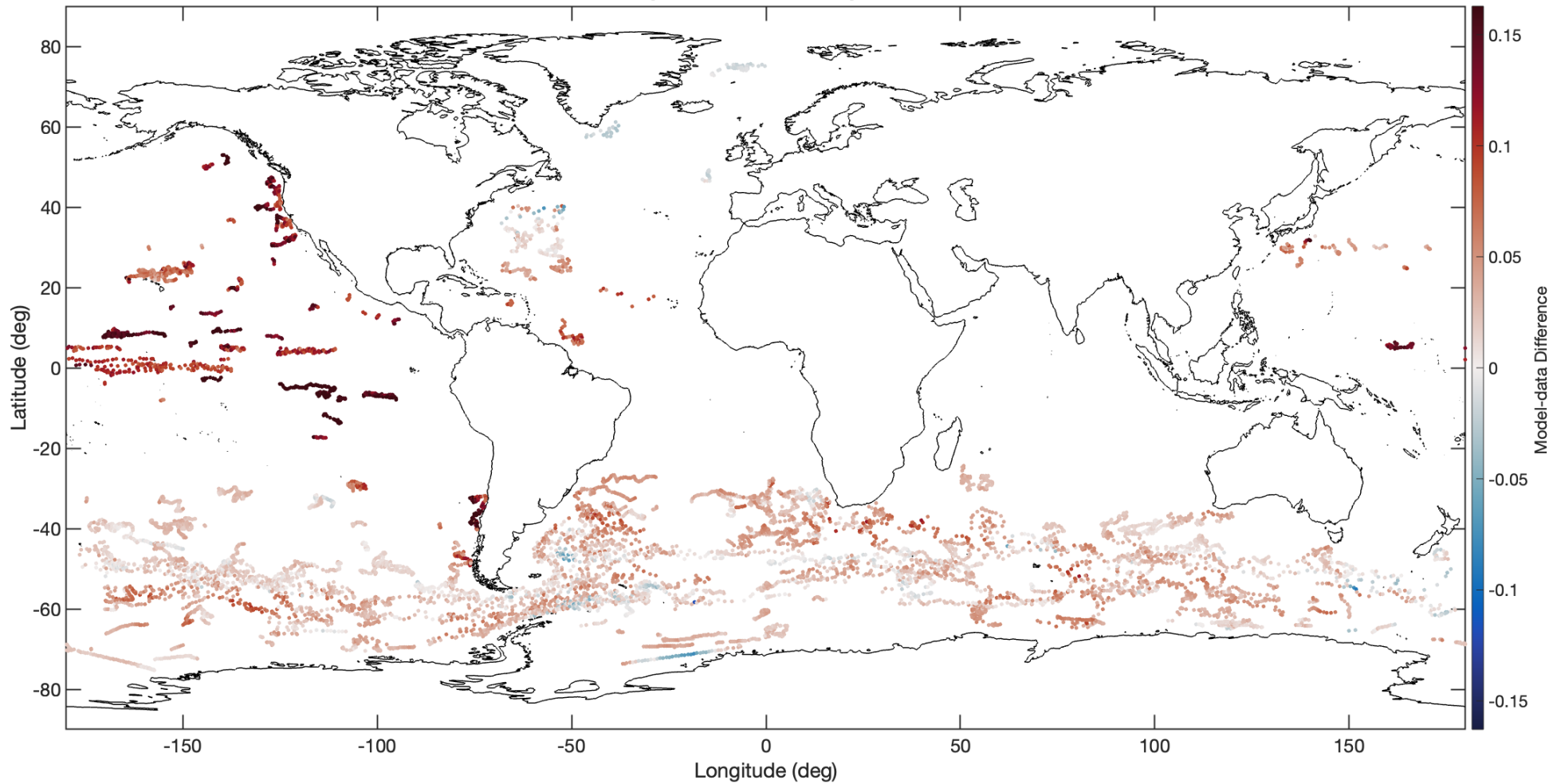


O_2 , 0 to 100-m Depth

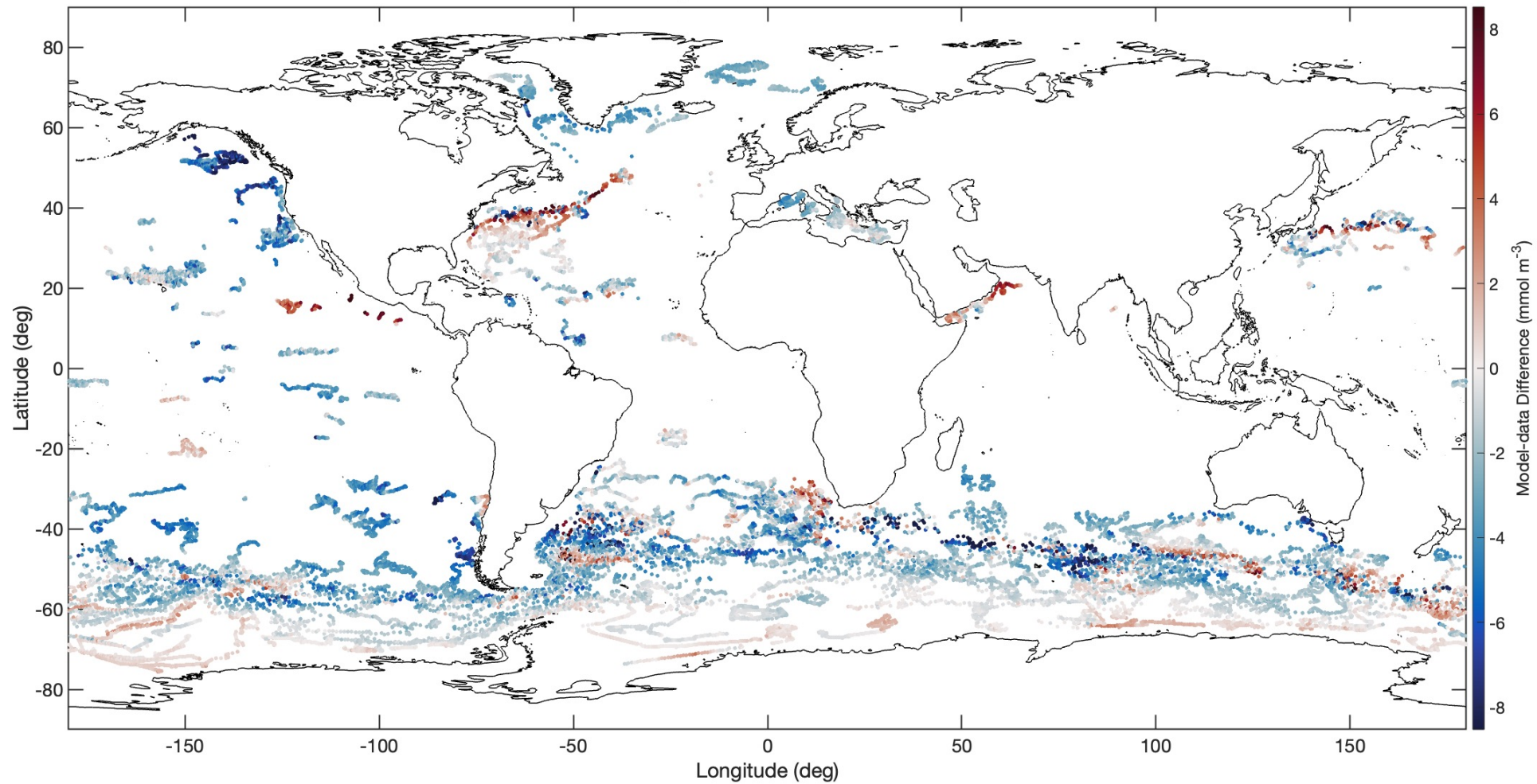


ECCO-Darwin vs. BGC-Argo model-data difference map: 100 to 500-m depth

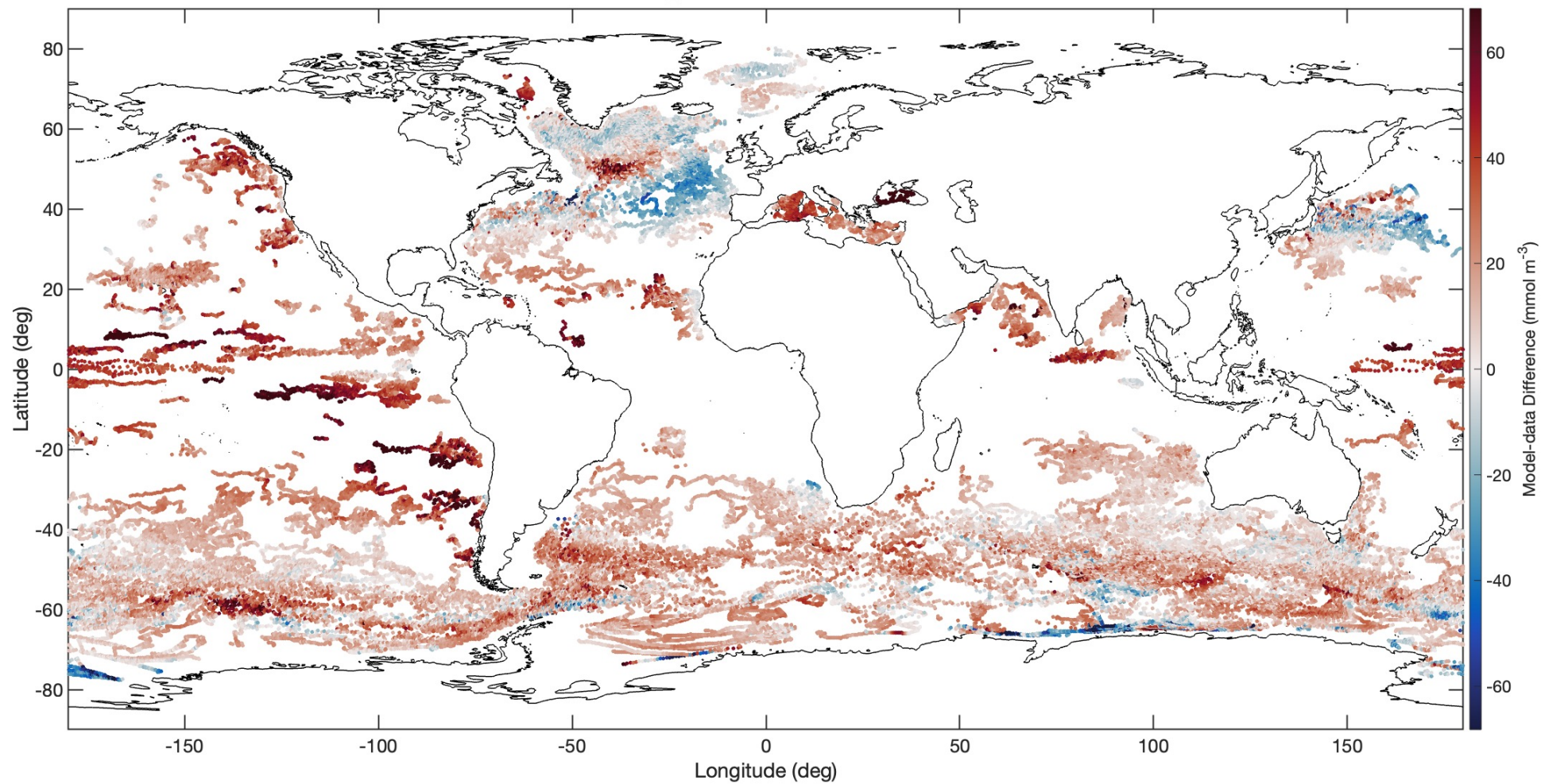
pH, 100 to 500-m Depth



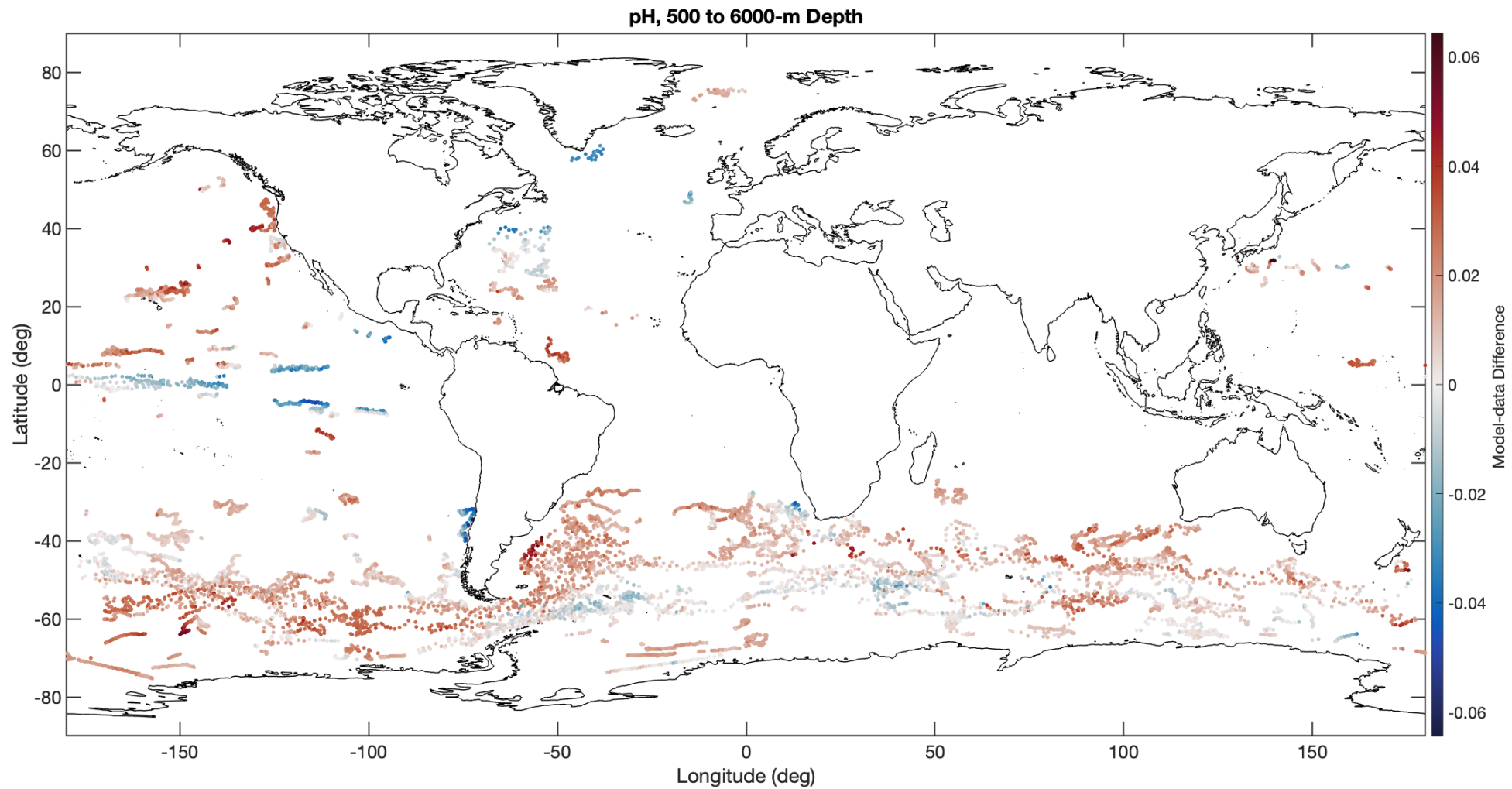
NO_3^- , 100 to 500-m Depth



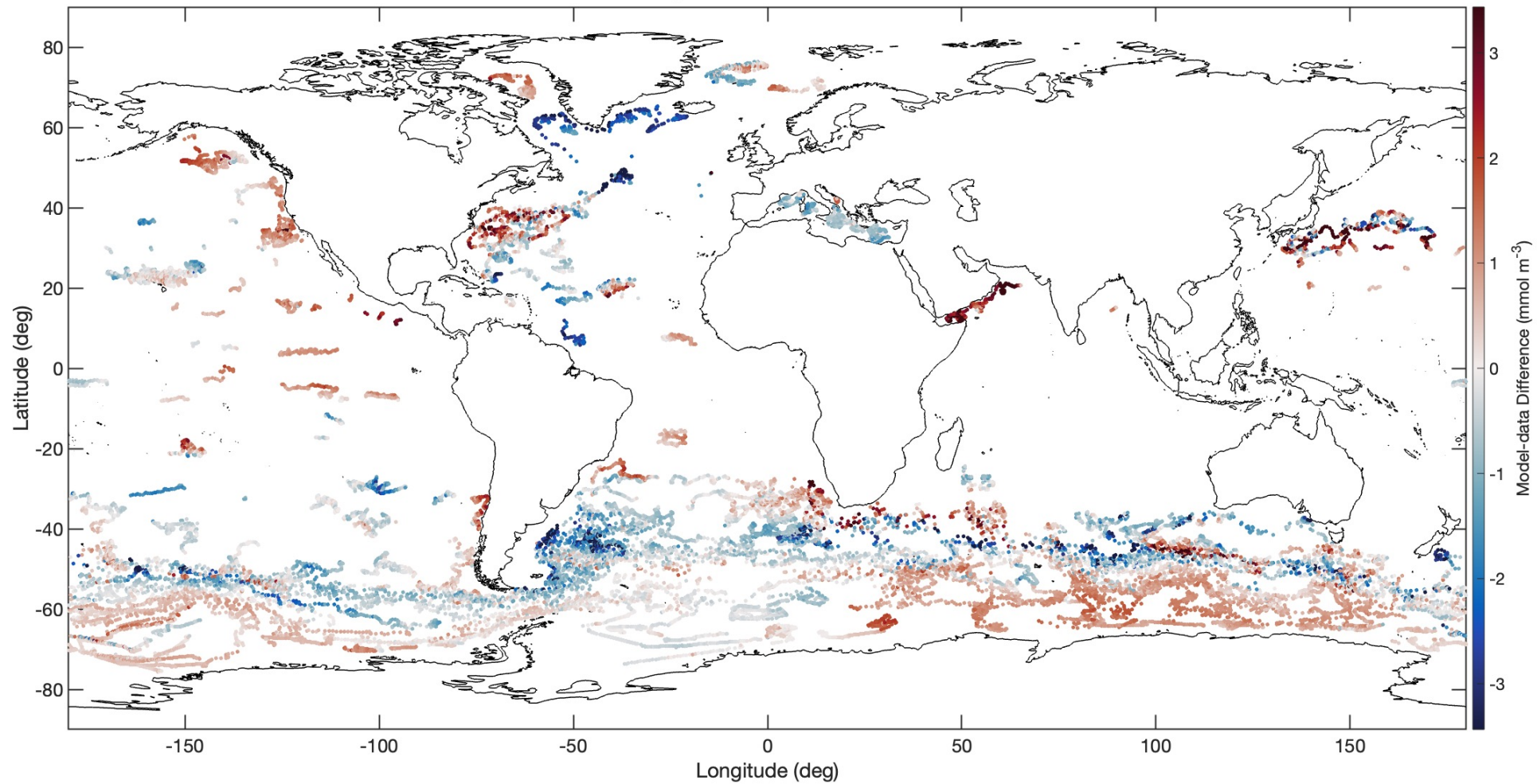
O₂, 100 to 500-m Depth



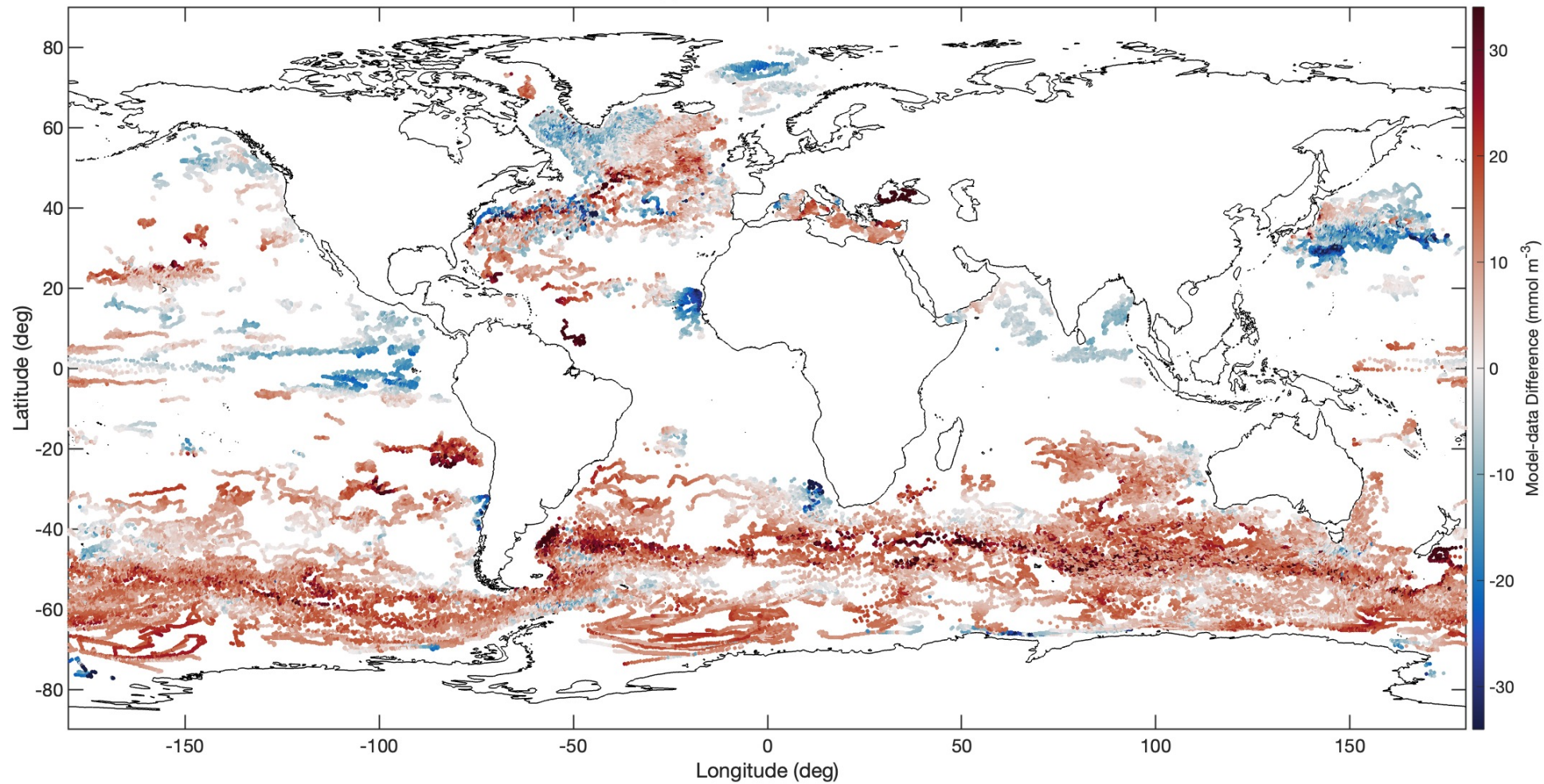
ECCO-Darwin vs. BGC-Argo model-data difference map: 500 to 6000-m depth



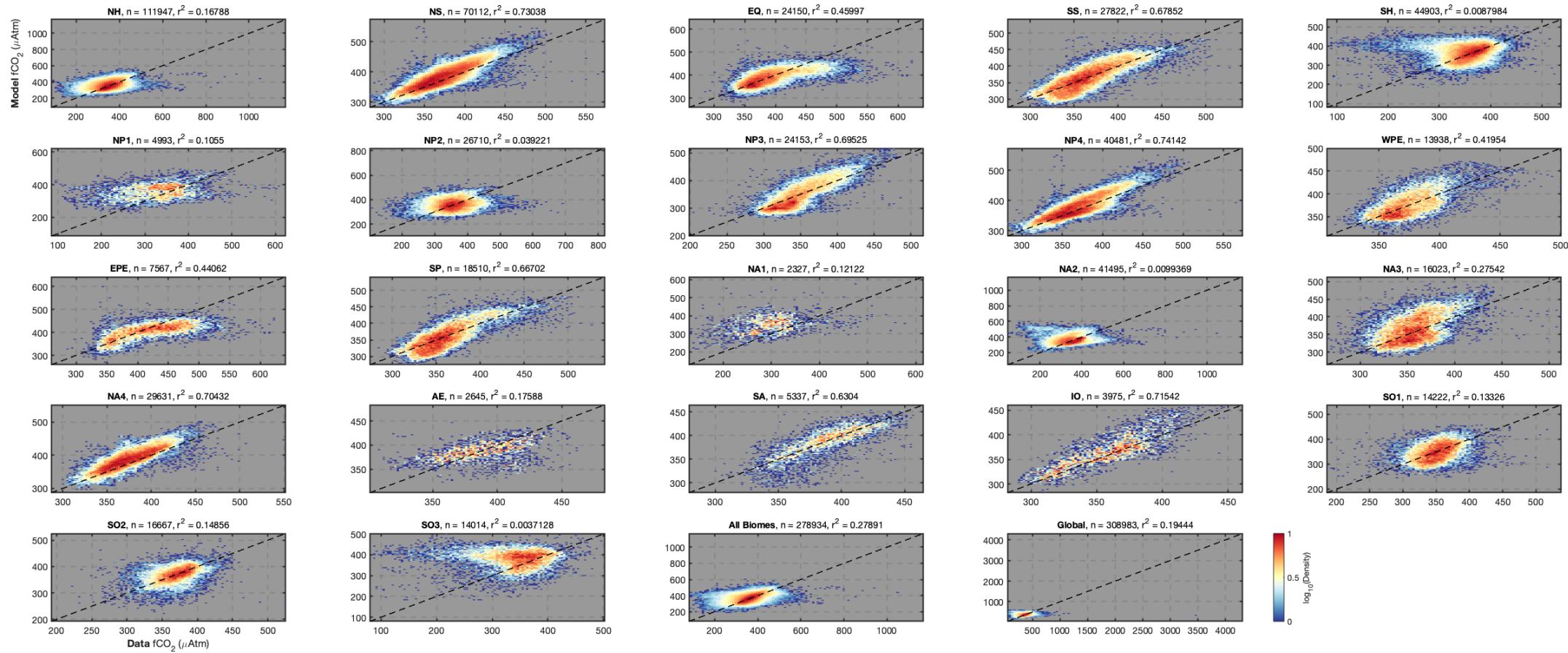
NO_3 , 500 to 6000-m Depth



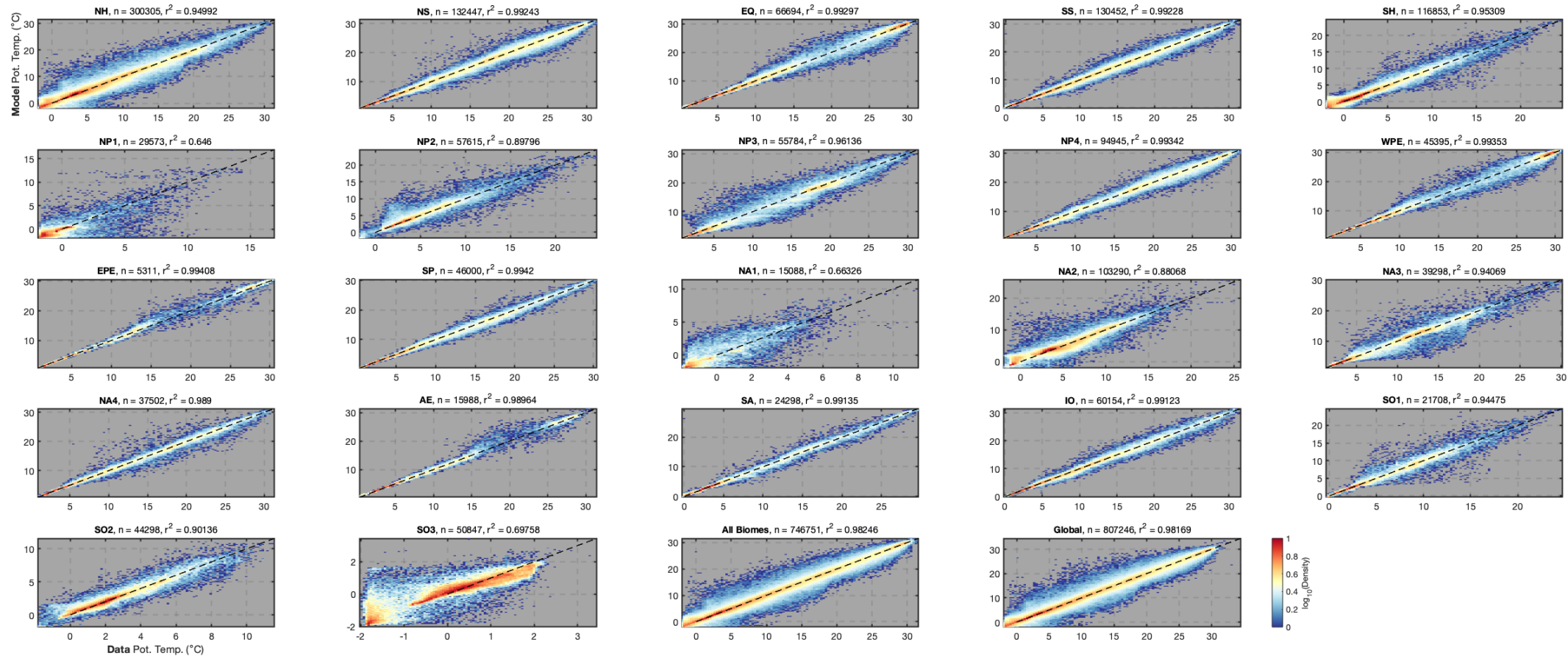
O₂, 500 to 6000-m Depth

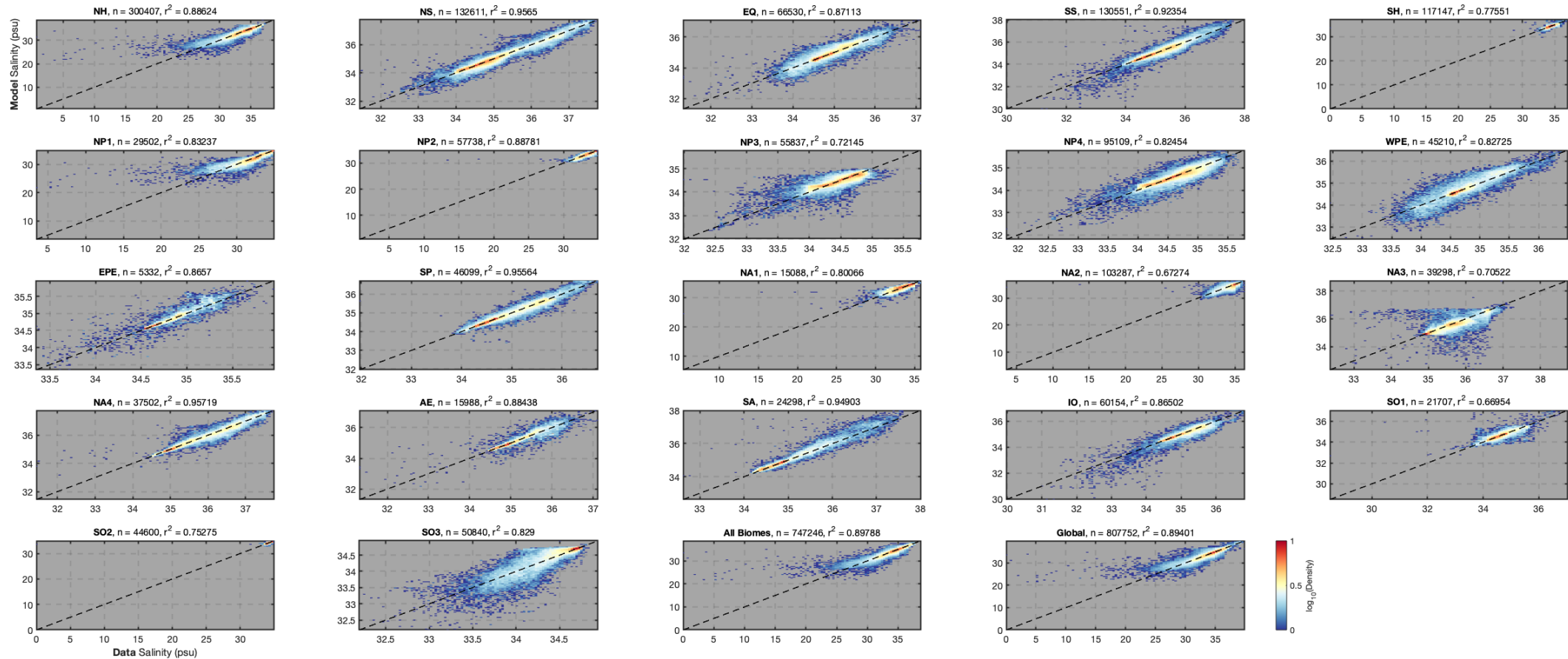


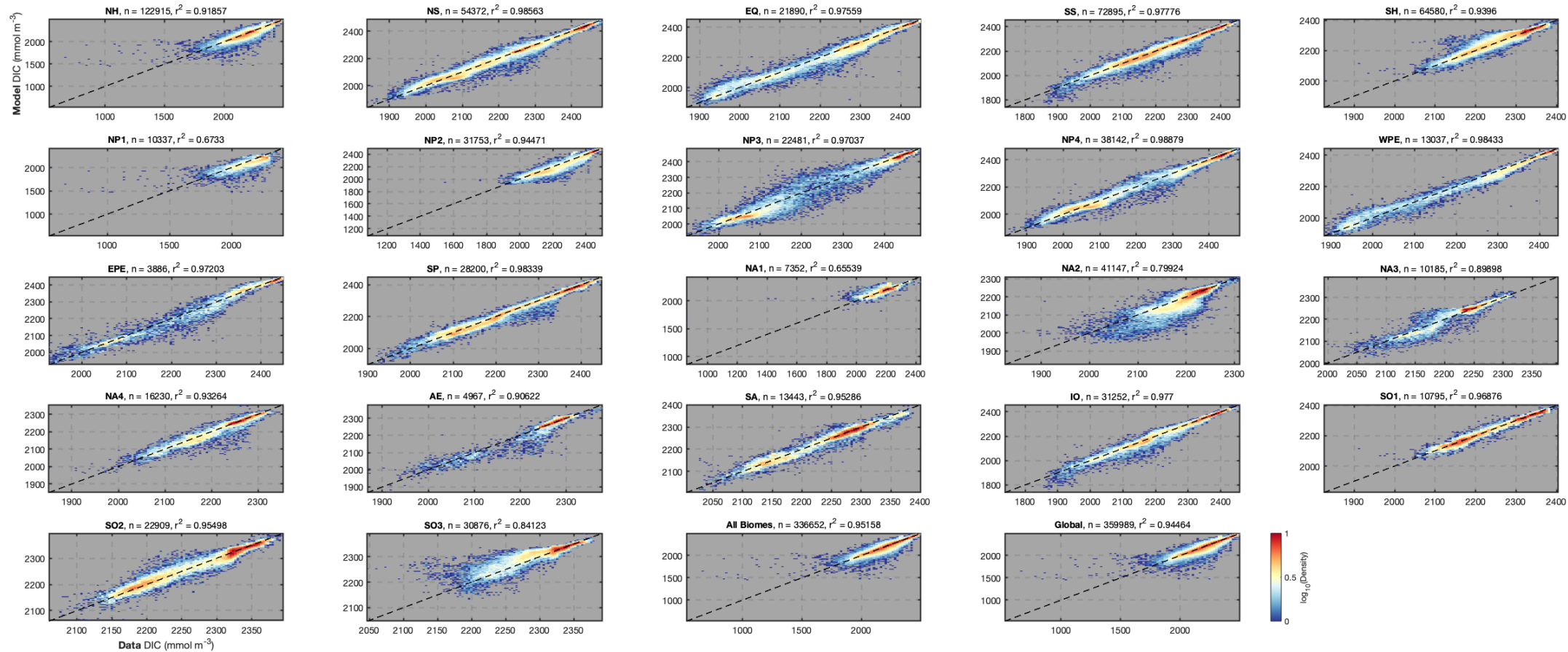
ECCO-Darwin vs. SOCAT scatter: surface ocean

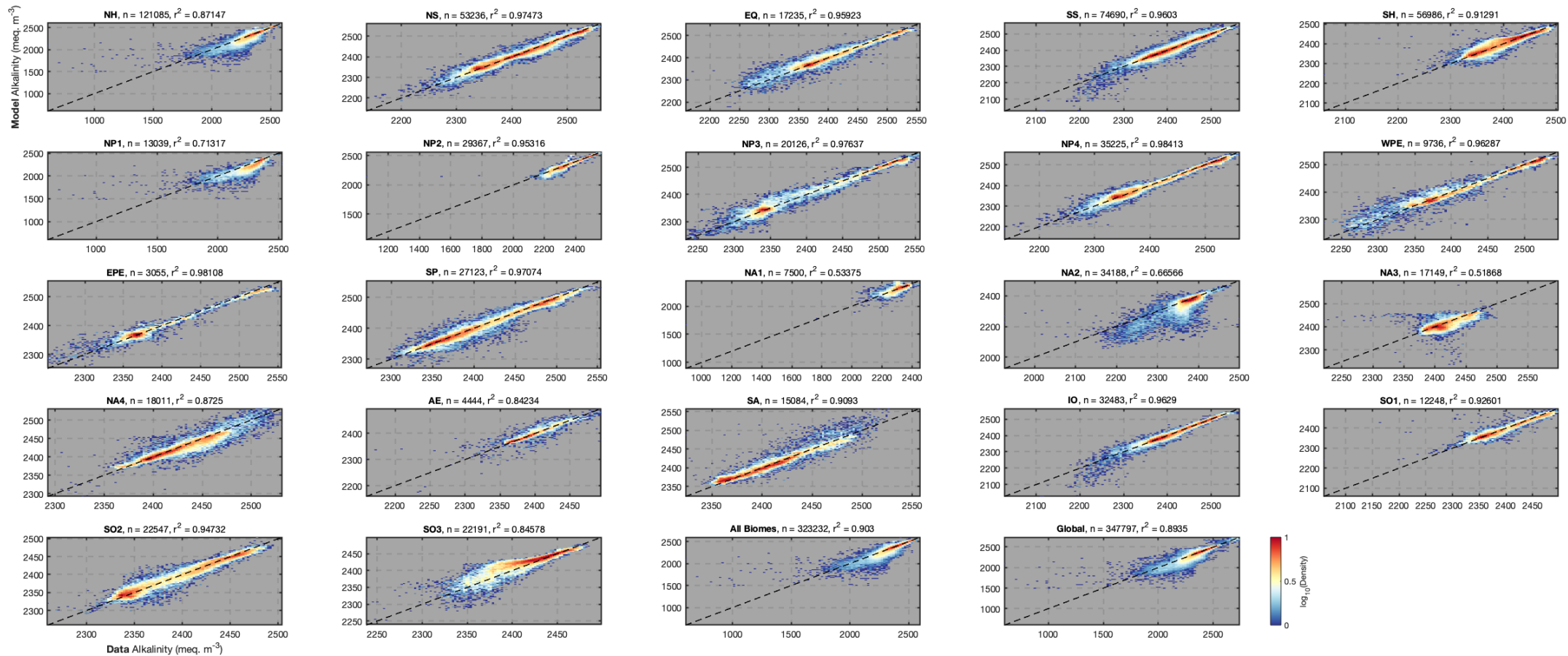


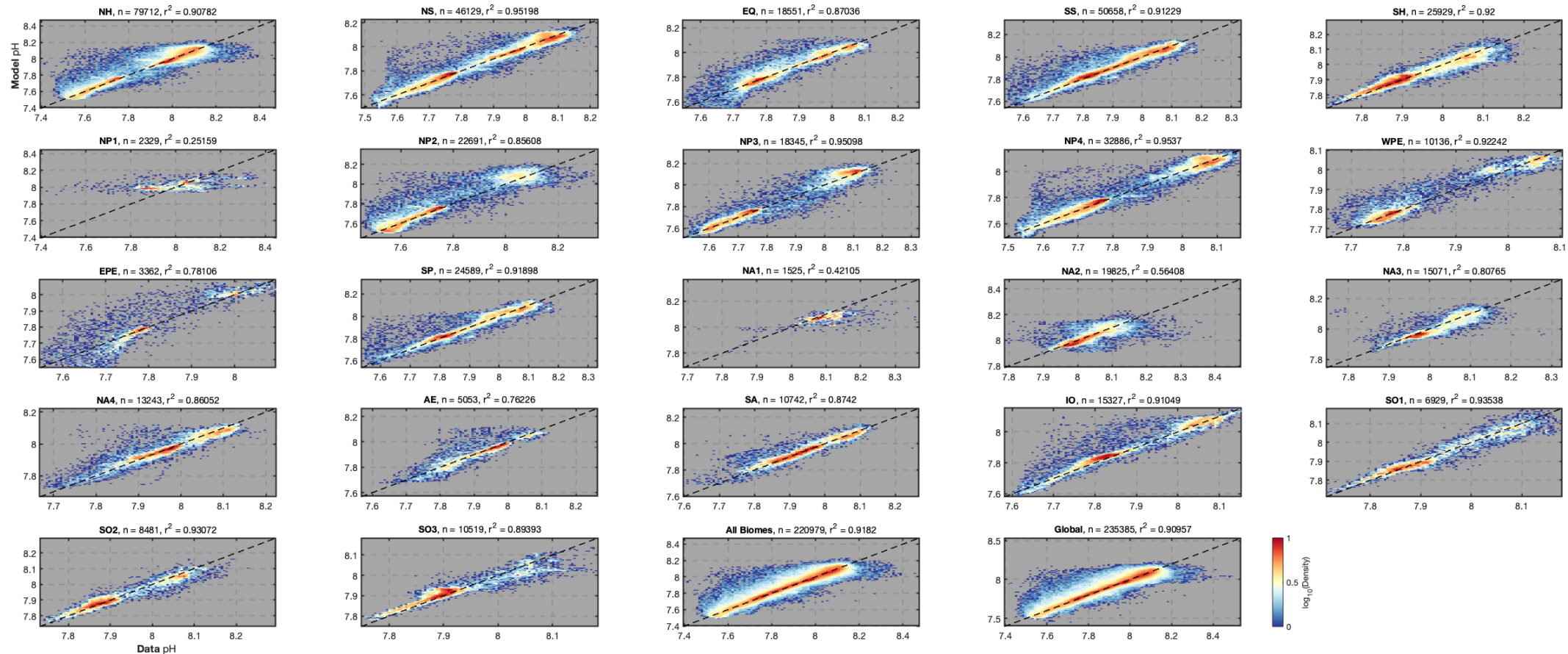
ECCO-Darwin vs. GLODAP scatter: all depths

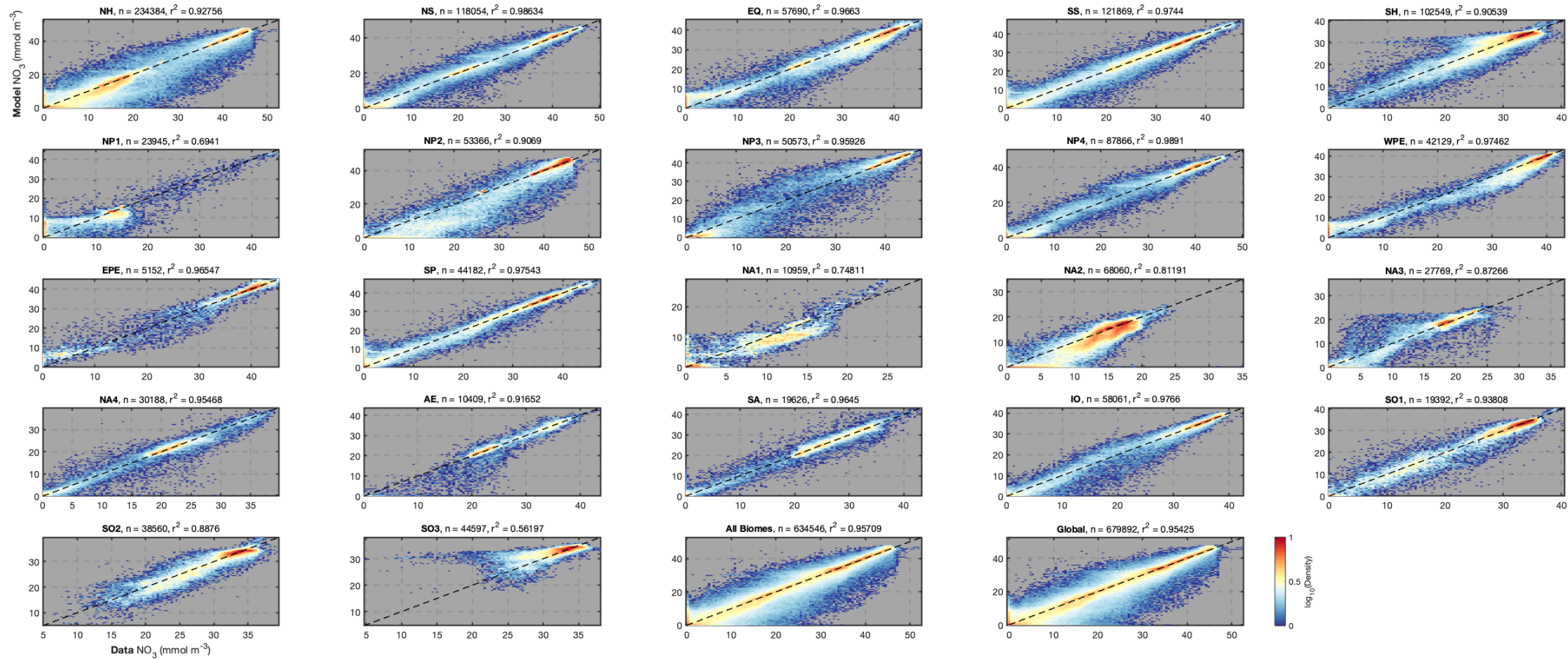


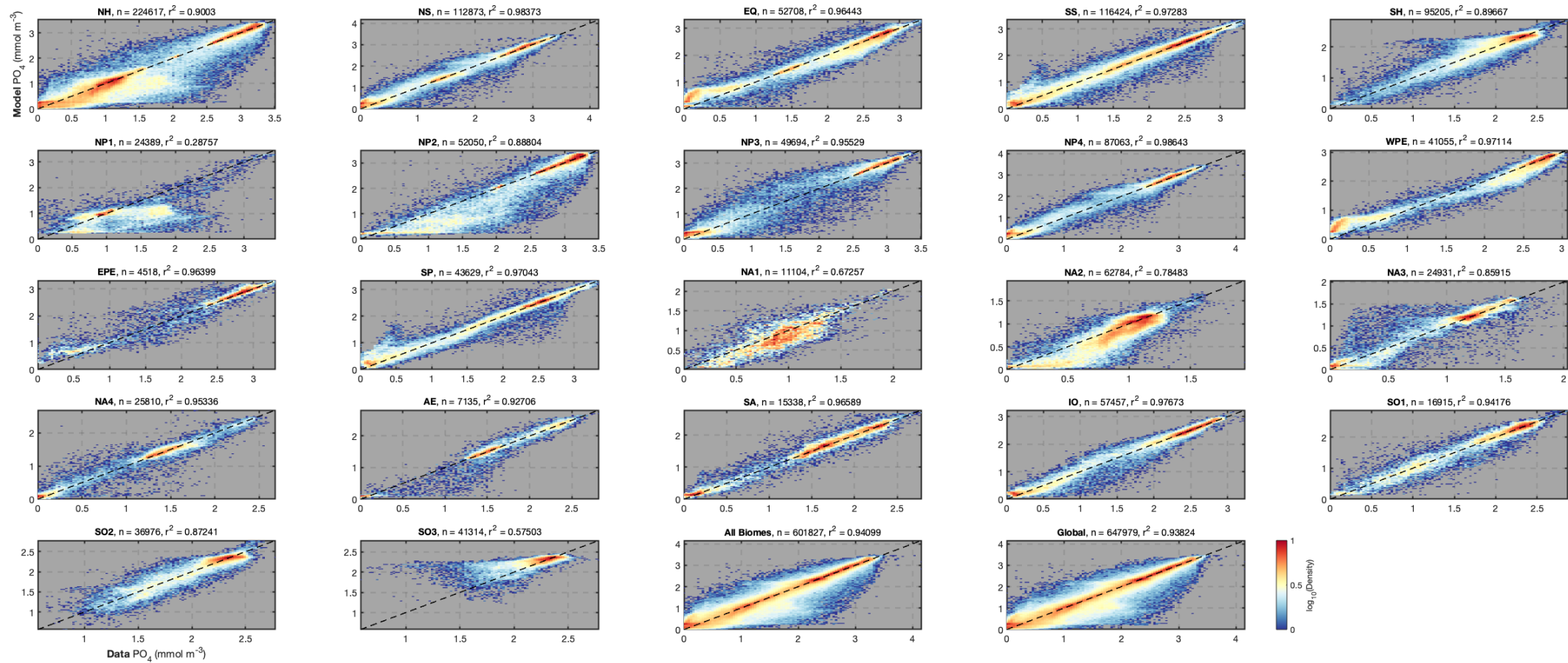


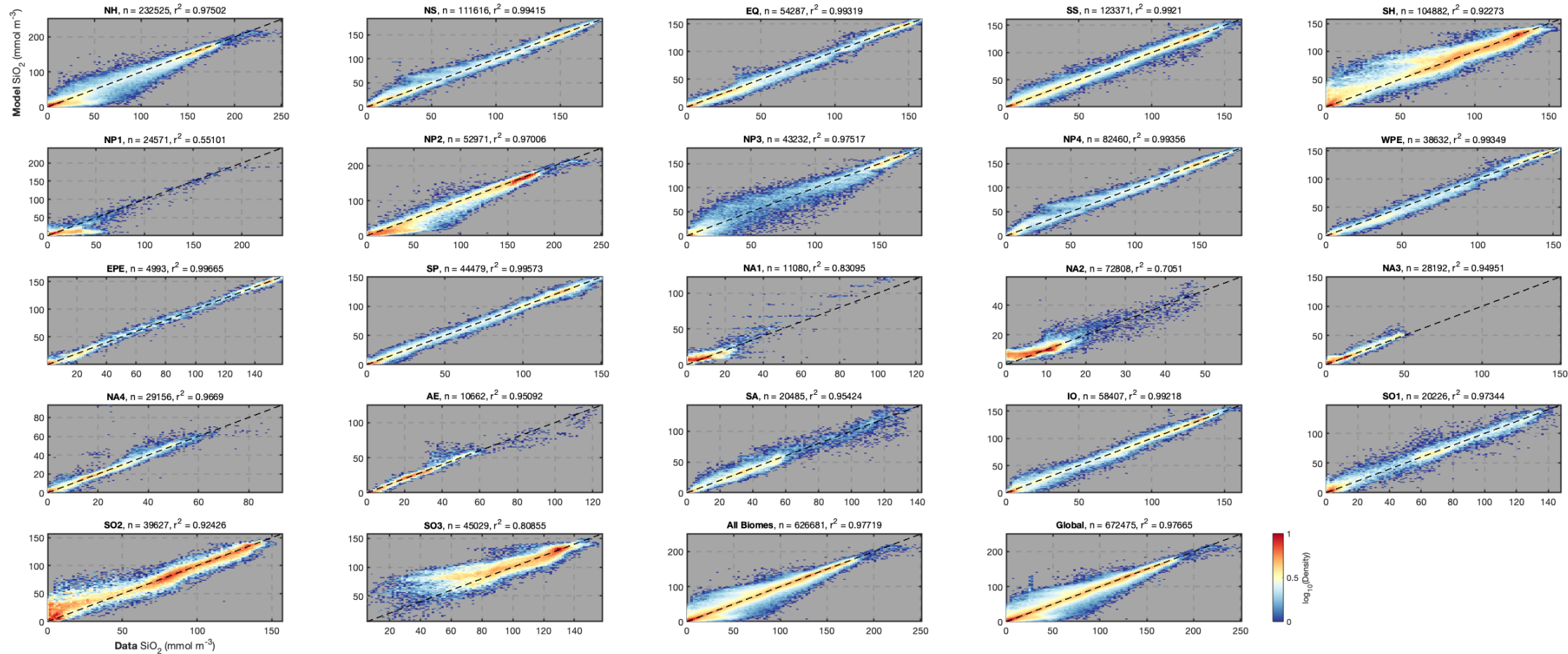


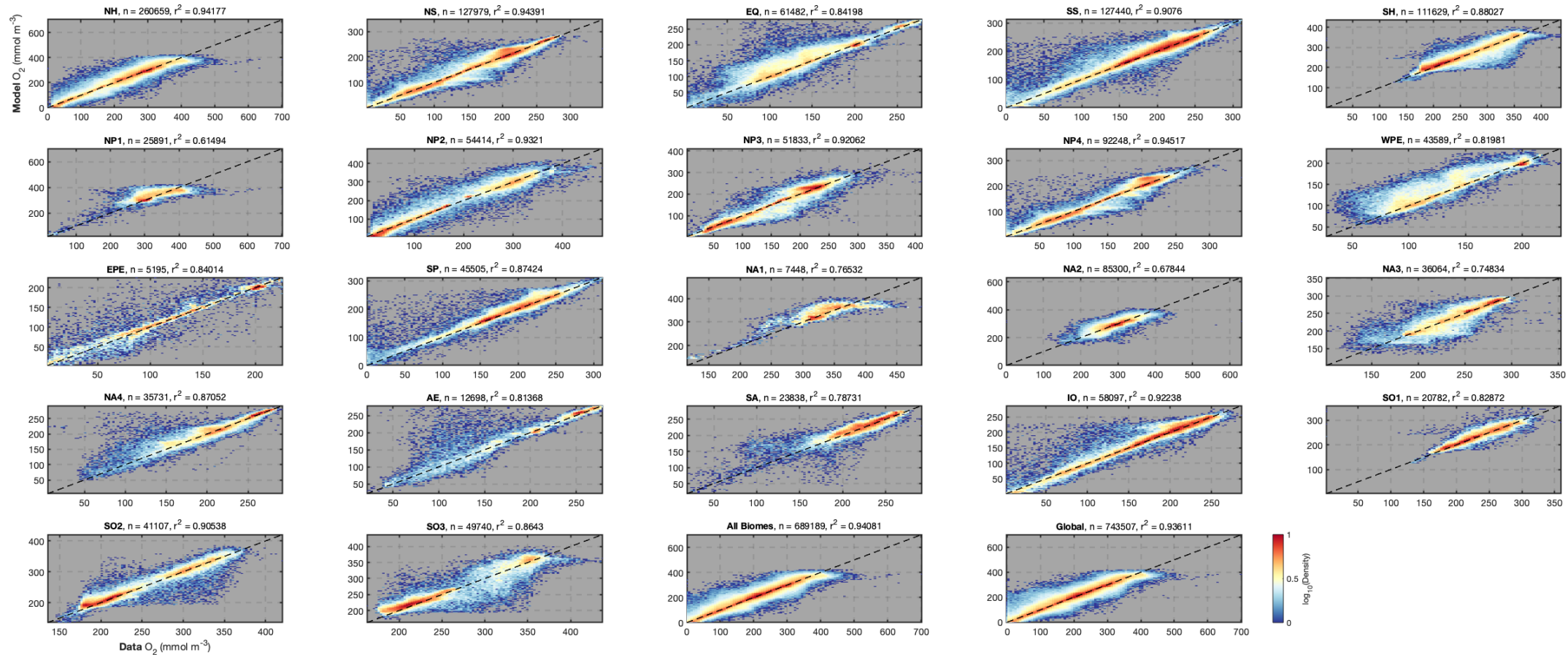




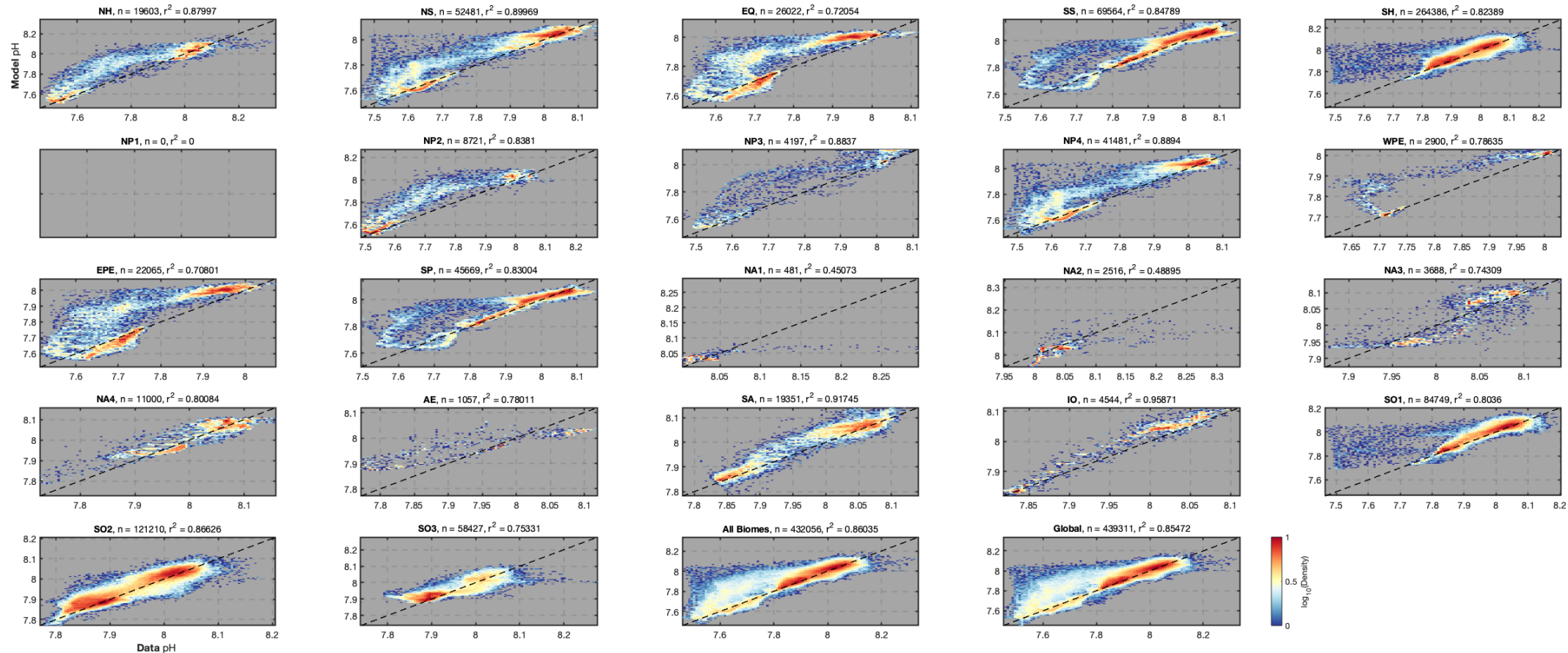


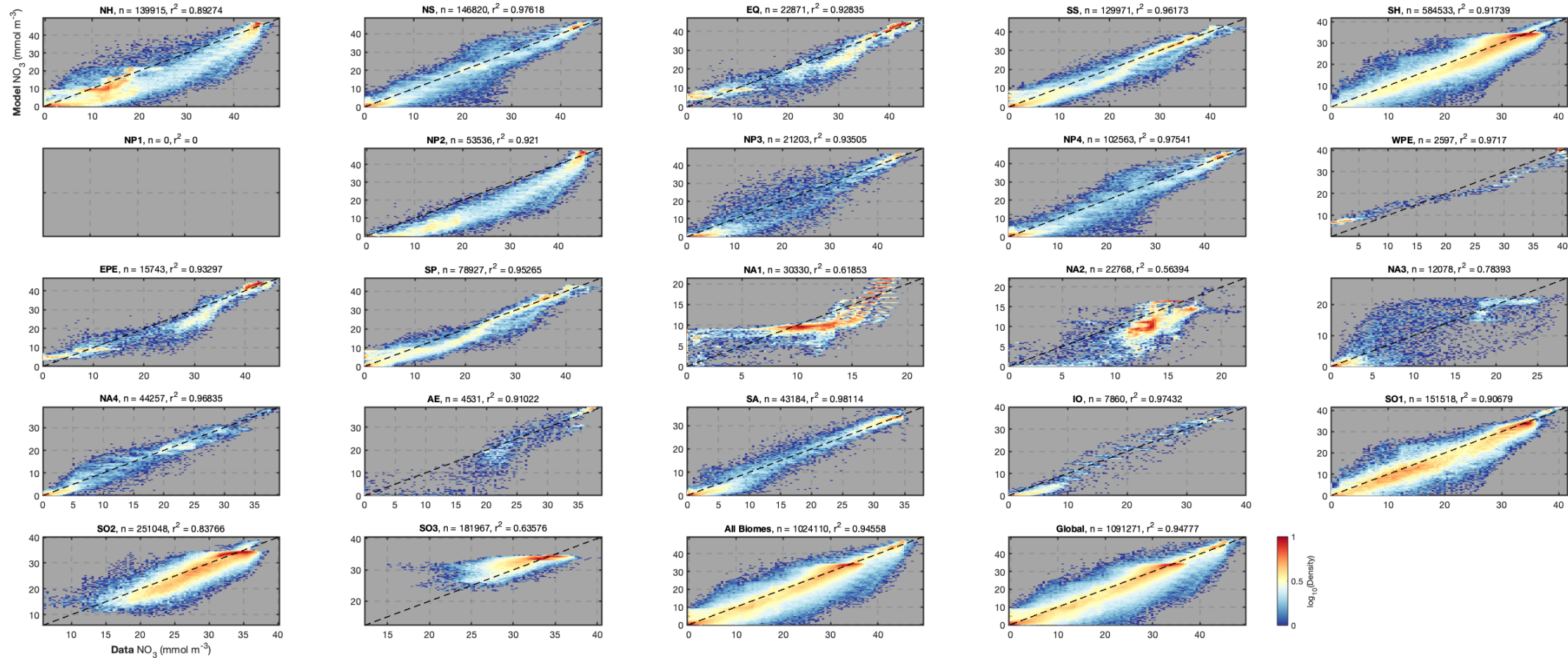


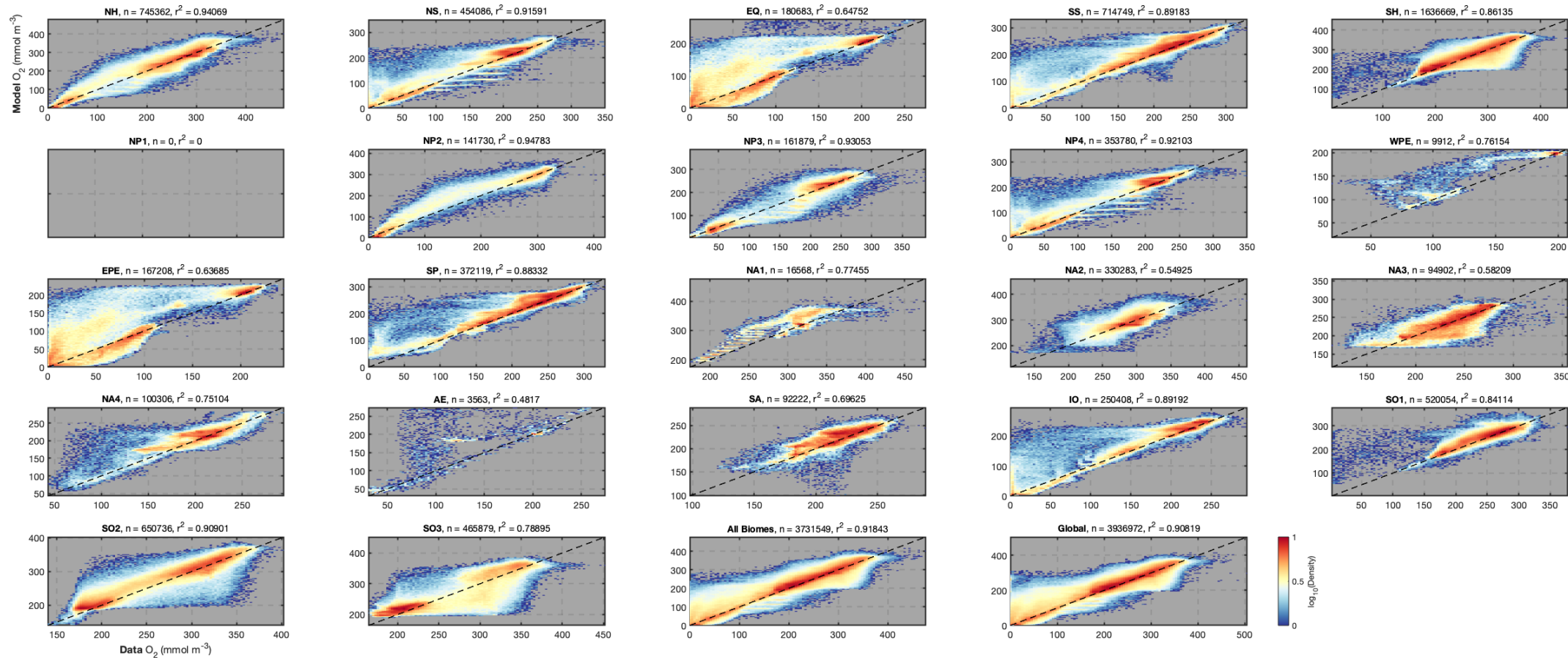




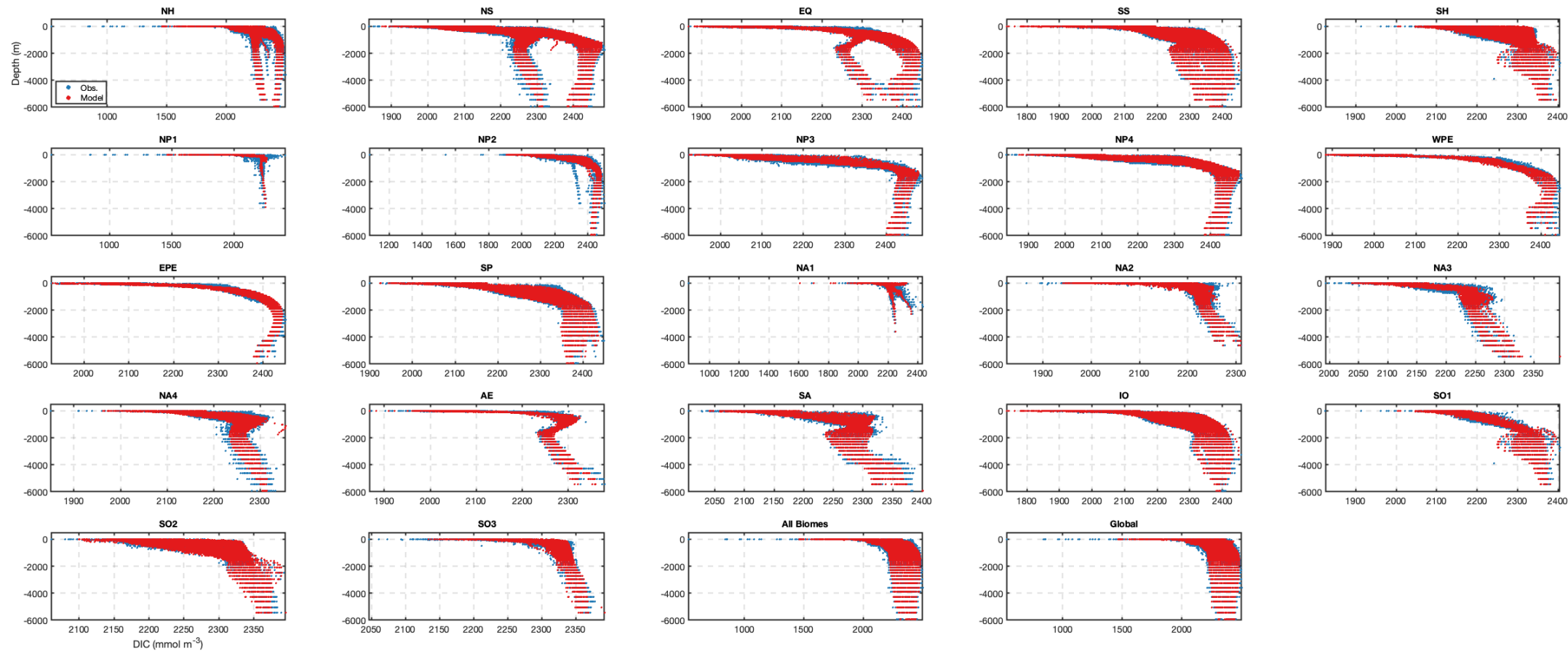
ECCO-Darwin vs. BGC-Argo scatter: all depths

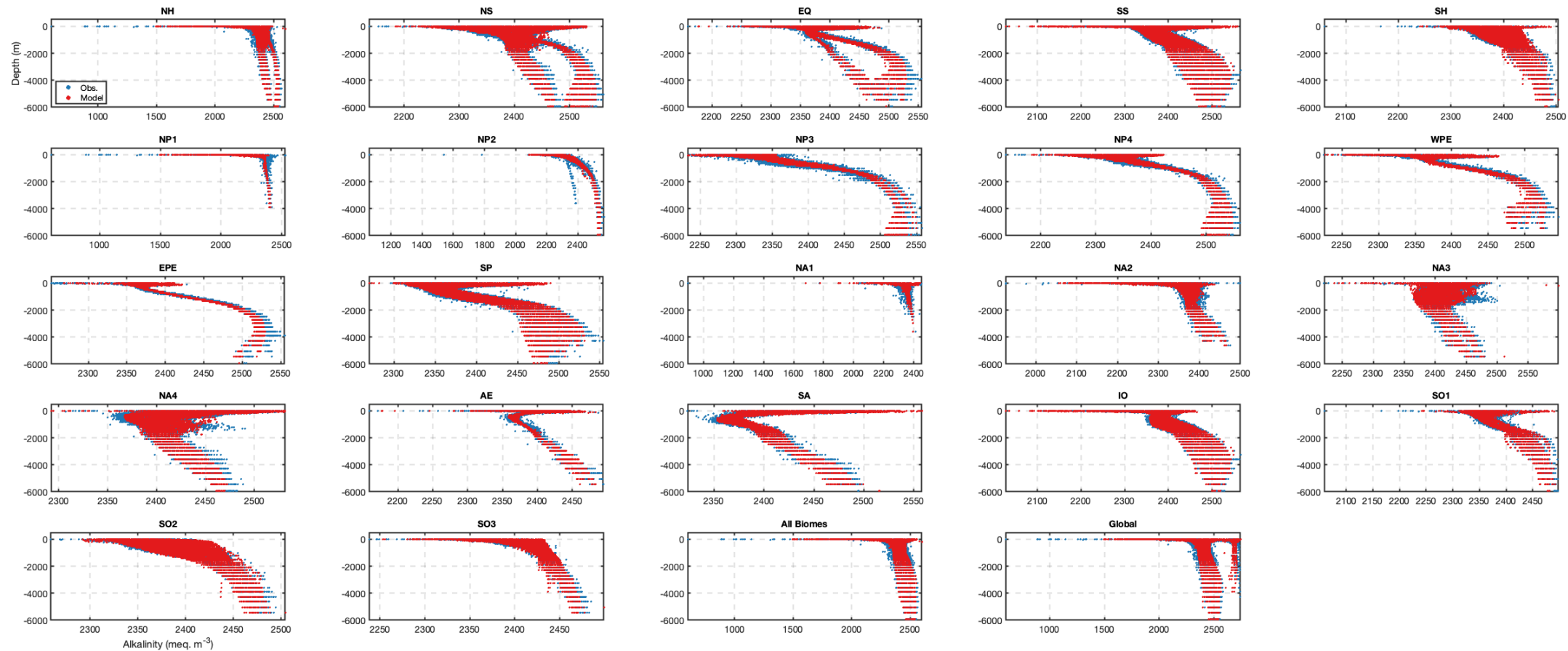


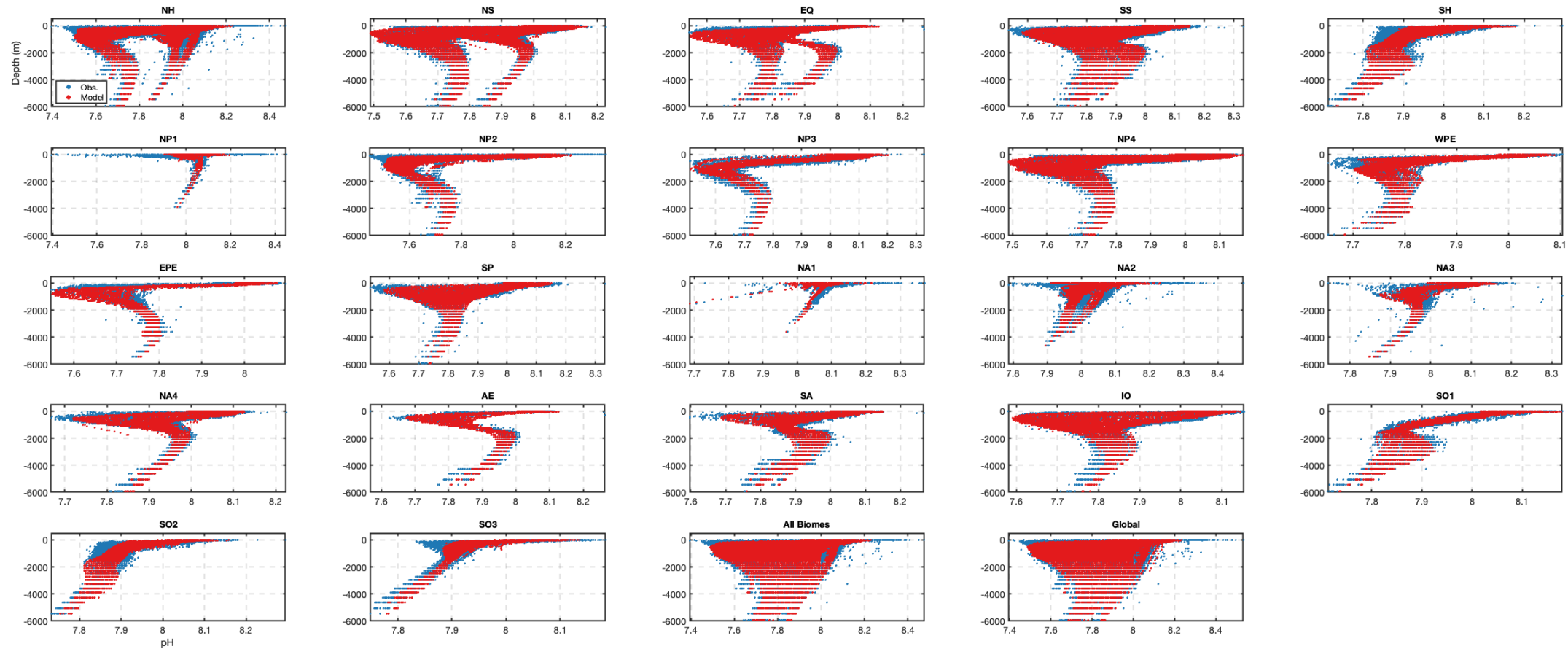


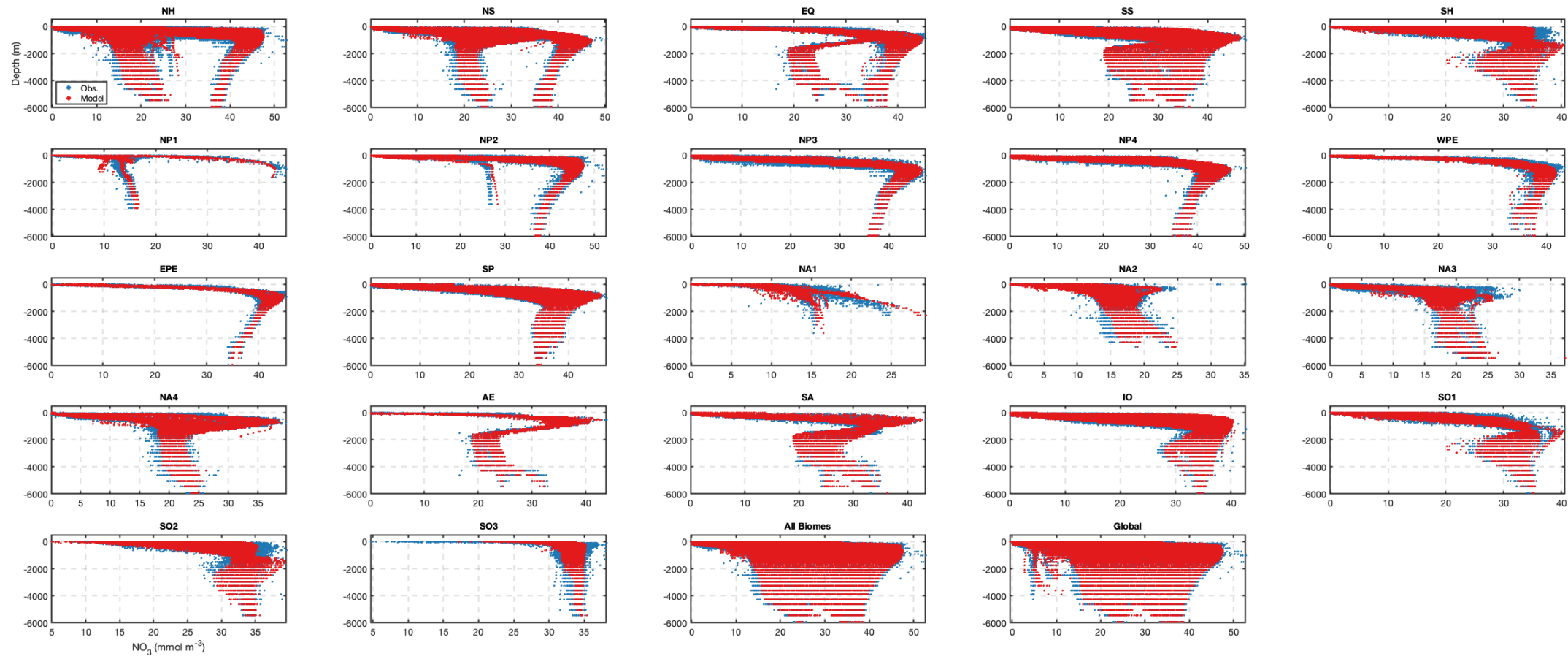


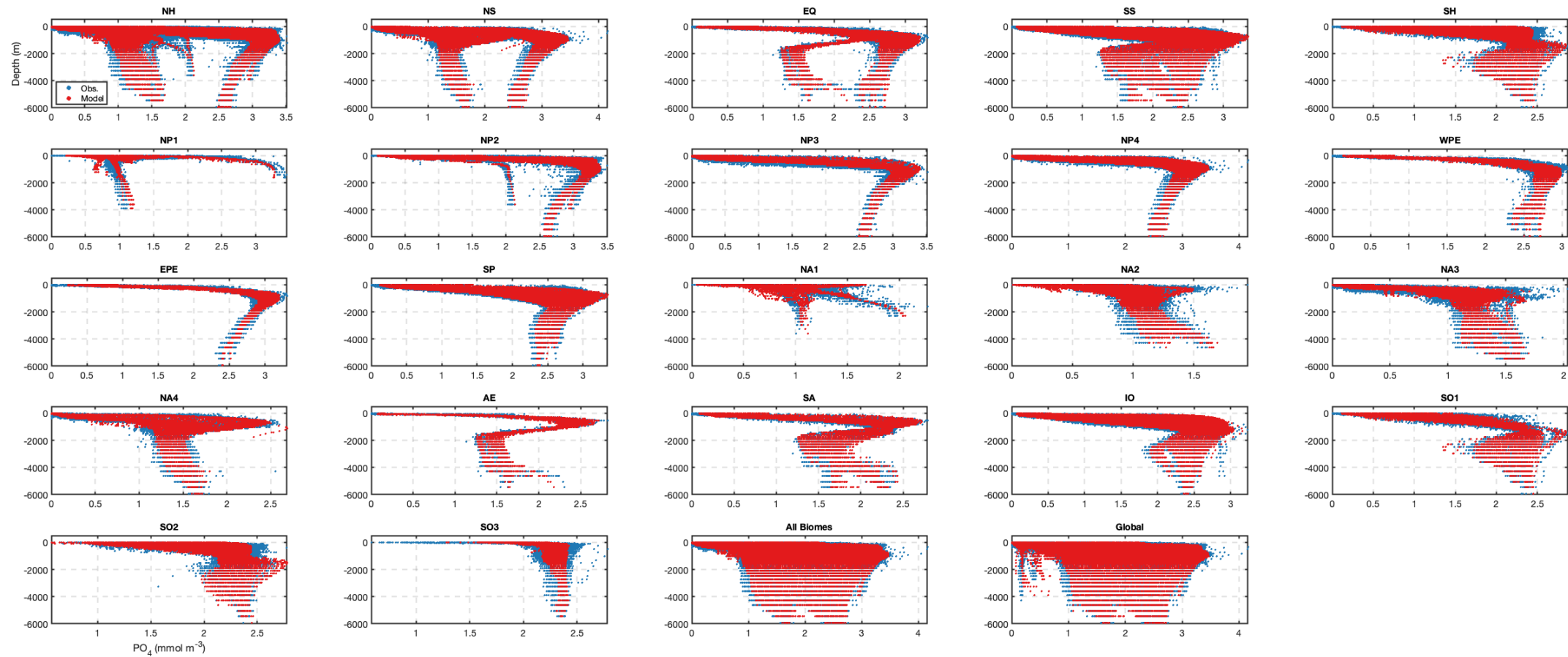
ECCO-Darwin vs. GLODAP vertical profiles: all depths

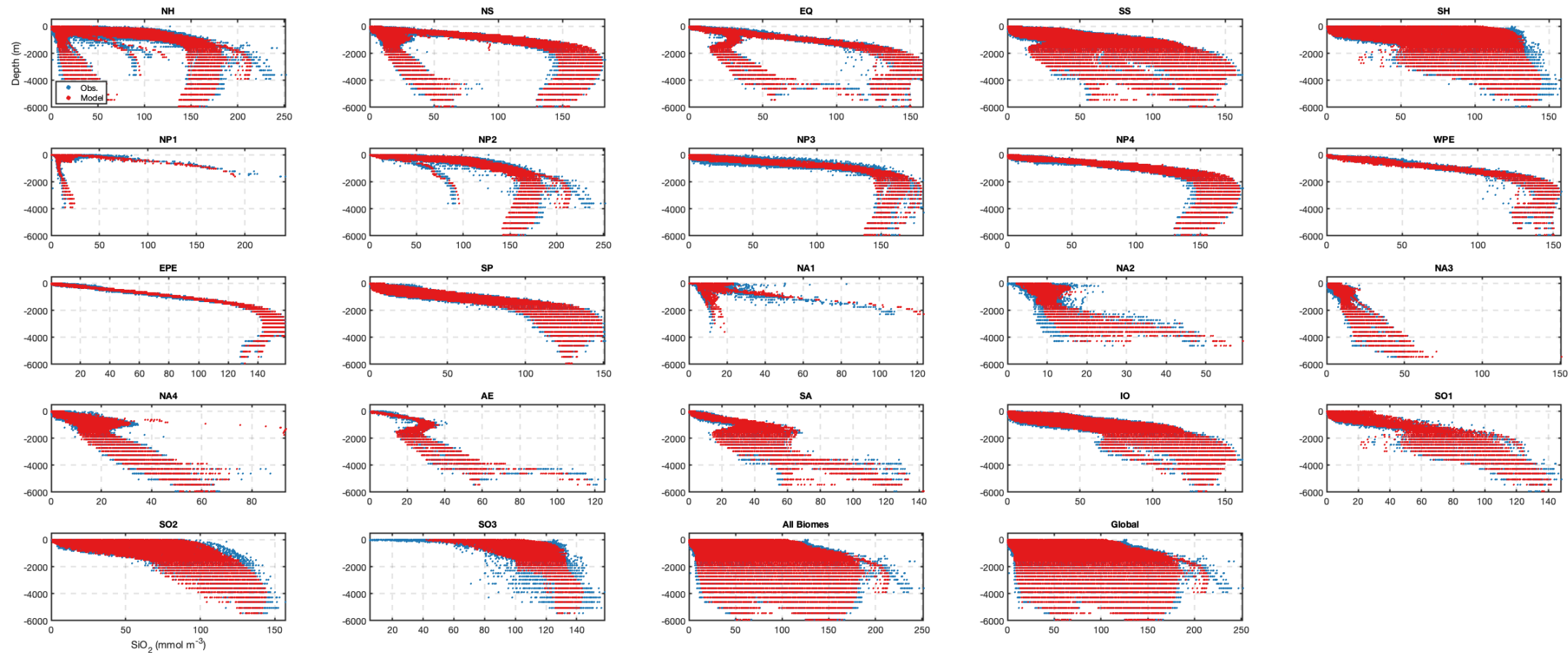


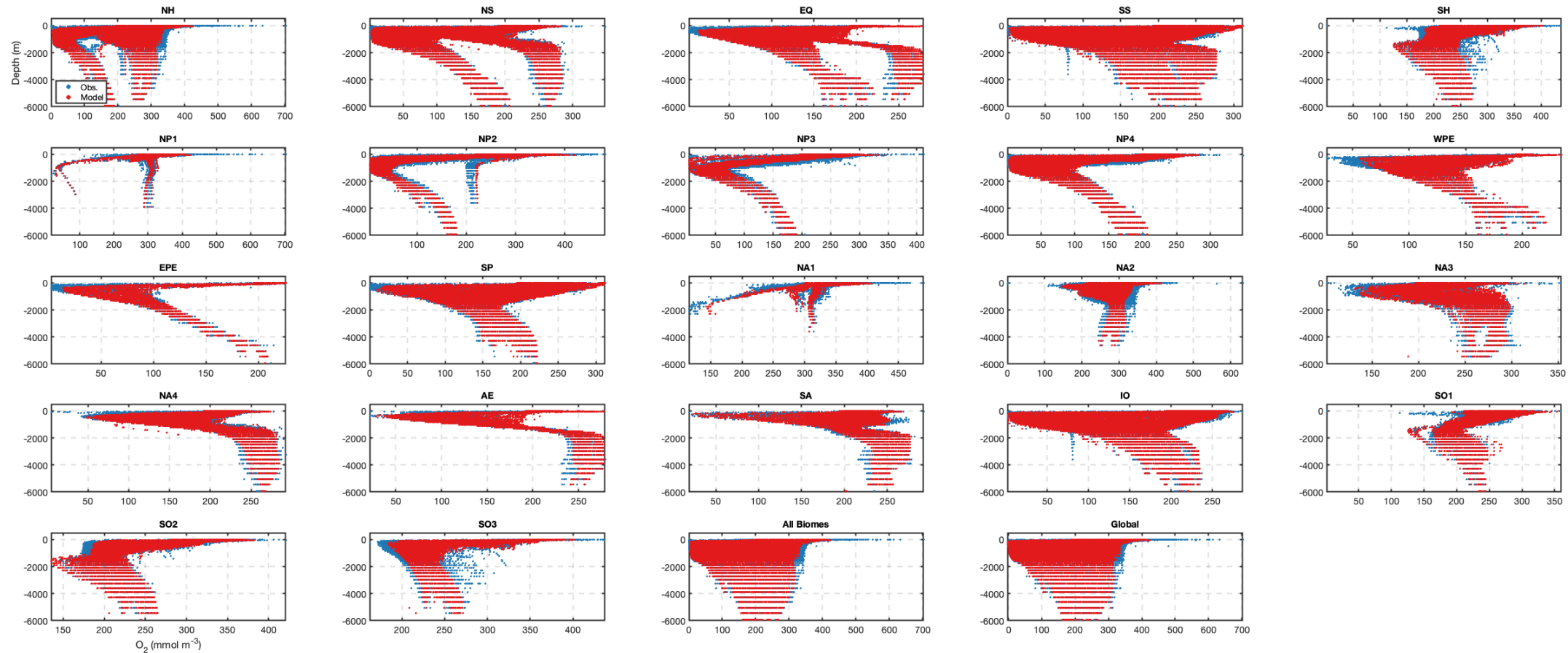




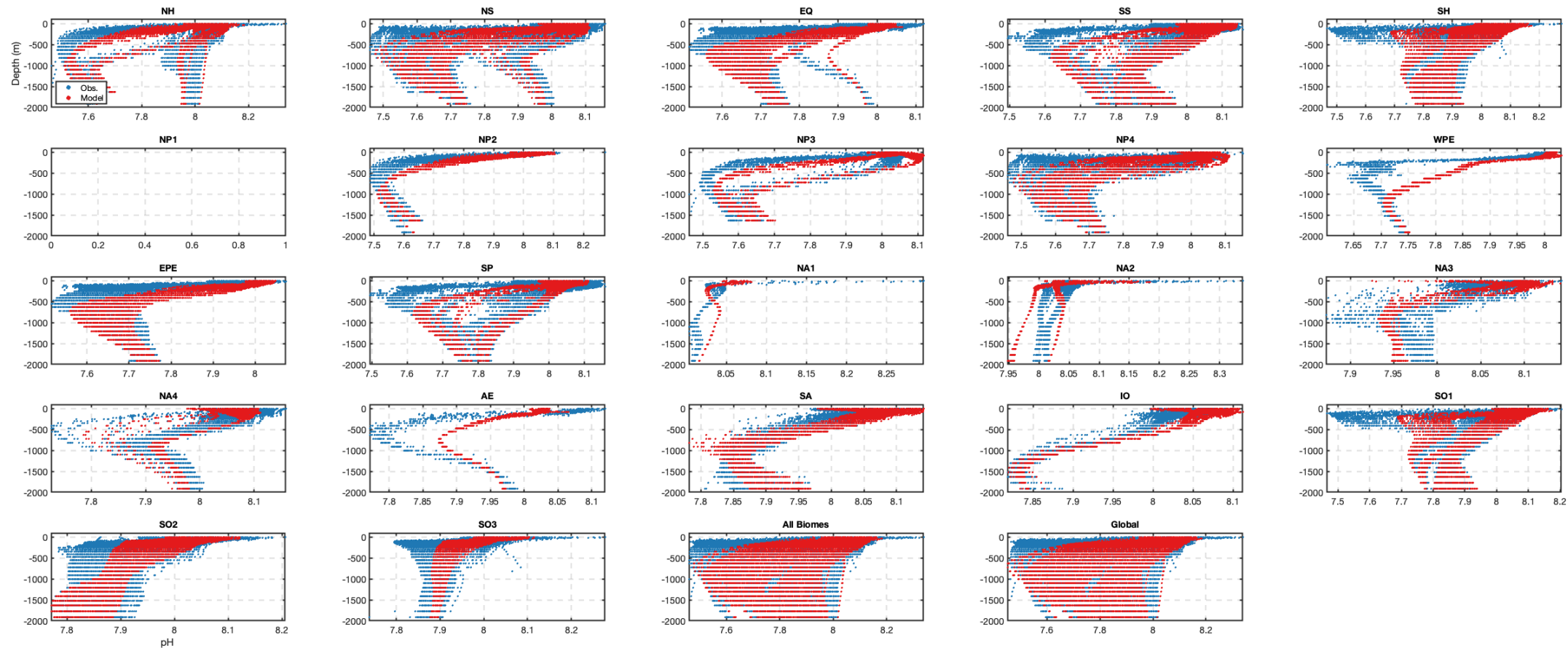


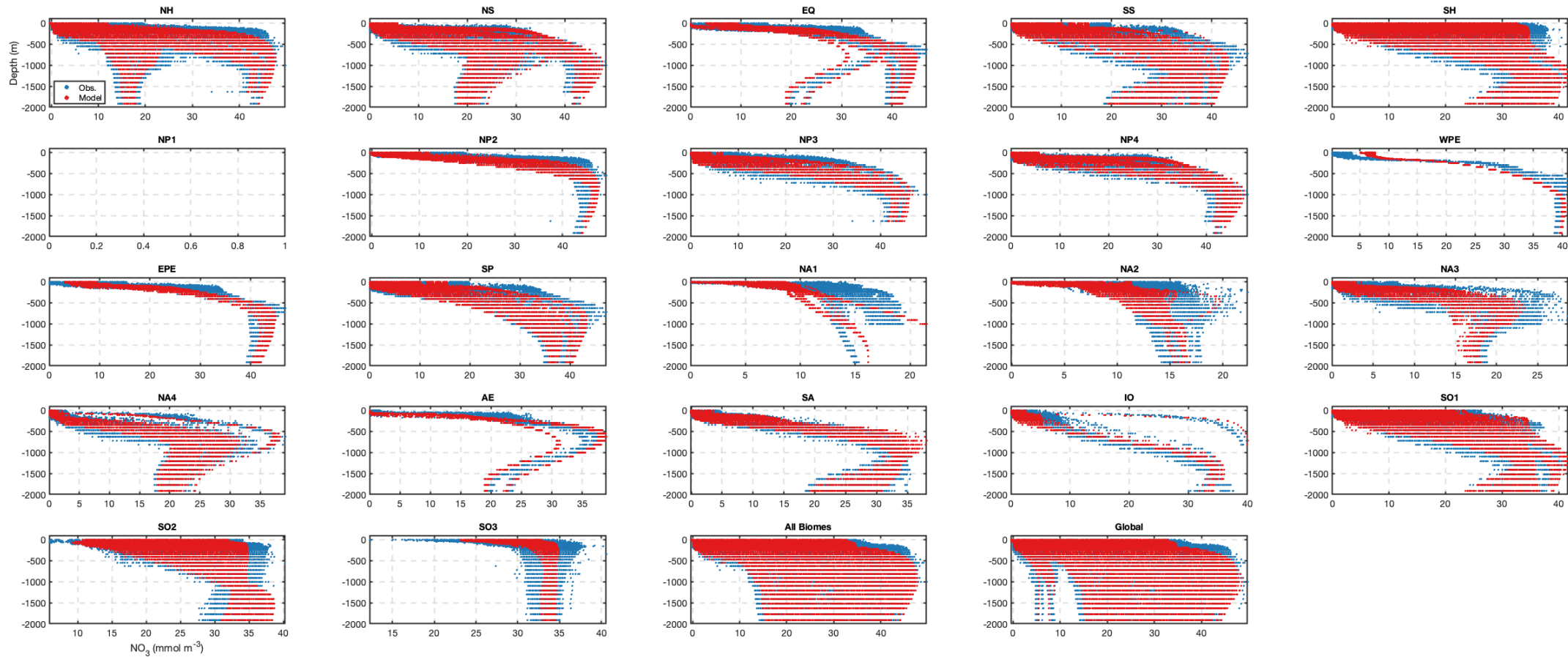


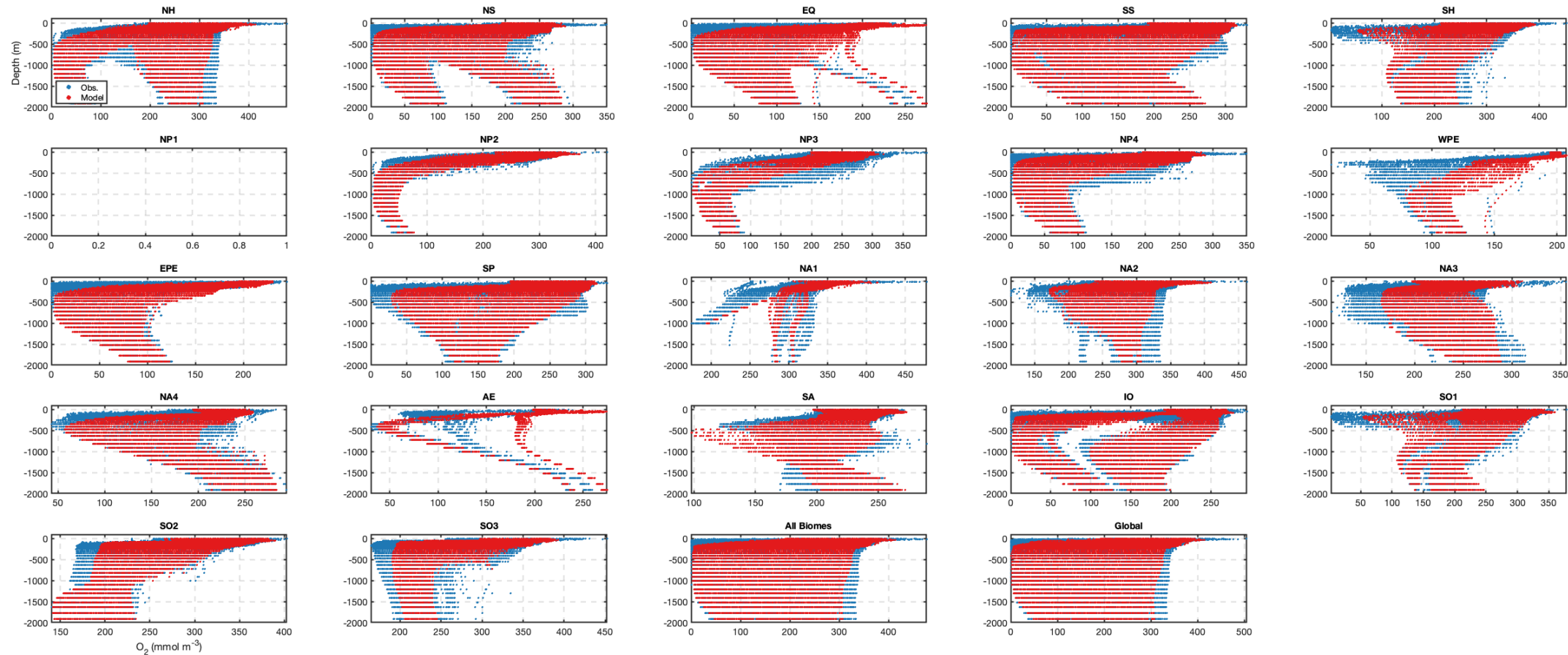




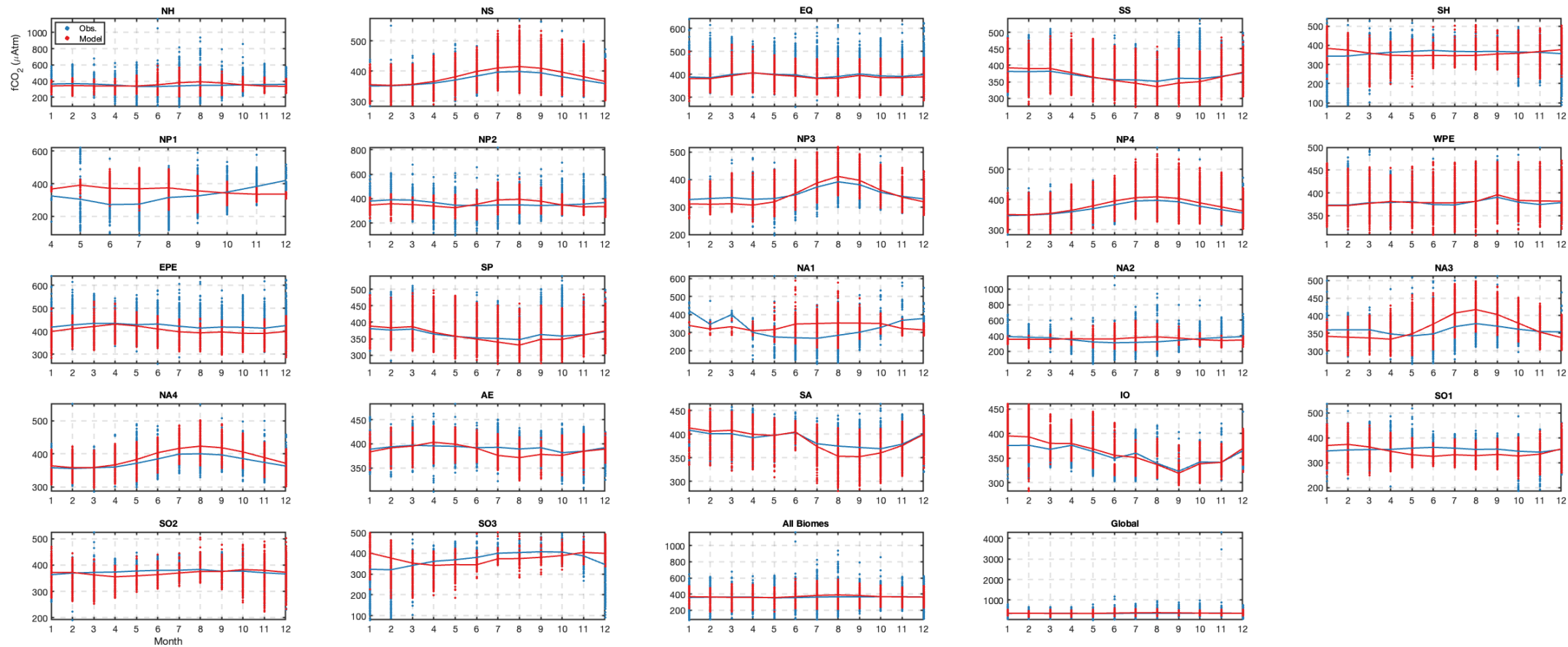
ECCO-Darwin vs. BGC-Argo vertical profiles: all depths



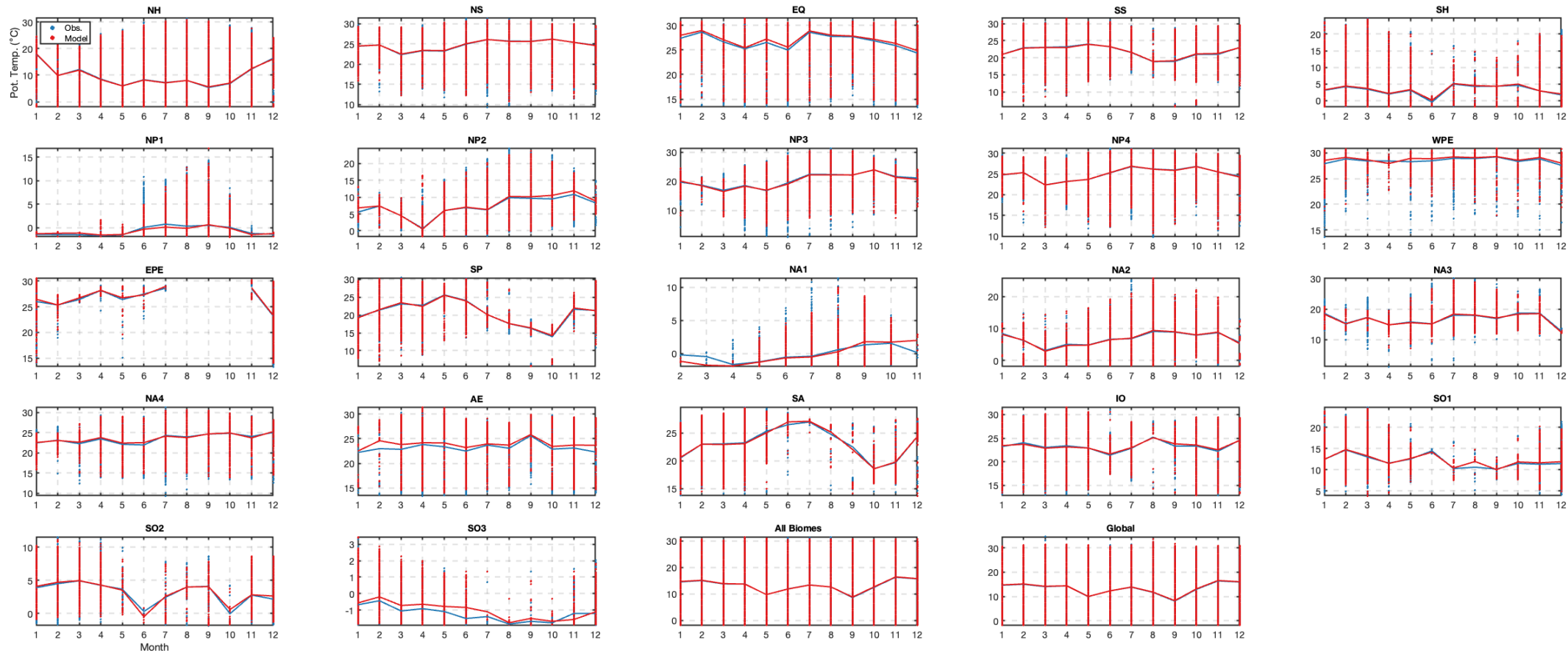


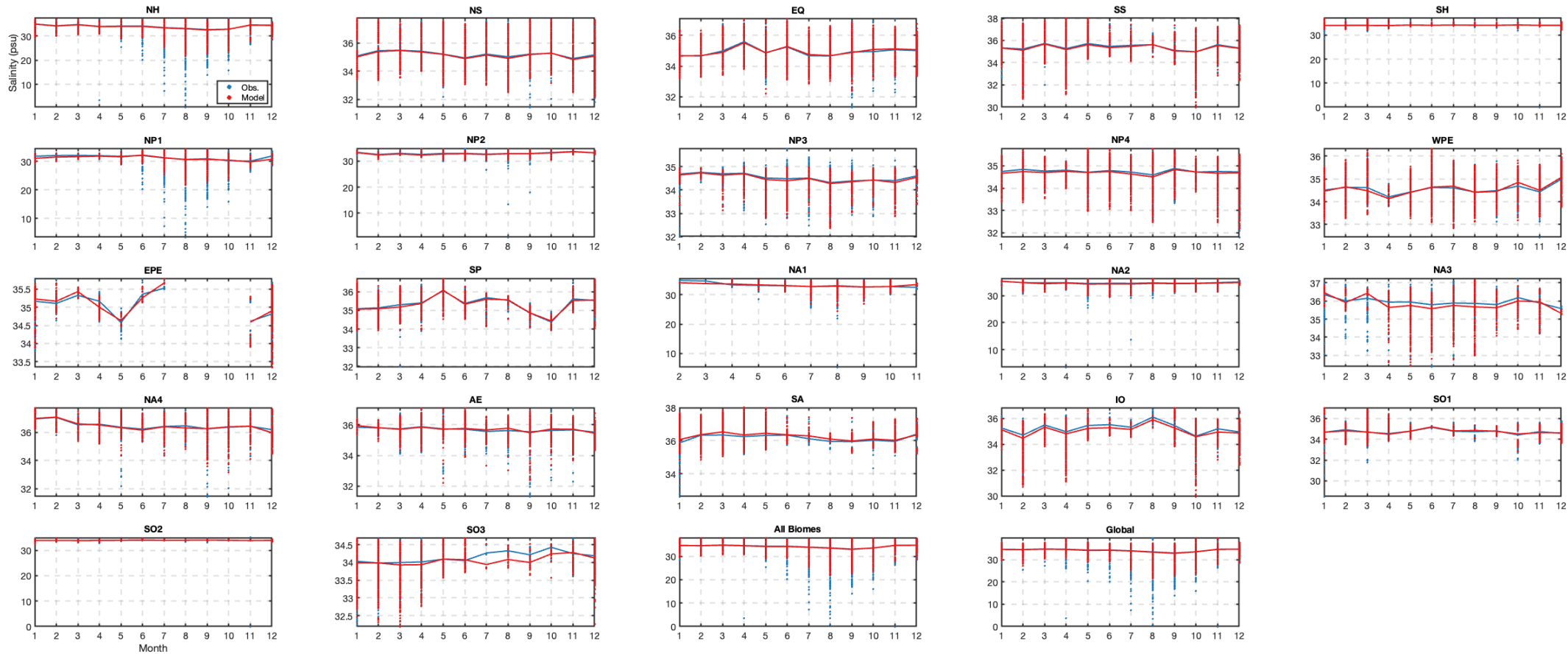


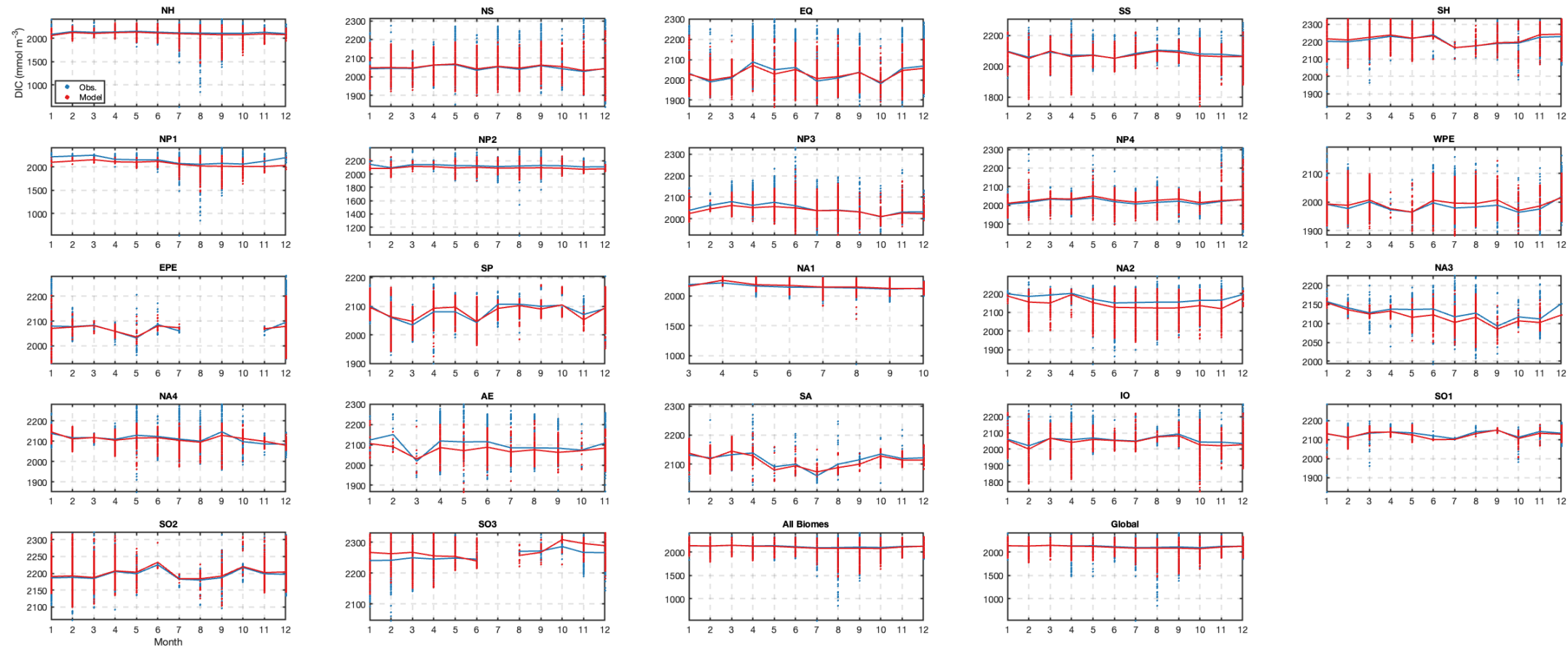
ECCO-Darwin vs. SOCAT seasonal climatology: surface ocean

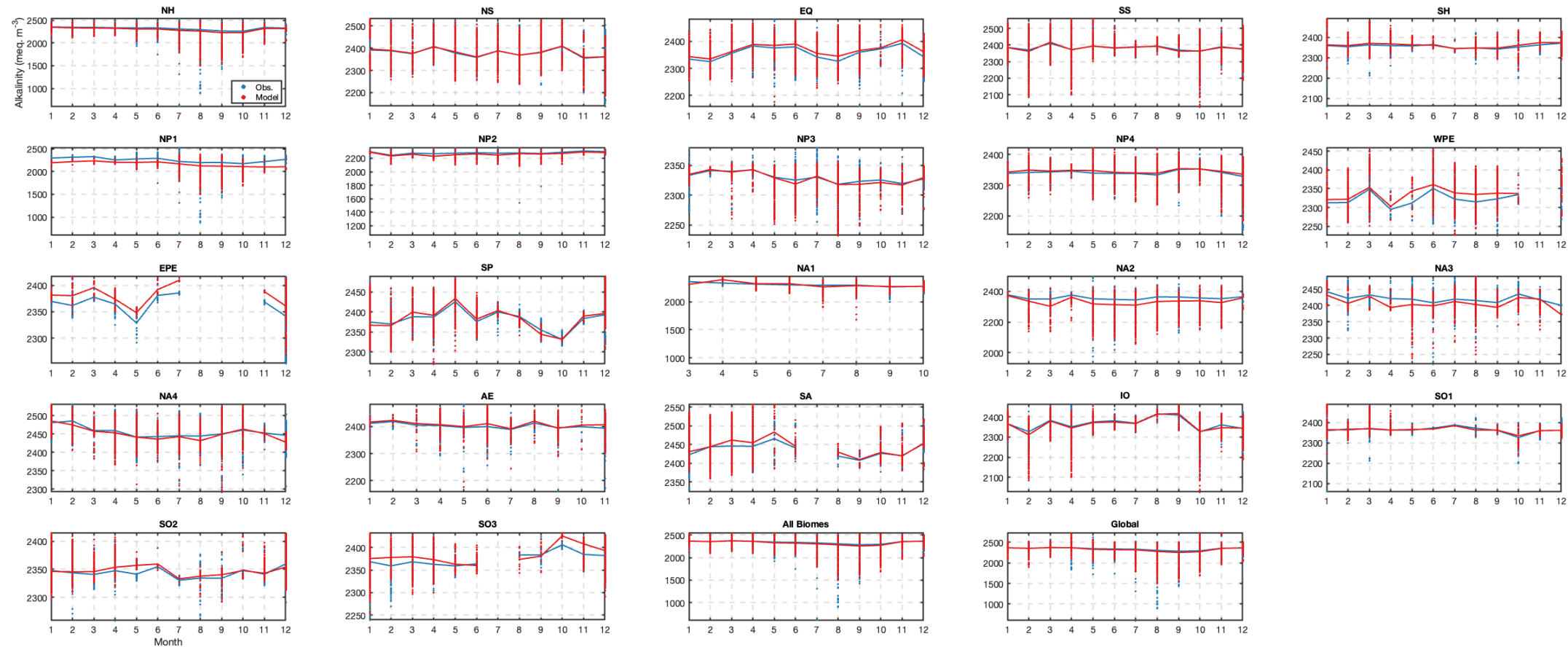


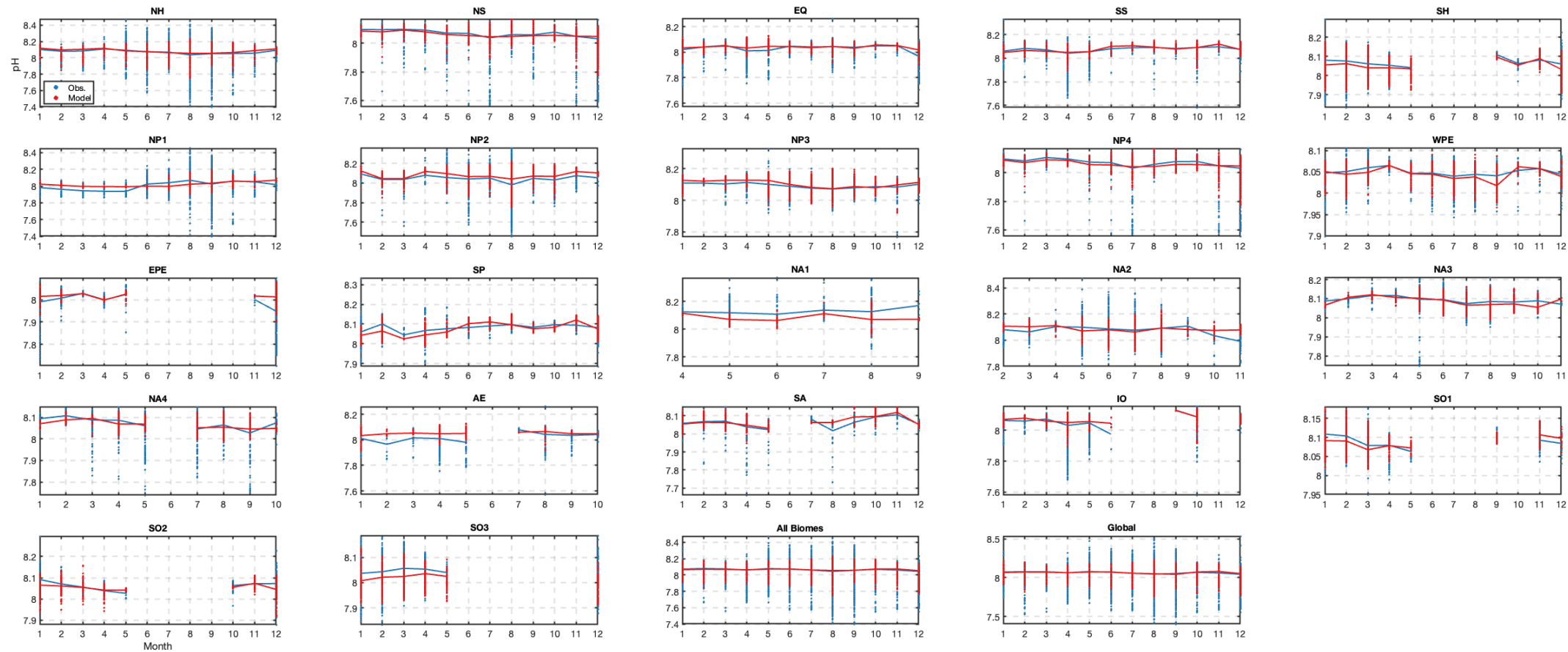
ECCO-Darwin vs. GLODAP seasonal climatology: 0 to 100-m depth

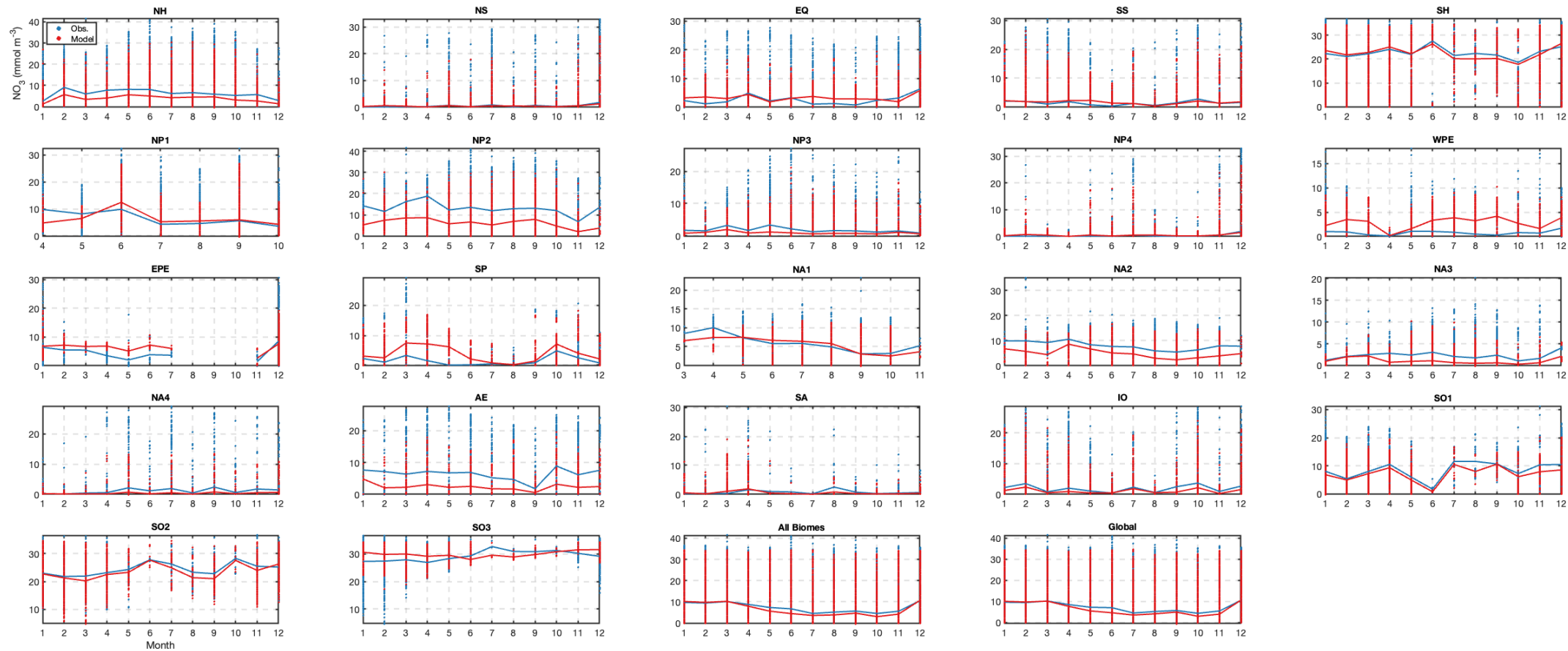


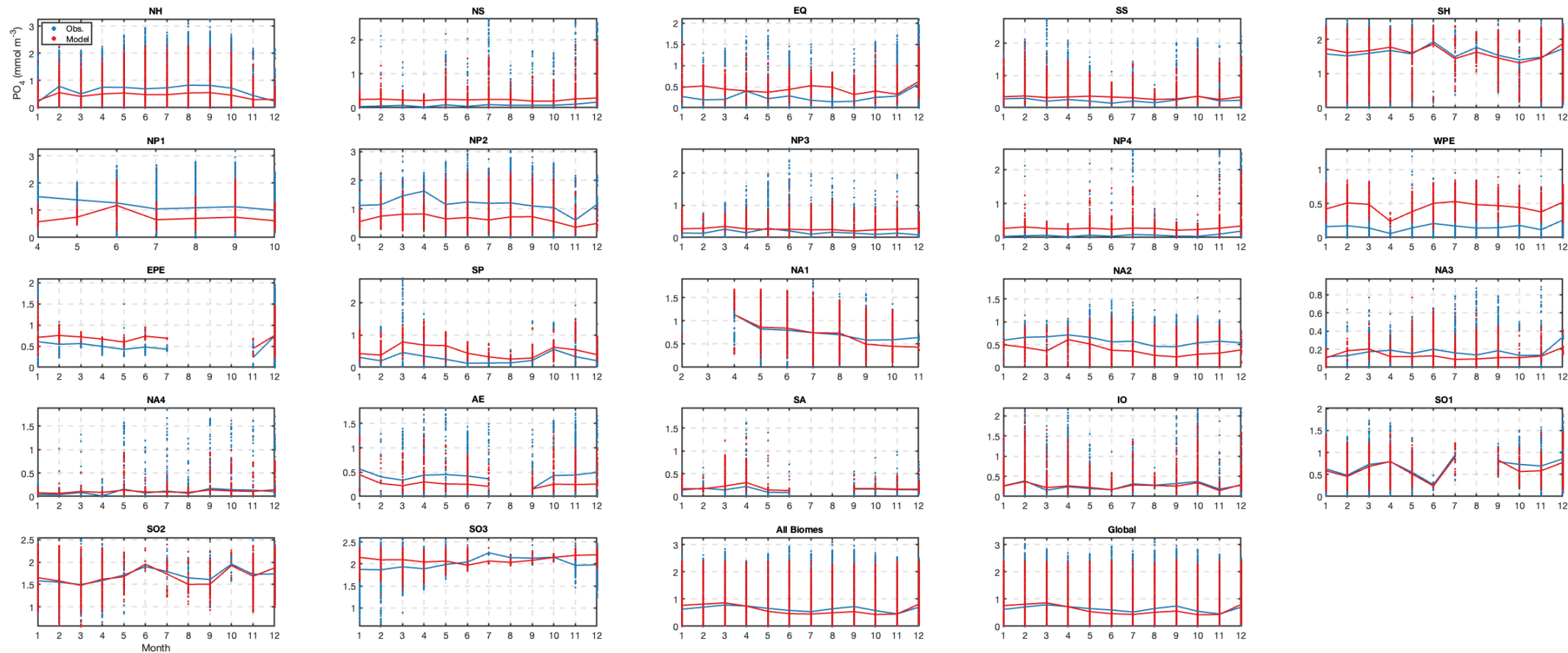


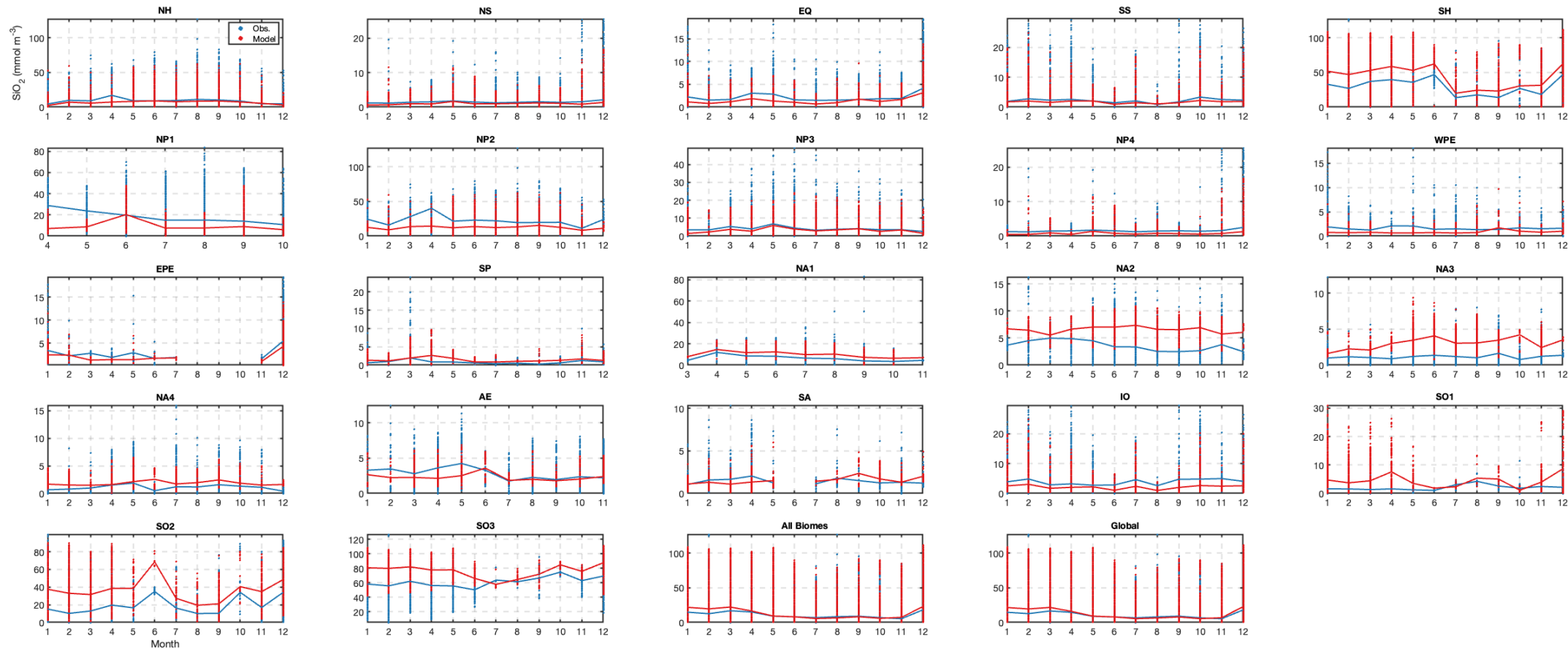


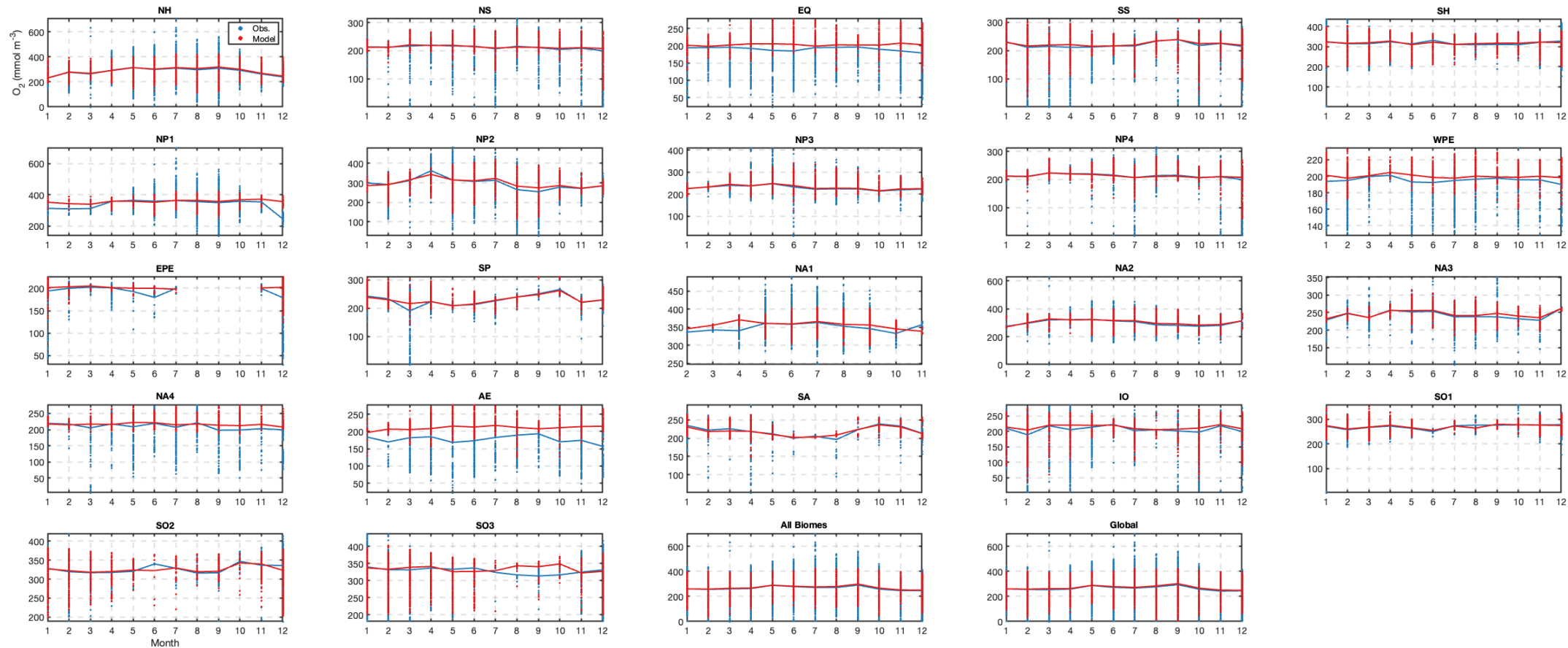




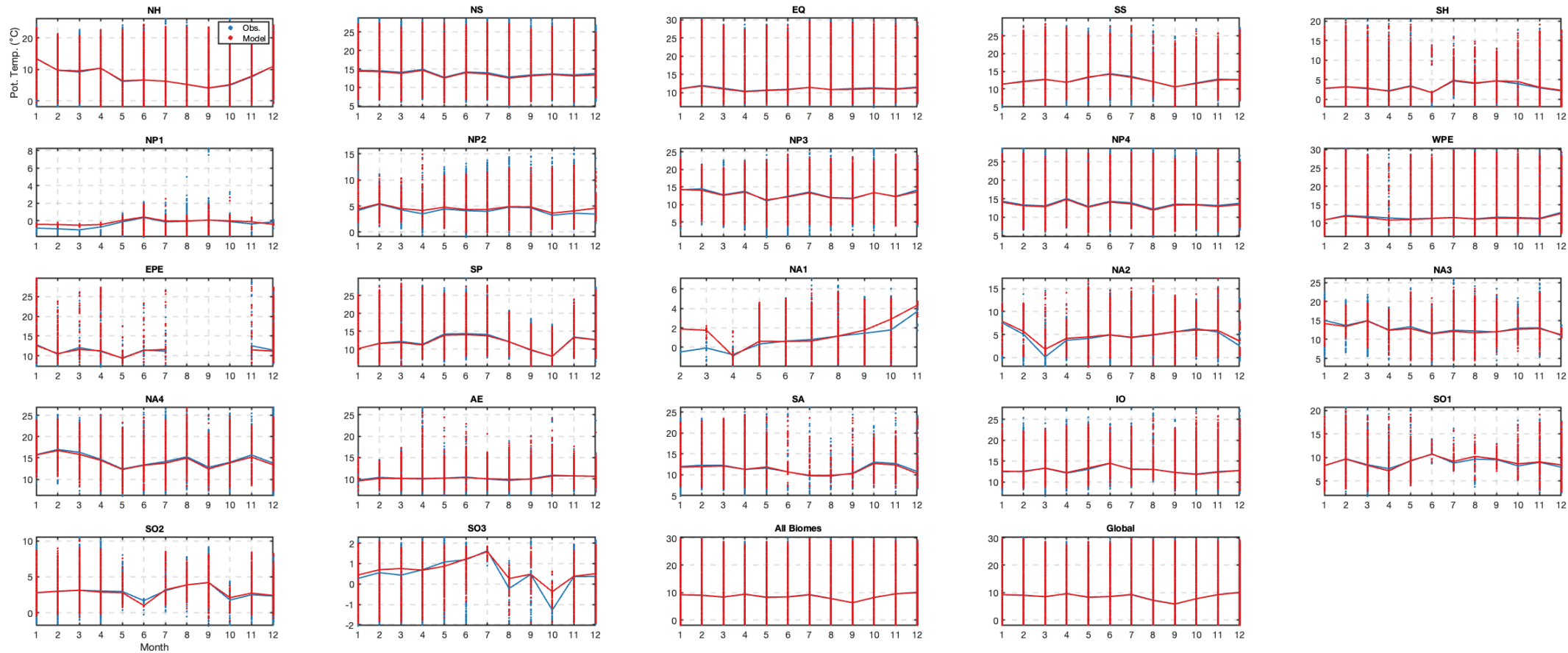


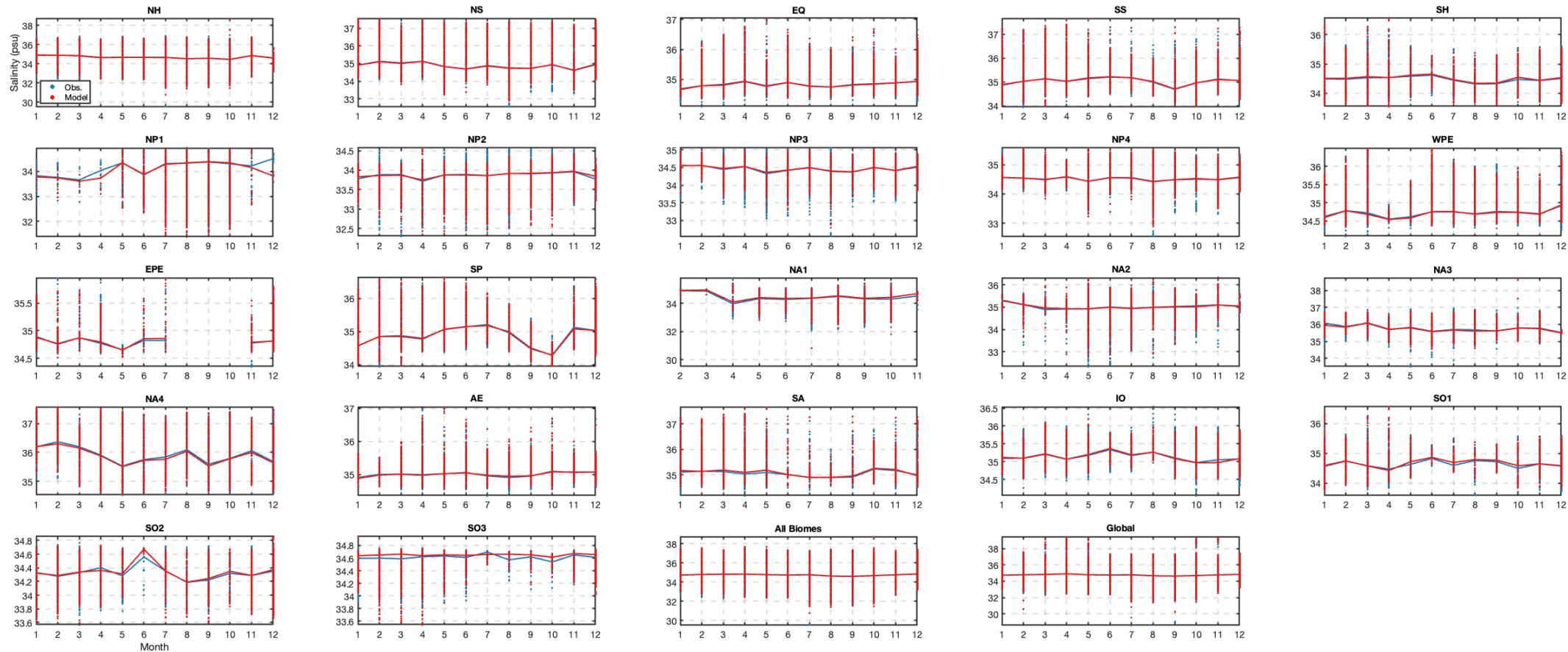


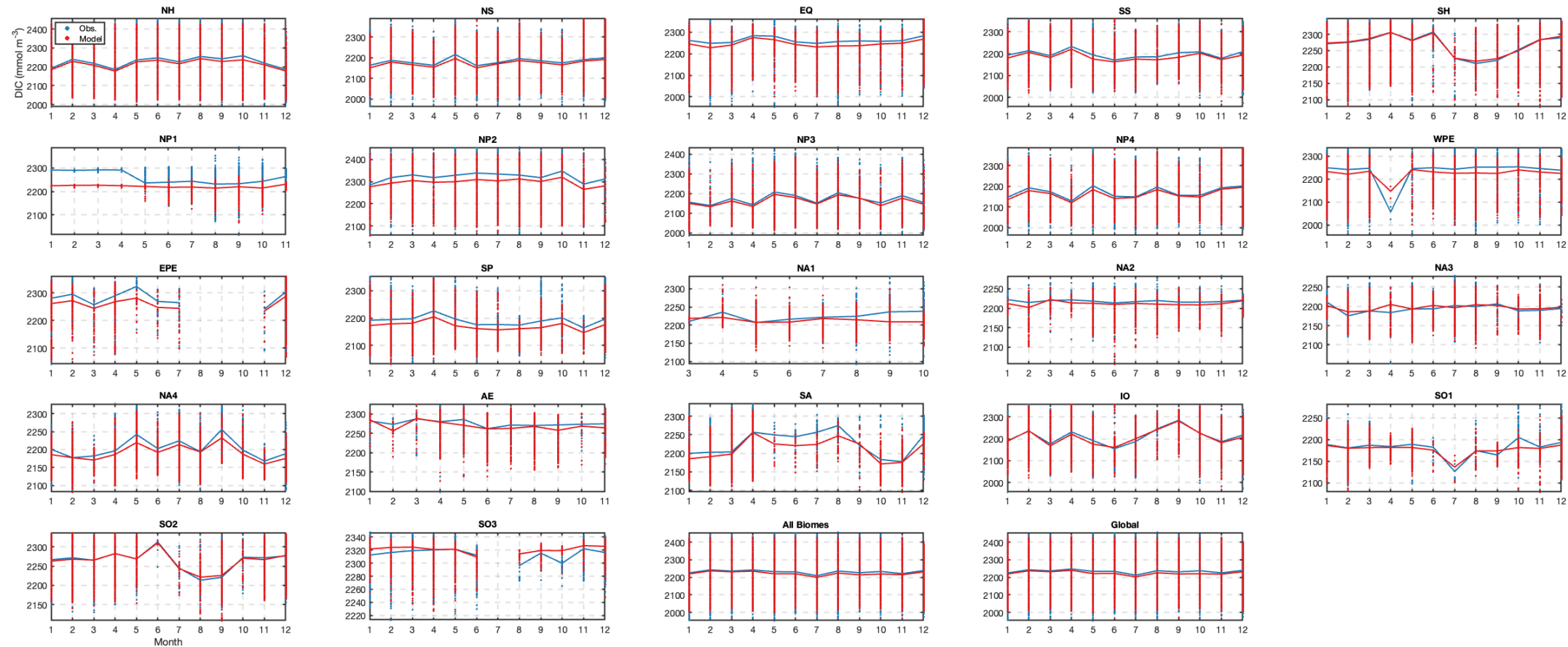


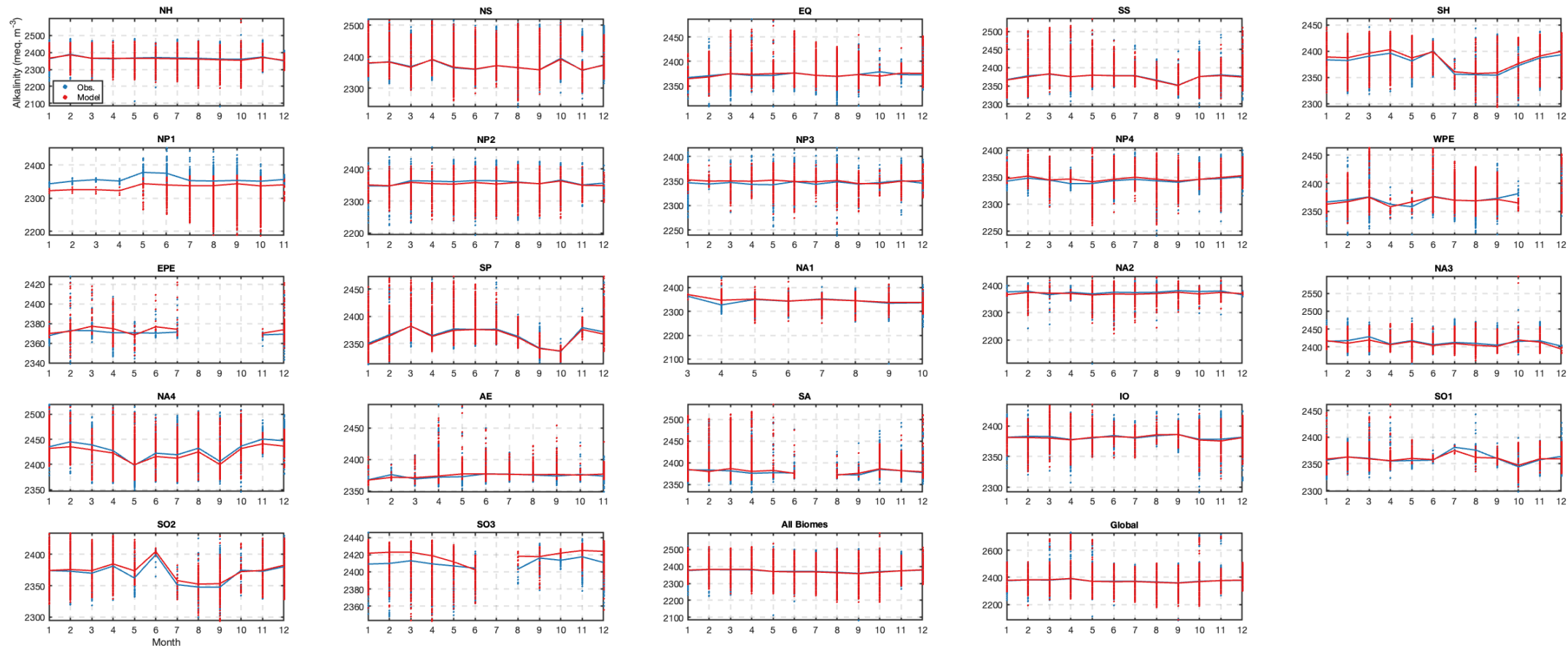


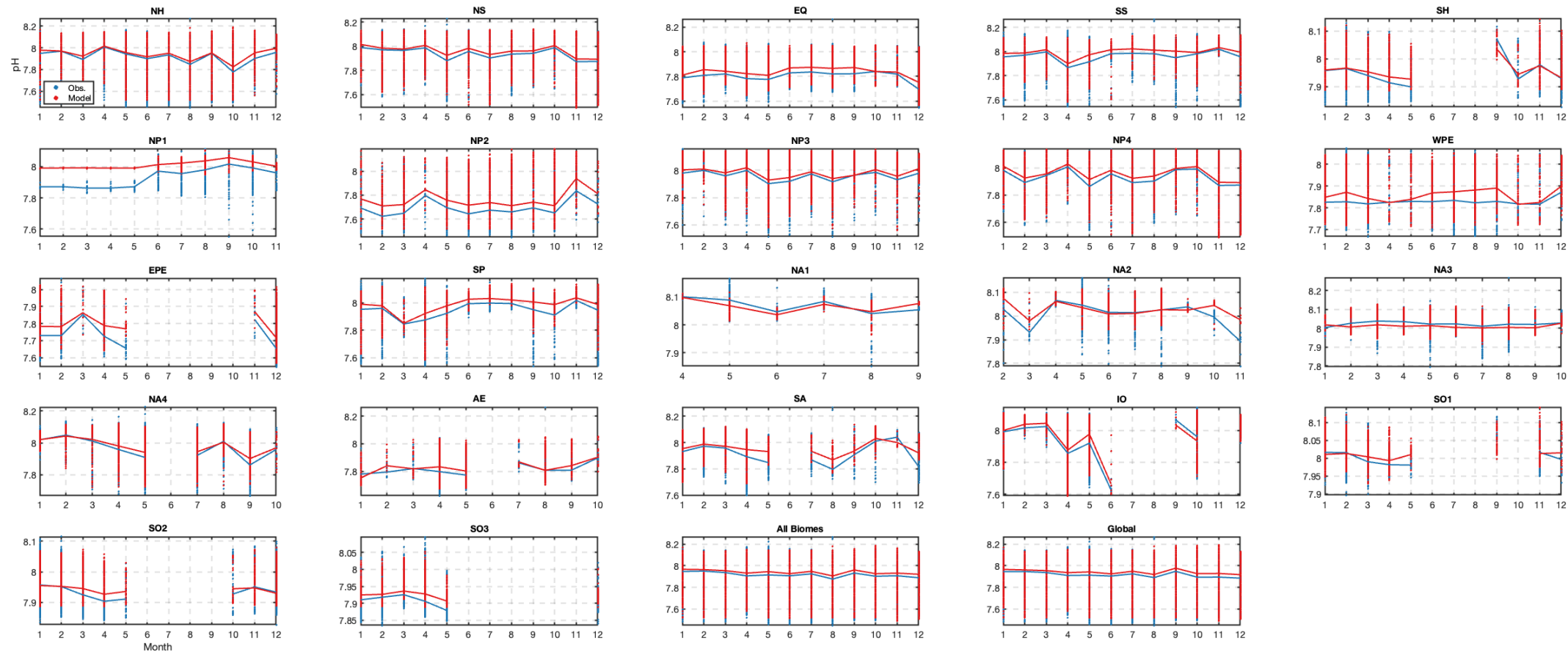
ECCO-Darwin vs. GLODAP seasonal climatology: 100 to 500-m depth

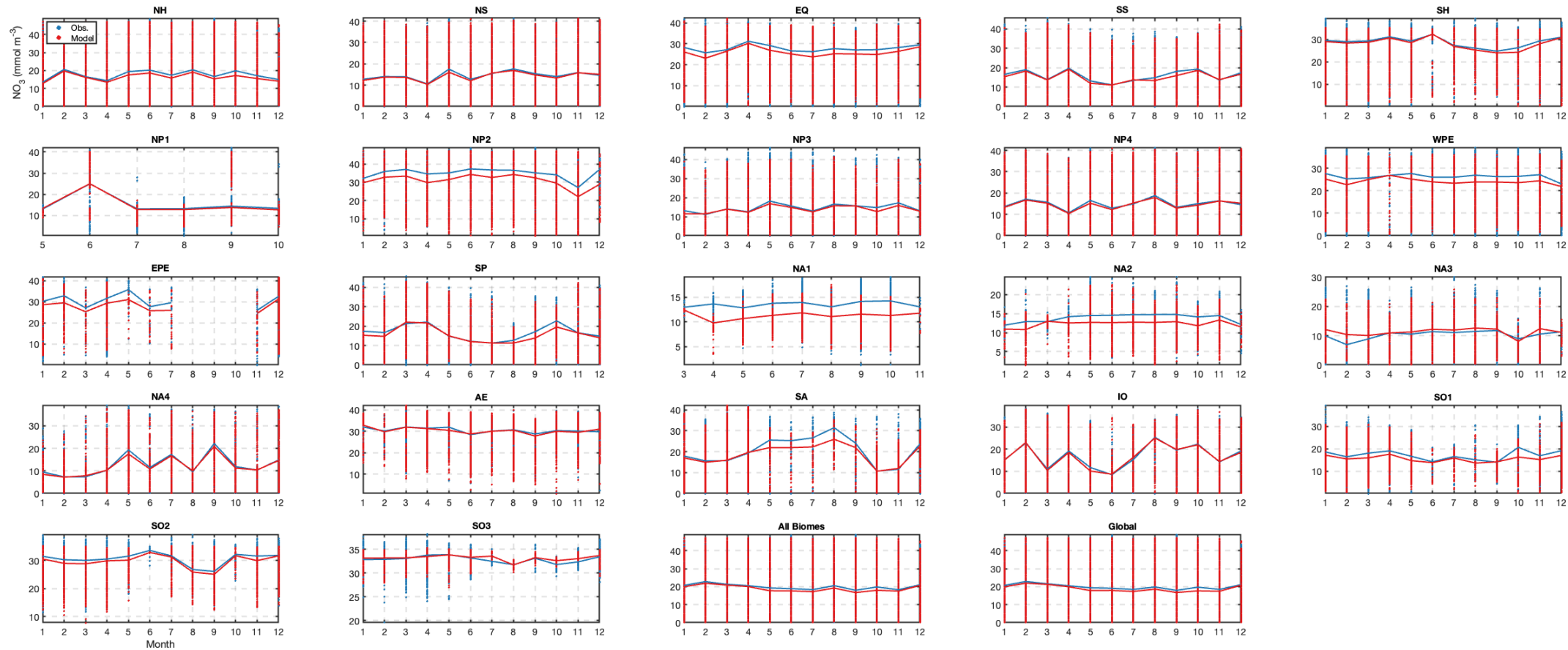


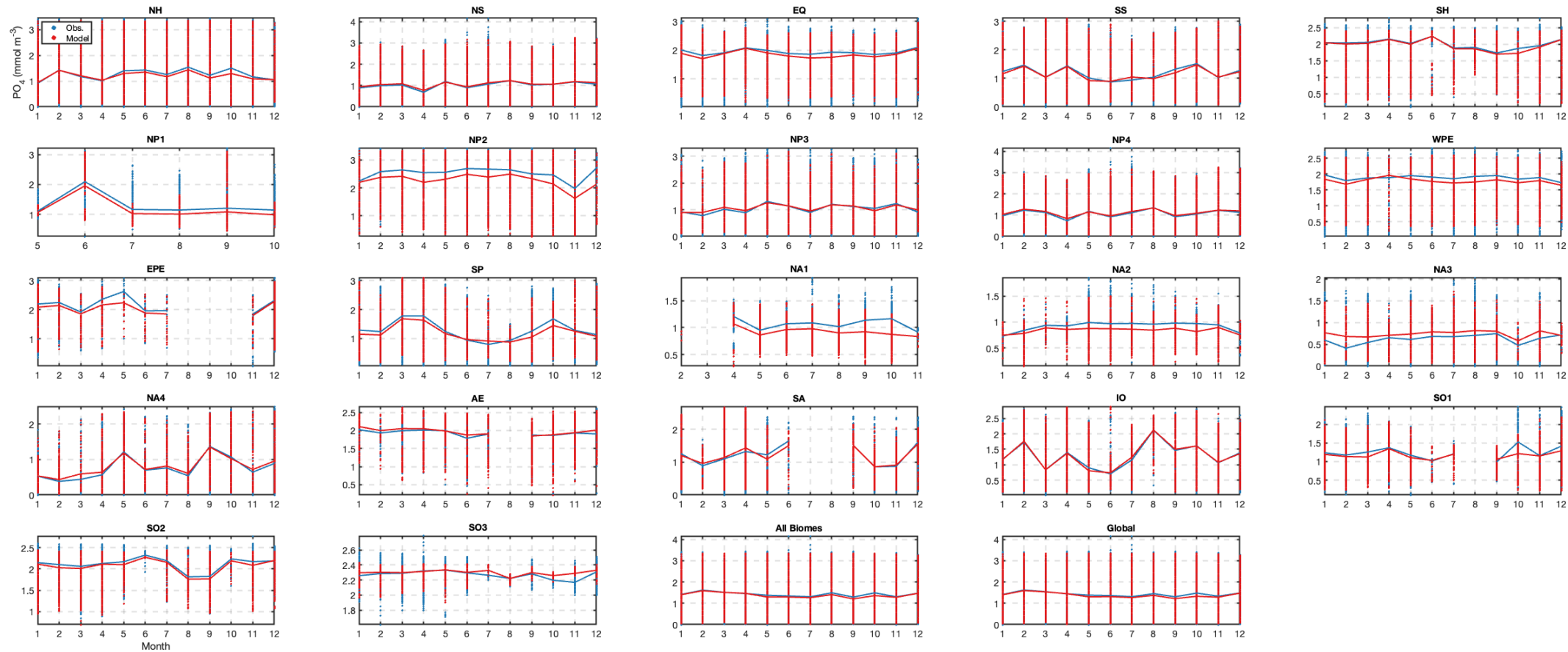


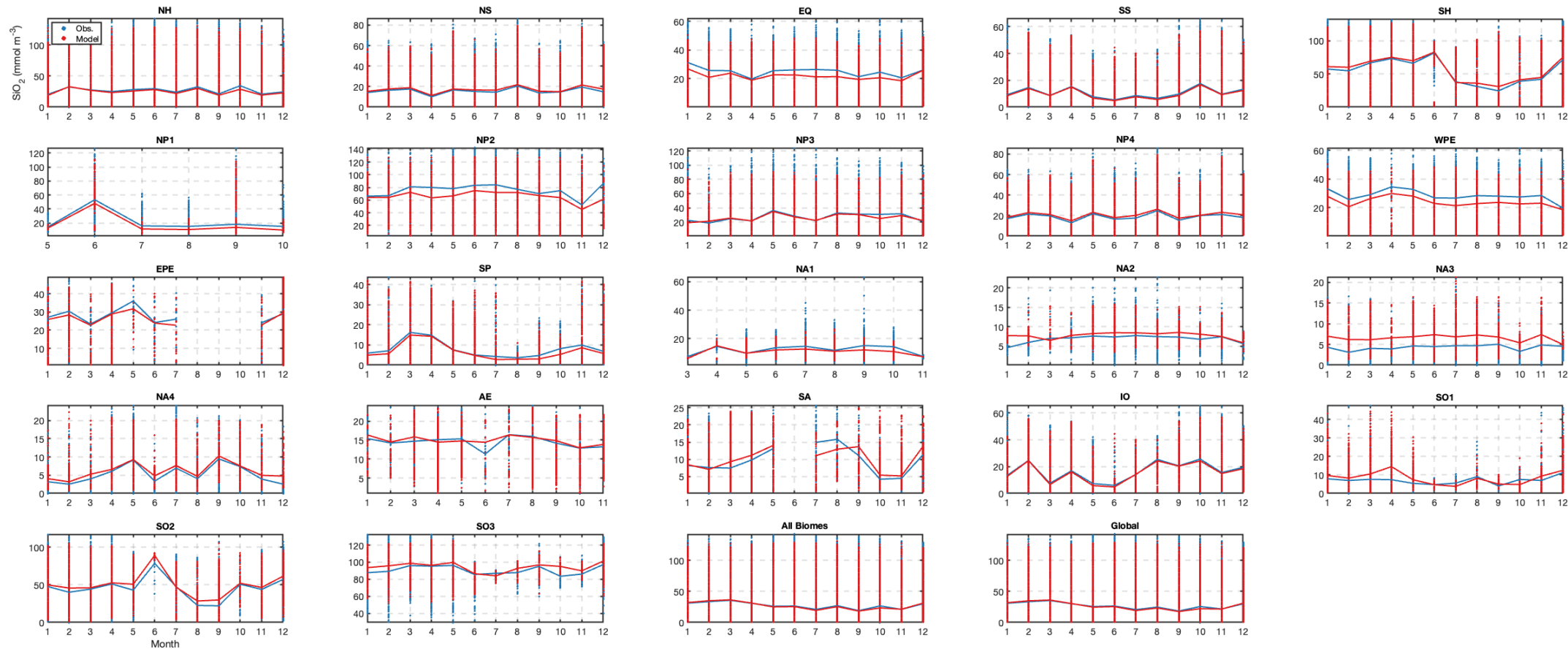


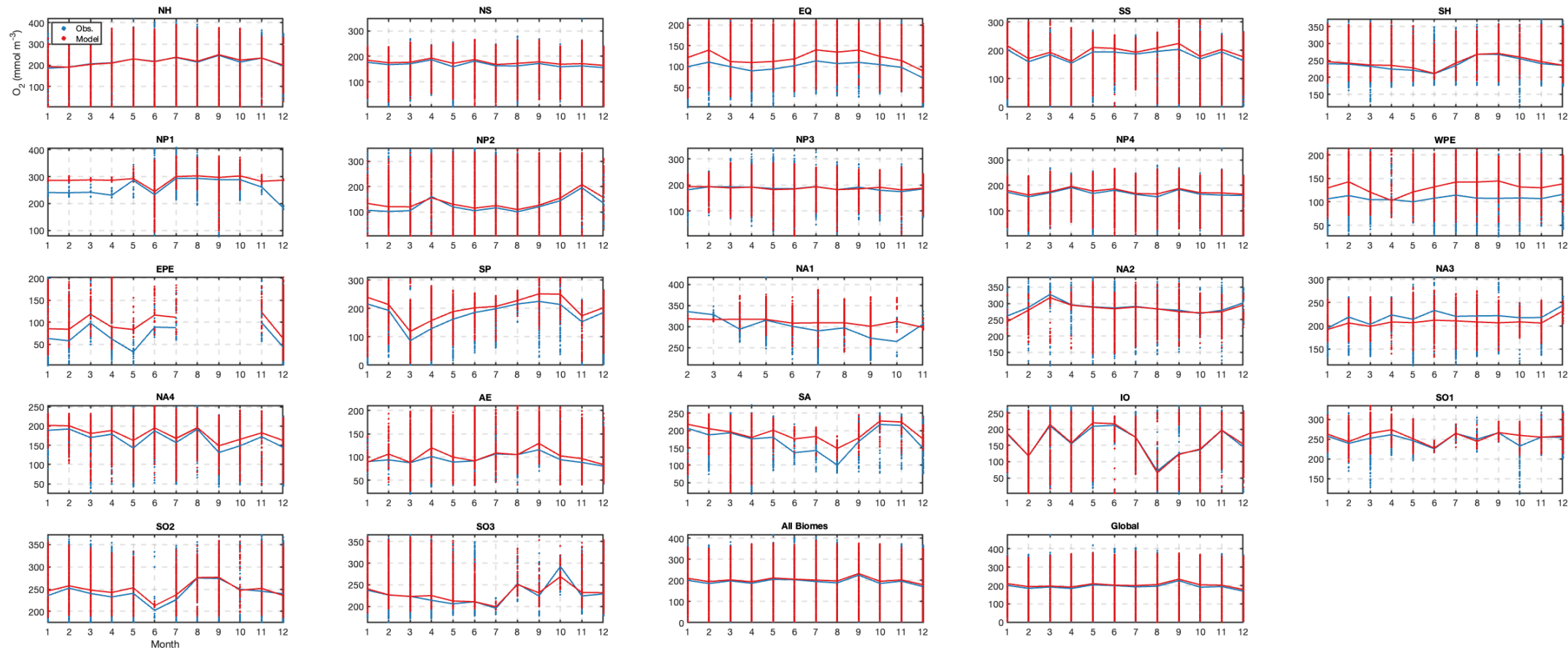




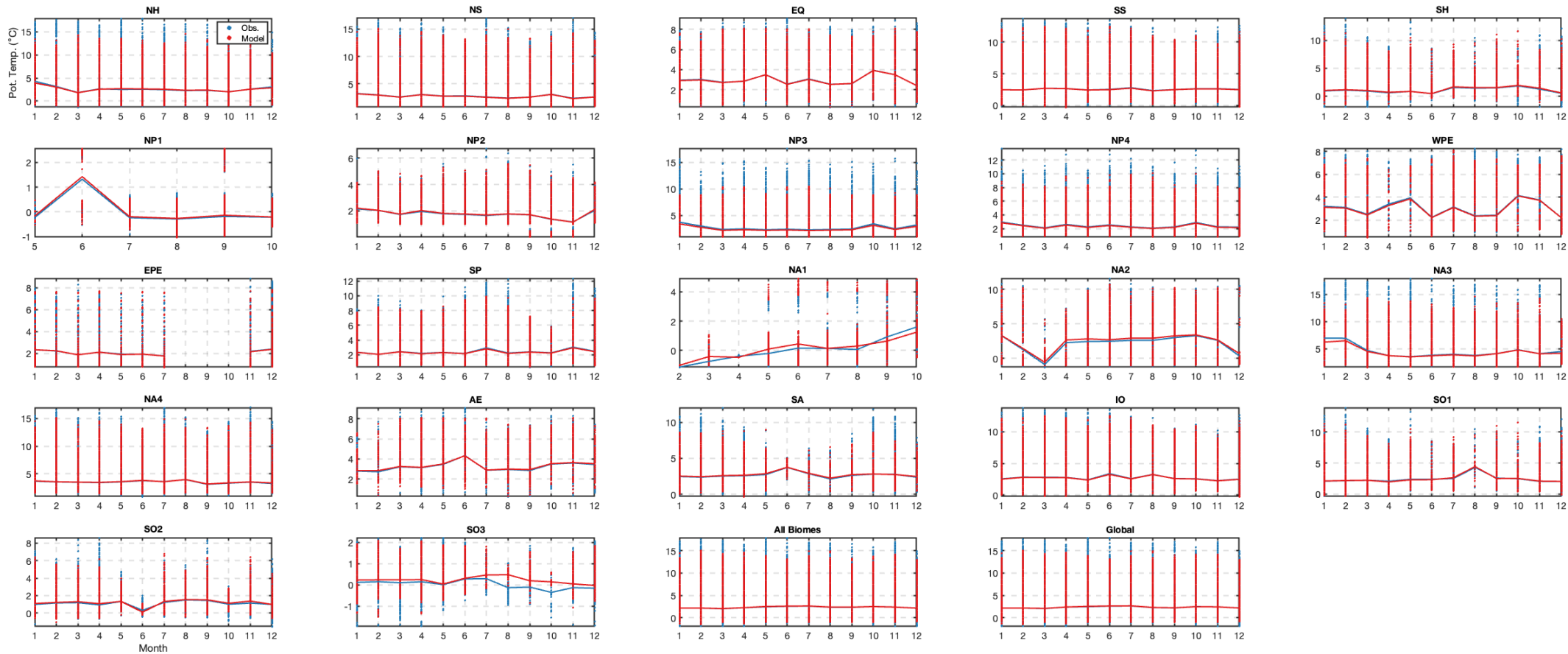


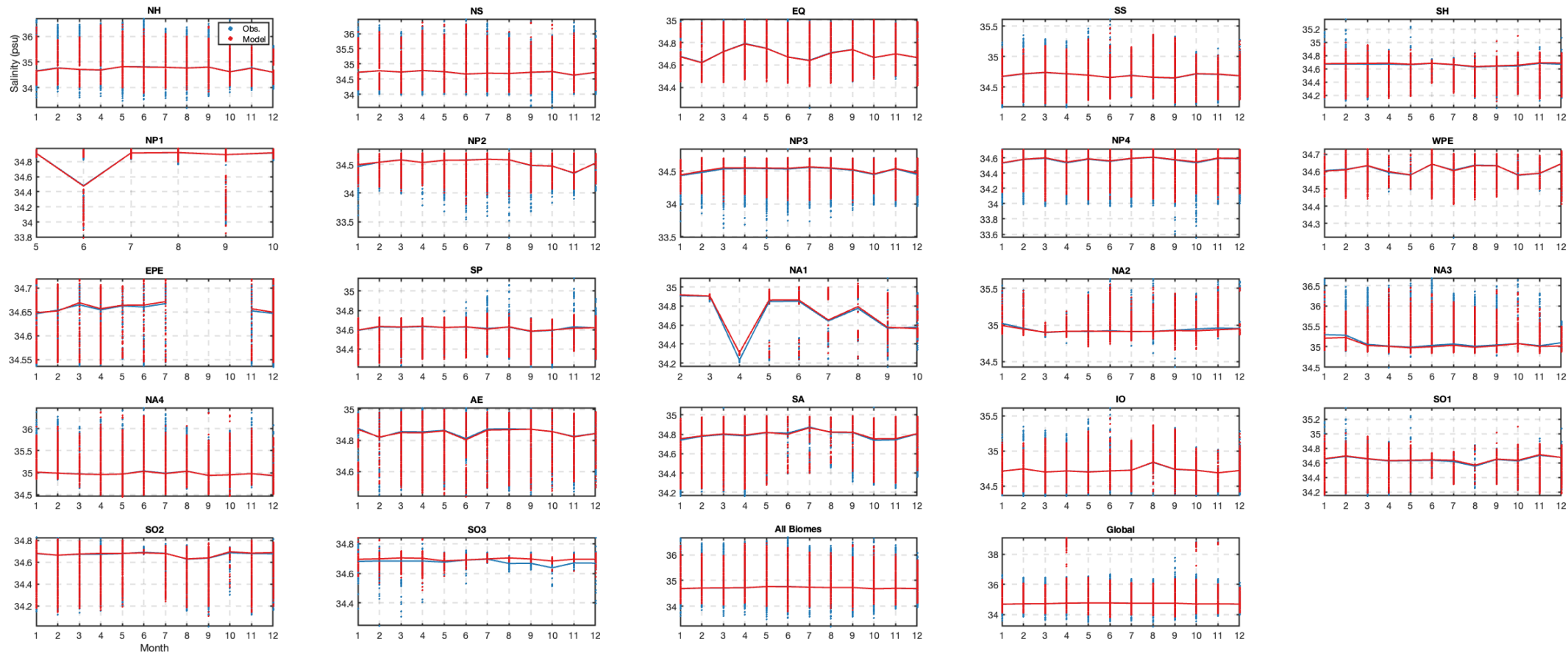


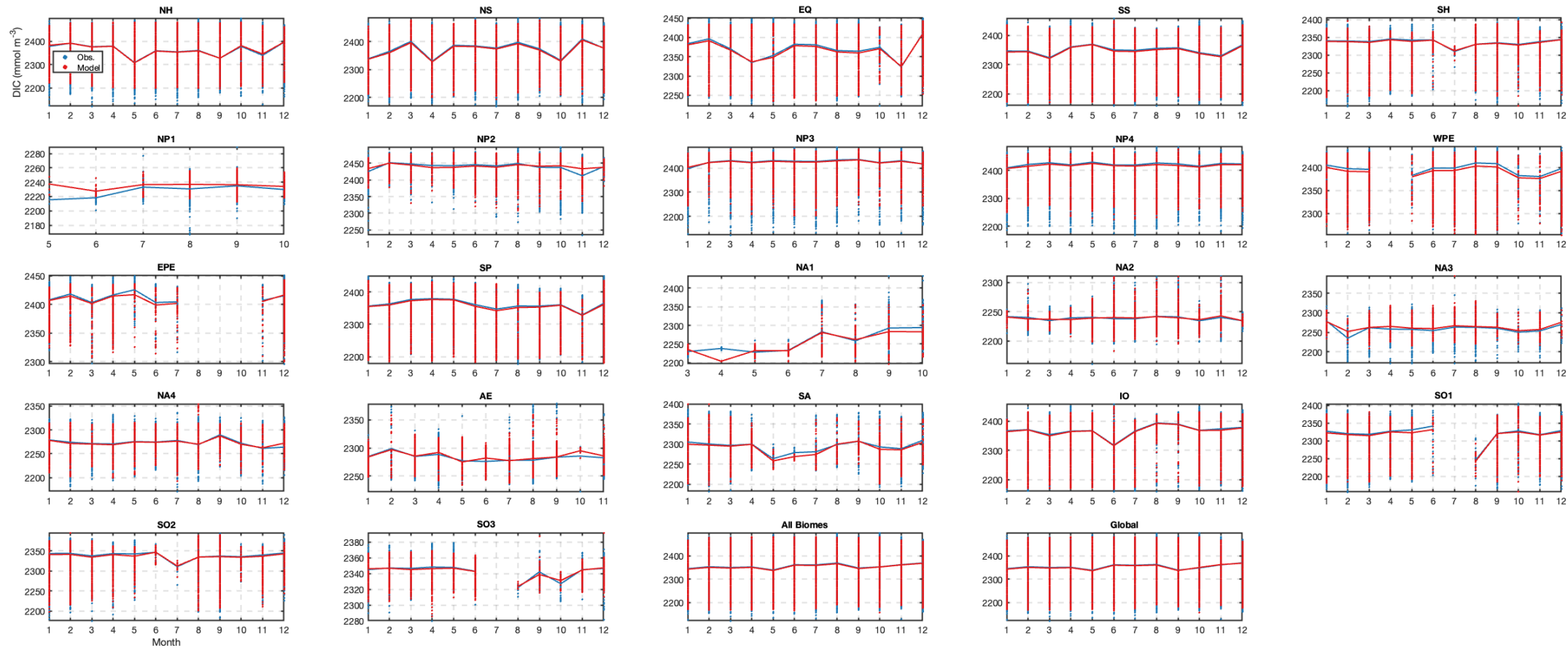


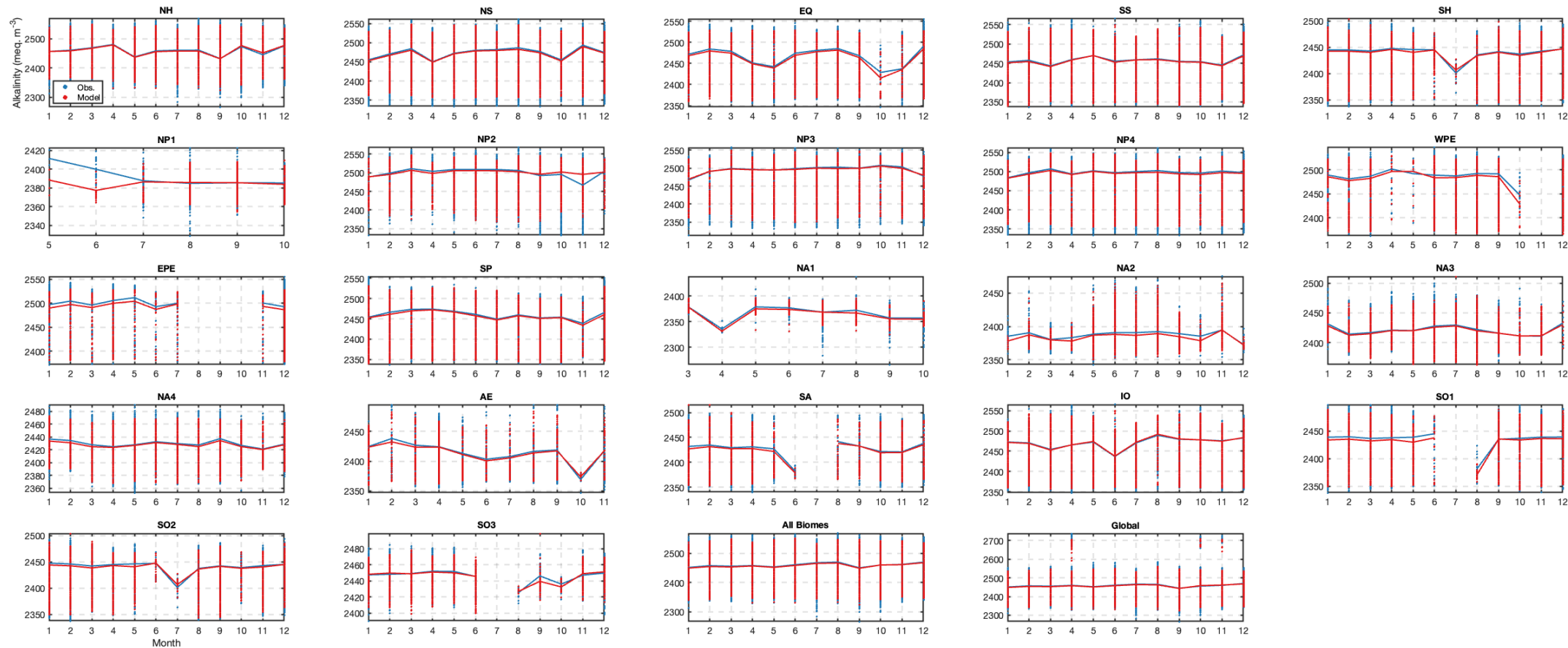


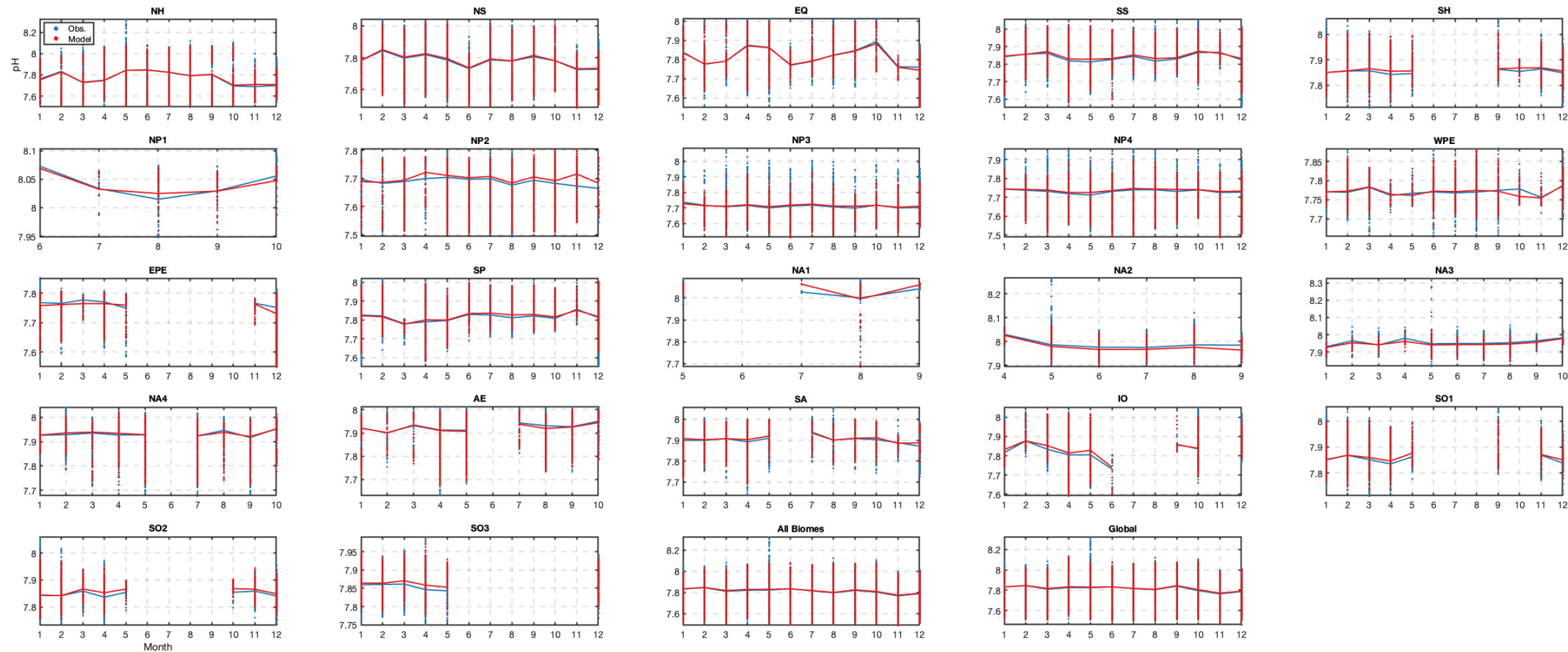
ECCO-Darwin vs. GLODAP seasonal climatology: 500 to 6000-m depth

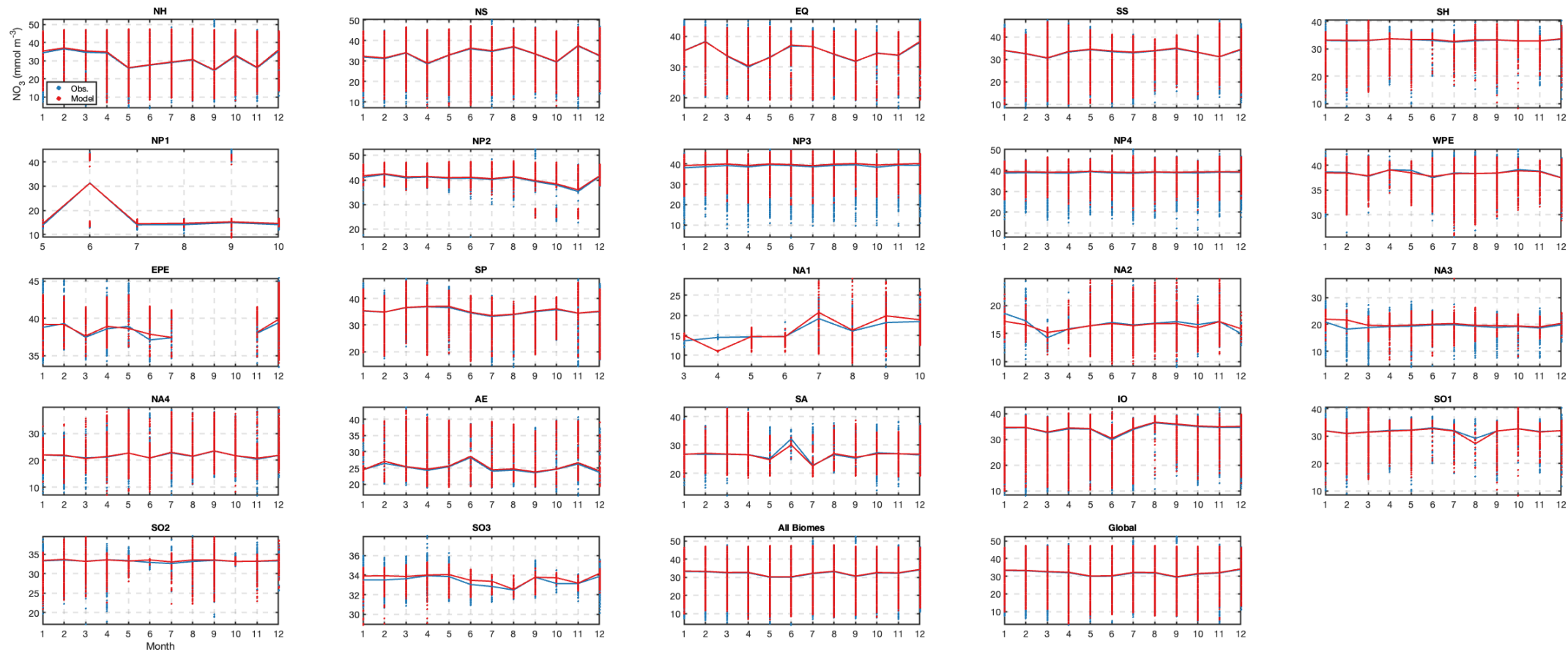


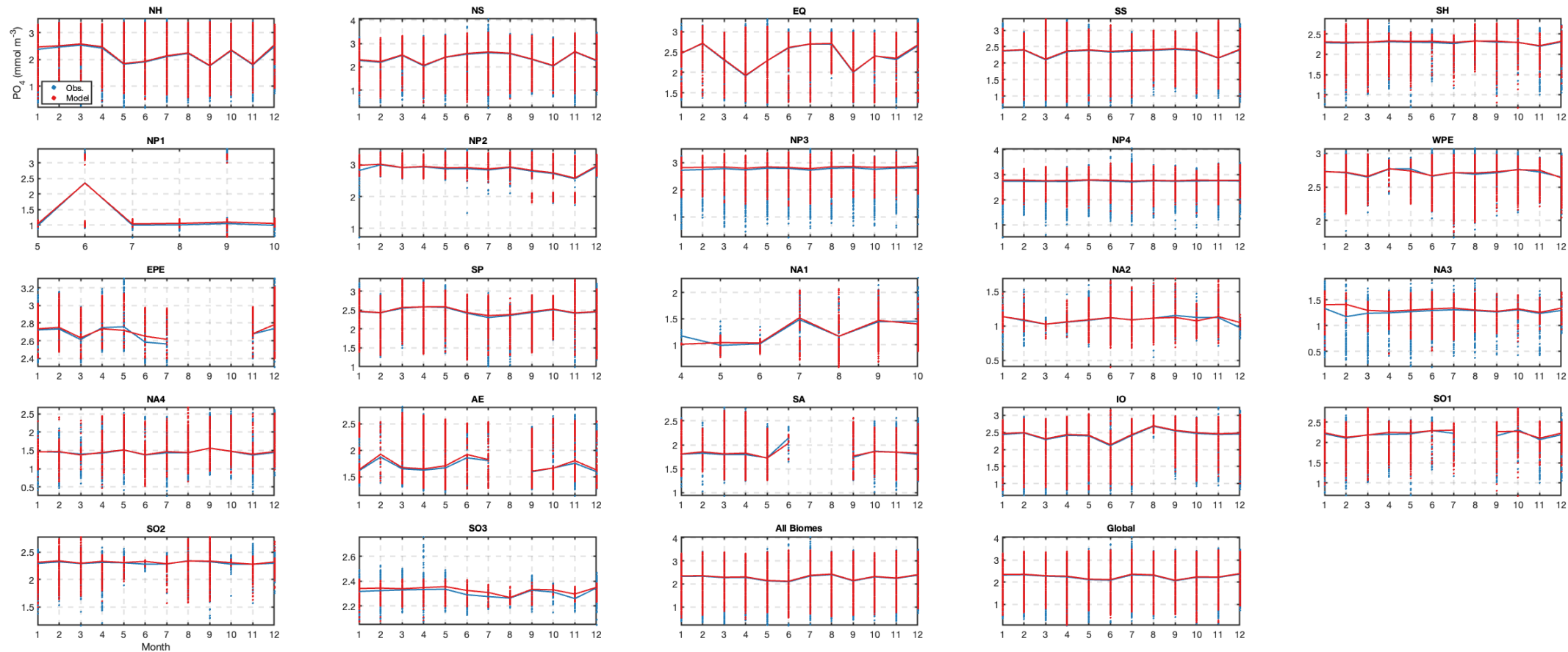


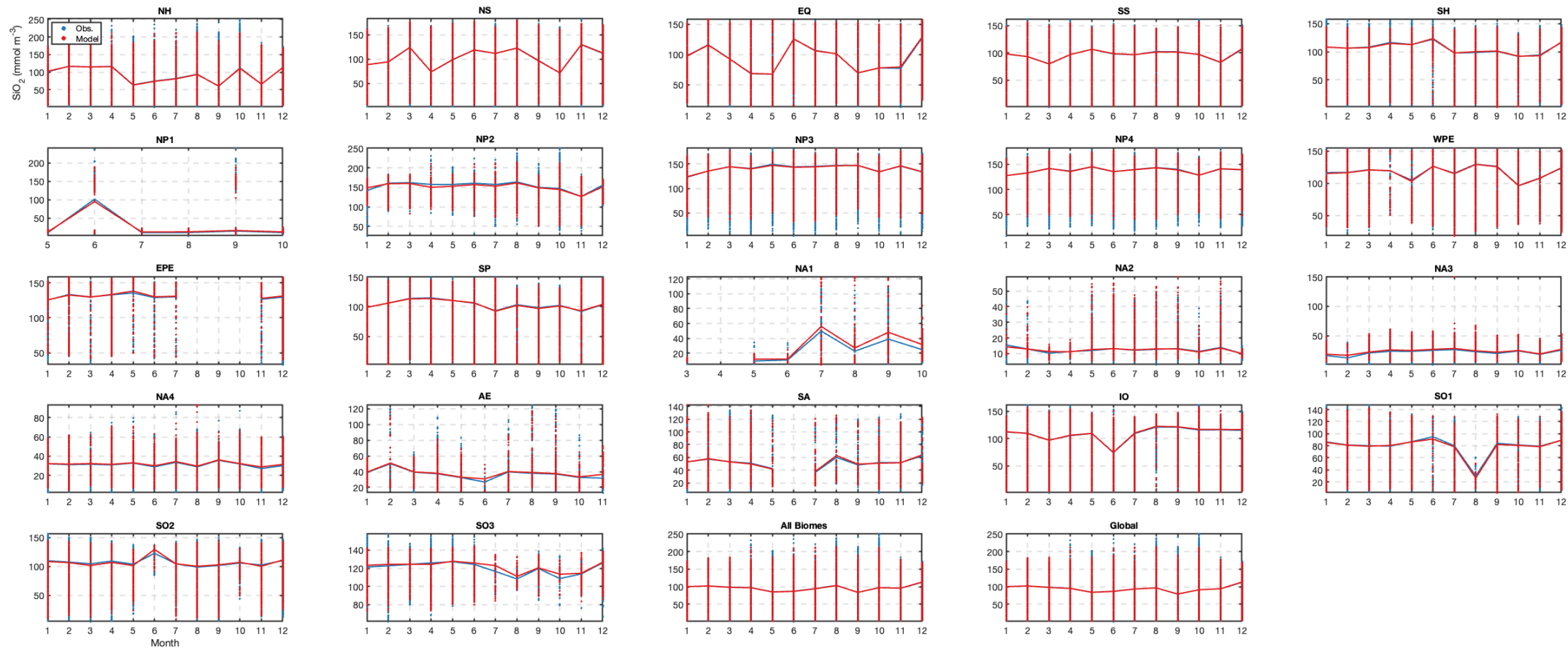


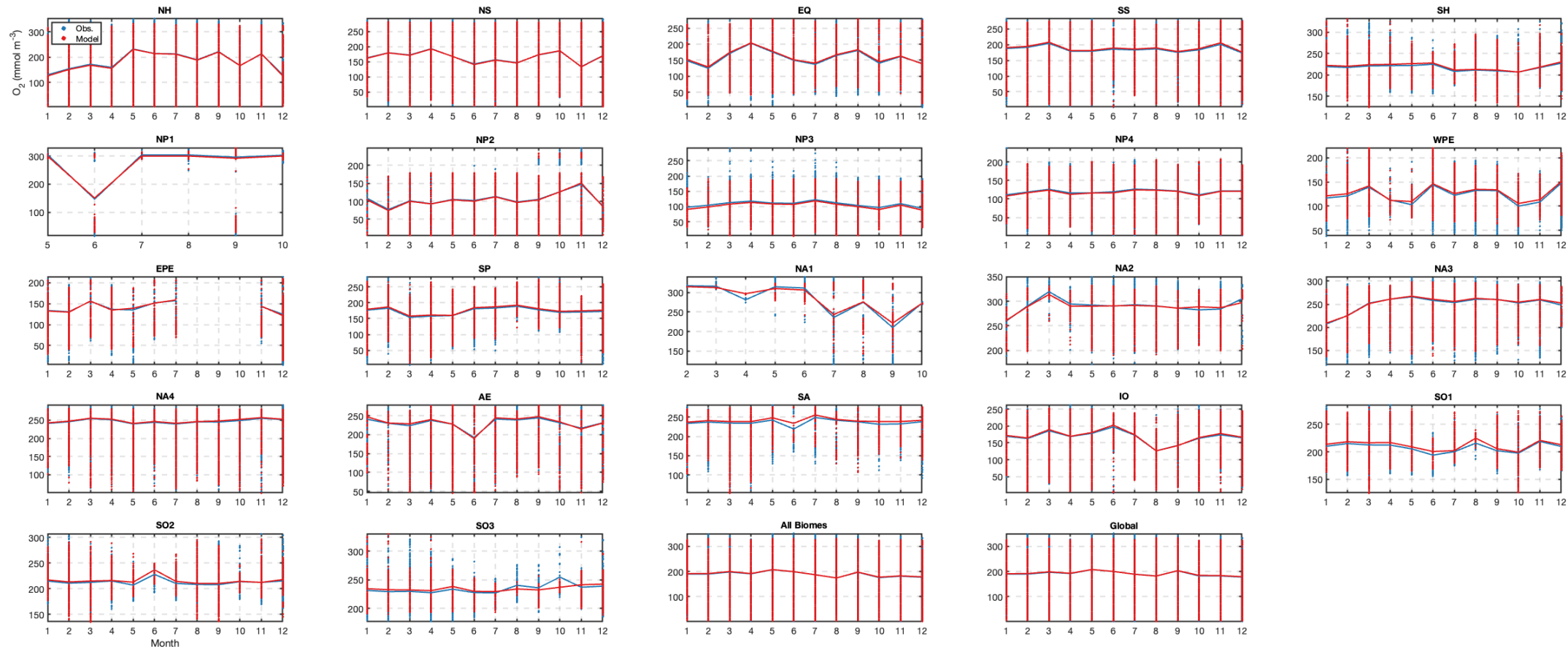




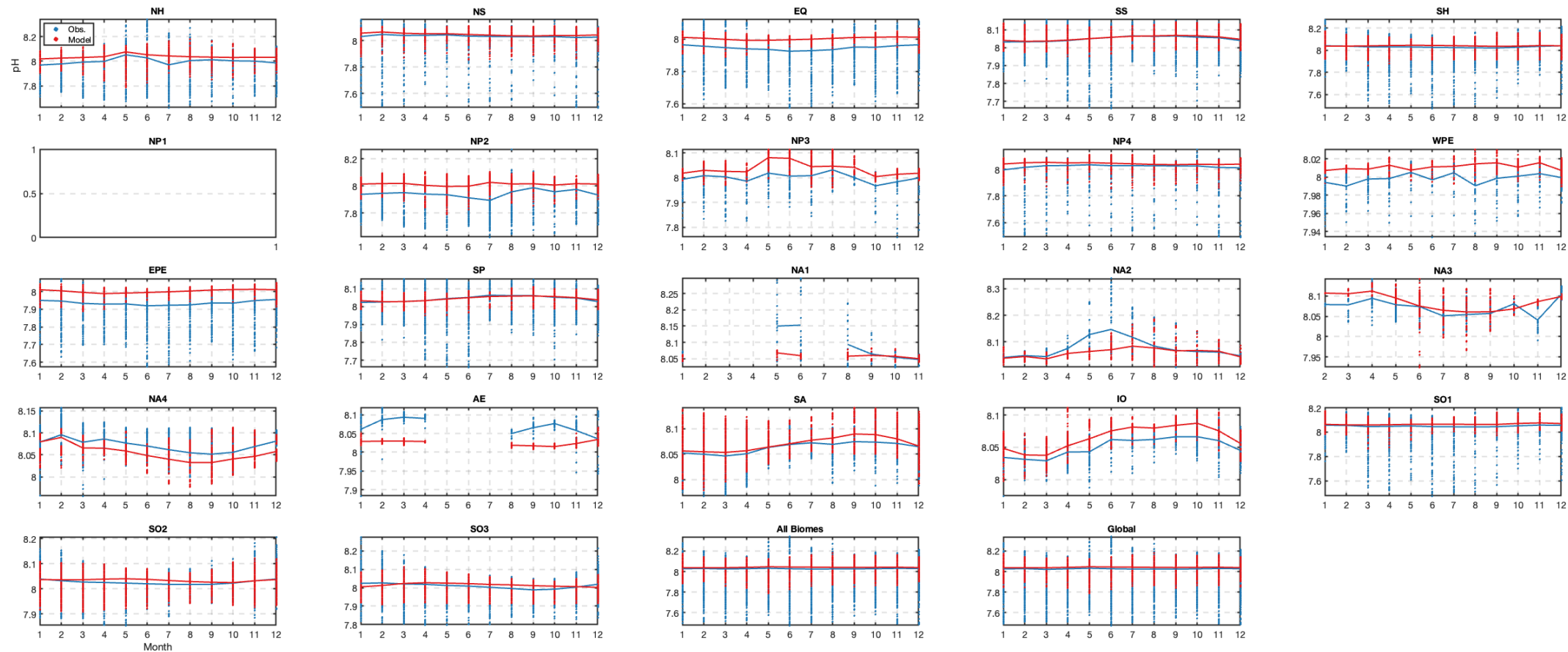


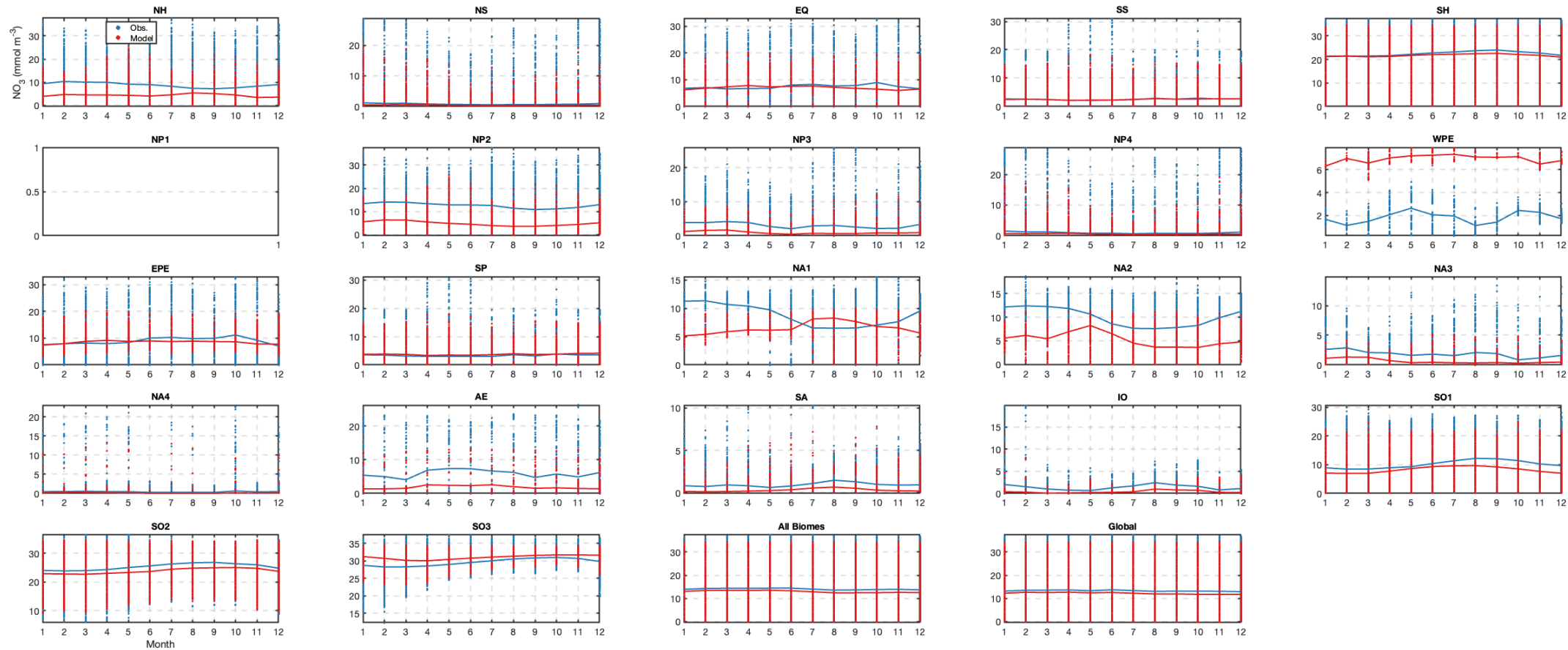


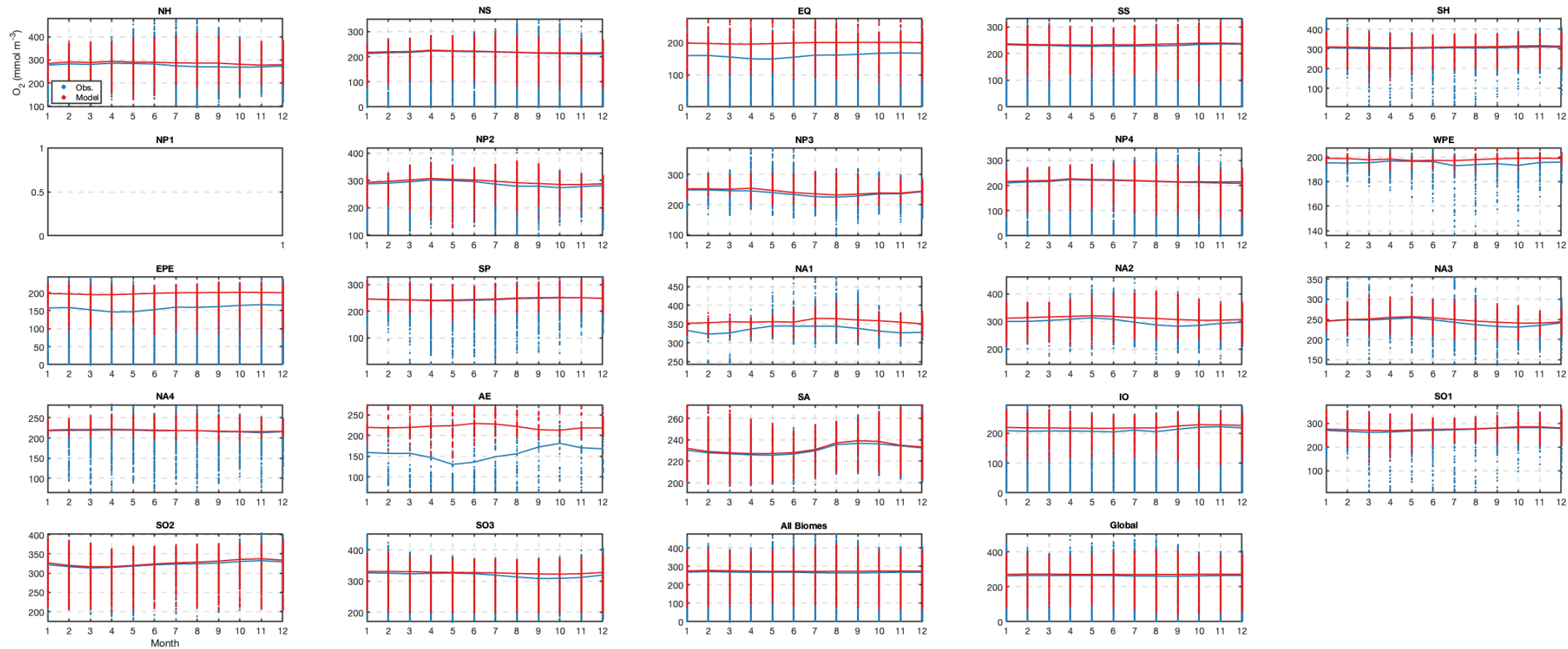




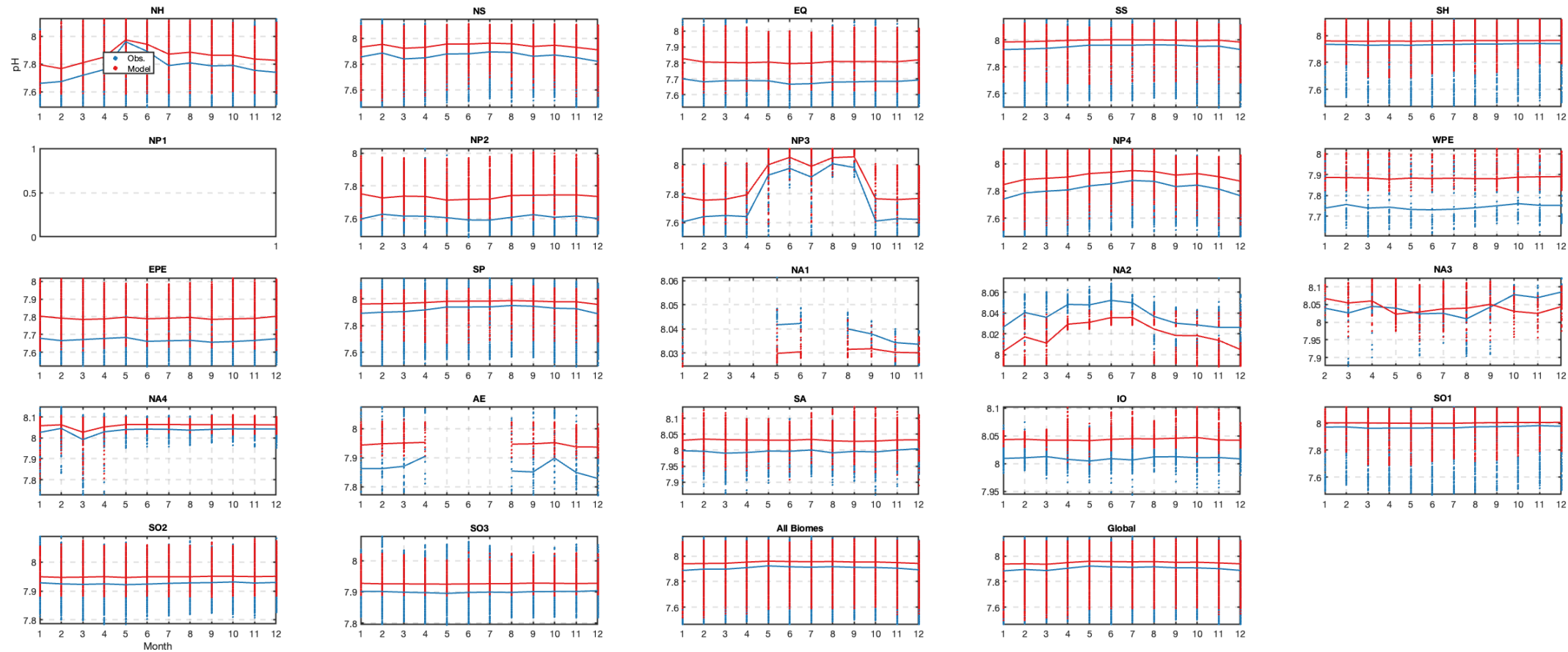
ECCO-Darwin vs. BGC-Argo seasonal climatology: 0 to 100-m depth

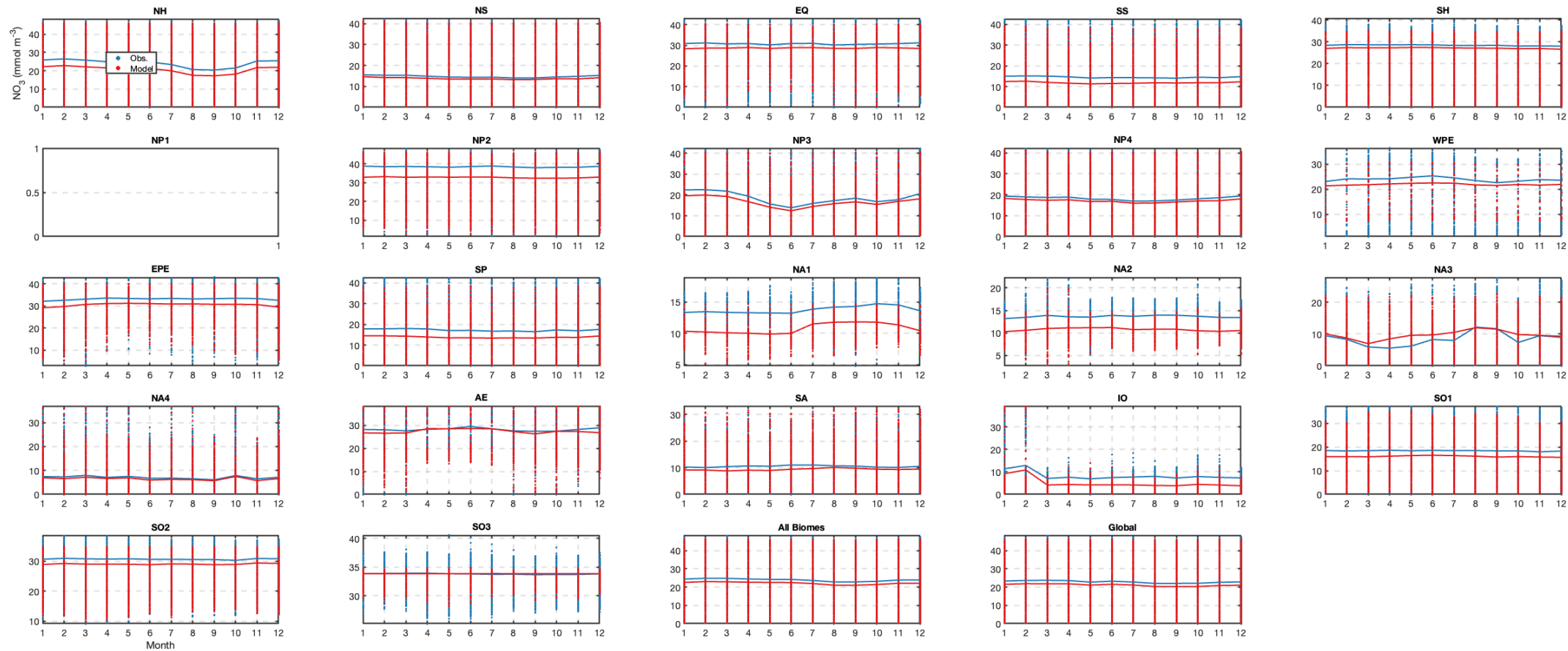


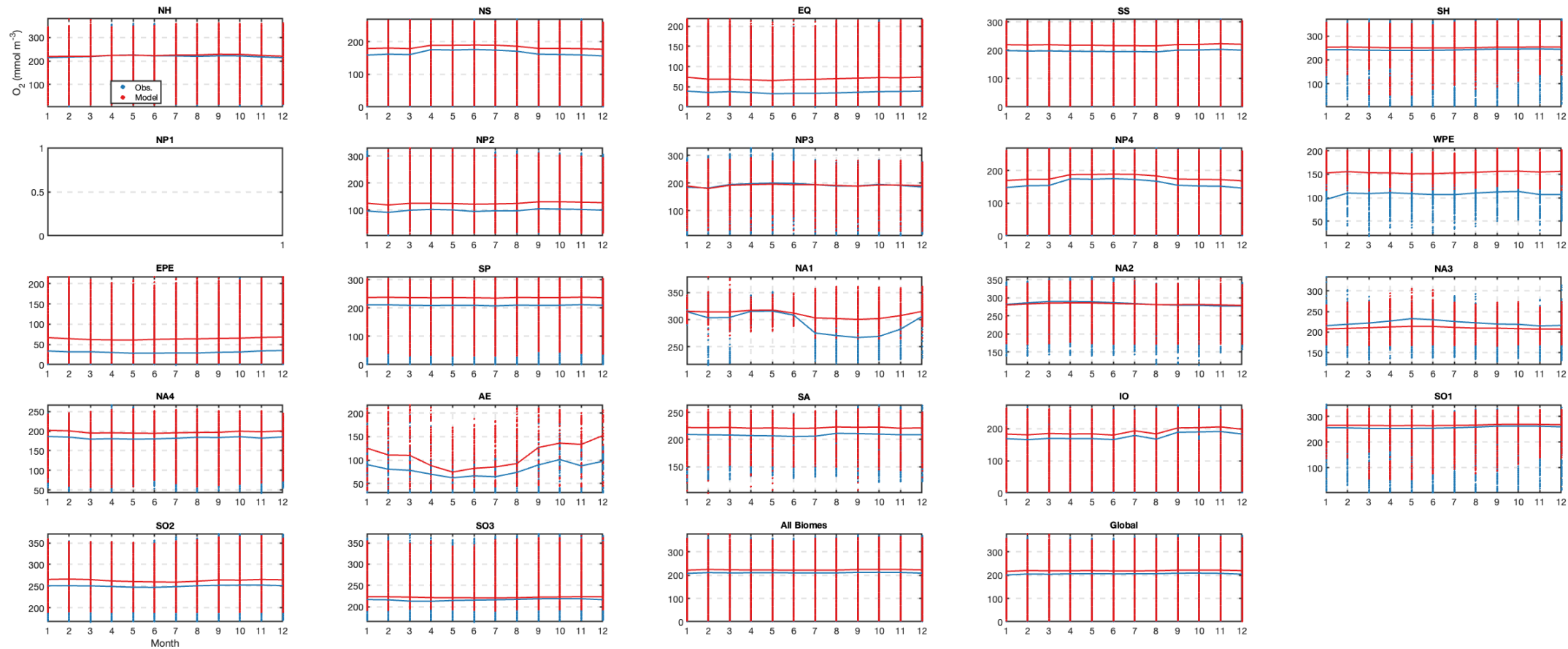




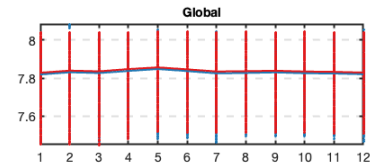
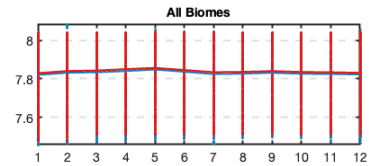
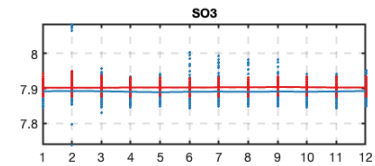
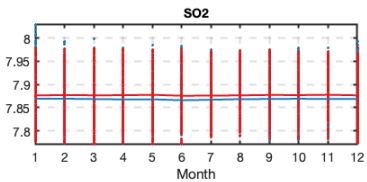
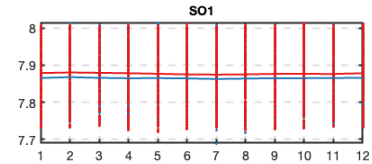
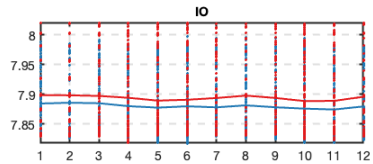
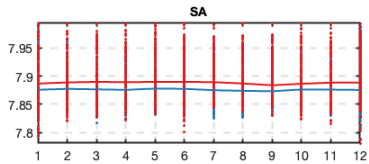
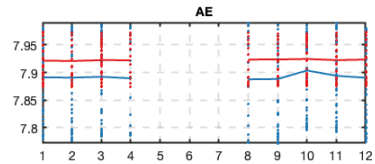
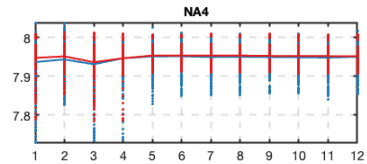
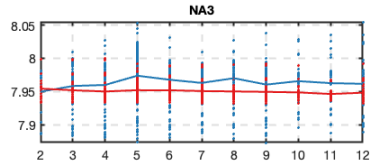
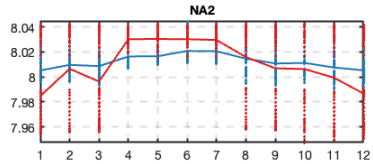
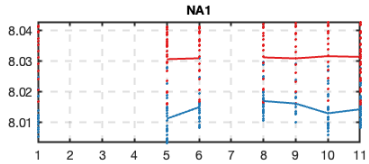
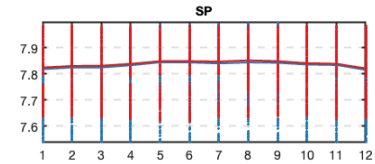
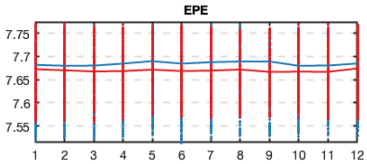
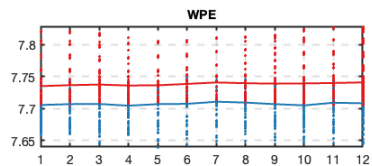
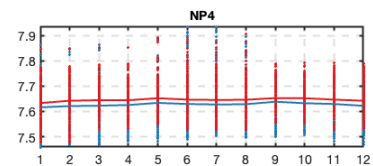
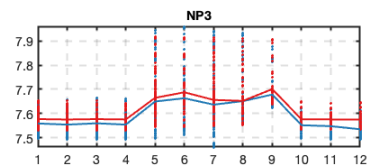
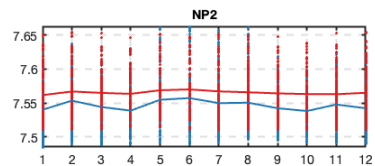
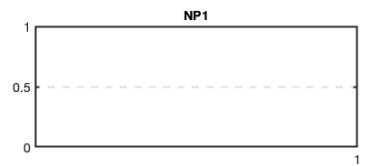
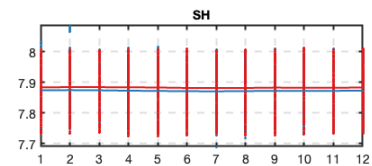
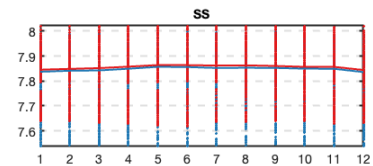
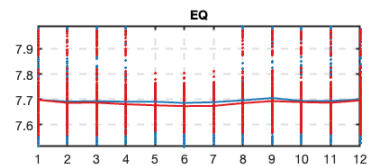
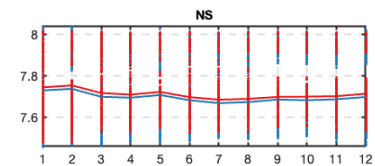
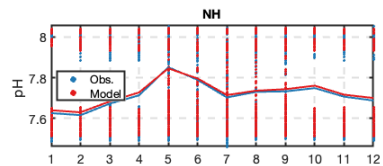
ECCO-Darwin vs. BGC-Argo seasonal climatology: 100 to 500-m depth

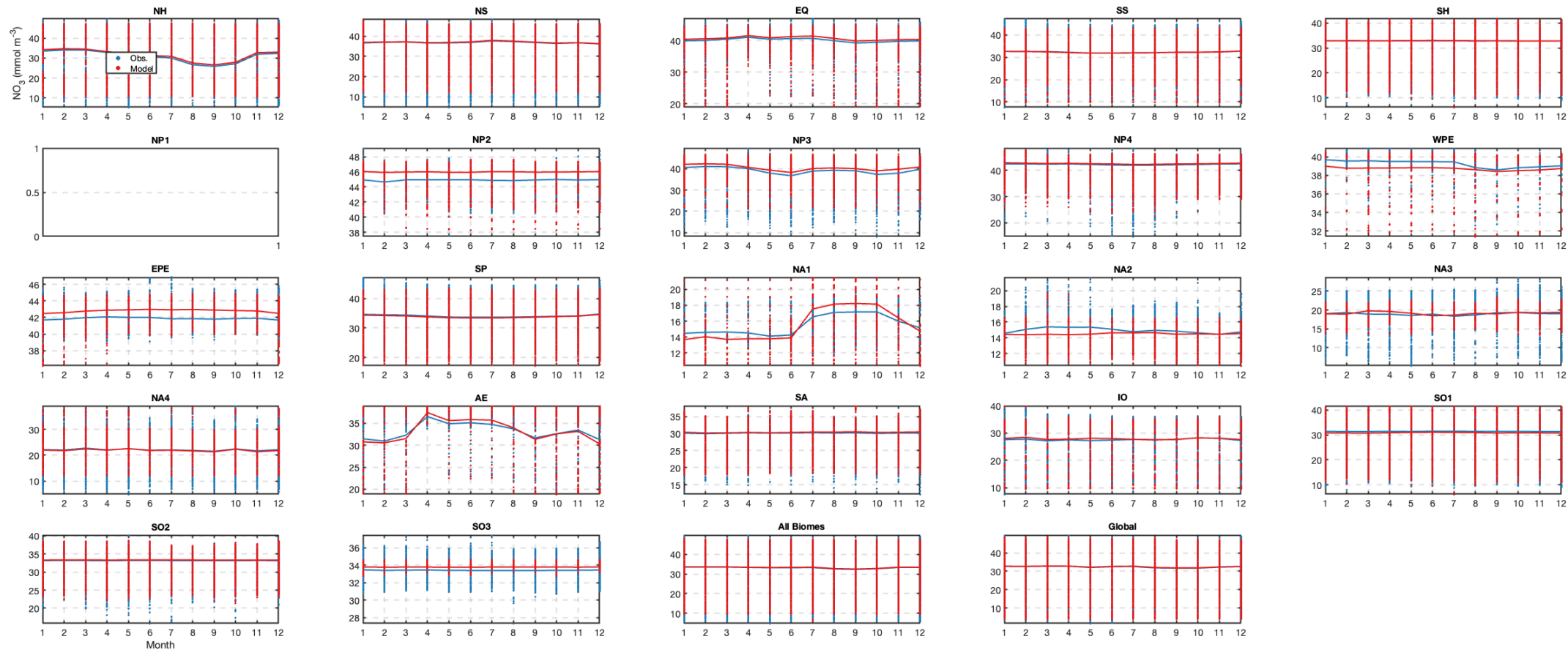


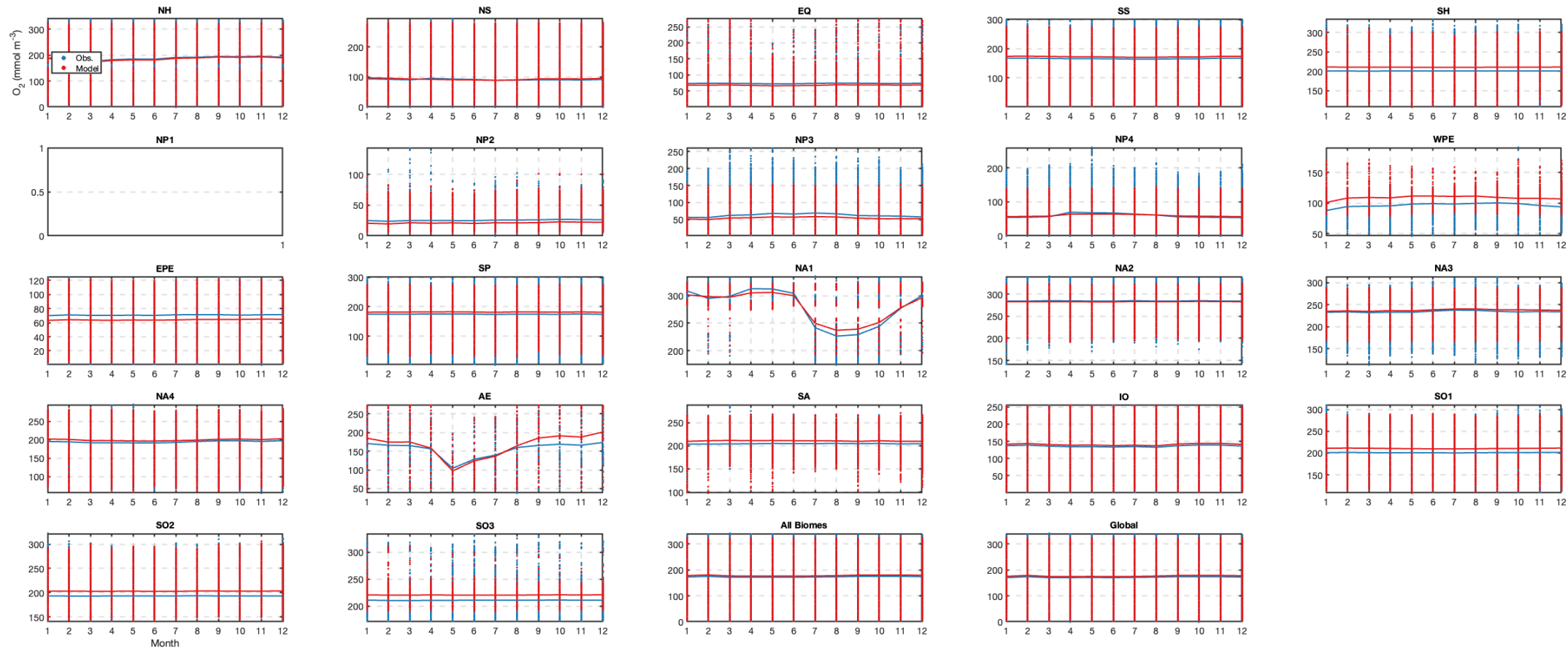




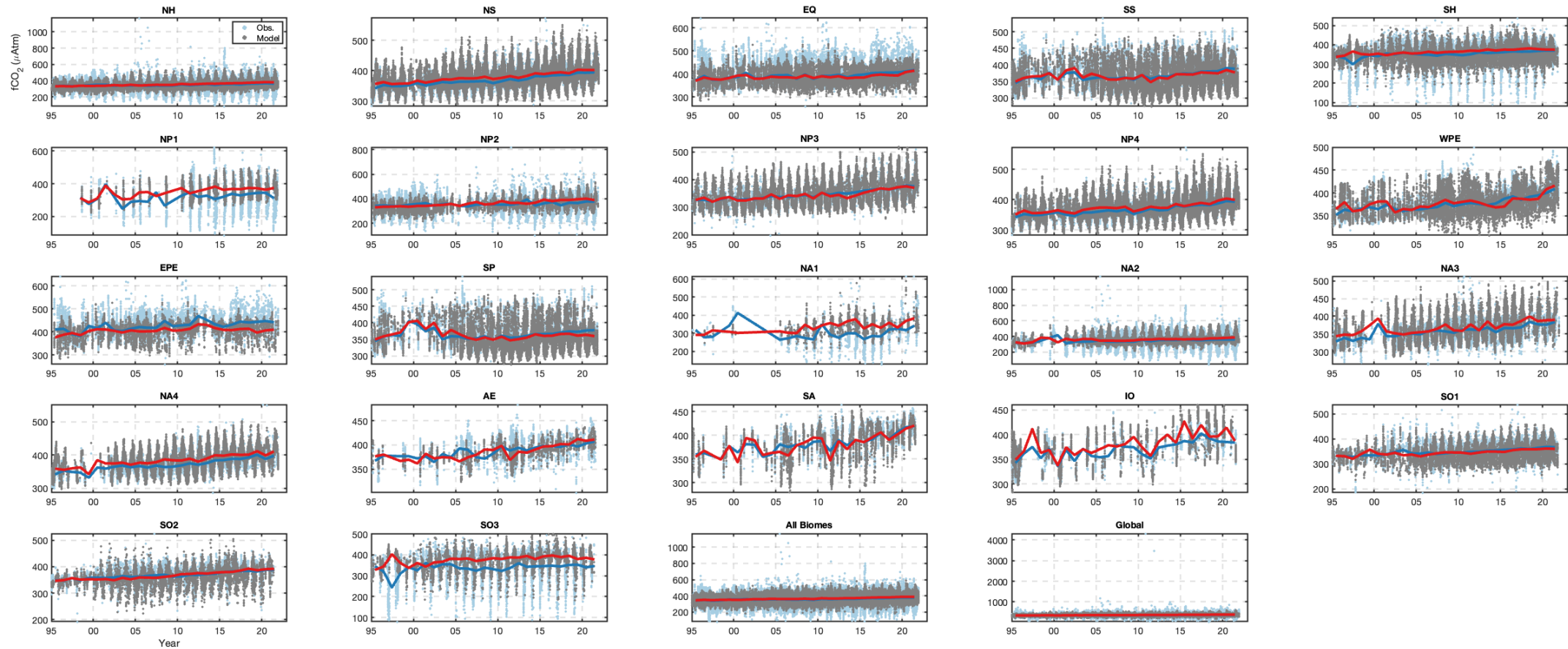
ECCO-Darwin vs. BGC-Argo seasonal climatology: 500 to 6000-m depth



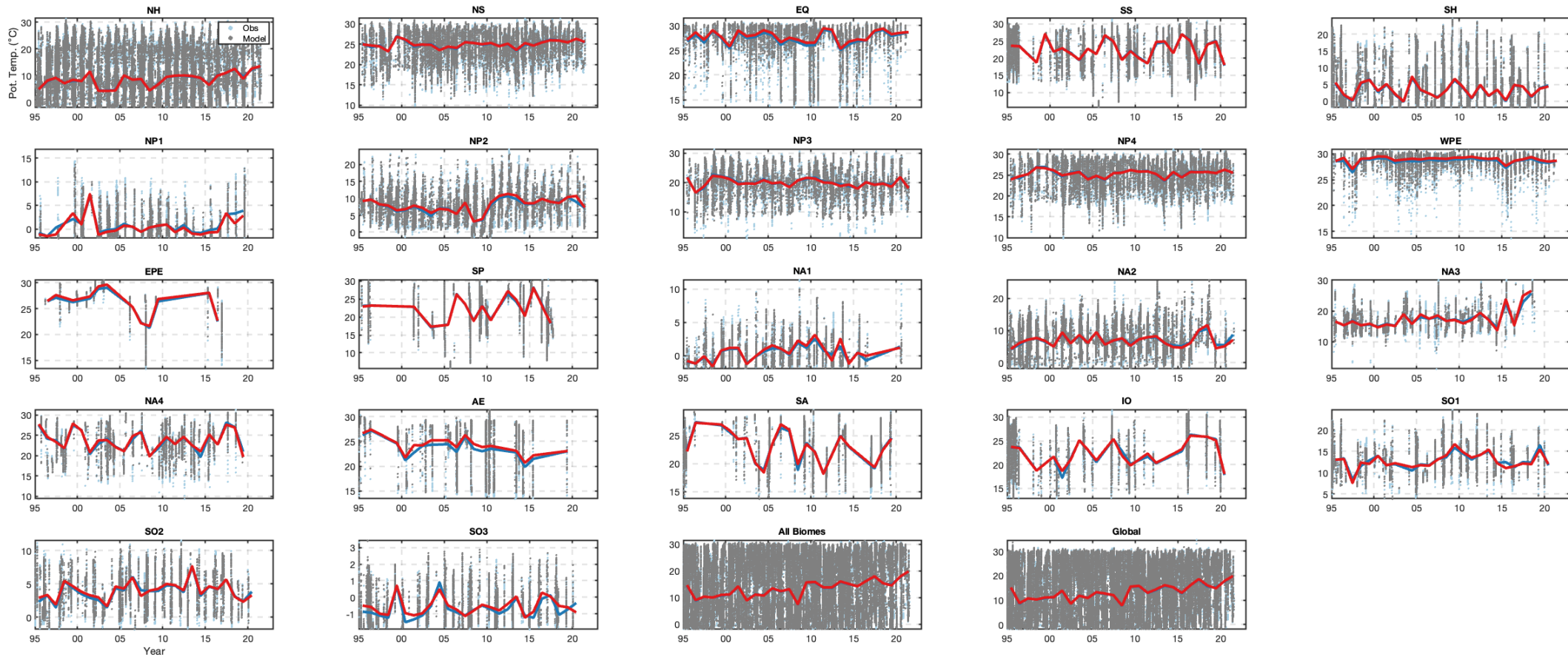


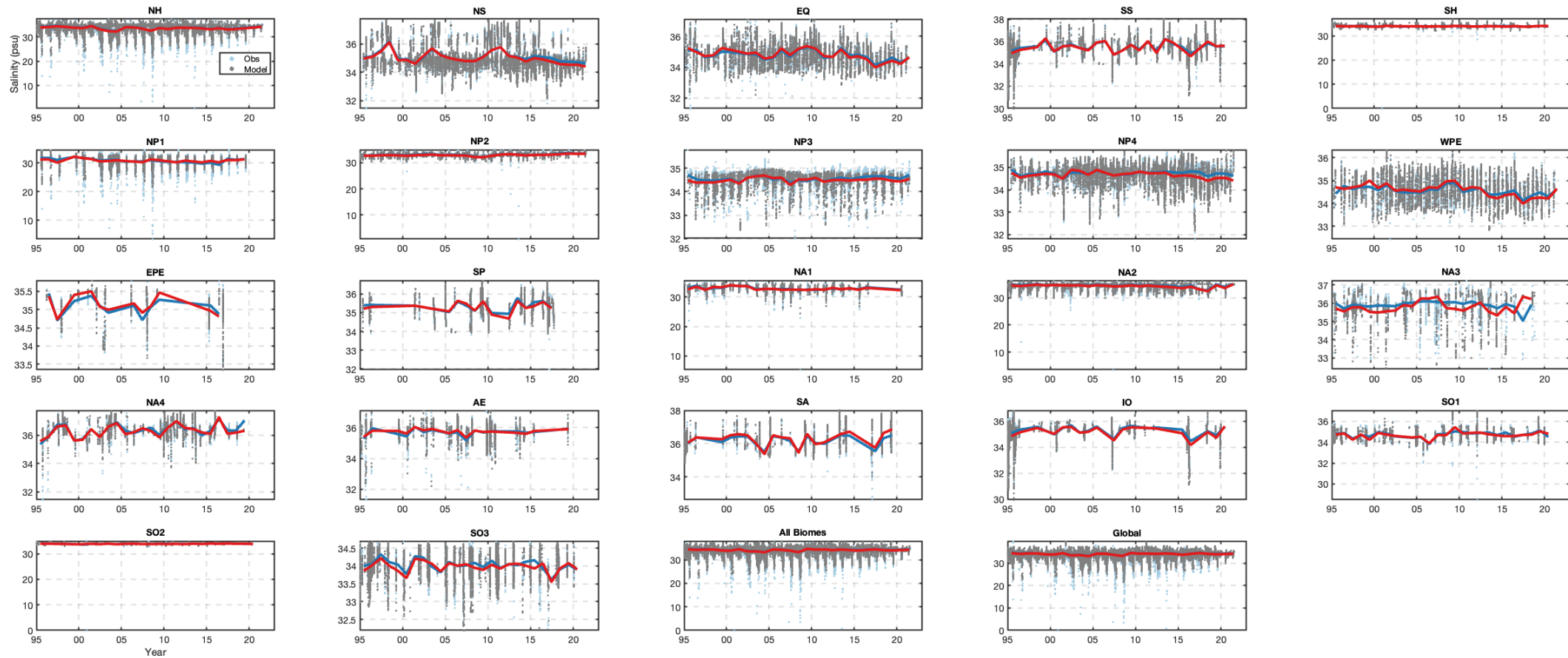


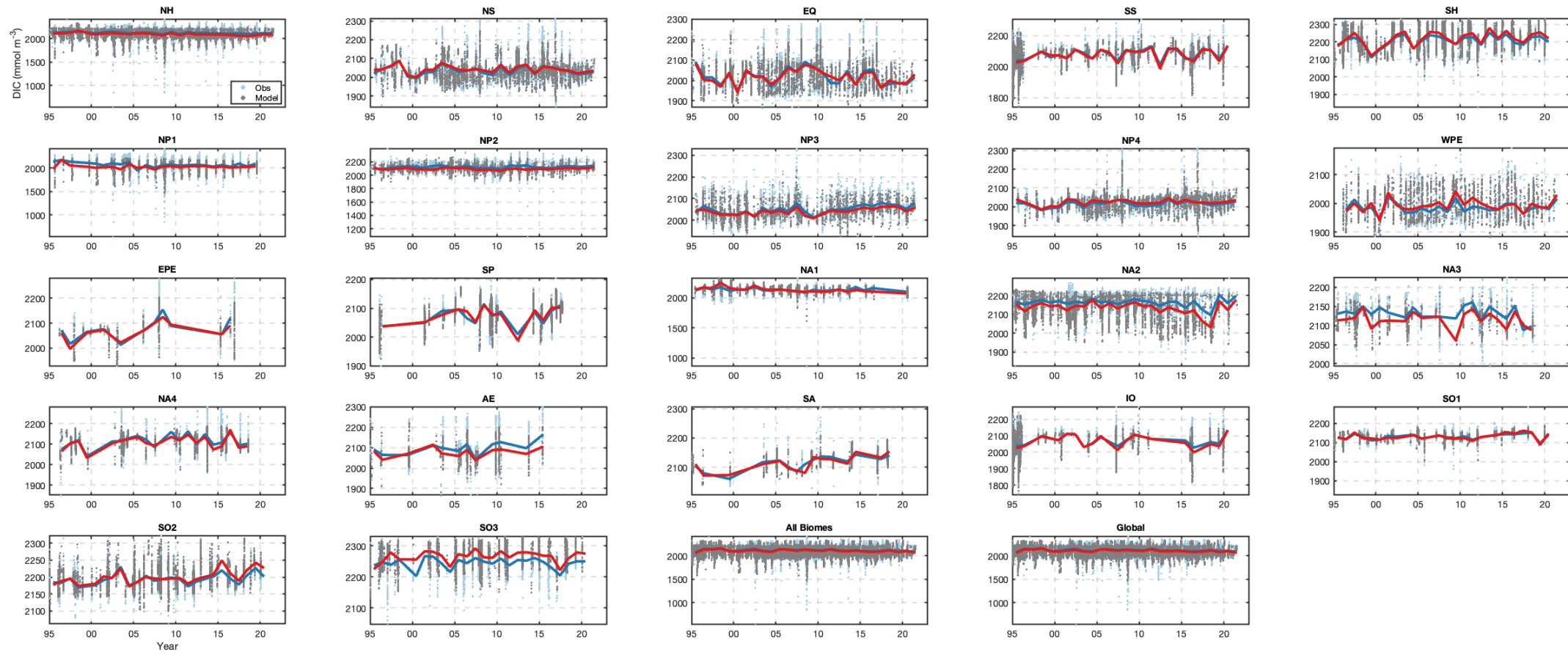
SOCAT time series: surface ocean

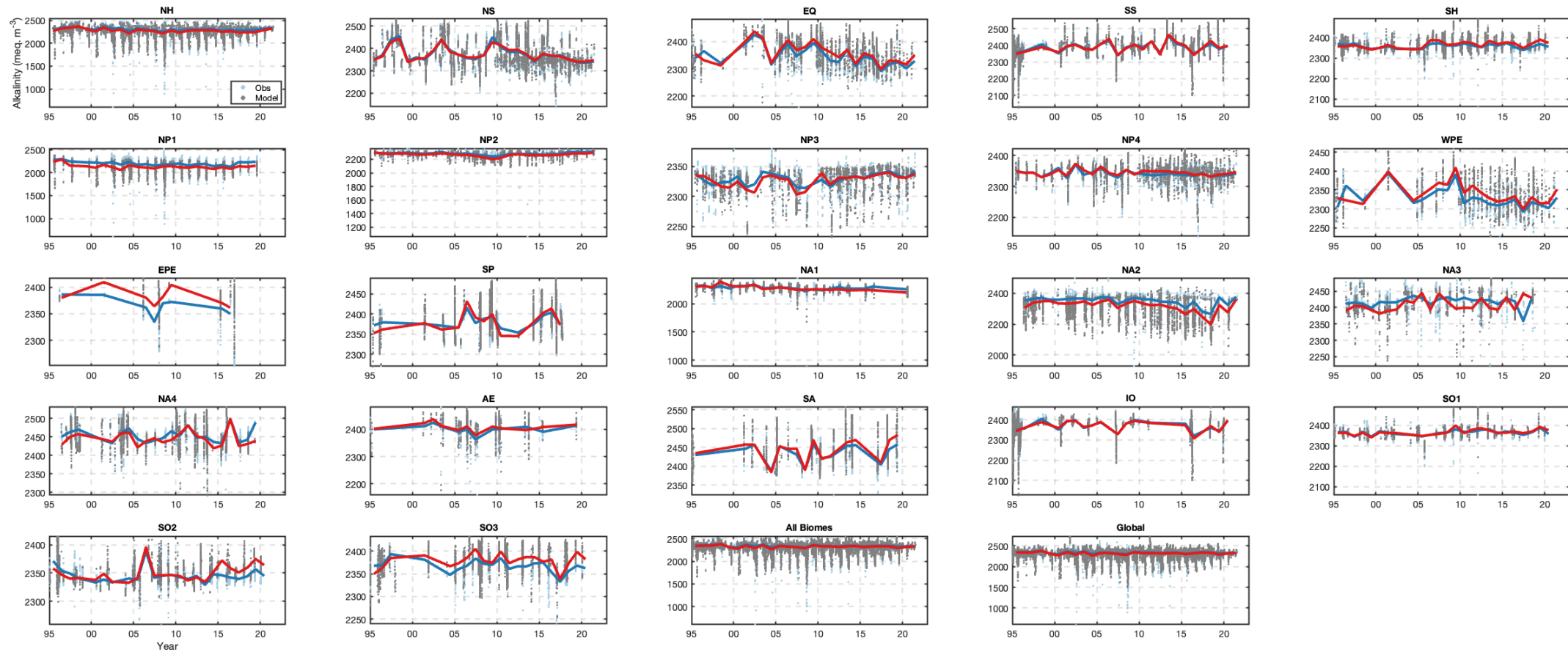


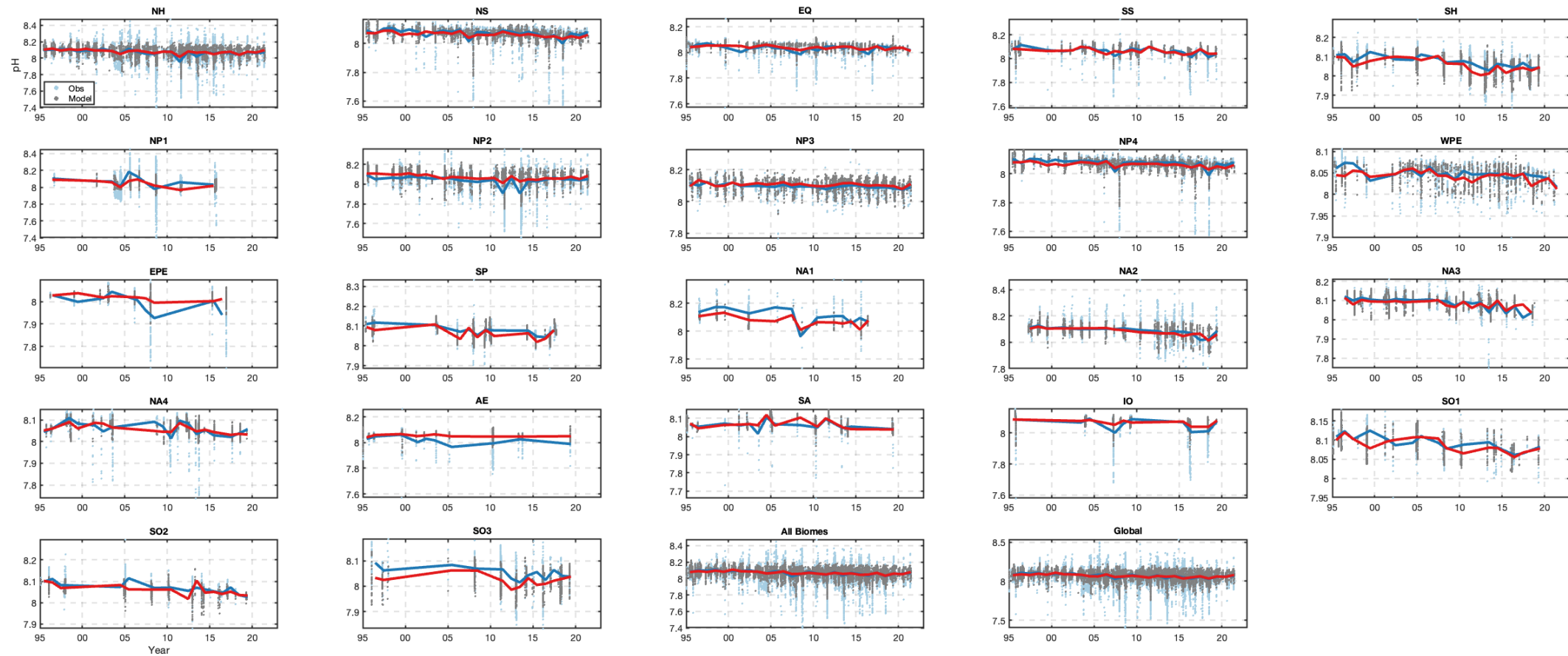
GLODAP time series: 0 to 100-m depth

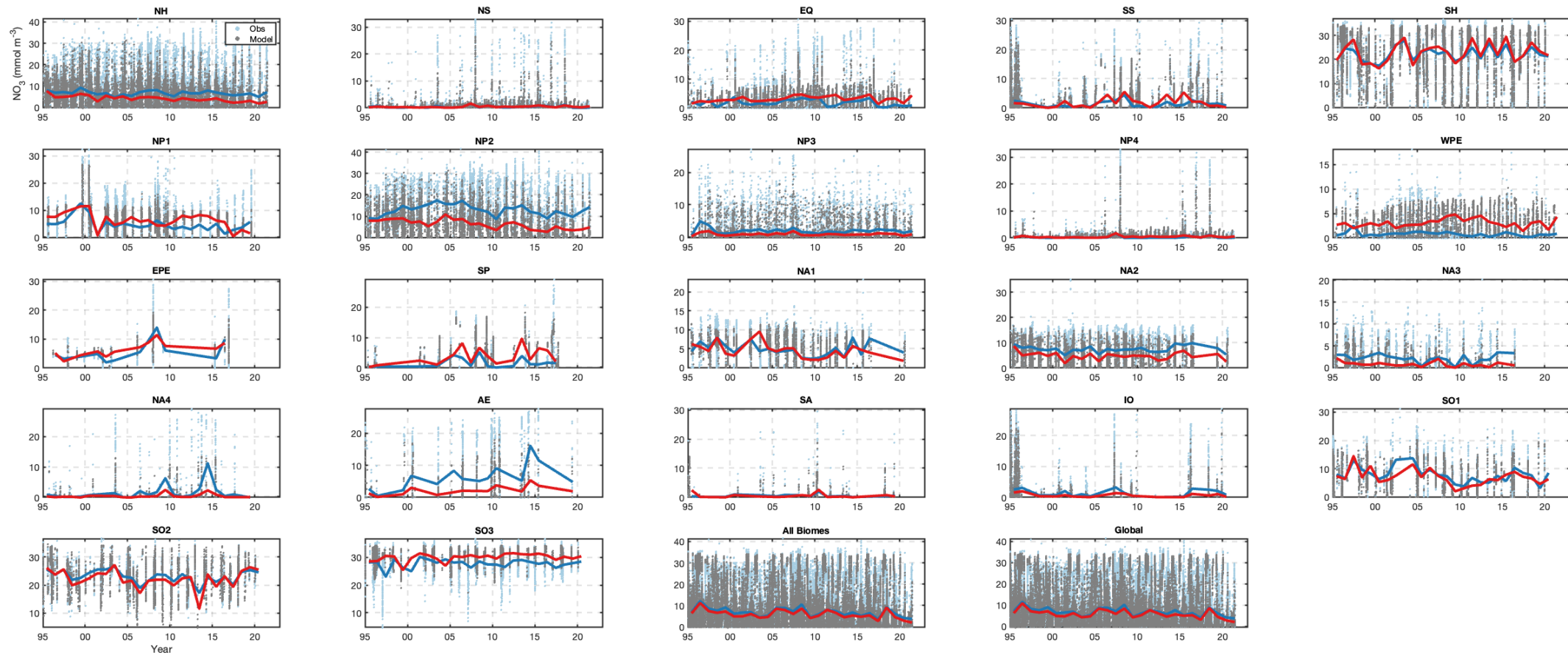


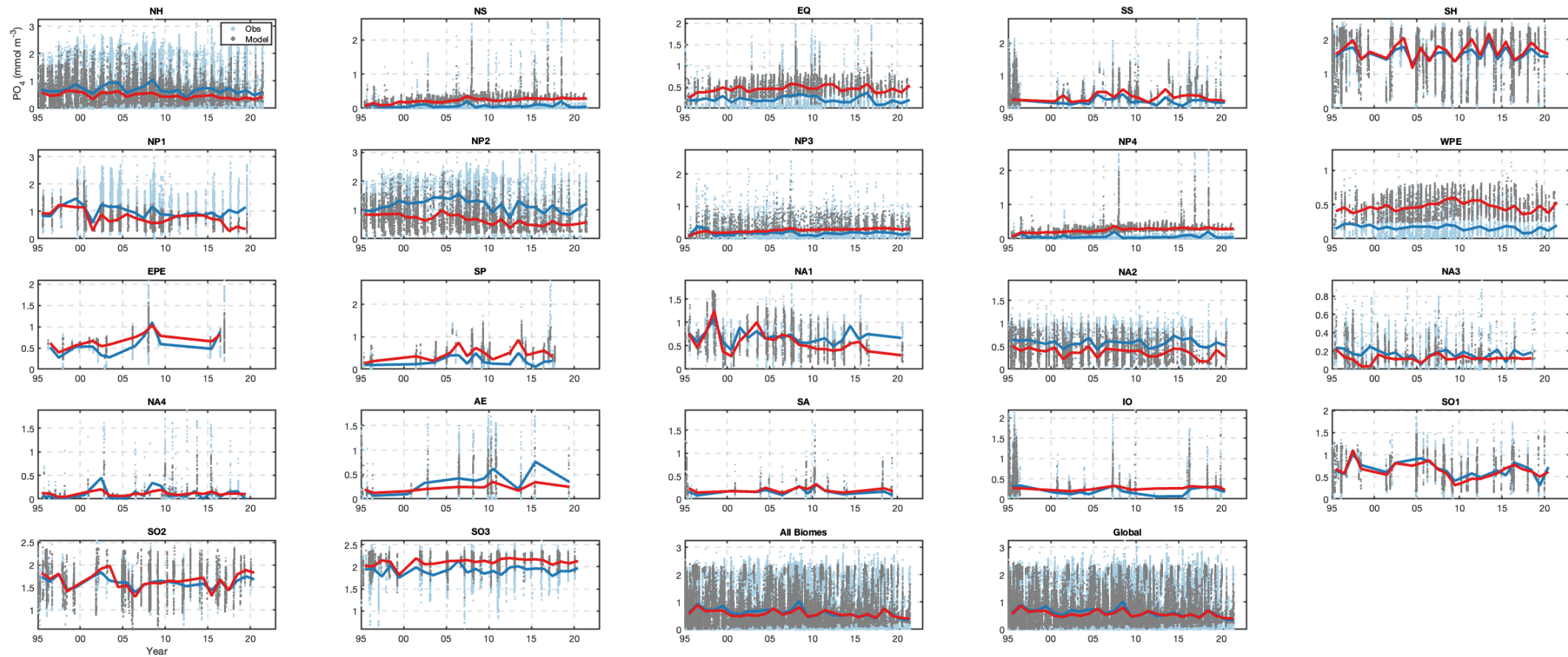


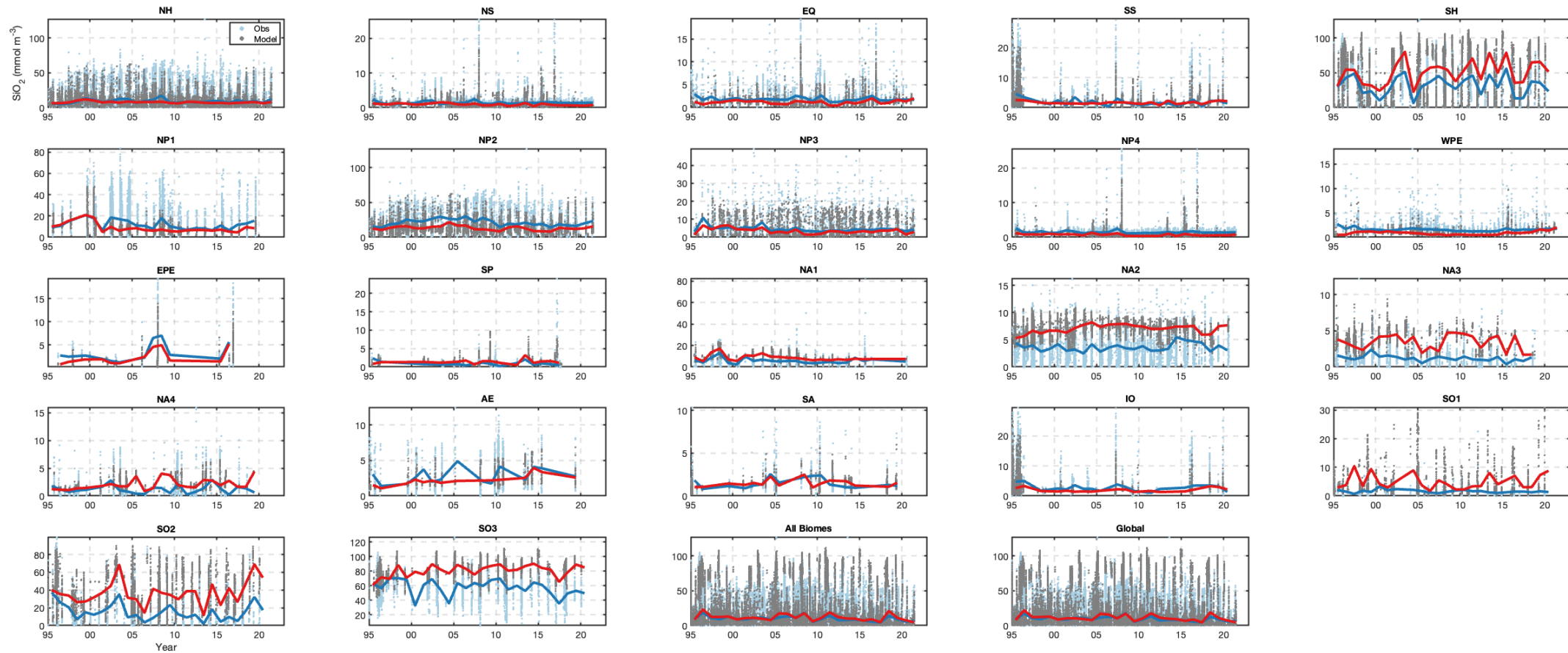


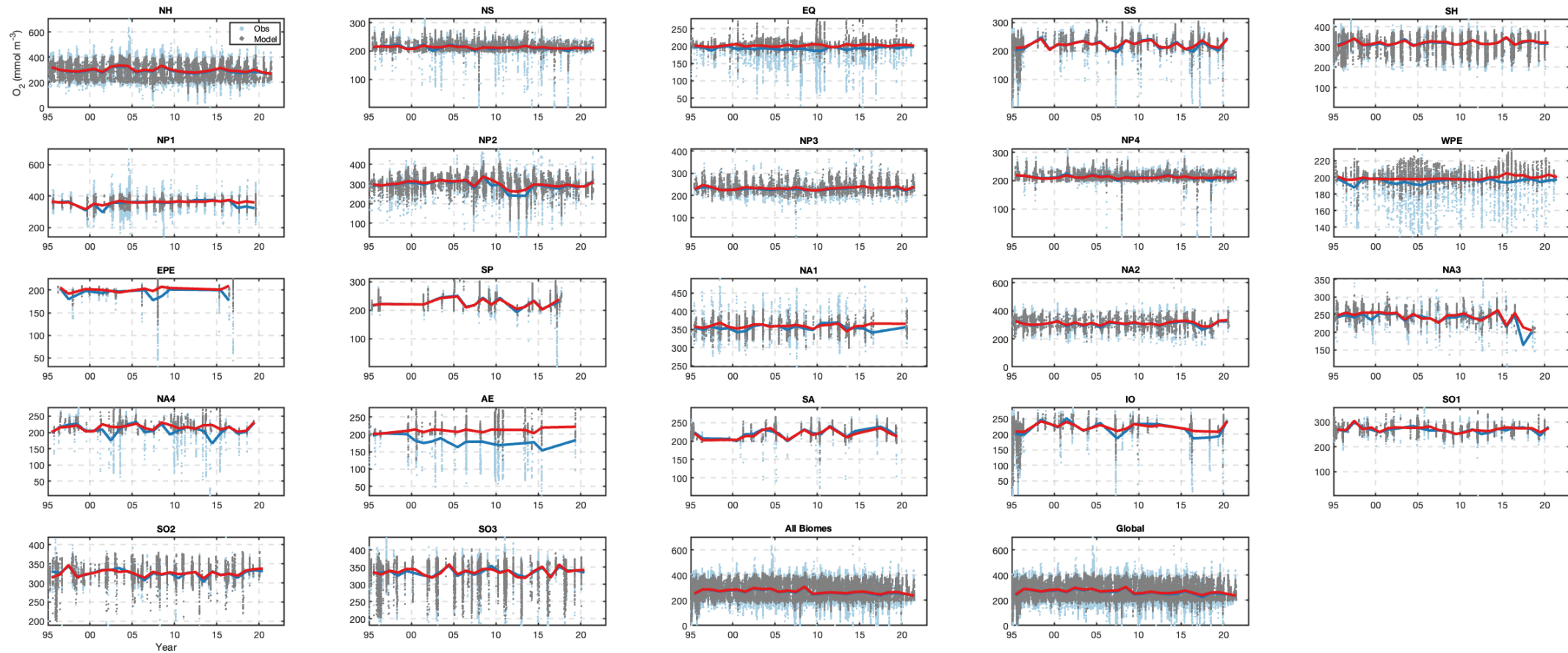




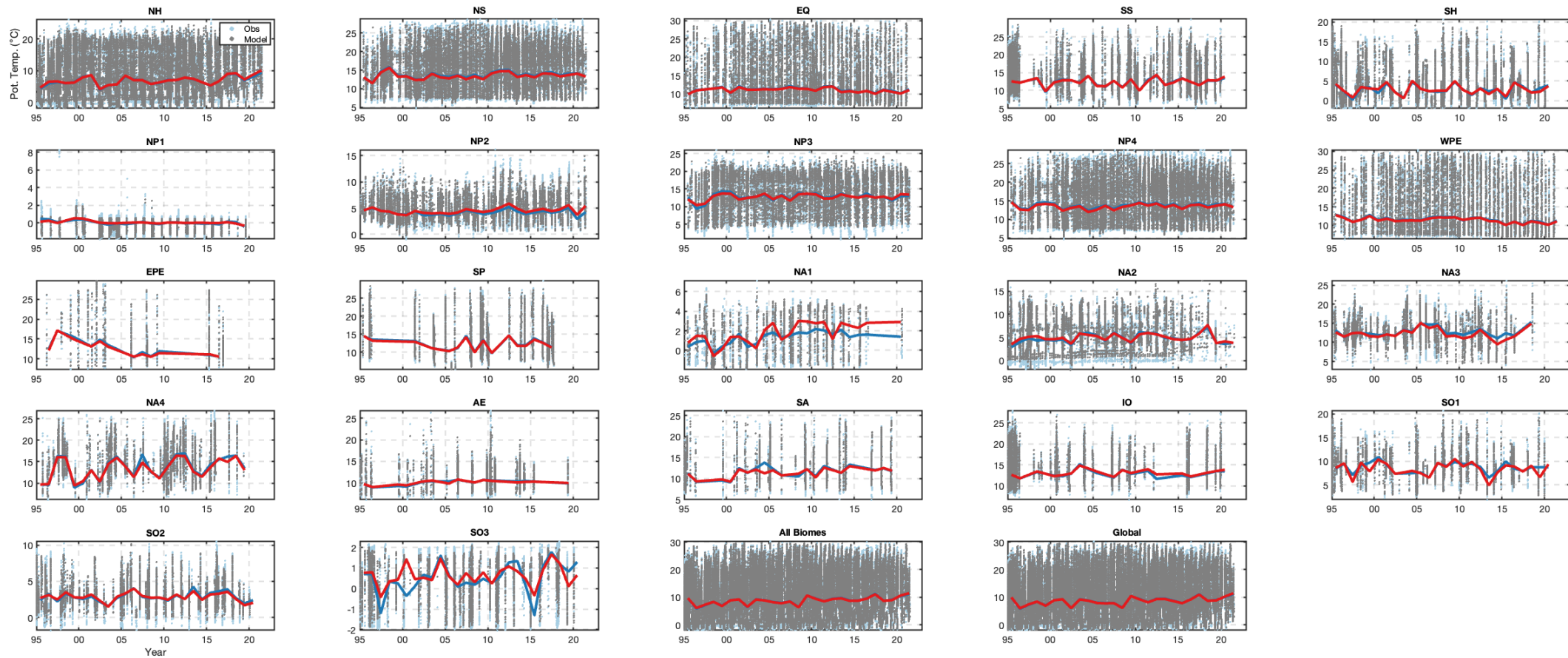


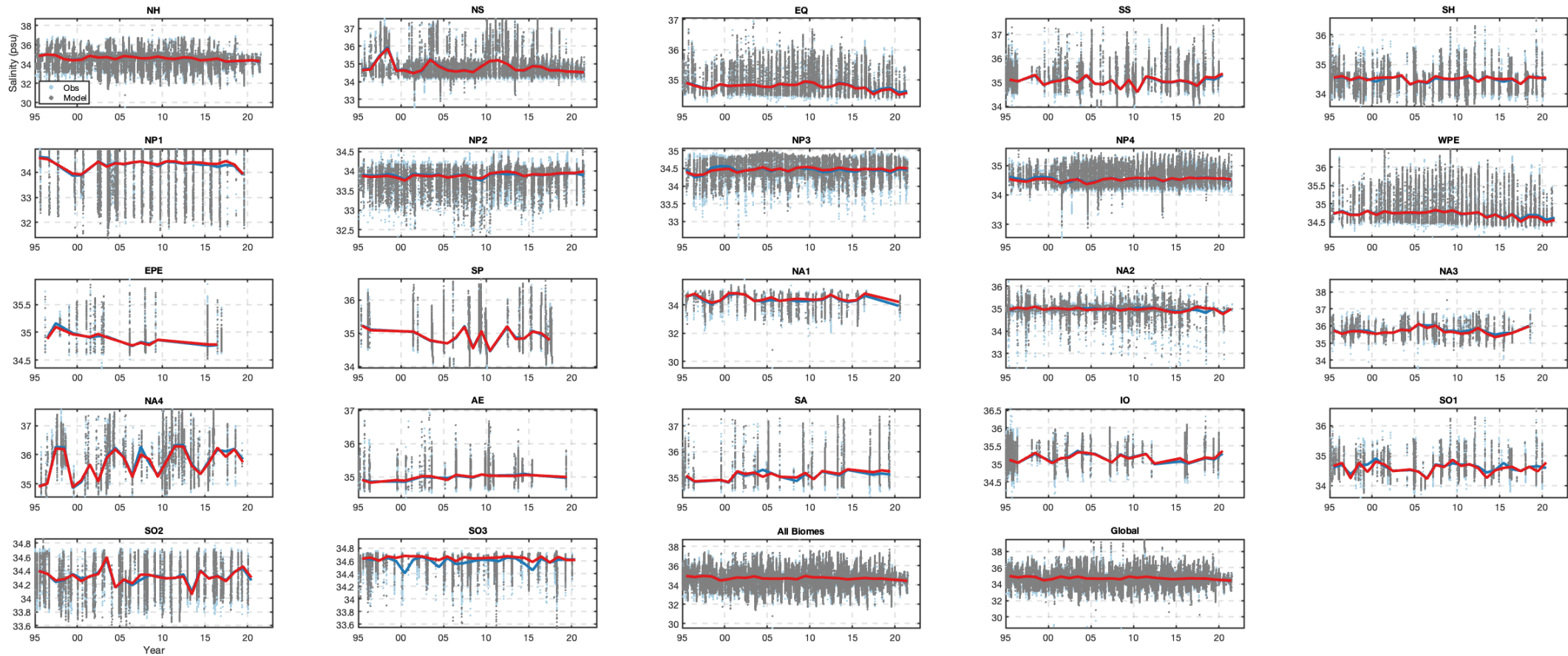


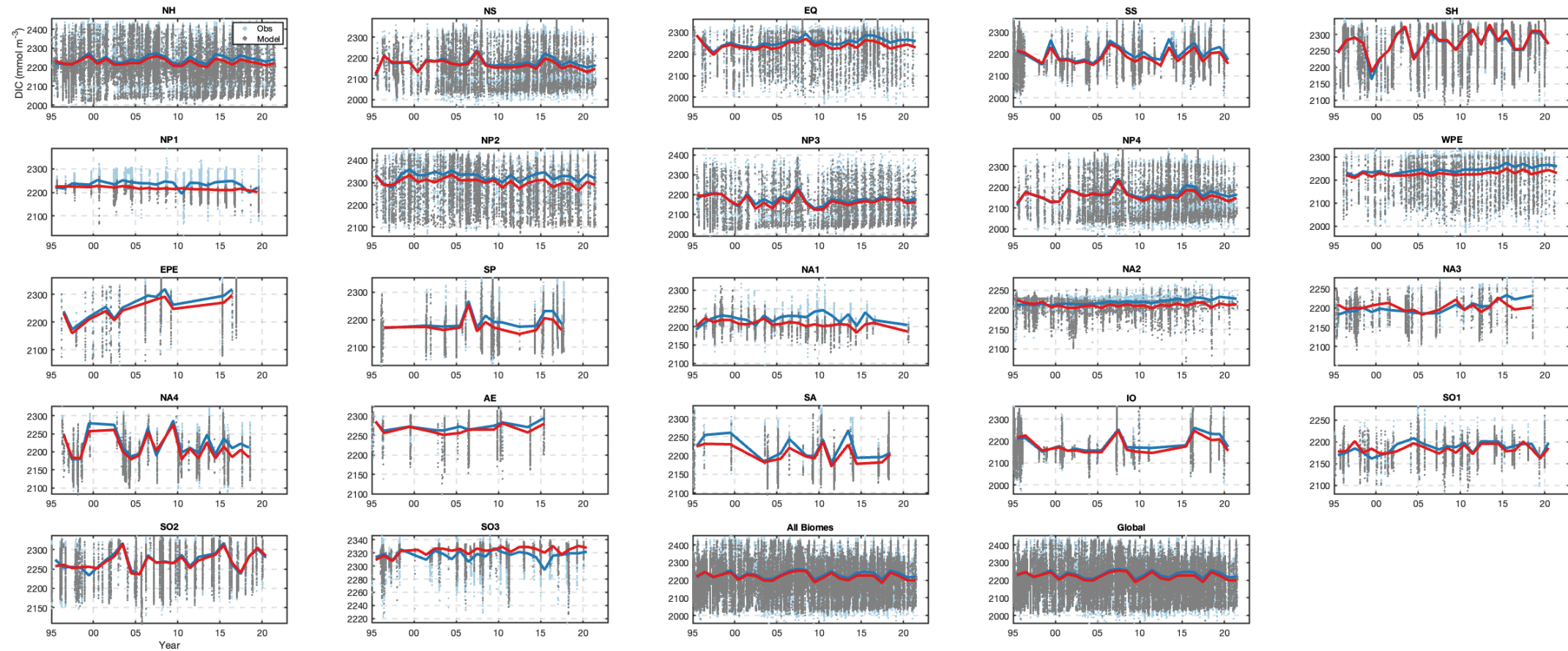


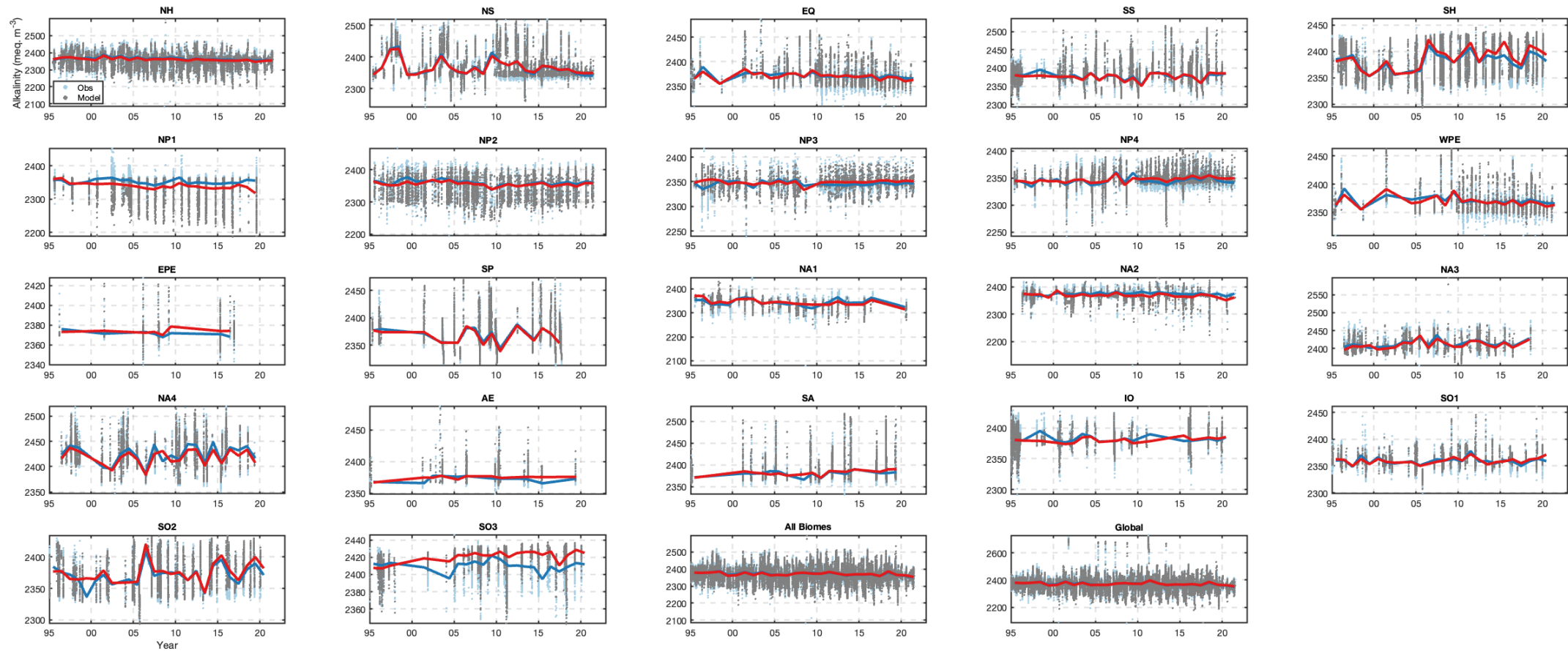


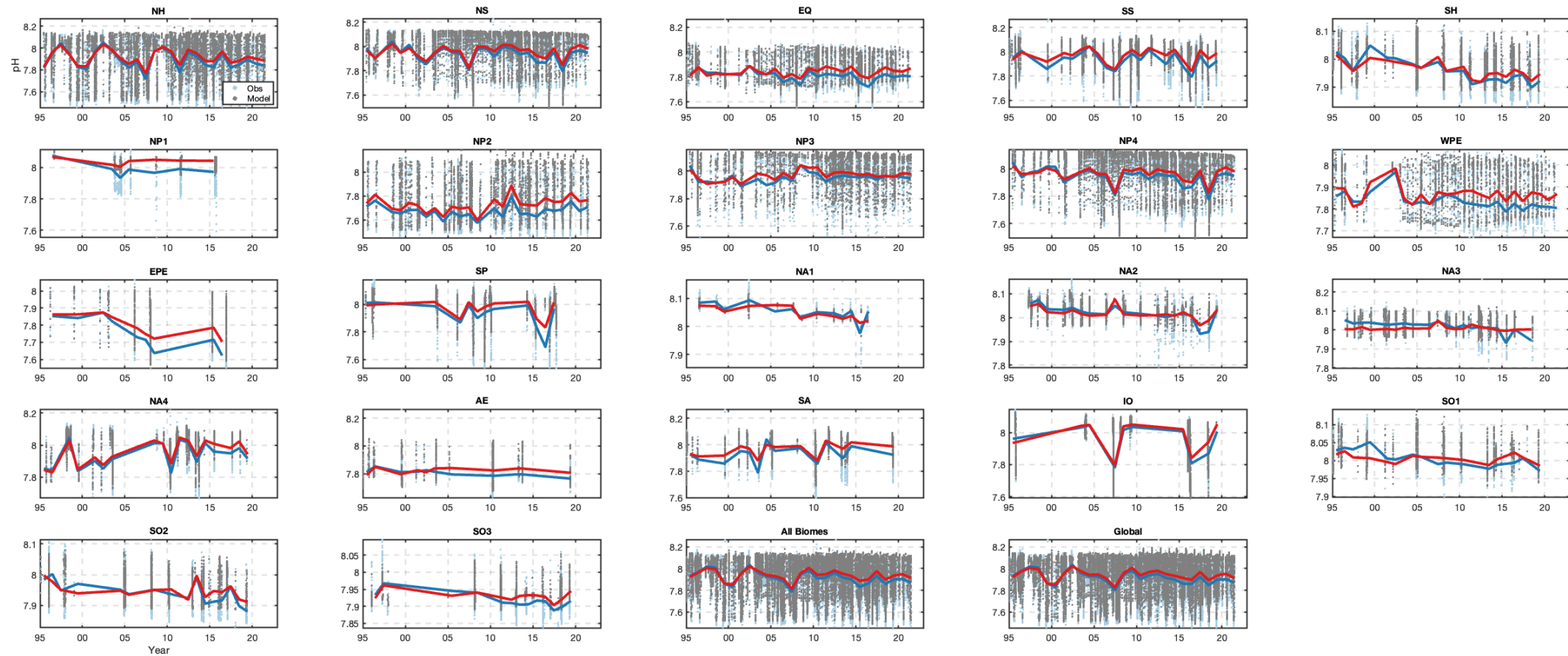
GLODAP time series: 100 to 500-m depth

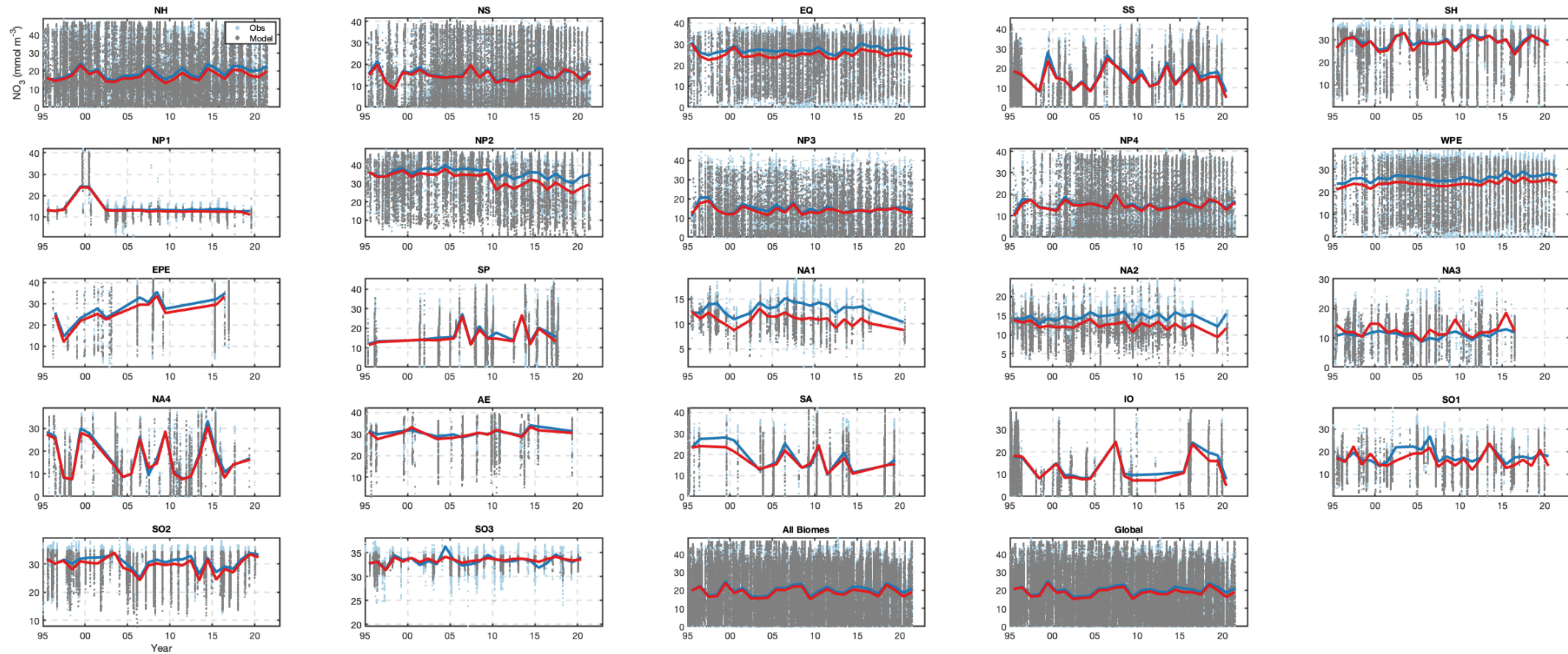


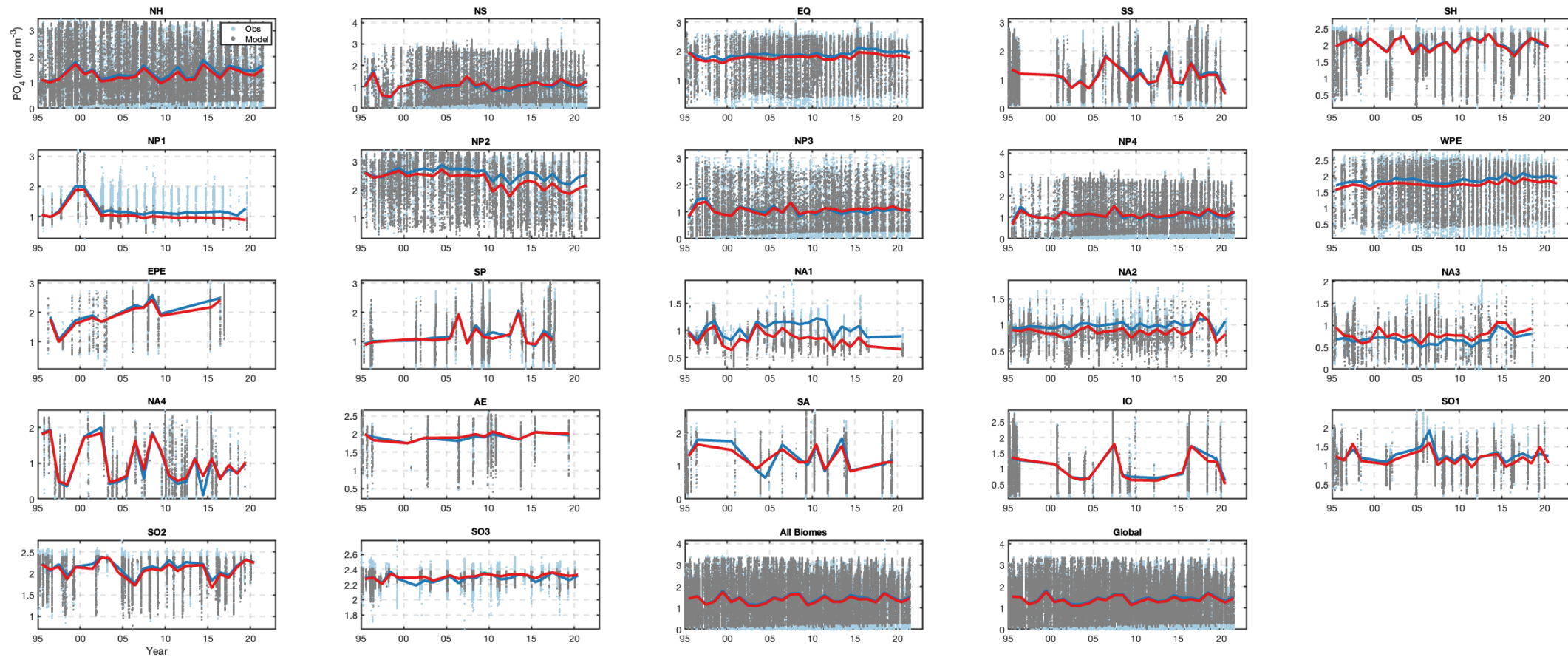


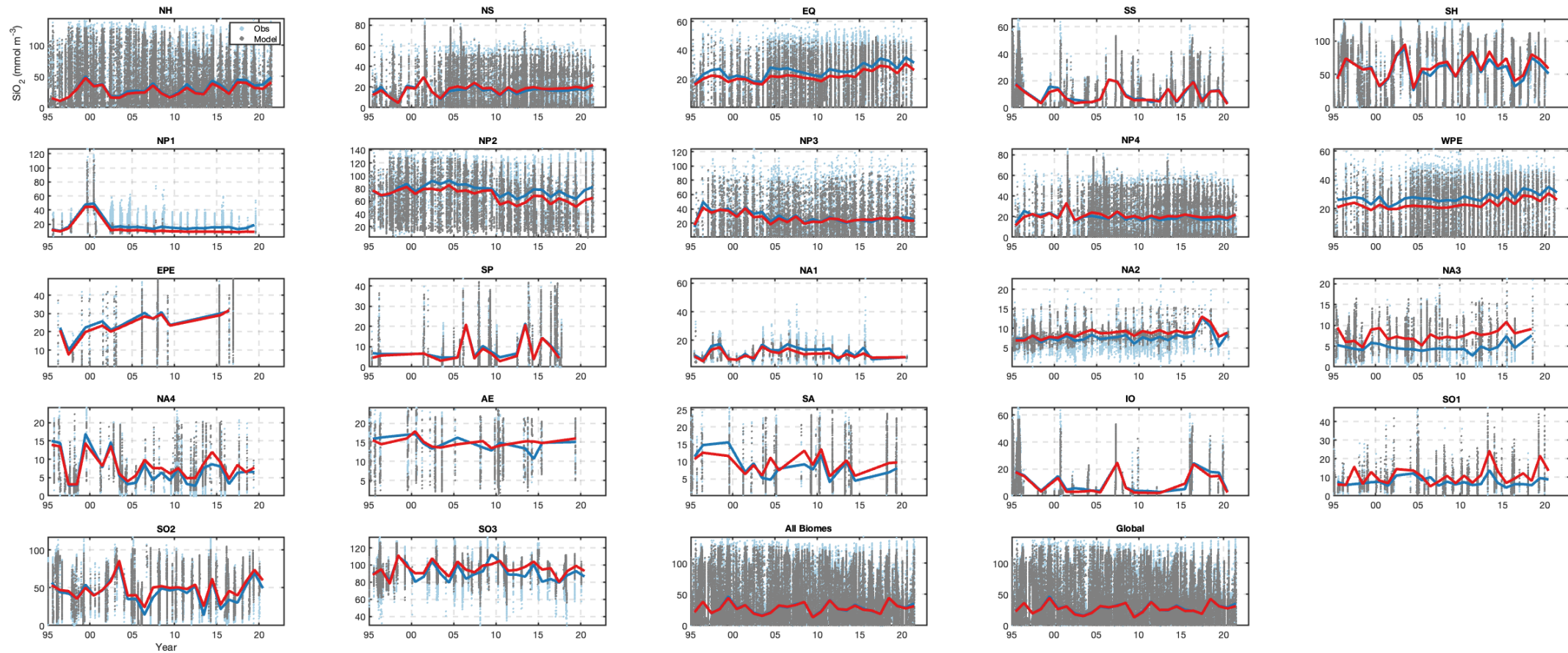


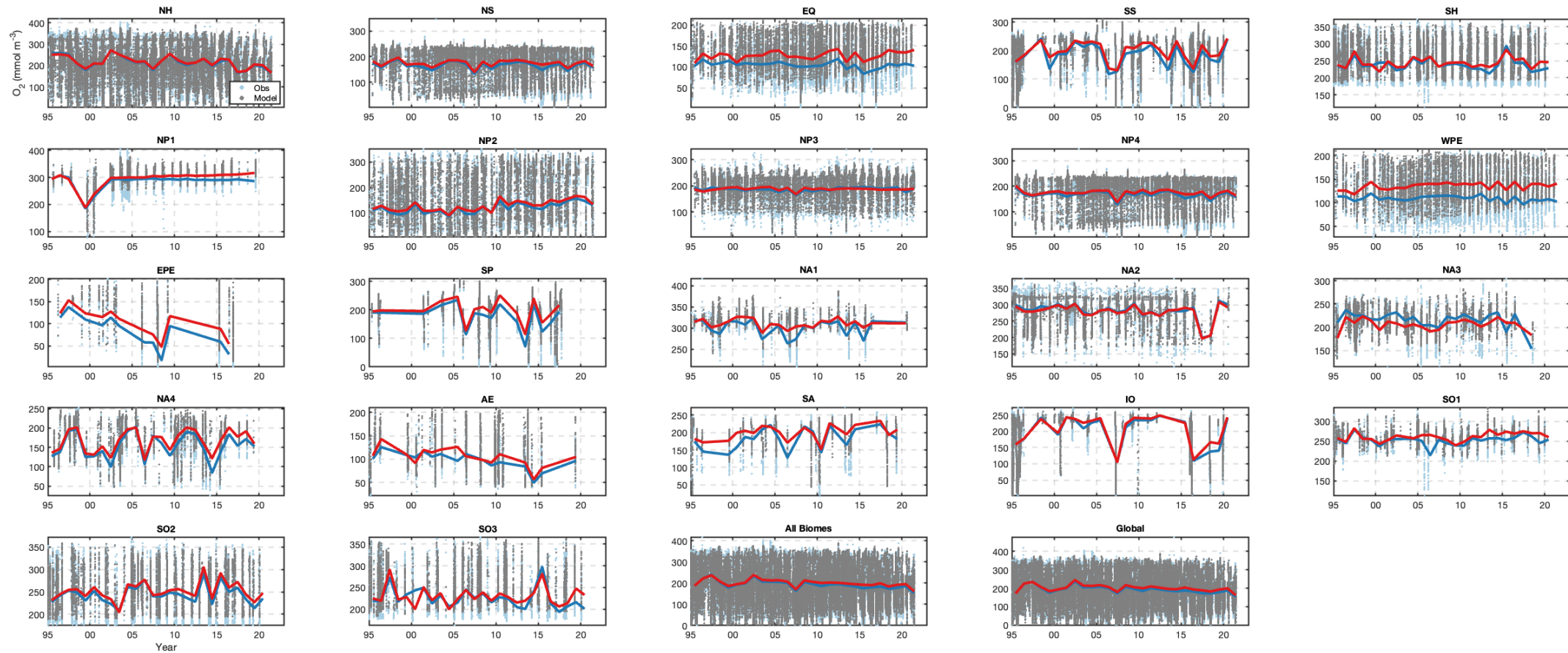




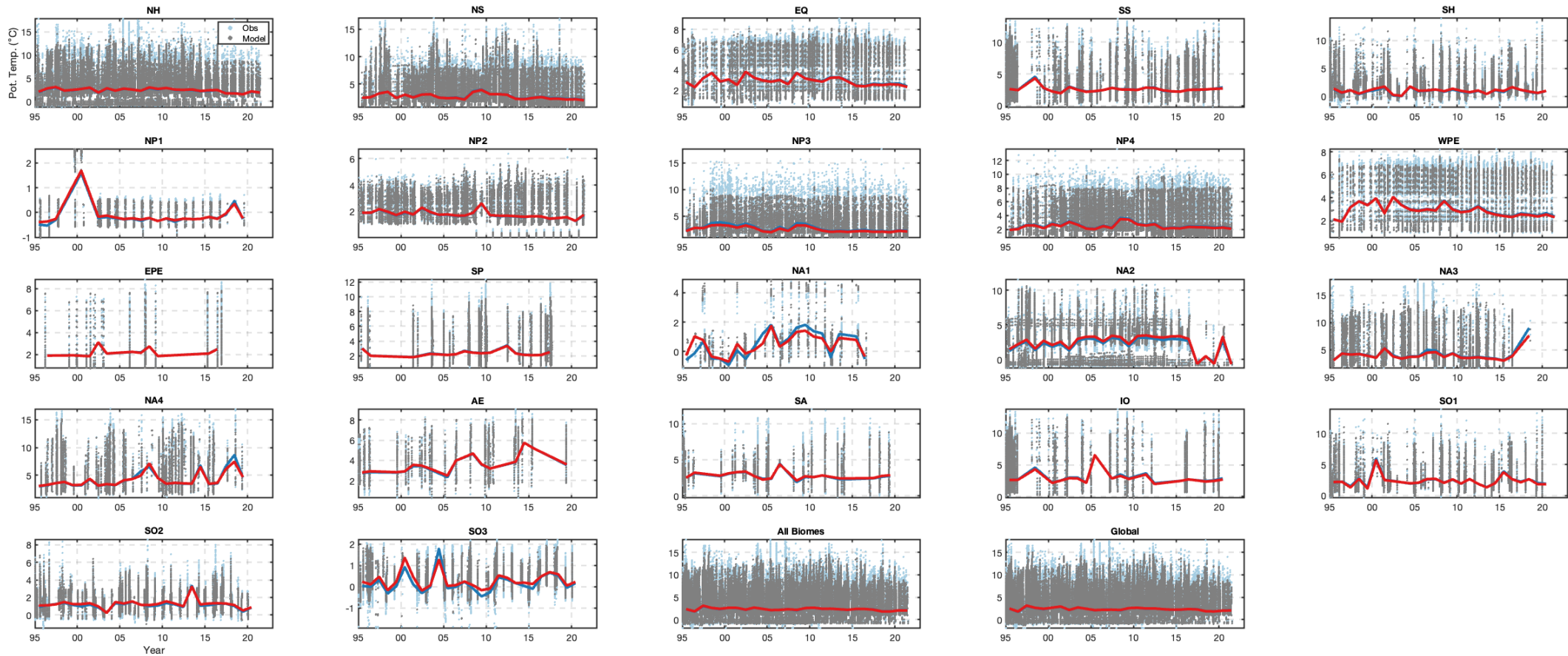


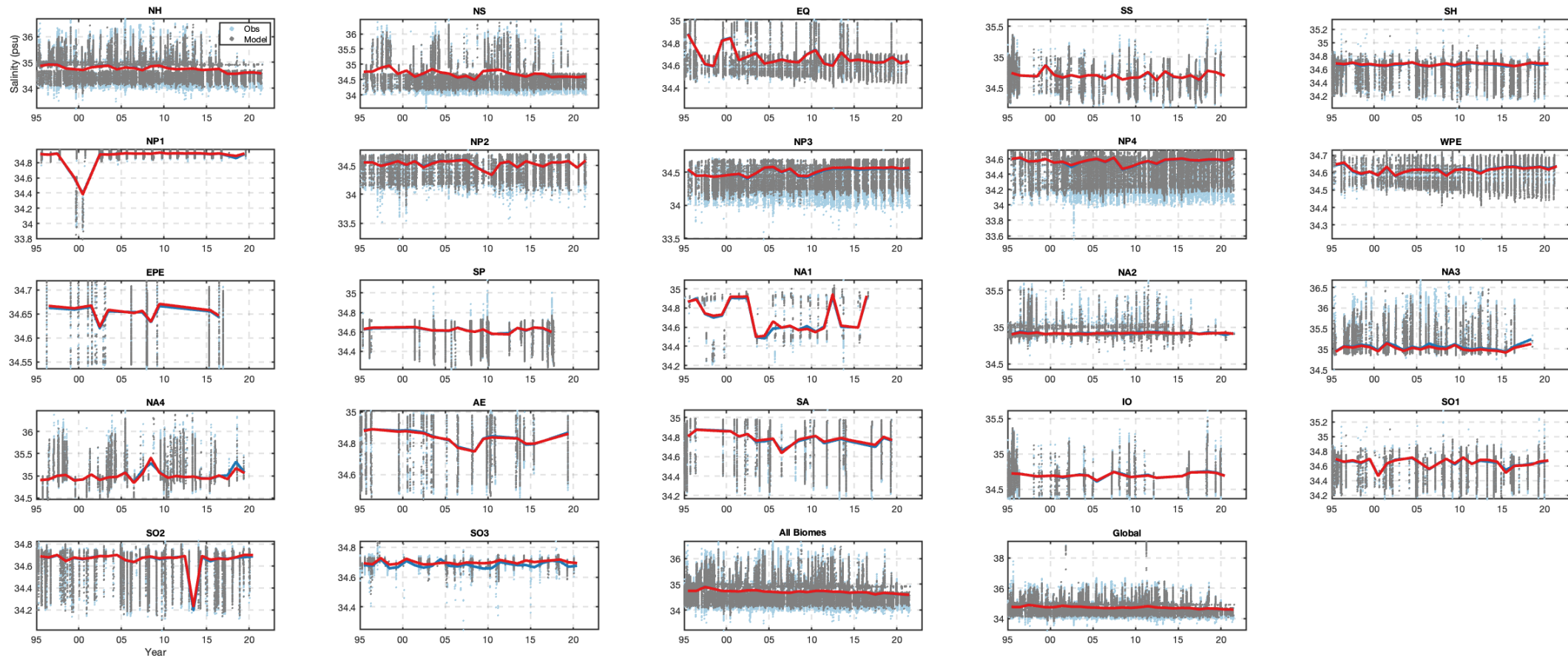


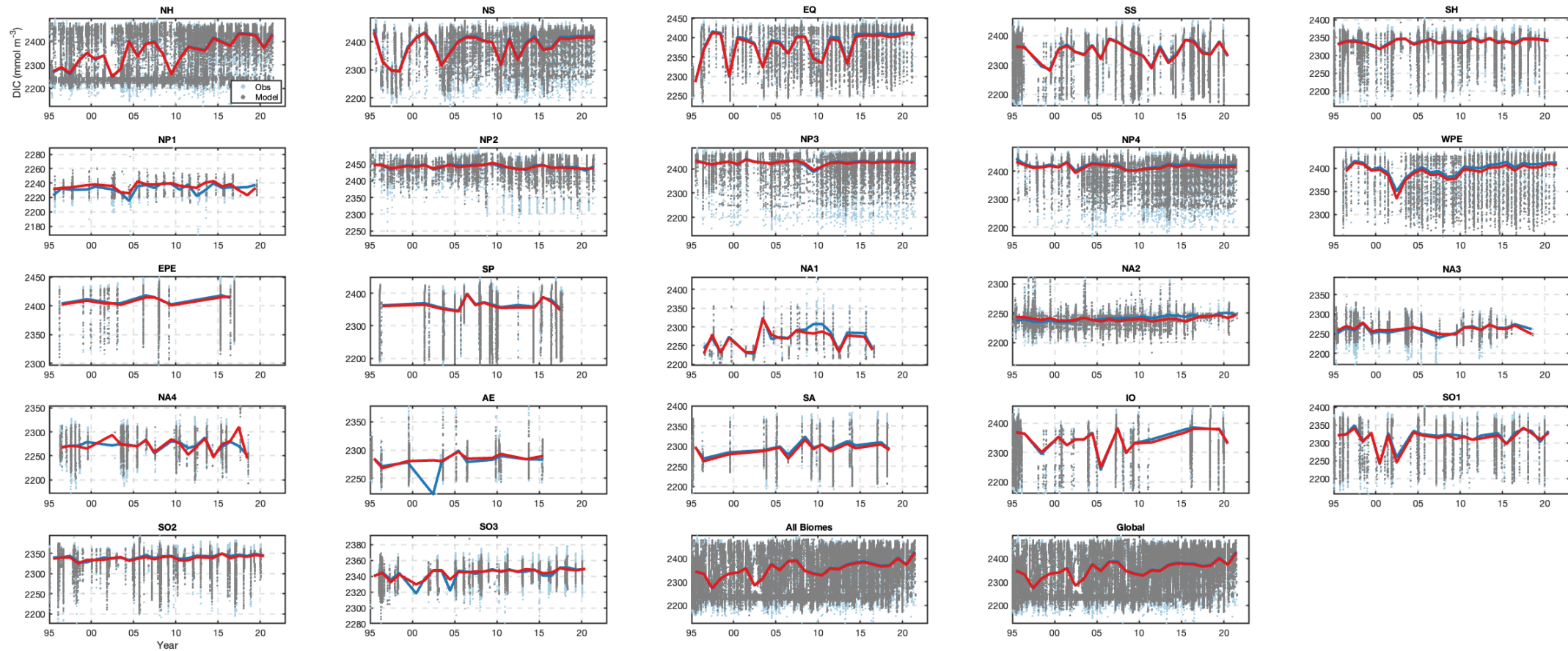


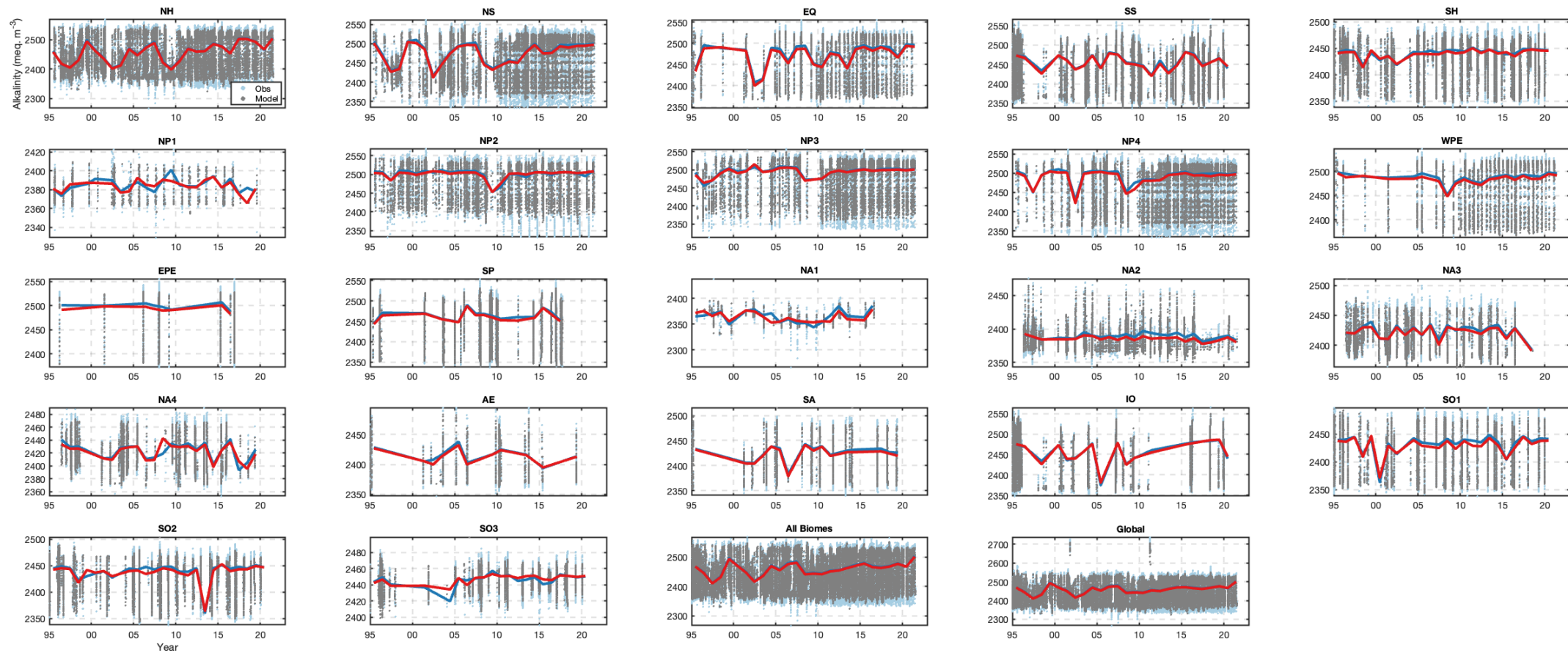


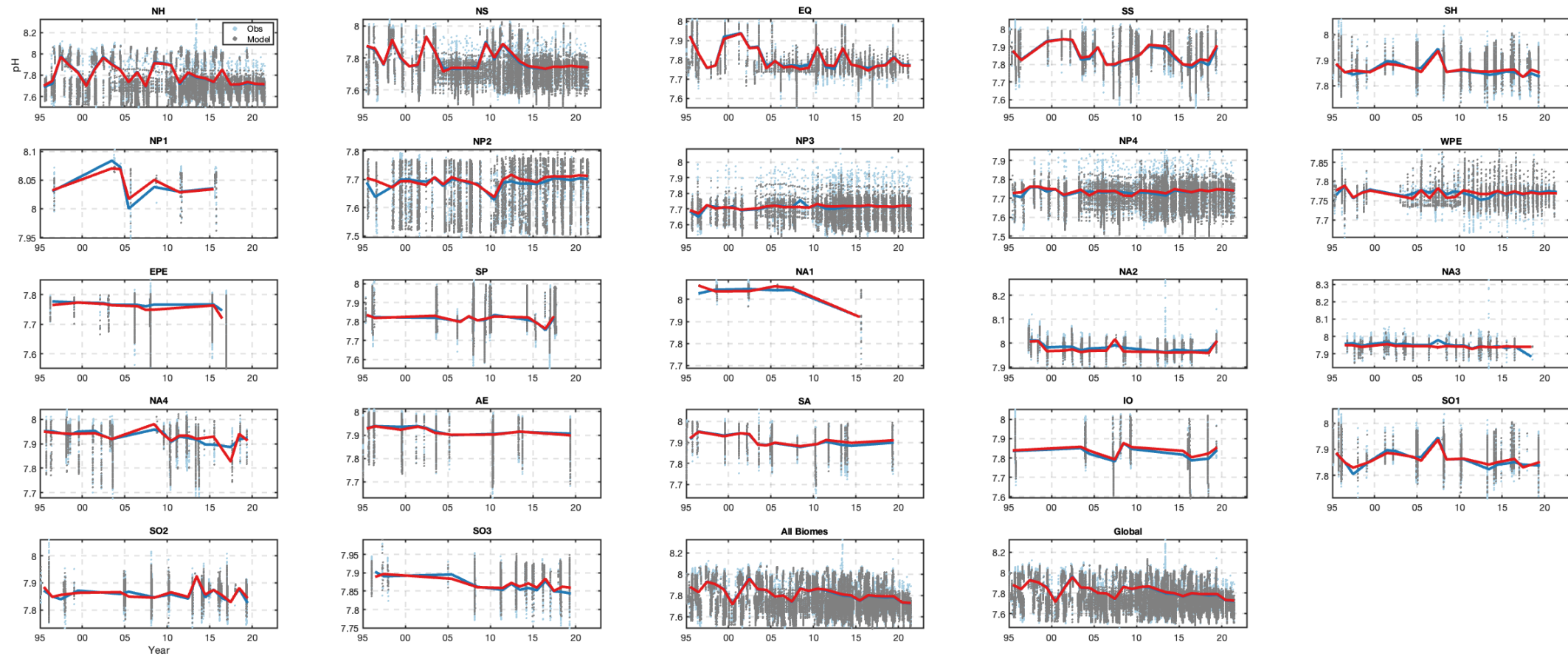
GLODAP time series: 500 to 6000-m depth

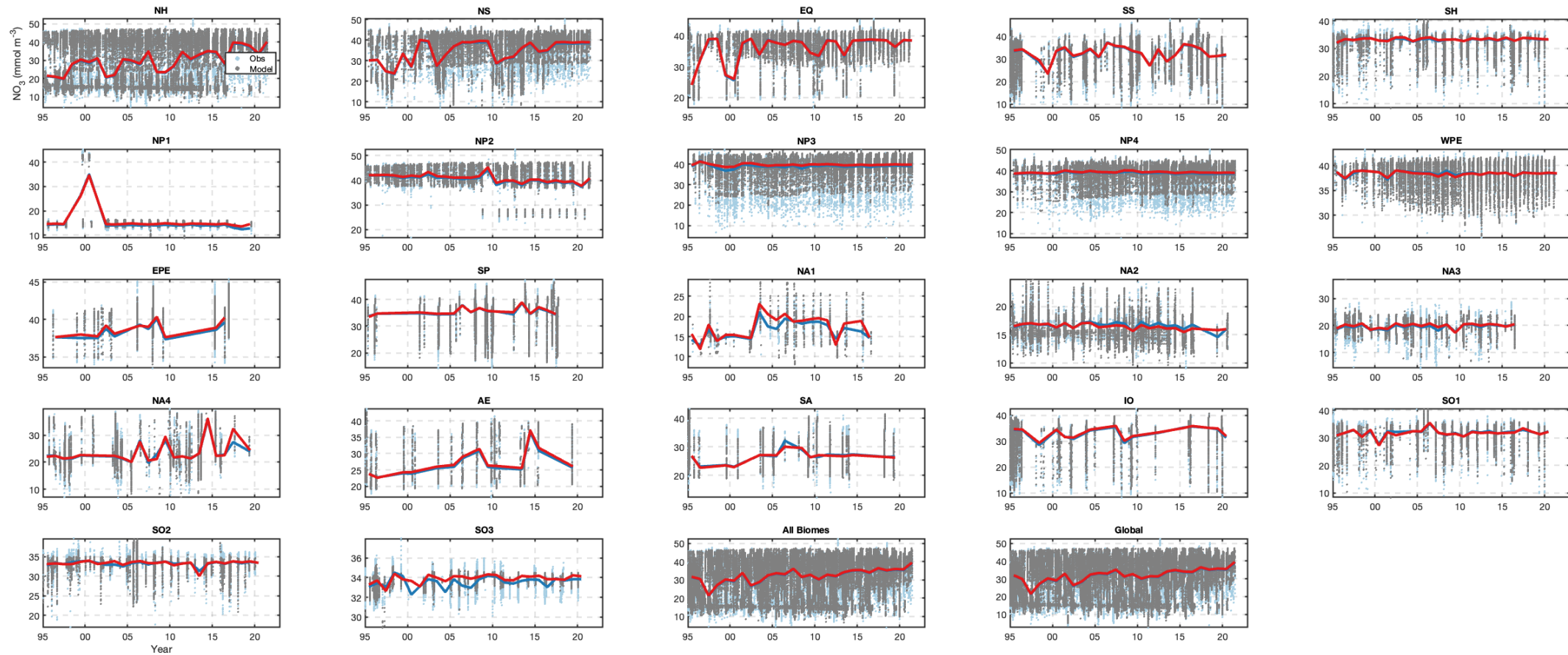


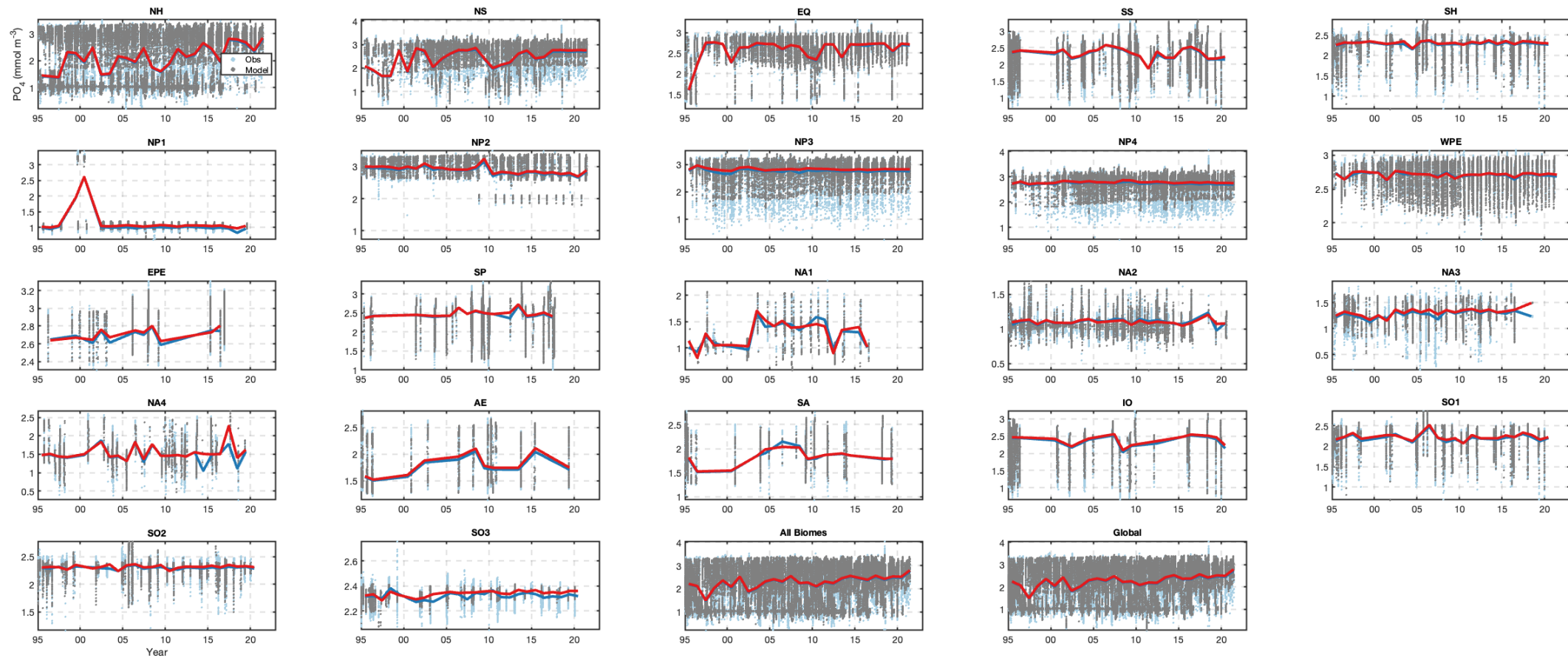


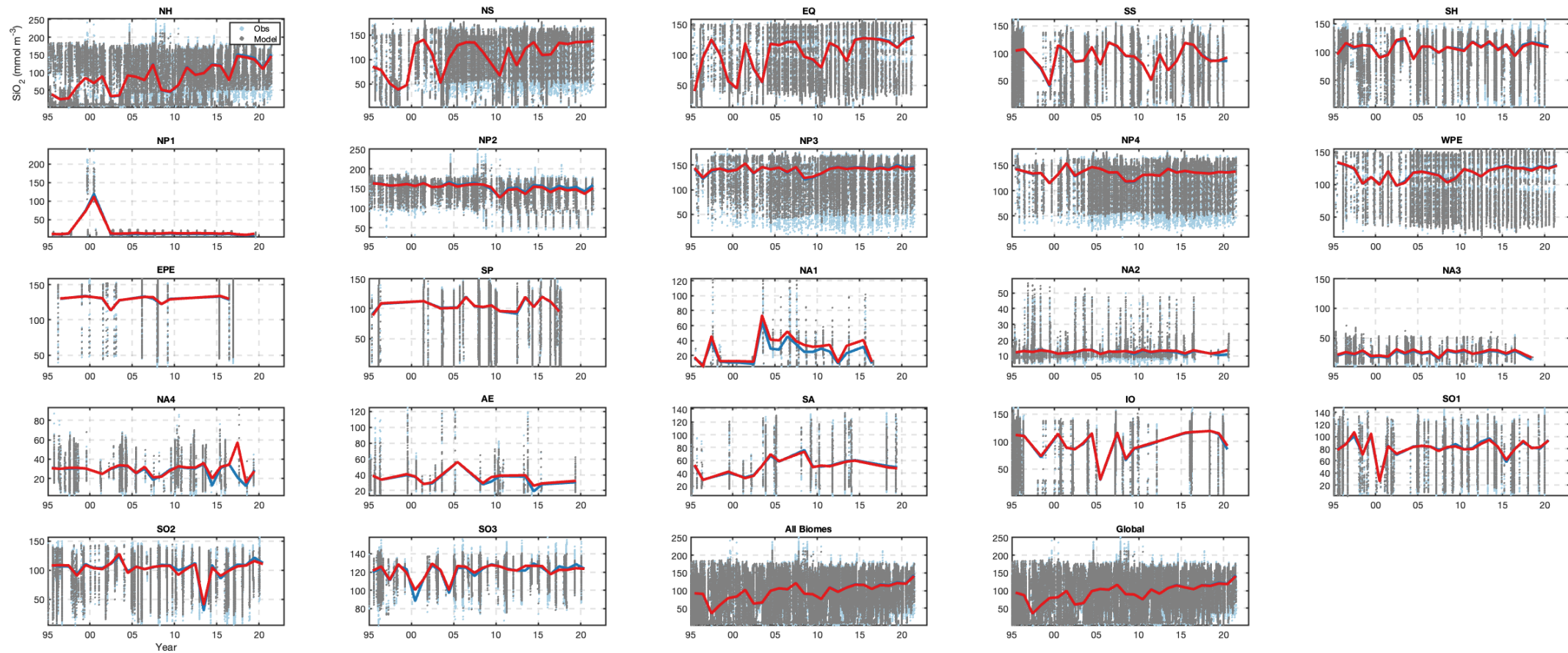


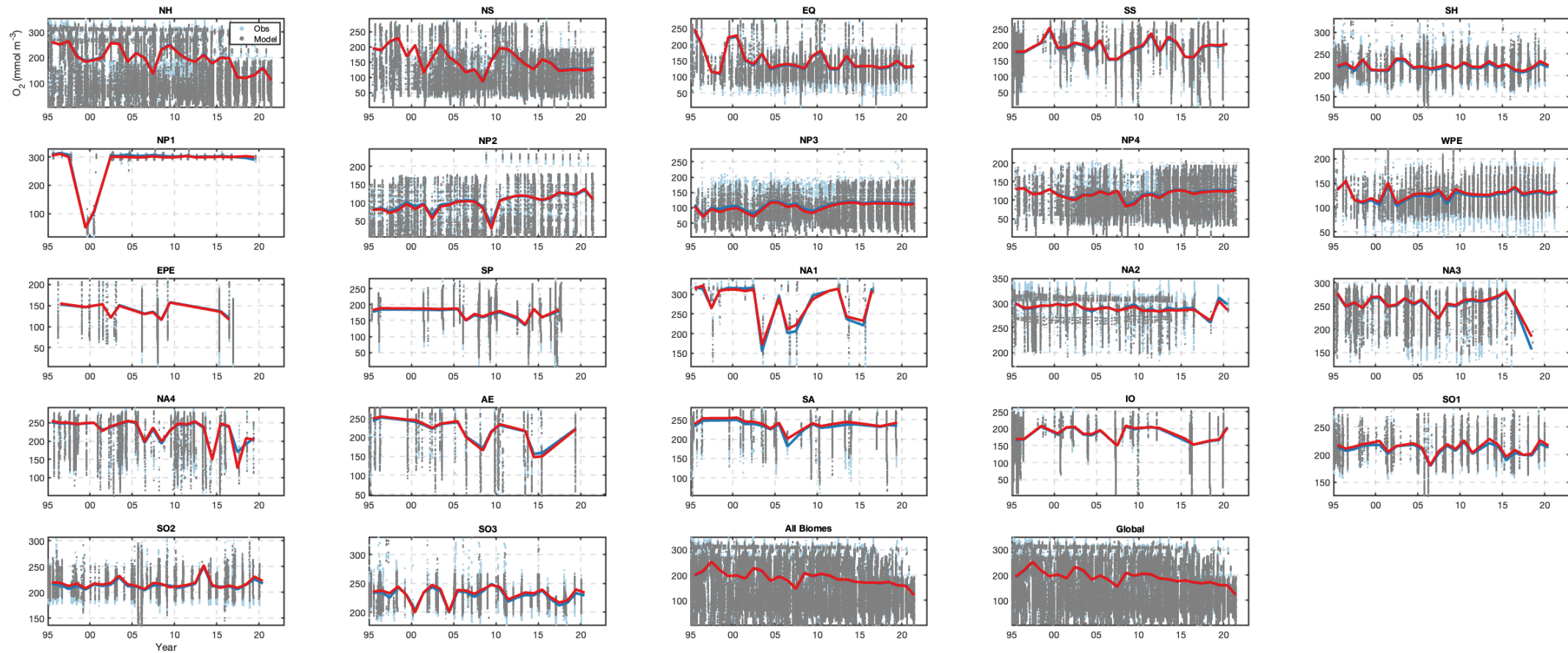




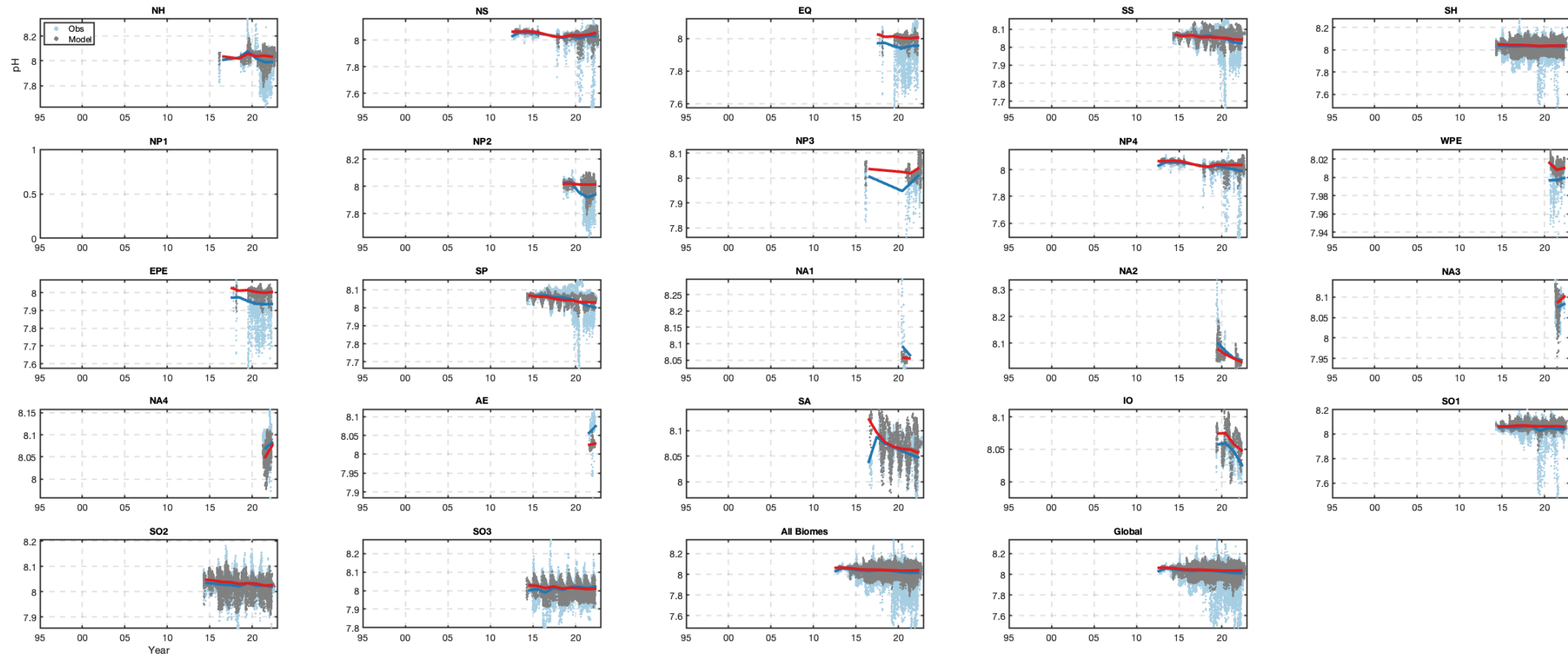


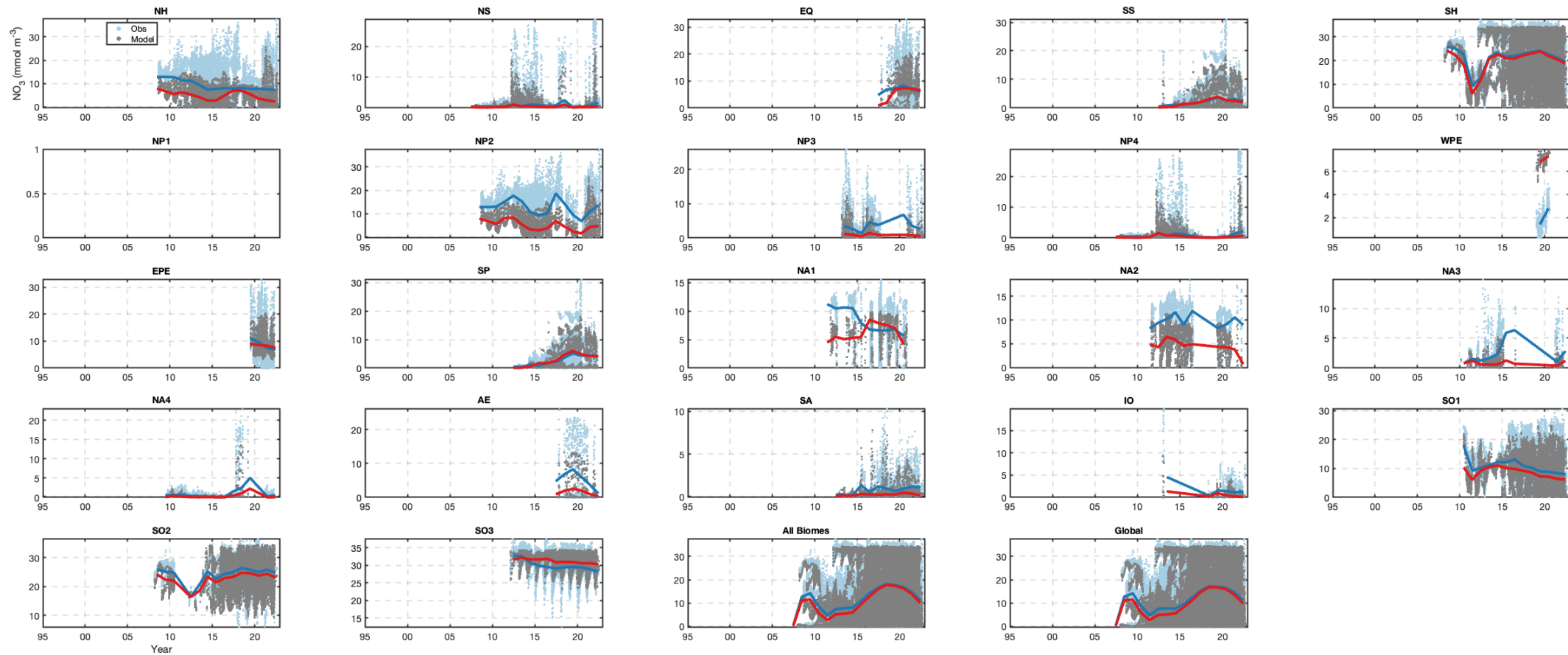


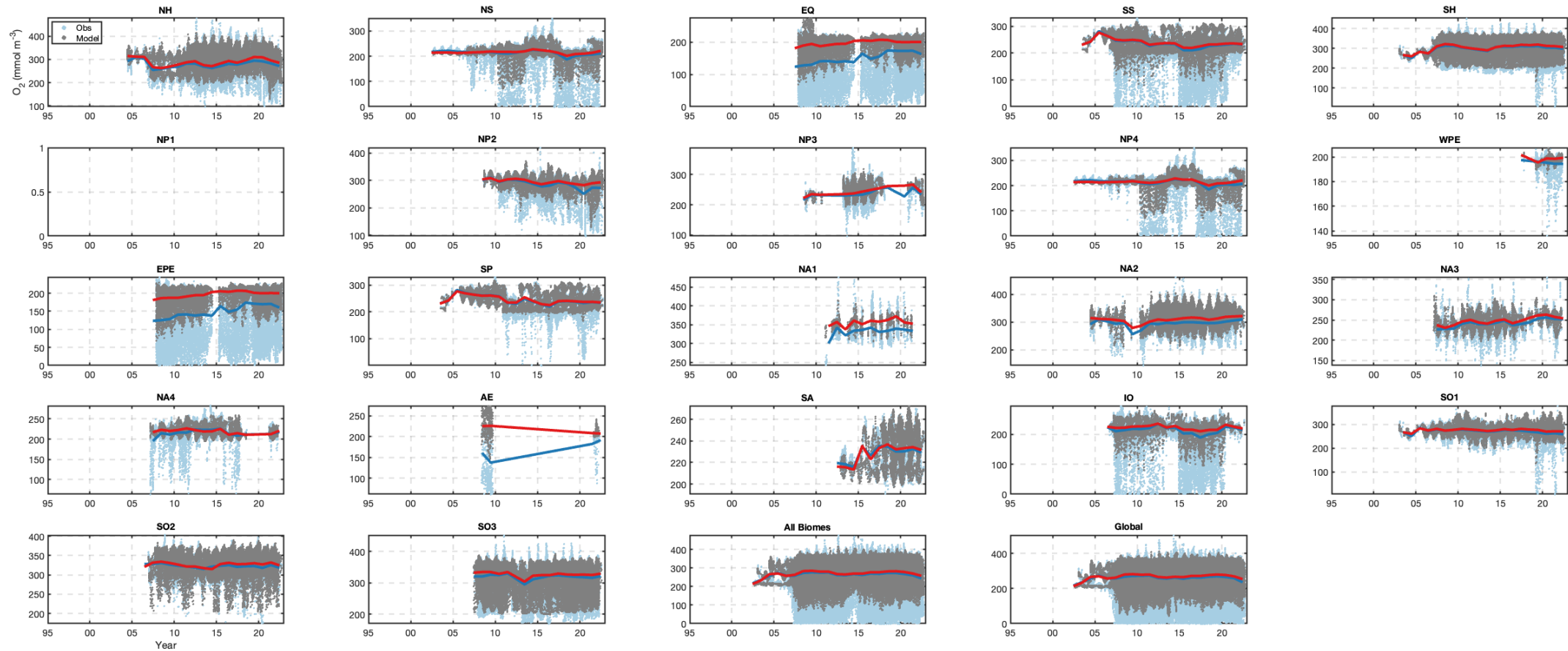




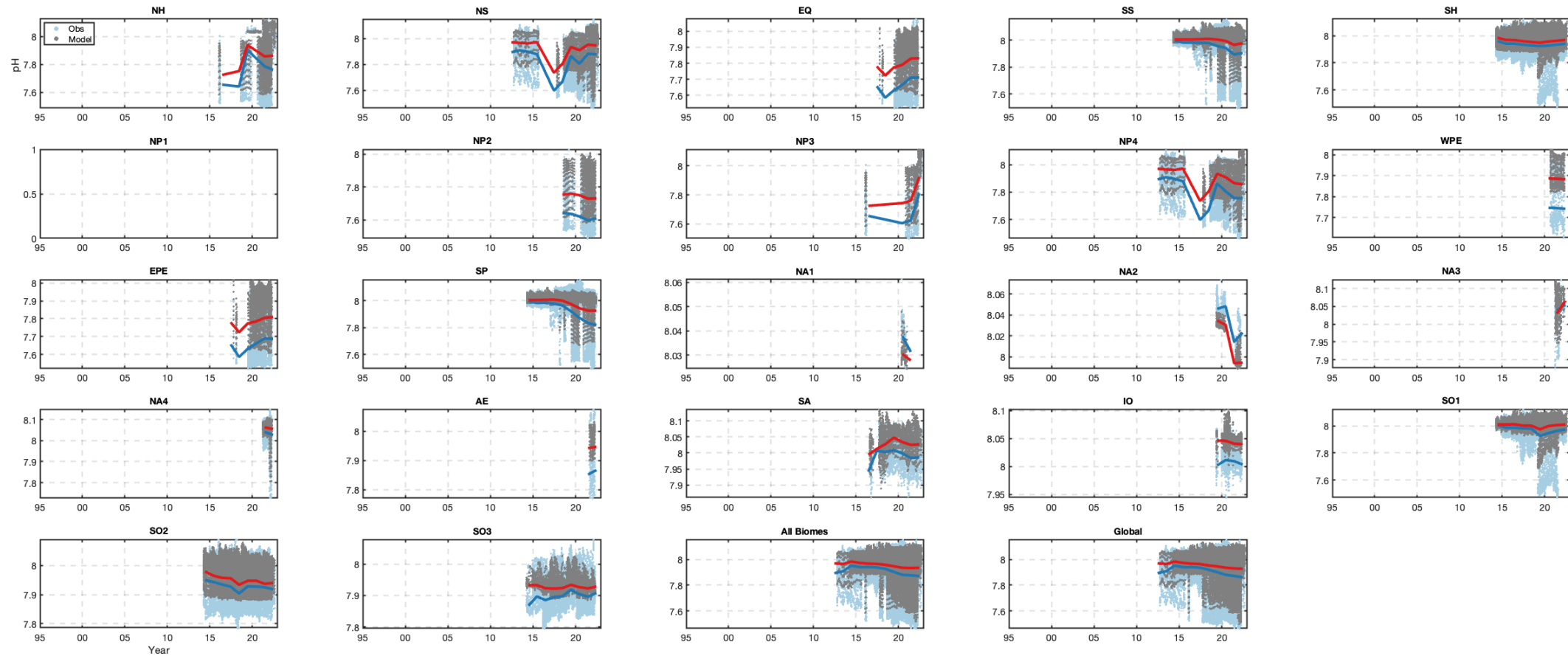
BGC-Argo time series: 0 to 100-m depth

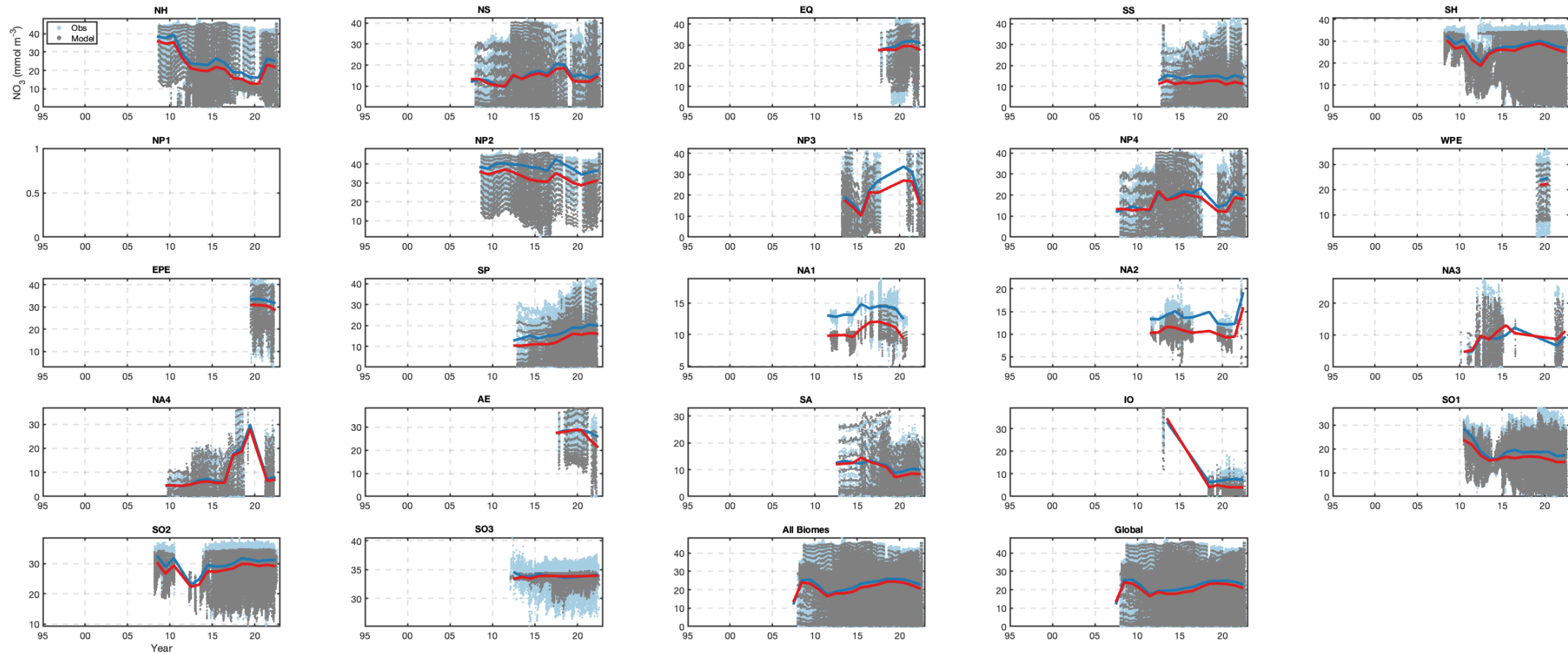


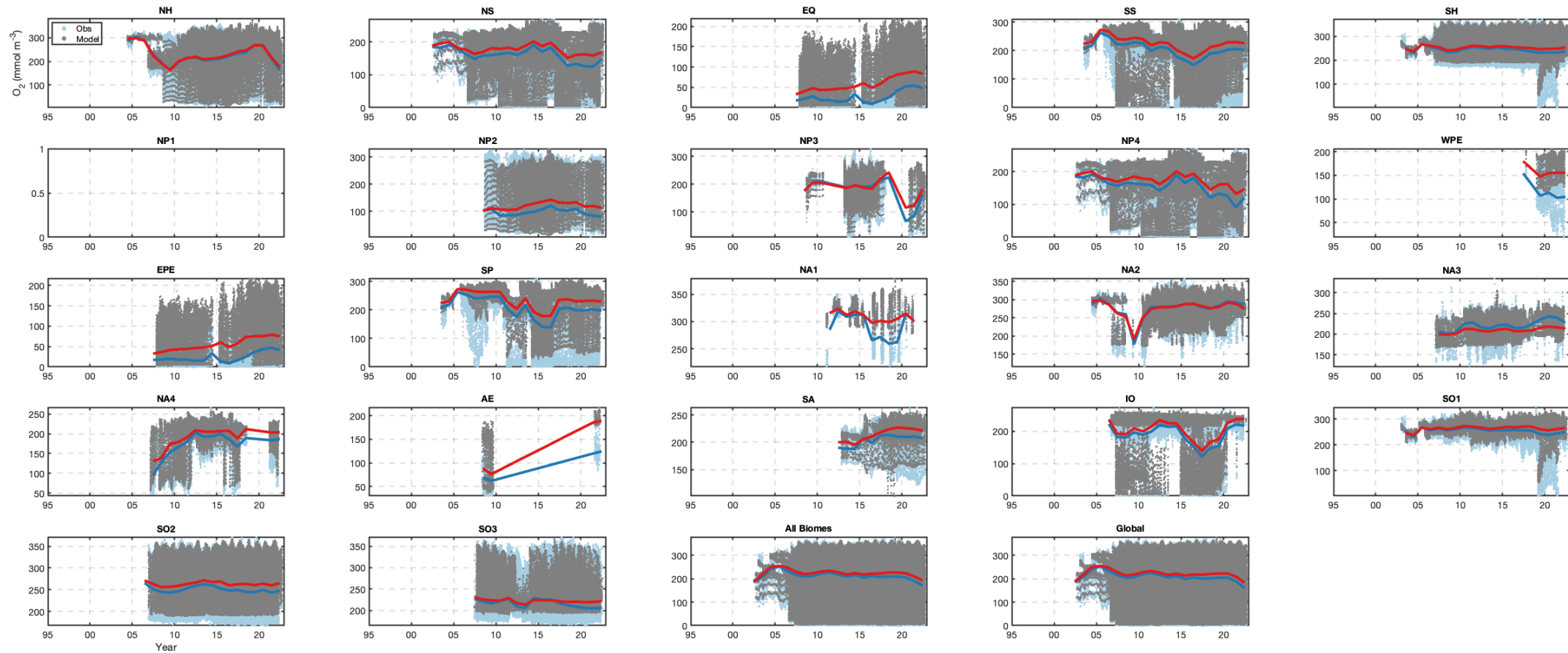




BGC-Argo time series: 100 to 500-m depth







BGC-Argo time series: 500 to 6000-m depth

